BIOCHAR FROM VACUUM PYROLYSIS OF AGRICULTURAL RESIDUES: CHARACTERISATION AND ITS APPLICATIONS

by

Ümit Uras

Thesis presented in partial fulfillment
of the requirements for the Degree

of

MASTER OF SCIENCE IN ENGINEERING
(CHEMICAL ENGINEERING)

in the Faculty of Engineering
at the University of Stellenbosch

Supervisor
Prof. J.H. Knoetze

December 2011

Declaration

By submitting this thesis electronically, I declare that the entirety of the work contained therein is my own, original work, that I am the sole author thereof (save to the extent explicitly otherwise stated), that reproduction and publication thereof by Stellenbosch University will not infringe any third party rights and that I have not previously in its entirety or in part submitted it for obtaining any qualification.

....

Signature Date

ABSTRACT

According to recent studies, biochar has the potential to improve soil fertility, mitigate climate change, reduce off-site pollution and assist in managing wastes. The application of biochar to soil is not a new concept; Amazonian dark earths are carbon-rich soils with high soil fertility that were created before 1541. Vacuum pyrolysis is a thermo-chemical conversion technique in which biomass is transformed into bio-oil, biochar and non-condensable gas. The objective of this work was to investigate the chemical and physical properties of biochar produced from vacuum pyrolysis of black wattle, vineyard annual prunings and sugar cane bagasse for their potential as soil amendment and adsorbent.

The vacuum pyrolysis of black wattle, vineyard prunings and sugar cane bagasse (pyrolysis temperature: 460°C, pressure: 8kPa$_{abs}$, heating rate: 17°C/min) resulted in biochar yields of 23.5%, 31.0% and 19.7% on a weight basis, respectively. The nature of the biomass had a substantial effect on yields of the products. High ash content combined with high lignin composition led to higher biochar yields for vineyard prunings.

The highest surface acidity was observed for sugar cane bagasse (2.3 mmol/g), whereas the lowest surface acidity was observed for vineyard biochar (1.67 mmol/g). Consequently, the pH of the biochars was in the order: vineyard (10.43)> black wattle (9.74)> sugar cane bagasse (6.56). The cation exchange capacities (CEC) of biochars were 122 cmol/kg, 101 cmol/kg and 65 cmol/kg for sugar cane bagasse, black wattle and vineyard, respectively. The electrical conductivities (EC) were highly correlated with feedstock nature. The Ca and K rich vineyard biochar resulted in the highest EC (0.83 dS/m), whilst EC values of black wattle and sugar cane bagasse were 0.67 dS/m and 0.17 dS/m, respectively. Biochars contained substantial amounts of plant-available nutrients, while being low in toxic inorganic content (Pb, As, Cd). The BET surface areas of sugar cane bagasse, black wattle and vineyard were 259 m^2/g, 241 m^2/g and 91 m^2/g, respectively.

The adsorption capacity was found to increase with increased contact time and initial solution concentration. The experimental equilibrium time were found to be 3505 min, 1350 min and 150 min for adsorption of 20 mg/L methylene blue solution for vineyard, black wattle and sugar cane bagasse, respectively. Equilibrium data were well fitted to Langmuir and Freundlich isotherms. The maximum adsorption capacities were found to be 15.15 mg/g, 14.49 mg/g and 19.23 mg/g for

vineyard, black wattle and sugar cane bagasse when modelled with Langmuir isotherms. The adsorption kinetics was found to follow the pseudo-second order kinetic model.

In summary, biochar from sugar cane bagasse is a promising adsorbent for the removal of basic dyes due to its high surface area and microporous structure. This biochar can be applied to slightly acidic soils for nutrient retention and the exchange of nutrients. On the other hand, possessing high amounts of nutrients, biochars from black wattle and vineyard are potential soil amendentment agents. Biochar from black wattle is more beneficial compared to biochar from vineyard due to its higher surface area, microporosity and cation exchange capacity.

OPSOMMING

Volgens onlangse studies, het houtskool die potensiaal om grond vrugbaarheid te verbeter, klimaat verandering te versag, besoedeling te verlaag en ondersteuning te verleen in die bestuur van afval. Die toevoeging van houtskool in grond is nie 'n nuwe konsep nie; Amazone donker gronde is koolstof ryk gronde met hoë vrugbaarheid wat voor 1541 geskep is. Vakuum pirolise is 'n termo-chemiese omskakelings tegniek waarin biomassa afgebreek word na bio-olie, houtskool en nie-kondenseerbare gasse. Die doelwit van hierdie werk was om die chemiese en fisiese eienskappe van houtskool, wat geproduseer is deur die vakuum pirolise van swart wattel, jaarlikse wingerd snoeisels, en suikerriet bagasse, vir hulle potensiaal vir grond verbetering en adsorpsie toepassings te ondersoek.

Die vakuum pirolise van swart wattel, jaarlikse wingerd snoeisels, en suikerriet bagasse (pirolise temperatuur: 460°C, druk: 8kPa$_{abs}$, verhittingstempo: 17°C/min) het houtskool opbrengste van 23.5%, 31.0% en 19.7% op massa basis, respektiewelik tot gevolg. Die tipe biomassa het 'n beduidende effek op die opbrengs van die produkte. Hoë as-inhoud, gekombineer met hoë lignien inhoud, lei tot hoër houtskool opbrengste vir wingerd snoeisels.

Die hoogste oppervlak suurheid is gevind vir suikerriet bagasse (2.3 mmol/g), terwyl die laagste waarde gevind is vir die wingerd snoeisels (1.67 mmol/g). Gevolglik, is die pH van die houtskole in die volgorde van: wingerd (10.43) > swart wattle (9.74) > suikerriet bagasse (6.56). Die katioon uitruiling vermoë (CEC) van die houtskole was 122 cmol/kg, 101 cmol/kg and 65 cmol/kg vir suikerriet bagasse, swart wattel en wingerd snoeisels respektiewelik. Die elektriese konduktiwiteite (EC) is gekorreleer met die eienskappe van die biomassas. Die Ca en K ryke wingerd snoeisel houtskool het die hoogste EC waarde (0.83 dS/m) tot gevolg, terwyl die EC waardes vir swart wattel en suikerriet bagasse bepaal is as 0.67 dS/ 0.16 dS/m respektiewelik. Die houtskole het groot hoeveelhede plant-beskikbare voedingstowwe bevat, terwyl dit laag was in toksiese anorganiese stowwe (Pb, As, Cd). Die BET oppervlak areas van suikerriet bagasse, swart wattel en wingerd snoeisels was 259 m^2/g, 241 m^2/g en 91 m^2/g respektiewelik.

Daar is gevind dat die adsorpsie kapasiteit toeneem met toenemende kontak tyd met die aanvanklike oplossing. Die eksperimentele ewewigs tye is gevind as 350 min, 1350 min en 150 min vir die adsorpsie van 'n 20 mg/L metileen blou oplossing vir wingerd snoeisels, swart wattel en suikerriet bagasse, respektiewelik. Die ewewigs data het die Langmuir en Freundlich isoterme goed

gepas. Die maksimum adsorpsie kapasiteite is gevind as 15.15 mg/g, 14.9 mg/g en 19.23 mg/g vir wingerd snoeisels, swart wattel en suikerriet bagasse wanneer dit gemodeleer is met Langmuir isoterme. Daar is bevind dat die adsorpsie kinetika ‘n pseudo-tweede orde kintika model volg.

In opsomming, houtskool van suikerriet bagasse is ‘n veelbelowende adsorpsie middel vir die verwydering van basiese kleurstowwe, as gevolg van die hoë oppervlak area en mikroporie-struktuur van hierdie houtskool. Dié houtskool kan gebruik word op effense suur gronde vir voedingstof behoud en uitruiling. Aan die ander kant, houtskole van swart wattel en wingerd snoeisels wat hoë hoeveelhede voedingsstowwe bevat, is potensiële grond verbeterings middels. Houtskool afkomstig van swart wattel is meer voordelig as die van wingerd snoeisels, as gevolg van die hoër oppervlak area, mikroporositeit en katioon uitruilings vermoë van die swart wattel houtskool.

ACKNOWLEDGEMENTS

Firstly, I would like to express my gratitude to my supervisor Prof. Knoetze for the opportunity he gave me to do this project and the financial support over the last year.

I am particularly indebted to Dr. Marion Carrier and Dr. Ailsa Hardie for their kindness, support and help during the project. I feel privileged to have worked with knowledgeable researchers who did not hesitate to answer my questions neither to give their precious time. Thank you for teaching me how to be a good researcher.

I would like to thank Hanlie Botha, Matt Gordon, Esme Spicer, Riana Rossouw, Susanne Causmann and Cathy Clarke for the analyses they did. They especially made me happy when the results were good.

I would like to thank my mom, dad and sister for supporting my decisions, believing in me and being there for me. I would like to thank them for calling me every second day and being as excited as I was during the thesis write-up. I love them all.

I would like to thank my dear friends, especially Dirk Postma for his kindness, help and support, and Jeanne du Preez for praying with me and encouraging me since we met. I would like to thank my dear friend, Makhosazana Sika for making my soil science adventure more enjoyable with her positive energy. I would also like to thank my officemates in A601, especially Frans van Schalkwyk, Derek Gerber, Jan-Erns Joubert, Stephen Danje, Mohsin Karimi and Takura Nyashanu. I count myself lucky to have met all of you.

Finally I would like to thank my God for all the love, hope, faith and strength He gave me.

TABLE OF CONTENTS

LIST OF FIGURES

CHAPTER 1: INTRODUCTION

CHAPTER 2: LITERATURE REVIEW

CHAPTER 3: MATERIALS AND METHODS

CHAPTER 4: RESULTS AND DISCUSSION

APPENDIX C: Calibration curves used for calculation of MB concentraction

APPENDIX E:Time (min) versus q (mg/g) equilibrium graphs for MB adsorption

APPENDIX F: Pseudo-second-order adsorption kinetics for overall adsorption of 20 ppm MB

LIST OF TABLES

CHAPTER 2: LITERATURE REVIEW

CHAPTER 3: MATERIALS AND METHODS

CHAPTER 4: RESULTS AND DISCUSSION

APPENDIX D: Adsorption raw data

LIST OF ABBREVIATIONS

Abbreviation	Abbreviated word
FC	Fixed carbon
AA	Activating agent
AC	Activated carbon
AIL	Acid insoluble lignin
BC	Before Christ
BP	British Petroleum
BW	Black wattle
daf	Dry and ash-free
dw	Dry weight
EPA	Environmental Protection Agency
FTIR	Fourier Transform Infrared Spectroscopy
GHG	Green house gas
GtC	Gigatons of carbon
HW	Hardwood
IEA	International Energy Agency
Liquid yield	All liquids from pyrolysis including water and oil fractions
MB	Methylene blue
MC	Moisture content
NMR	Nuclear Magnetic Resonance
NOC	Neutral Organic Contaminants
PB	Pine Bark
PC	Pine Chip pellets
PN	Pine hull pellets
SAWIS	South Africa Wine Industry and Systems
SCB	Sugar cane bagasse
SD	Pine sawdust
SOM	Soil Organic Matter
SSE	Sum of Square Errors
Tarry phase	The viscous phase which is collected from room temperature condenser and pipes
TGA	Thermogravimetric Analysis
UIPAC	International Union of Pure and Applied Chemistry
UNFCCC	United Nations Framework Convention on Climate Change
V	Vineyard
VM	Volatile matter
wt.%	Weight percentage
Y	Yield

LIST OF SYMBOLS

Abbreviation	Name	Unit
AC_0	Ash content of biomass	%
AC_f	Ash content of biochar	%
b	Langmuir constant	L/mg
BET surface area	Brunaur-Emmett-Teller surface area	m^2/g
C	Concentration of solution	ppm or mg/L
C	Intraparticle diffusion constant	mg/g
C_0	Initial concentration of solution	ppm or mg/L
C_e	Concentration at equilibrium	ppm or mg/L
CEC	Cation exchange capacity	meq/g
C_s	Solubility of adsorbate concentration	ppm or mg/L
EC	Electrical conductivity	dS/m
HR	Heating rate	°C/min
HT	Hold time	min or h
k_1	Pseudo-first-order rate constant	1/min
k_2	Pseudo-second-order rate constant	g/mg min
K_F	Freundlich equilibrium constant	$mg^{1-1/n}.L^{1/n}.g^{-1}$
k_p	Intraparticle diffusion rate constant	$mg/g\ min^{1/2}$
$\dot{M}$	Mass flow rate	kg/h
m_0	Initial biomass mass	g
m_f	Biochar mass	g
m_{RTC}	Mass of room temperature condenser	g
n	Freundlich constant	-
P	Pressure	kPa, Pa or atm
q	The amount adsorbed per unit mass	mg/g
q_e	Adsorption capacity at equilibrium	mg/g
q_m	value of q corresponding monolayer coverage	mg/g
R_L	Correlation factor	-
SA	Surface acidity	mmol/g
SB	Surface basicity	mmol/g
T	Temperature	°C or K
t	Time	min
V	Solution volume	mL
Vporosity	volume of porosity	m^3/g
WC_0	Water content of biomass	%
WC_1	Water content of water phase	%
WC_2	Water content of tarry phase	%

CHAPTER 1: INTRODUCTION

Climate change caused by greenhouse gas (GHG) emissions is now widely recognised as a serious threat to human civilisation and natural ecosystems (Woolf, 2008). It is known that fossil fuel and land use can contribute significantly to GHG emissions (Pratt & Moran, 2010). Therefore, the increasing GHG emissions and rising fossil fuel prices have led researchers to consider the utilisation of renewable energy resources. One of the potential ways to contribute to GHG mitigation is the sequestration of carbon through pyrolysis processes (Woolf, 2008).

Pyrolysis is one of the thermo-chemical conversions that can be used to convert unused agricultural residues into useful products, namely biochar, bio-oil and non-condensable gas by heating in the absence of oxygen (Demirbaş, 2008). Vacuum pyrolysis differs from slow and fast pyrolysis in terms of operating conditions and product yields. The installation of a vacuum pump provides reduced pressure, thereby removing primary volatile products from the hot reaction zone and restricting secondary decomposition reactions (Shafizadeh, 1982). Regarding main products, while fast pyrolysis yields high amounts of oil, biochar is the main product of slow pyrolysis (Mohan *et al.*, 2006). Studies have shown that biochar yield is between 19-35% and bio-oil yield ranges between 20 and 43% via vacuum pyrolysis (Garcìa-Pèrez *et al.*, 2007; Garcìa-Pèrez *et al.*, 2002; Bouchar *et al.*, 2000; Darmstadt *et al.*, 2000).

Biochar can be used as a fuel, an adsorbent or as a soil conditioner. Adsorbents are especially preferred in wastewater treatments for the removal of heavy metals or colour, which is released from industrial activities. Biochars can be activated by steam, CO_2 or their mixtures or by using chemical activating agents (Bansal, 1988). Production of activated carbon from biochars and their adsorption abilities has been widely studied (Sharma & Uma, 2010; Raposo *et al.*, 2009; Ioannidou & Zabaniotou, 2007). However, the application of biochar to soil has recently been a reconsidered concept in the scientific community. The studies done on biochar as soil amendments have pointed out that biochar can improve soil fertility, structure, nutrient availability and carbon sequestration (Roberts *et al.*, 2010). Pyrolysis can convert approximately half of the carbon in biomass into more recalcitrant forms (Lehmann, 2006); consequently the half-life of stable C in soil is estimated to be over 1000 years (Laird, 2008). Sequestration of carbon into soil can offset the CO_2 emissions, which would otherwise have entered the atmosphere through fossil fuel production, combustion, fertiliser production or composting. From an energy point of view, the production of bio-oil and gas from pyrolysis can be used as fuels which can off-set the fossil fuel usage (Lehmann, 2006).

Facing the energy crisis, thermo-chemical processes in South Africa have become a topic of interest for conversion of cheap agricultural wastes into clean energy and valuable products. Sugar cane is one of the major harvested crops in the world and annually 6 million tonnes of sugar cane bagasse are generated in South Africa (IEA, 2010). Pyrolysis of sugar cane bagasse, especially for activated carbon production has been widely studied (Devnarain, 2003; Darmstadt *et al.*, 2001; Bernardo *et al.*, 1997), but sugar cane bagasse biochar as a soil amender has not received much attention. Likewise, there is a lack of information on the pyrolysis of wood based prunings such as black wattle and vineyard. Black wattle is an invasive tree covering a 2.5 Mha (IEA, 2010). On the other hand, South Africa has 101 259 ha under vines for wine production (SAWIS, 2009). This study will focus on the biochar production via vacuum pyrolysis of sugar cane bagasse, black wattle and vineyard prunings and their potential as adsorbents and soil amenders by determining their physical and chemical properties.

1.1 Motivation and objectives of the study

Biochar production and applications of biochar can provide numerous benefits to the environment and economy. However, to be able to obtain these benefits, the understanding of the physico-chemical structure of this valuable product has to be improved. The motivation behind this research is the fact that this topic has received little attention in South Africa even though the country produces a wide range of biomasses such as vineyards, invasive plants and sugar cane bagasse etc. that can be used in pyrolysis processes. Additional to this, there is no physico-chemical characterisation data for biochars from vacuum pyrolysis in the open literature.

The project has two principle objectives. Firstly, it aims to evaluate the chemical and physical properties of biochars produced from various sources of agricultural wastes, namely sugar cane bagasse, black wattle and vineyard prunings by using vacuum pyrolysis. The chemical and physical properties that are investigated in the biochar will focus on those properties that affect soil fertility.

The second main objective of the project is to investigate the potential of biochars as adsorbents for wastewater treatment using methylene blue as a model compound. In general, the performance of adsorption systems for textile wastewater is evaluated based on the equilibrium, isotherms and kinetics from experimental data (Gerçel *et al.*, 2007). For this purpose the Langmuir and Freundlich isotherm models and the first order, pseudo-second-order kinetic and intraparticle diffusion models have been used to fit the adsorption isotherms and kinetics, respectively.

1.2 Mind map

Figure 1.1 illustrates the mind map of the thesis.

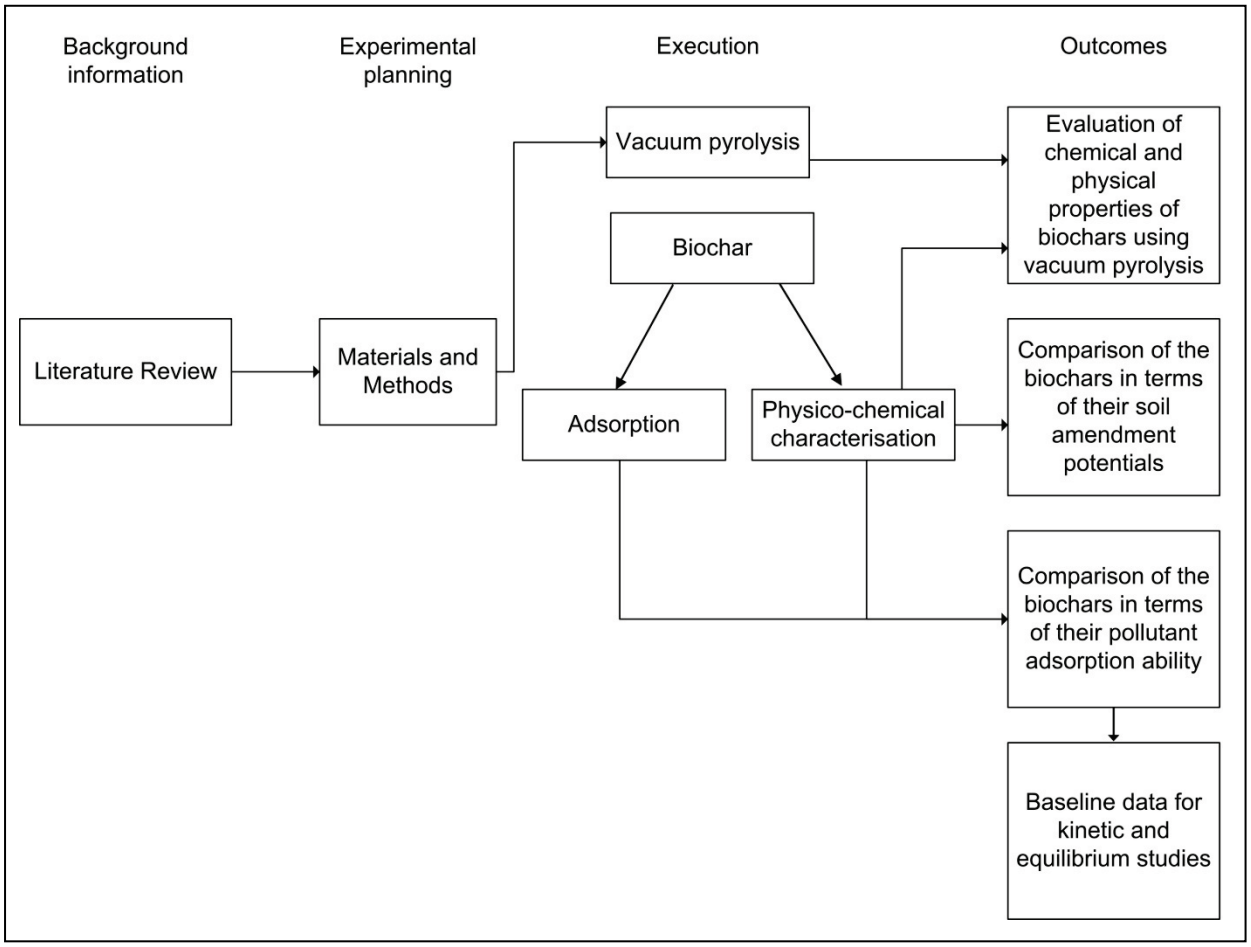

Figure 1.1: Mind map of the thesis

The thesis is structured in four main sections. The first section is Literature Review (Chapter 2), which is composed of three main sub-sections. The first sub-section provides an introduction to the biomasses used and their structural compositions are compared. The second sub-section discusses vacuum pyrolysis and the key properties that affect the process and product yields. The third sub-section debates the biochar and its applications. These sub-sections all together provide an extensive summary of the relevant knowledge and research results that have been published to date.

Chapter 3 describes the materials and experimental methods used in this research. These methods were mostly based on information from the literature survey.

Chapter 4 (Results and Discussion) tackles the objectives of the research. In this section, vacuum pyrolysis results are given and discussed by means of product yields. Afterwards, attention is given to the biochar characterisation, namely physico-chemical characterisation and adsorption results. The physico-chemical characterisation results deals with the first objective of the project, whilst adsorption copes with the second objective of the project. The results are compared to the results presented in Chapter 2.

Conclusions of the study are summarised in the final section (Chapter 5). The outcomes of the study are firstly, evaluation of the chemical and physical properties of biochars from vacuum pyrolysis for soil amendment and wastewater treatment purposes. Secondly, baseline data for adsorption equilibrium and kinetics are obtained. Finally, the comparison of the physico-chemical properties of biochars and adsorption abilities lead one to decide which biochar is superior to another. The recommendations which direct further research are given in this chapter after conclusions.

CHAPTER 2: LITERATURE REVIEW

In this chapter, readers will be introduced to biomasses that were used in this study. These biomasses are vineyard prunings (agricultural residues), black wattle prunings (harvested invasive plant residues) and sugar cane bagasse (industrial herbaceous residues). The production rates, utilisation areas, lignocellulosic compositions, and the chemical compositions of the biomasses will be discussed in this chapter.

2.1 Biomass

Biomass can generally be defined as any hydrocarbon matter that is derived from natural ecosystems such as forests, grasslands and aquatic ecosystems or any kind of lignocellulosic residues or the products from energy crops (Goyal *et al.*, 2008). The residues from agriculture are potential renewable energy resources as they can be used for the production of biogas, bio-oil and biochar (Demirbaş, 2008). Agricultural wastes and energy crops can also be used to produce other valuable products with various conversion methods as it is illustrated in Figure 2.1. Currently, 5.1 billion dry tonnes of agricultural wastes are produced globally (IEA, 2010).

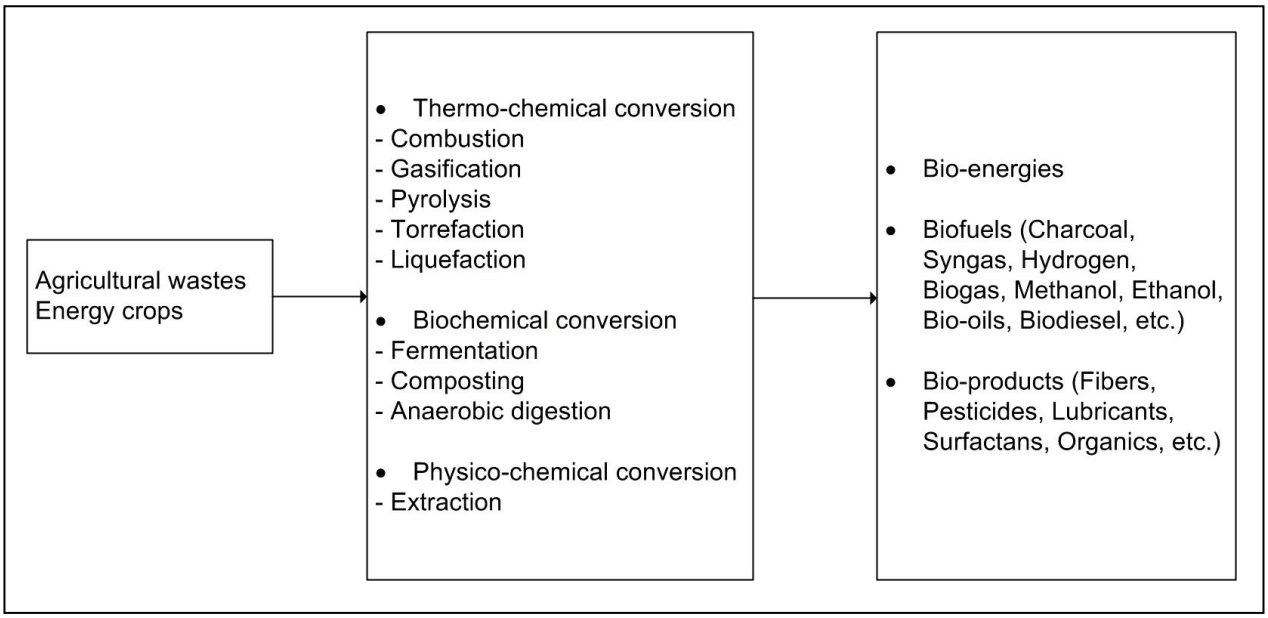

Figure 2.1: Biomass conversions for useful and valuable products (Redrawn from Diaz, 2006)

The chemical structure and major organic components in biomass are very important for the conversions that are used and for the development of the process for the specific application. Cellulose, hemicelluloses and lignin build the cell walls of woody plants and they are the major organic components of these biomasses. General composition of plant biomass is depicted in Figure 2.2.

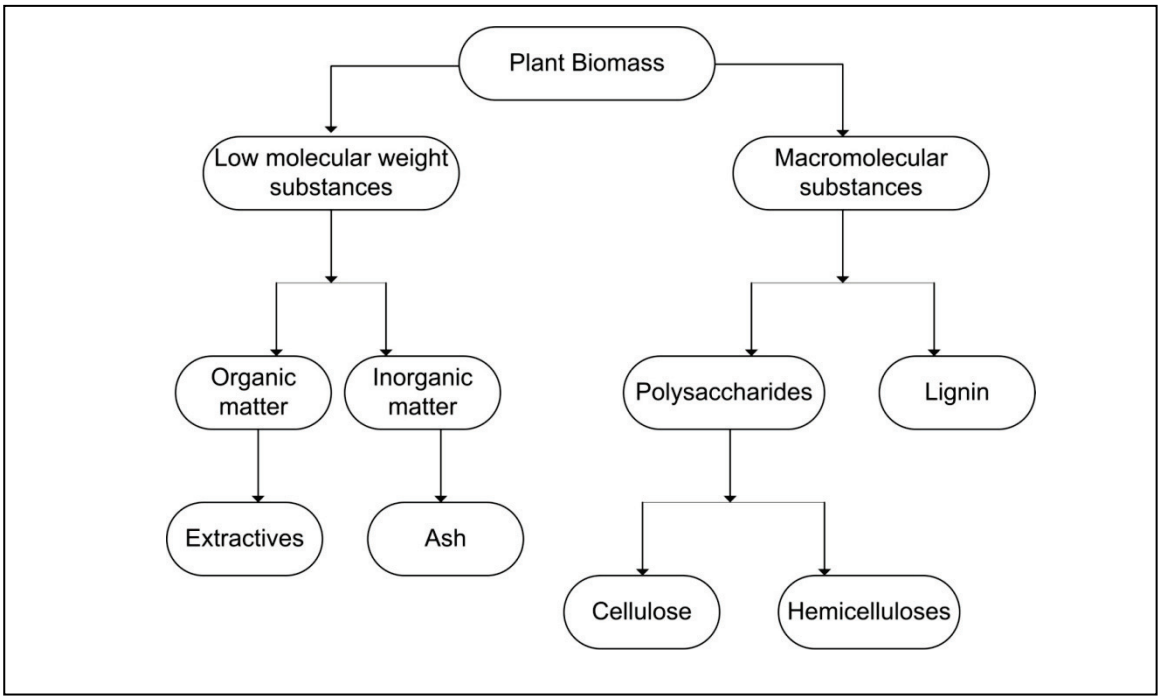

Figure 2.2: General components of plant biomass (Redrawn from Mohan *et al.*, 2006)

Cellulose is the major wood component and the main structural component of the plant cell walls (Fengel & Wegner, 2003). Cellulose is a homopolysaccharide, containing β-D-glucopyranose units which are connected by (1 → 4) - glycosidic bonds. Cellulose molecules are completely linear and show a strong tendency to crystallize and form intra- and intermolecular hydrogen bonds. Generally, 40-45 % of the dry substance is cellulose in most species (Browning, 1963; Sjöström, 1981). The chemical structures of (a) β-D-glucose and (b) cellulose are given in Figure 2.3.

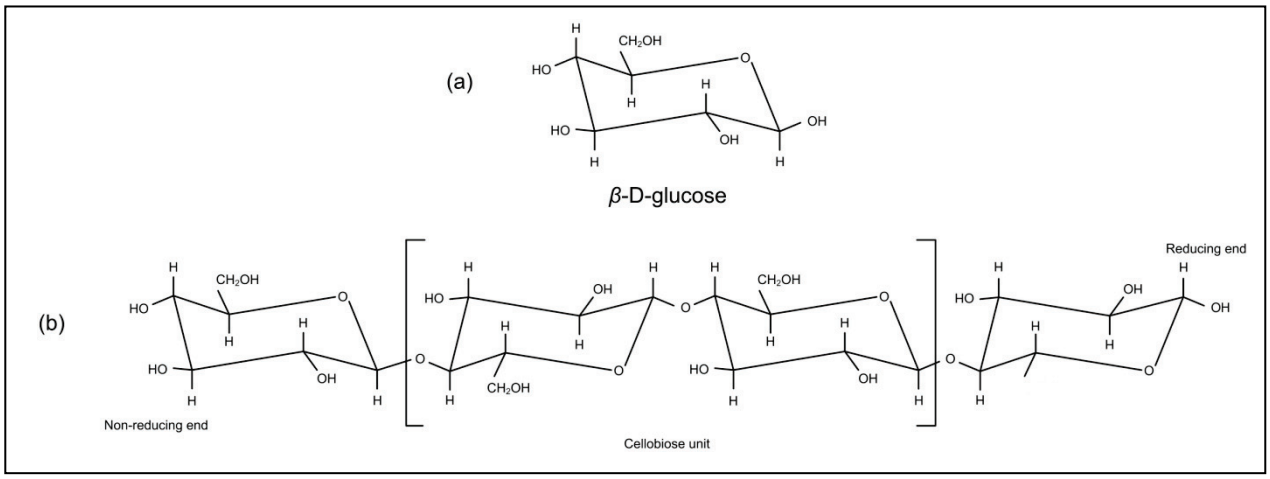

Figure 2.3: Chemical structures of cellulose (Redrawn from Bierman, 1996)

Hemicelluloses are heteropolysaccharides that can be extracted by water or aqueous alkali from plant tissue. Hemicelluloses are more readily hydrolysed by acids to their monomeric components than cellulose. Many of them have the general formula $(C_5H_8O_4)_n$. Main constituents of hemicelluloses are D-glucopyranose, D-xylopyranose, L-arabinofuranose, D-xylopyrahose, D-glucuronic acid (Figure 2.4). Hemicelluloses form hydrogen bonds with cellulose and covalent bonds with lignin. The hemicelluloses content of wood is usually between 20 and 30% on a dry basis (Sjöström, 1981).

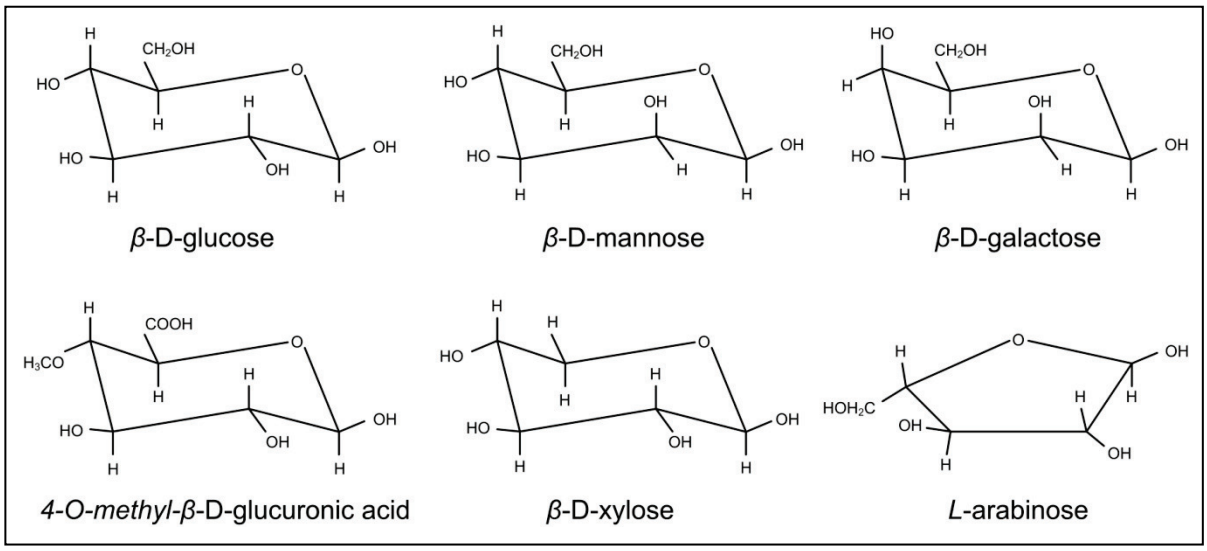

Figure 2.4: Chemical structures of hemicelluloses (Redrawn from Bierman, 1996)

Schulze derived the name lignin from the Latin word for wood (*lignum*) in 1865, while Peter Klason studied the composition of lignosulfonates in 1897 and postulated that lignin is a macromolecular substance in 1907 (Sjöström, 1981). Basically, lignins are polymers of phenyl propane units, namely p-coumaryl, coniferyl and sinapyl alcohols (Figure 2.5) (Bierman, 1996). Softwood usually contains

26-32% lignin, while the lignin content of hardwood exceeds 30% on a dry basis (Sjöström, 1981). The variety of the lignin in softwood and hardwood is due to the number of methoxy groups on the phenolic ring (Shen *et al.*, 2010). One of the proposed lignin structures is given in Figure 2.6.

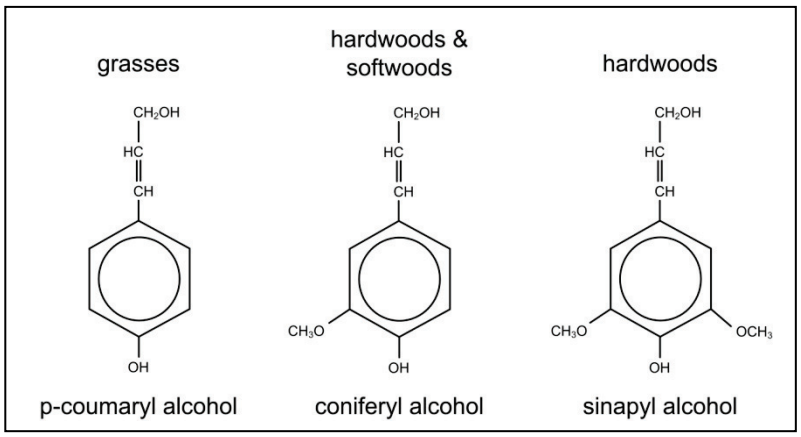

Figure 2.5: Lignin building blocks (Redrawn from Bierman, 1996)

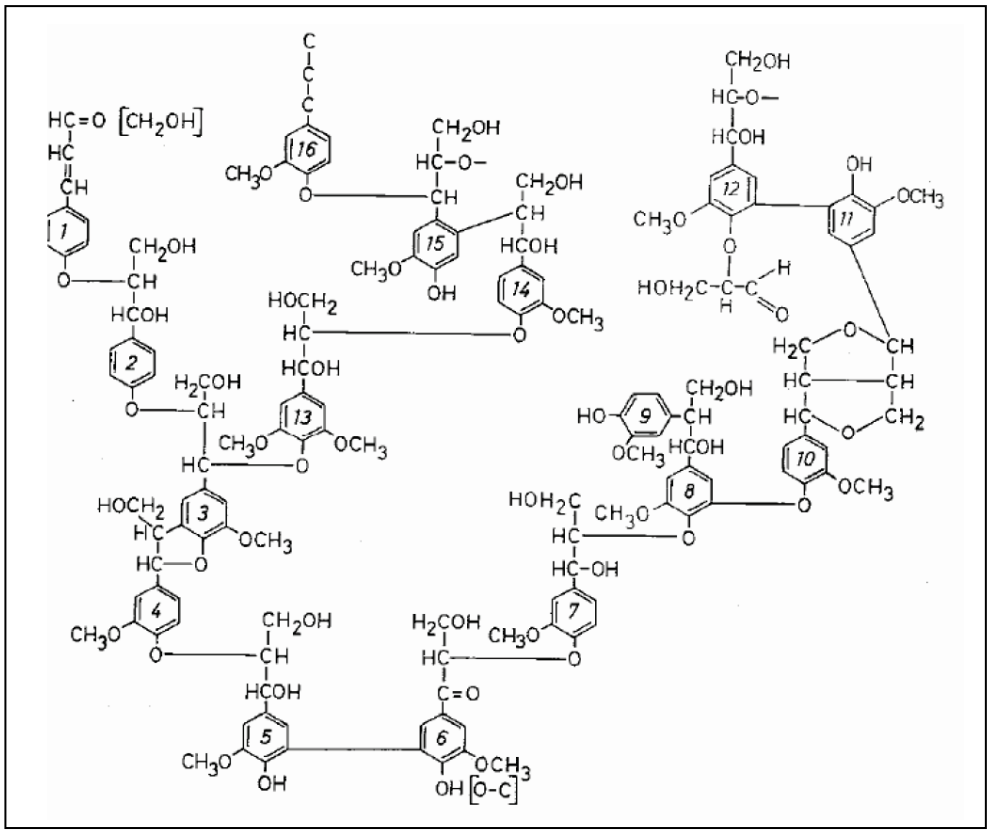

Figure 2.6: Chemical structure of lignin (Fengel & Wegner, 2003) (Granted permission from Kessel Verlag)

2.1.1 Black wattle (*Acacia mearnsii*)

Black wattle is a fast growing invasive tree which was introduced to South Africa 150 years ago from Australia to provide bark products. Approximately 18 Mha of total South African lands are invaded by alien vegetation and black wattle is considered to be a major invasive tree covering 2.5 Mha (IEA, 2010; Moyo *et al.*, 2009). Other than South Africa and Australia, black wattle is cultivated in other countries such as China, Brazil, Zimbabwe, India, Kenya and Tanzania (Brown & Ko, 1997). Black wattle threatens native habitats by competing with indigenous vegetation, replaces grass communities and is estimated to use 25% of the total water supply, ranking first in water use among invasive species (Moyo *et al.*, 2009). Nevertheless, black wattle has a nitrogen fixation property that builds up soil fertility and is also considered as a soil stabiliser to decrease erosion. Black wattle has various utilisation areas, of which tannin compound extraction from the bark for use in the production of soft leather is the most important. Other uses of black wattle are resin, thinners and adhesive production from extracts, building materials from the timber, biochar production from wood for fuel and the wood chips are used in pulp and paper production (Chenje & Mohamed-Katerere, 2006). Black wattle is especially widely spread in the Eastern Cape and KwaZulu-Natal provinces of South Africa (de Neergaard *et al.*, 2005). The ash content of black wattle is 0.36%, lignin 21.2%, cellulose 63.9% (Brown & Ko, 1997) and hemicelluloses 12.7% (Lachke *et al.*, 1987) on dry basis. Izabel *et al.* (2008) studied the thermogravimetric analysis (TGA) of black wattle and observed that the profile of the mass loss shows two macro stages for all heating rates used (2 to 50°C/min), related to the decomposition of cellulose and hemicelluloses. A third step was observed at lower heating rates, which were attributed to the decomposition of the remaining lignin. However, no specific studies done on the pyrolysis of black wattle could be found in the open literature.

2.1.2 Vineyard

Annually 2 to 4 tonnes per hectare of vineyard prunings are generated from a vineyard. These agricultural residues are burned or used as fuel, organic fertiliser or feed and the rest are dumped (Corcho-Corral *et al.*, 2006). Bustos *et al*. (2004) reported that prunings contain 34.1% cellulose, 19% hemicelluloses and 27.1% lignin on dry weight basis. The pH of prunings is 5.13 with an ash content of 2.82% (Ntalos & Grigoriu, 2002). Thermogravimetric analyses (Hernandez *et al.*, 2010; Tartarelli *et al.*, 1987), gasification, pyrolysis for furfural production (di Blasi *et al.*, 2010) and Branuer-Emmett-Teller (BET) surface area determinations for use in adsorption processes (Deiana *et al.*, 2009) have been done on vineyard prunings. Tartarelli *et al.* (1987) observed the elimination of moisture at

temperatures between 60-100°C. Volatiles release was observed from 200-300°C up to 700°C. Hernandez *et al.* (2010) divided the temperature profile into three stages. First stage took place around 100°C, which was attributed to the elimination of highly volatile organics and unbound moisture. The second stage was observed at temperatures between 200-400°C, corresponding to the pyrolysis of lignocellulosic contents of the biomass. At temperatures above 400°C, the third area of weight loss was evidence of the progressive degradation of heavy lignin fractions and chars. Regarding BET surface area, Tartarelli *et al.* (1987) determined the surface area as 18 m^2/g, whereas Deiana *et al.* (2009) improved the surface area by activating the carbonized material with steam (412 m^2/g) or phosphoric acid (1500 m^2/g). A leaching step was also performed before the steam activation step to compare the influence of ash content on the surface area of activated carbon and it was found that the leaching step improved the surface area (700-900 m^2/g) (Deiana *et al.*, 2009).

2.1.3 Sugar cane bagasse

Sugar cane bagasse is the solid waste left after extraction of juice from sugar cane (Bilba & Ouensanga, 1996). Sugar mills generate approximately 135 kg of bagasse per metric ton of sugar cane on dry weight basis. These residues can be used for heat, power generation or ethanol production (Brienzo *et al.*, 2009). Currently 423 000 ha are used for sugar cane production in South Africa. Annually 6 million tonnes of sugar cane bagasse (dry weight) are generated and 90% of the residues are burned to produce heat and electricity. KwaZulu Natal has the highest production of sugar cane bagasse with 83 % of annual production (IEA, 2010). Pyrolysis, TGA, activated carbon, and bio-ethanol production from sugar cane bagasse have been studied by various researchers (Carrier *et al.*, 2011; Inyang *et al.*, 2010; Souza *et al.*, 2009; Okuno *et al.*, 2005; Garcìa-Pèrez *et al.*, 2002; Darmstadt *et al.*, 2001). Garcìa-Pèrez *et al.* (2002) determined fixed carbon content as 16.3% on dry weight basis, while Souza *et al.* (2009) reported a value of 25.66%. Regarding ash content, Devnarain *et al.* (2002) and Garcìa-Pèrez *et al.* (2002) determined the ash content of sugar cane bagasse as 1.8% and 1.6%, respectively. A later sample of sugar cane bagasse with ash content 5.9% was used by Devnarain *et al.* (2002) and inorganic elements were reported as follow: 1.47% aluminium, 2.67% silicon, 0.7% phosphorus, 0.04% potassium, 0.58% calcium and 0.4% iron. A possible explanation for high Al and Si contents is that the sample was contaminated by soil. However, higher ash contents have been observed (Souza *et al.*, 2009). Biochar derived from sugar cane bagasse has been extensively studied for the production of activated carbon (Liou, 2010; Jaguaribe *et al.*, 2005; Tsai *et al.*, 2001; Bernardo *et al.*, 1997). In the study of Liou (2010), optimum BET surface area (2289 m^2/g) was reached with $ZnCl_2$ activation at 500°C. Tsai *et al*. (2001) studied the removal of acidic dyes with

$ZnCl_2$ activated carbons. Even though surface area was quite high (905 m^2/g), the removal was low. If the pore size is smaller than or close to the molecular dimensions of the dye molecules, low adsorption efficiencies can be observed as Tsai *et al*. (2001) also concluded. Jaguaribe *et al*. (2005) and Bernardo *et al*. (2001) reached BET surface areas with steam activation of 806 m^2/g and 931-1394 m^2/g, respectively.

2.1.4 Biomass composition

The elemental, proximate and lignocellulosic composition analyses indicate the chemical structure of a biomass. As was mentioned, the major organic components of a biomass are cellulose, hemicelluloses and lignin. The main elements which compose a biomass are carbon, oxygen, hydrogen and nitrogen. These elements are determined by elemental analysis. On the other hand, proximate analysis gives information on moisture content, volatile matter, fixed carbon and ash content. All this data helps one to compare a certain biomass to another and to determine a suitable application for this biomass. Table 2.1 shows the compositional differences of the biomasses, which were compiled from open literature.

Table 2.1: Elemental, proximate analyses and lignocellulosic compositions of biomasses (dry,wt.%)

Biomass	%VM	%Ash	%FC	%C	%H	%N	%O*	%Cellulose	%Hemicelluloses	%Lignin
Black wattle		[a]0.36						[a]63.9	[b]12.7	[b]17.9 - [a]21.2
Vineyard	[c]76.6 - [d]91.9	[e]2.6 - [c]6.3	[c]17.02 – [e]20.0	[c]46.3 - [d]50.07	[c]5.3 - [d]5.91	[d]0.52 – [e]0.81	[c]41.6 – [e]43.5	[f]34.1	[f]19.0	[f]27.1
Sugar cane bagasse	[g]66.0-[h]82.1	[h]1.6-[g]8.0	[h]16.3 – [g]26.0	[i]47.6 - [h]48.8	[h]5.9 - [i]6.03	[i]0.29 – [h]0.49	[h]43.1 – [i]43.4	[j]41.7 - [h]42.4	[h]35.2 - [j]37.4	[j]19.3 - [h]20.8

*obtained by difference

[a] Brown & Ko (1997)

[b] Lachke *et al.* (1987)

[c] Hernandez *et al.* (2010)

[d] Covalaglio & Cotana (2007)

[e] Jenkins & Ebeling (1985)

[f] Bustos *et al.* (2004)

[g] Souza *et al.* (2009)

[h] Garcìa-Pèrez *et al.* (2002)

[i] Okuno *et al.* (2005)

[j] Brienzo *et al.* (2009)

2.1.5 Conclusion

Plant biomass contains cellulose, hemicelluloses, lignin, extractives and ash. Useful and valuable products can be derived from biomass via thermo-chemical, bio-chemical and physico-chemical conversions. In this project, three biomasses were used; namely, sugar cane bagasse, vineyard and black wattle prunings.

Black wattle has the highest cellulose content, whilst vineyard has the lowest cellulose content. Sugar cane bagasse contains higher amounts of hemicelluloses compared to the other biomasses. The highest volatile matter (VM) content was observed in vineyard with value of 91.9%. Regarding ash content, black wattle has the lowest ash content. From the gathered studies, sugar cane bagasse ash content goes up to 8% on moisture free basis. In general, industrial and agricultural residues are more reactive than wood due to their higher ash content (Zanzi *et al*., 2001).

Fixed carbon (FC) contents of the biomasses are pretty close to each other, but the highest FC content (26%) was observed for sugar cane bagasse. Carbon, hydrogen, nitrogen and oxygen contents of the biomasses are quite similar. Bagasse residues are generated in high amounts annually and most of them are burned.

TGA studies of the agricultural wastes showed that there were three main stages; elimination of moisture, elimination of highly volatile matters (cellulose, hemicelluloses and lignin) and the third stage; further degradations of lignin residues. Finally, as temperature increases, the organic matter is completely eliminated leaving an incombustible residue known as ash. Biochar is one of the products from pyrolysis of the agricultural residues which can be used as adsorbent due its high surface area or as soil amendment.

2.2 Vacuum pyrolysis

Pyrolysis is used for the thermo-chemical conversion of agricultural residues. In this section pyrolysis will be briefly explained along with the influence of process parameters. The aim of vacuum pyrolysis is the production of high quality biochar. Therefore, effects of the process parameters on char yields and properties will be discussed.

2.2.1 Principle

Pyrolysis is the thermal decomposition of organic molecules in the absence of air to obtain solids (biochar or charcoal), liquids (tar, bio-oil and pyrolytic water) and gaseous products, which can be used as fuels, solvents and chemicals. It is known that Cro-Magnon man discovered the production of charcoal, indicating the early usage of the pyrolysis of biomass (Grønli & Antal, 2003; Bridgewater, 2008). The mechanism of pyrolysis is very complex; however, pyrolysis of biomass can be divided into three stages. The first stage includes the elimination of water, bond scission, appearance of free radicals, formation of carbonyls, carboxyls and hydroperoxide, carbon monoxide, carbon dioxide and solid residue which occurs at temperatures between 200 °C and 400 °C (Shafizadeh, 1982). Temperatures above 400°C cause decomposition of the primary products and formation of aromatic pyrolysis products, which are accepted as secondary stage products of pyrolysis (Demirbaş & Arın, 2002; Fisher *et al.*, 2002). Secondary decomposition reactions occur at a high rate. Finally, during the third stage, char decomposes at a very slow rate and carbon enrichment is achieved due to further scission of C-H, C-O bonds and devolatilisation (Koufonas *et al.*, 1989). The pyrolysis pathways, which were developed by Radlein are given in Figure 2.7 (Bridgwater, 1994).

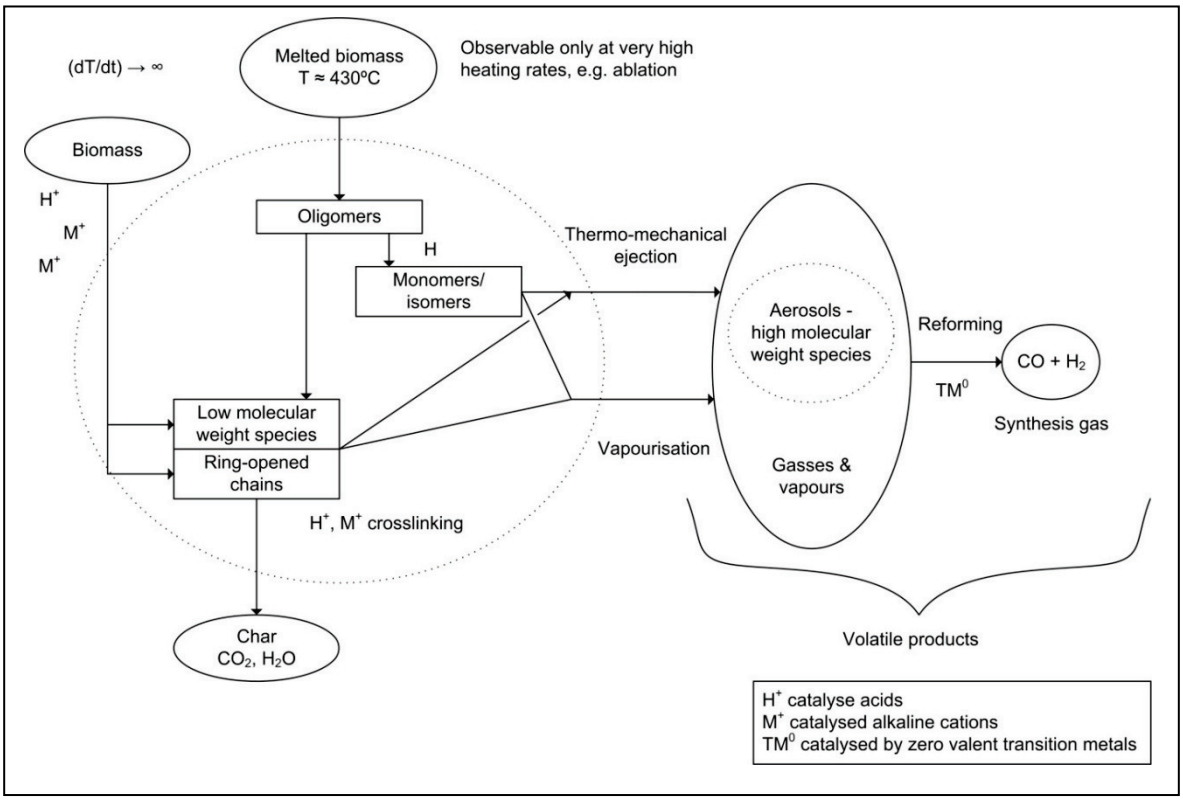

Figure 2.7: Pyrolysis pathways at elevated temperature (Redrawn from Bridgwater, 1994)

As Demirbaş & Arın (2002) showed, the pyrolysis reaction is basically described by the following reaction:

$$\text{Biomass} \longrightarrow \text{Char} + \text{Volatile products}$$

Vacuum pyrolysis is operated at reduced pressure under vacuum. It is known that the first person to use vacuum was Klason in 1914 (de Jongh, 2001). Vacuum restricts secondary decomposition reactions removing the primary volatile products from the hot reaction zone (Shafizadeh, 1982). In this way further cracking and re-condensation reactions are prevented (Goyal *et al.*, 2008), resulting in less gas production. Miranda *et al.* (1999) stated that biomass decomposes between 450 and 550°C under a pressure between 2 and 15 kPa abs.

A number of studies using *Populus tremuloides* (Ahmed *et al.*, 1989), tyres (Benallal *et al.*, 1995), oil shales (Pakdel *et al.*, 1999), PVC (Miranda *et al.*, 1999), maple bark (Darmstadt *et al.*, 2000), softwood bark residues (Cao *et al.*, 2002; Boucher *et al.*, 2000), sugar cane bagasse (Garcìa-Peréz *et al.*, 2002; Carrier *et al.,* 2011), pistachio-nut shells (Lua&Yang, 2004), teak sawdust (Ismadji *et al.*, 2005), hardwood residues (Garcìa-Peréz *et al.*, 2007), olive wastes (Petrov *et al.*, 2008), durian peel (Nuithitikul *et al.*, 2010), etc. have been done on vacuum pyrolysis. Pyrolytic chemistry differs as the

chemical composition of feedstock used differs, for instance pyrolytic reactions would be different for PVC than wood (Mohan *et al.*, 2006).

Vacuum pyrolysis differs from slow pyrolysis as it can be used with fast or slow heating rates (Mohan *et al.*, 2008). In slow pyrolysis, vapor residence time is between 5 and 30 min with the vapour phase that continue to react with each other as solid and liquid products are formed, whilst residence time is between 2-30s in vacuum pyrolysis. Fast pyrolysis where biomass decomposes to generate vapours and aerosols, requires high temperature and high heating rates and short residence times (0.5-5s) (Mohan *et al.*, 2006). Figure 2.7 shows the pyrolytic pathways for biomass pyrolysis at high temperatures. The first part is mainly char production at low temperatures. The main product is char for slow pyrolysis, while fast pyrolysis yields high amounts of bio-oil. Vacuum pyrolysis results in mostly bio-oil and considerable amounts of biochar.

2.2.2 Parameters affecting vacuum pyrolysis

Process parameters such as temperature, pressure, particle size, heating rate, pyrolysis time and nature of feedstock (ash content, lignocellulosic composition, etc.) have a substantial effect on pyrolysis products (Grønli & Antal, 2003).

2.2.2.1 Temperature

At high temperatures, secondary cracking reactions of the pyrolysis vapours lead to an increase in gaseous products. The greater primary decomposition of the solid biomass or the further decomposition of the char results in a decrease in char yield with a higher fixed carbon content. The further decomposition of char at higher temperatures contributes to an increase in gas yield due to the production of non-condensable gases (Parihar *et al.*, 2007).

The effect of temperature on pyrolysis product yields has been investigated by many researchers on different biomasses such as olive wood sawdust, sugar cane bagasse, corn cobs and corn stalks (Ioannidou *et al.*, 2009; Demirbaş & Arin, 2001; Figueiredo, 1989). From these studies, it was concluded that, for high yield of biochar, lower temperatures should be chosen. Figure 2.8 shows the temperature effect on slow pyrolysis products from olive bagasse. A decrease in solid product yield and an increase in volatiles with increased temperature were observed for the vacuum pyrolysis of sugar cane bagasse by Carrier *et al.* (2011).

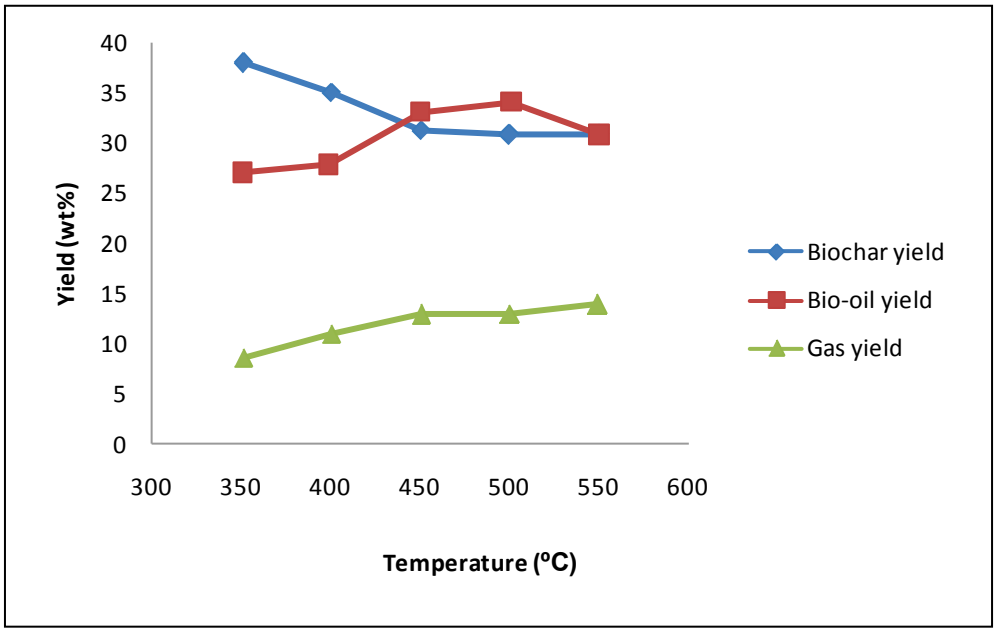

Figure 2.8: Effect of temperature on product yields from slow pyrolysis of olive bagasse (Redrawn from Şensöz *et al.*, 2006)

2.2.2.2 Pressure

According to Cetin *et al*. (2004), high pressure leads to the decrease in total surface area and swelling at low pressures. Pyrolysis pressure influences the size and shape of the char due to changes in the void fraction in the char (Cetin *et al.*, 2004). Increased pressure during pyrolysis of cellulose favoured the formation of char and CO_2 and reduced the CO content (Mok & Antal, 1983a). High pressure increases the rate of decomposition reactions and prolongs the residence time for vapour-particle interaction. Under vacuum (40-400 Pa), volatiles do not have an opportunity to interact with un-pyrolysed material thereby limiting secondary reactions (Ward & Braslaw, 1985). Figure 2.9 shows the effect of pressure on char yield from slow pyrolysis of cellulose from the study of Mok & Antal (1983b).

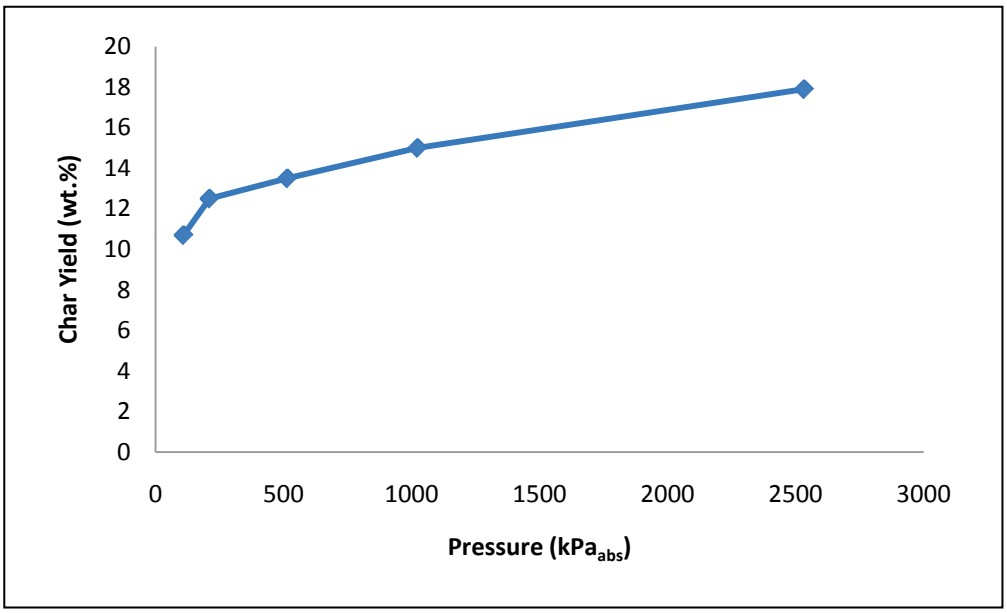

Figure 2.9: Effect of pressure on char yield from slow pyrolysis of cellulose at 500°C with 20 cm^3/min flow of argon gas (Redrawn from Mok & Antal, 1983b)

2.2.2.3 Heating rate

Heating rate is one of the most important parameters that affect pyrolysis products, their structure and chemistry. Uzun *et al.* (2010) studied the effect of heating rate on product yields from the pyrolysis of tea waste. High heating rates caused a sharp increase in the yield of the liquid products due to heat and mass transfer limitations. Char yield decreased from 34.3 to 27.1% when heating rate increased from 5 to 700 °C/min. This decrease in char yield has been reported by many researchers (Uzun *et al.*, 2010; Sensöz *et al.*, 2006; Brunner & Roberts, 1980).

Çetin *et al.* (2004) reported that very high heating rates result in melting of the char particles and the creation of smoother surfaces and spherical cavities. Brunner & Roberts (1980) investigated the effect of heating rate on pyrolysis of powdered cellulose and concluded that micropore volume and openings are highly affected by the heating rates deducing that high heating rate chars mainly consist of macropores. The similar conclusion was also drawn by Çetin *et al.* (2004) for *Eucalyptus* biochars (Figure 2.11). According to Lua & Yang (2004), the BET surface area and micropore volume increase for increasing heating rate up to 10°C/min, but these values decrease for further increases in heating rate for vacuum pyrolysis of pistachio-nut shells (Figure 2.11).

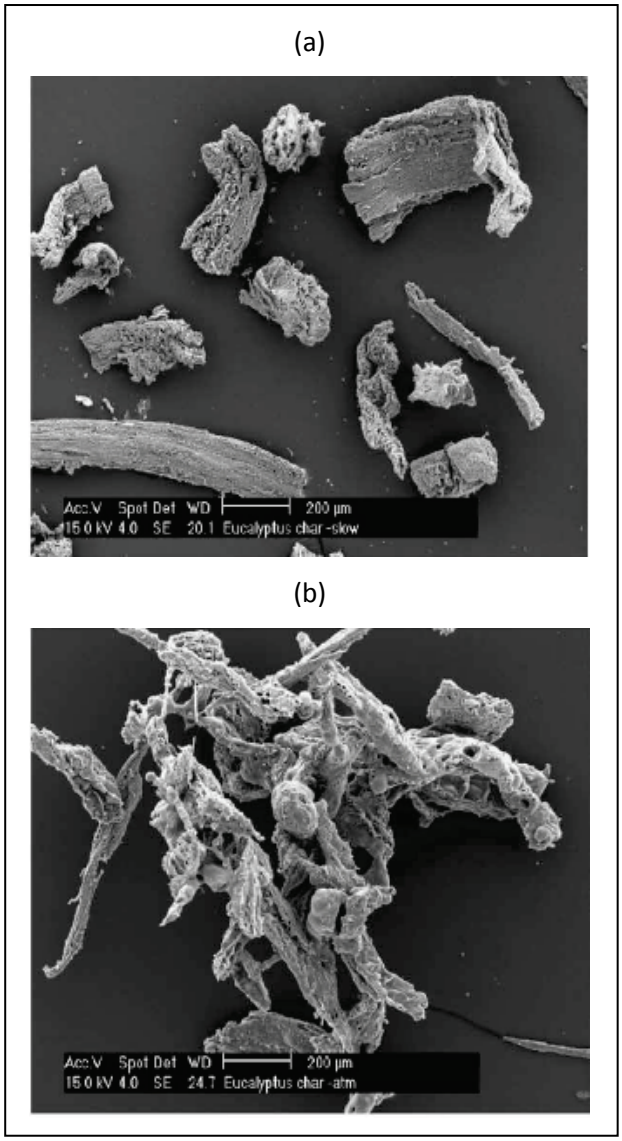

Figure 2.10: SEM images of *Eucalyptus* chars produced at (a) low HR, (b) high HR (Cetin *et al.*, 2004)

(Granted permission from Elsevier Ltd.)

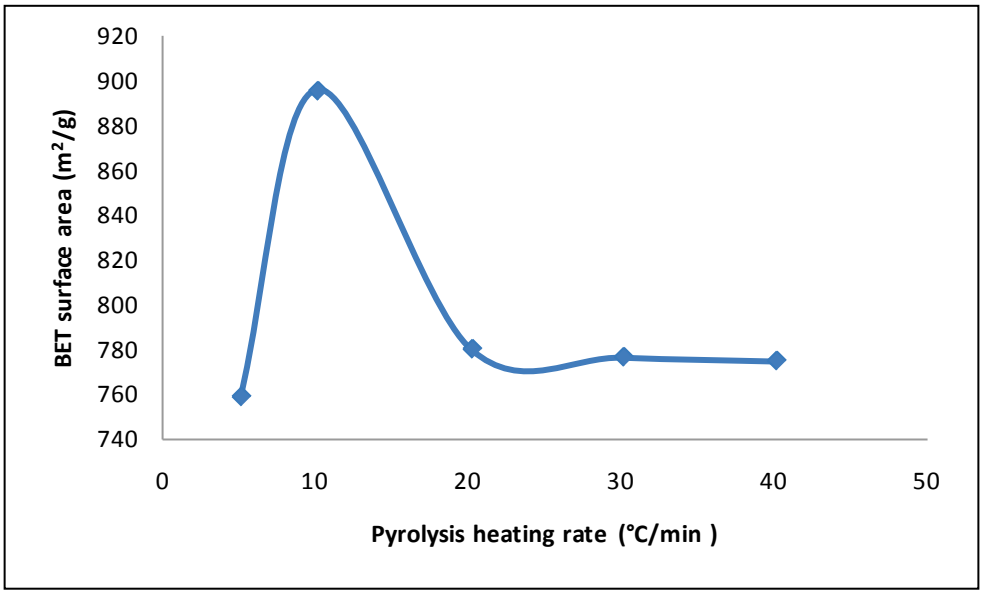

Figure 2.11: Effect of vacuum pyrolysis heating rate on the BET surface area of activated carbons from pistachio-nut shells (T: 500°C, P: 8kPa$_{abs}$, HT: 2h) (Redrawn from Lua & Yang, 2004)

2.2.2.4 Hold time

Hold time refers to the period of reaction. Lua & Yang (2004) reported that at longer hold times, more volatiles from char are released corresponding to an increase in fixed carbon content of the char. Lu *et al*. (1995) investigated the pyrolysis of sewage sludge and the influence of temperatures (450-850°C) and the effect of hold time (0.5-3h) on the BET surface areas of the chars. At lower temperatures (550 and 450°C), a maximum hold time gave the highest surface area. The overall highest surface area was approached at 850°C and a 2h hold time. When hold time increased to 3h, surface areas decreased due to the blockage of pores by sintering at high temperatures and long hold time.

2.2.2.5 Particle size

It is generally assumed that an increase in particle size causes greater temperature gradients inside the particle. Due to the temperature gradient, at a given time the temperature of the core is lower than the surface temperature (Şensöz, 2006; Beaumont, 1984). The cores of larger particles become carbonised but cannot be decomposed completely, which results in an increase in char yield but a decrease in liquids and gases. Smaller particles provide a greater reaction surface and a high heating rate, which allows a quicker decomposition of the biomass (Islam *et al.*, 2010).

Pütün *et al.* (1996) reported that the highest char yield was obtained at the highest particle size (D_p >1.8 mm) from slow pyrolysis of sunflower bagasse at 500°C, but there was no significant effect on the liquids yield. In other research, olive husk, corn cob and tea waste were used to determine the effect of particle size on char yield at a temperature of 677°C. The biochar yields increased as the particle sizes of the biomasses increased from 0.5 mm to 2.2 mm. A substantial percentage yield increase, namely 66%, was observed for corn cob biochar (Demirbas, 2004). In the pyrolysis study of Mani *et al.* (2010), the biochar yield from wheat straw increased as the particle size increased from 250 to 475 µm and remained the same for further increases in the particle size. However, some researchers observed that particle size exerts a negligible influence on yields (Ertas & Alma, 2010; Şensöz *et al.*, 2006; Encinar *et al.*, 1996; Pütün *et al.*, 1996).

Researchers agree that moisture, ash and volatile contents vary depending on the particle size of feedstock. Studies have shown that moisture content, volatile matter and fixed carbon decrease with reduced particle size, however ash content increases for smaller particle sizes for slow and vacuum pyrolysis (Mani *et al.*, 2010; Garcìa-Peréz *et al.*, 2002). Buah *et al.* (2007) mentioned that an increase in particle size increases the BET surface area for biochars from slow pyrolysis of municipal solid waste at various temperatures (400°C-700°C) with a heating rate of 10°C/min and a minimum hold time of an hour.

It is suggested to remove fine particles to reduce the entrainment of fines in the process gas. Through entrainment, fine particles get retained in condensates and cause an increase in methanol insoluble material in the oil (Garcìa-Peréz *et al.*, 2002).

2.2.2.6 Ash content

Mineral matter of biomass in combination with lignocellulosic composition plays an important role in determining pyrolysis product yields. It has been reported that ash content suppresses the formation of tar (Gray *et al.*, 1985). Raveendran *et al.* (1995) worked on different biomasses to understand the effect of ash content on pyrolysis product distribution. They concluded that char yield increases due to the demineralisation of coir pith, groundnut shell and rice husk, whilst biochar yields of wood and corn cob decrease. A substantial increase in yields of liquids was observed for above-mentioned biomasses once they were demineralised. For biomass with high lignin content, potassium acted as a catalyst for char gasification reacting with CO_2 and H_2O to form CO and H_2 and thus decreases char yield (Raveendran *et al.*, 1995).

Regarding temperature effect on ash content, Shinogi & Kanri (2003) showed that ash content increases with increasing temperature for all the feedstocks that were used (Figure 2.12). Elements such as N, C, H, O, S are volatilised during heating to varying temperatures, while inorganic salts are not volatilised, which is the main reason for increased ash content in the biochar.

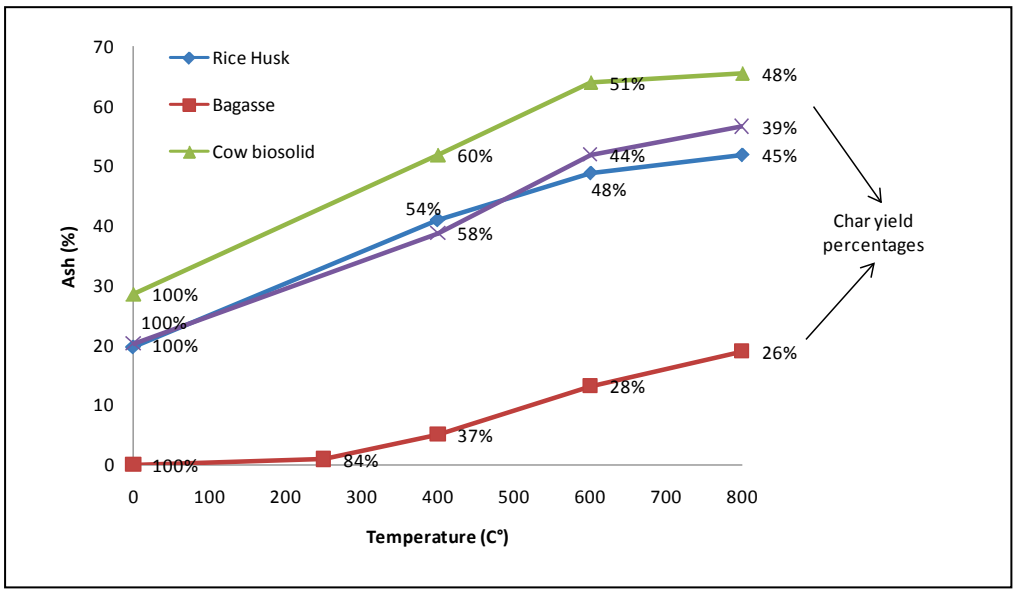

Figure 2.12: Effect of temperature on ash content (Redrawn from Shinogi & Kanri, 2003)

Demirbas (2004) studied pyrolysis of corn cob and olive husk and concluded that biochar from olive husk was more reactive in gasification than the biochar from corn cob due to higher ash content of the former. It is reported that for wood based feedstocks; carbon begins to volatilise around 100°C, nitrogen above 200°C, sulphur above 375°C, potassium and phosphorus between 700°C and 800°C and magnesium, calcium and manganese volatilise above 1000°C during pyrolysis (Lehmann & Joseph, 2009).

Knowledge of ash content of biochar is also important for reactor designs. The understanding of ash-related issues such as fly-ash and ash-deposit formation or ash disposal, storage and utilisation are important when biochar is used for heat and energy production. Ash deposition could cause reduction in heat transfer, corrosion and blockage in boilers (Abdullah *et al.,* 2010; Valmari *et al.*, 1999).

2.2.2.7 Lignocellulosic composition

The pyrolysis of lignocellulosic materials has been studied by many researchers (e.g. Çağlar, 2007; Demirbas, 2004; Fisher *et al.*, 2002; Raveedran *et al*., 1996; Antal & Varhegyi, 1995). The lignocellulosic composition affects the nature and quality of the pyrolysis products. During the pyrolysis process, hemicelluloses, cellulose and lignin decompose to their monomer and monomer-related molecules. Holocellulose (hemicelluses and cellulose) favours the production of furans and carbohydrates, whereas lignin leads to the formation of phenolics (Demirbaş, 2007).

Raveendran *et al*. (1996) studied the pyrolysis characteristics of biomass components, namely Whatman cellulose, wood cellulose, alkaline lignin, acid lignin, hemicelluloses, and extractives. They observed that below 100°C moisture volatilisation takes place, extractives start decomposing at temperatures between 100 and 250°C, hemicelluloses decomposition predominantly occurs between 250 and 350°C, while cellulose and lignin decompose mostly from 350-500°C and finally, at temperatures above 500°C it is predominantly lignin that decomposes. This shows that lignin is more resistant to thermal degradation than cellulose and hemicelluloses. It was concluded that cellulose decomposition rate was the highest with the lowest char yield (14 wt.%). Char yield from lignin was the highest, namely 45-50 wt.%. Hemicelluloses are thermally the most unstable, with with a char yield of 30 wt.%.

Antal & Varhegyi (1995) mentioned that vapour-solid reactions are the only effective source for char production during pure cellulose pyrolysis. There are two pathways recognised for the pyrolysis of cellulose. The first pathway is the levoglucosan formation, especially from vacuum pyrolysis while the second pathway is glycolaldehyde formation. Levoglucosan is known to be polymerised to polysaccharides, which are then converted into char and then degraded to some lower molecular weight products (Kawamoto *et al.*, 2003). Piskorz (1986) reported glycolaldehyde as a major product of fast pyrolysis. The increase in temperature favours the second pathway of cellulose pyrolysis, namely glucolaldehyde formation, due to the further decomposition of monomer units of cellulose to a two carbon and a four carbon fragments (Piskorz, 1986).

Lv *et al.* (2010) studied the effect of cellulose and lignin contents on biomass pyrolysis and observed that the main product from cellulose was tar, whereas lignin contributed to the char yield. When cellulose content increases, the yields of char and tar decrease with an increase in gas yield. Cellulose forms more CO, whereas lignin has higher H_2 and CH_4 yields. Sugar cane bagasse (with cellulose as

the largest component) yielded 15.5 wt.% of char and rice-husk (with the highest lignin content) resulted in 47.9 wt.% of char yield from fast pyrolysis at 500°C.

Worasuwannarak *et al*. (2007) reported that the large amount of water production during slow pyrolysis was due to the high content of hemicelluloses. On the other hand, the interactions between cellulose and lignin contributed to an increase in char yield but a decrease in tar yield.

Table 2.2 shows the vacuum pyrolysis conditions and product yields of various studies. Comparing the results from the study of Garcìa-Peréz *et al*. (2007), softwood bark residue yielded higher amounts of biochar and gas, but a lower liquid phase yield than hardwood, because softwood bark contains larger amounts of lignin and extractives. Hardwood is rich in cellulose which can also be the reason for the higher liquid yield. In the study of Darmstadt *et al*. (2000), maple bark yielded higher char and liquid yields but lower gas yield than softwood bark residues. It is evident that the different lignocellulosic composition of the materials led to different yields of pyrolysis products.

Garcìa-Peréz *et al.* (2002) also observed that pyrolysis runs in a large scale reactor yielded higher char and gas but less liquid phase than a lab scale reactor. The reactors used also affect the yields due to the heat and mass transfer phenomena which occur during the pyrolysis reactions.Using the same biomass, Boucher *et al*. (2000) and Garcìa-Peréz *et al*. (2007) obtained different char yields which could be explained by the use of batch mode against a continuous system.

Table 2.2: Vacuum pyrolysis conditions and product yields of various biomasses (dry, wt.%)

Material	Conditions	Char yield(%)	Liquid Yield(%)	Gas Yield(%)	Reference
Softwood bark residue	$\dot{M}$= 15 kg/h P= 15 kPa_{abs} T=500°C	27.6	45	27.4	Garcìa-Pérez *et al.,* 2007
Hardwood rich in fibres	M= 4.2kg P= 8 kPa_{abs} T=500°C HR=12°C/min	26.2	53.9	19.9	
Softwood bark residue	M=92 kg P= 14 kPa_{abs} T=500°C	35	44	20	Boucher *et al.,* 2000
Maple bark	M=1 kg P= 4- 6 kPa_{abs} T=501.85°C HR= 10°C/min	31	63.4	5.6	Darmstadt *et al.,* 2000
Softwood bark		28.4	57.1	14.5	

Material	Conditions	Char yield(%)	Liquid Yield(%)	Gas Yield(%)	Reference
Sugar cane bagasse	M= 80g P= 8 kPa_{abs} T=500°C HR=12°C/min	19.4	62	17.6	Garcìa-Pérez *et al.*, 2002
	M=20 kg P= 12 kPa_{abs} T= 530°C	25.6	51.3	22.0	

2.2.3 Conclusion

- Pyrolysis is the thermal decomposition of biomass into solid, liquid and gaseous products in the absence of oxygen. Vacuum pyrolysis is performed under reduced pressure instead of using an inert gas, leading to a decrease of gas production and an increase of bio-oil yield due to the limitation of secondary thermal decomposition. Pyrolysis process conditions and the feedstock characteristics affect the yields of pyrolysis products.

- High temperatures lead to an increase in the gas yield, but a decrease in the biochar yield. The ash and fixed carbon contents in the biochar also increase with an increase in pyrolysis temperature, combined with a decrease in volatile matter content due to the further decomposition of the biochar.

- The size and shape of biochar are affected by pressure. High pressures decrease the total surface area of biochar, while low pressures lead to swelling. Increasing pressure favours the formation of char.

- High heating rates favour the polymerisation reactions and formation of volatiles but limit the char formation. Therefore, high heating rates increase the yield of liquid products but decrease char yield with lower surface areas. The porosity of biochar is also affected by heating rates. High heating rates enlarge the micropores, resulting in biochar production with a macroporous structure.

- At longer hold times more volatiles are released from biochar, which leads to higher fixed carbon content of the biochar. Long hold times with low temperatures, lead to an increase in surface area of the biochar, while high temperatures and long hold times cause sintering thereby decreasing the surface area of the biochar.

- Large particle sizes favour the formation of biochar due to the incomplete decomposition of biomass particles. Smaller particle sizes provide more surface reactions, allowing a high heating rate which leads to faster decomposition of the biomass. Ash content increases with a decrease in particle size.

- Ash content and lignocellulosic composition of a biomass increase the yield of the biochar. Also the increase in ash content favours the reactivity of the biochar in processes such as gasification.

- Lignin is more heat resistant than cellulose and hemicelluloses. Higher lignin contents of the biomass favour the biochar yield, while higher cellulose contents lead to the formation of tar. A large amount of water production is attributed to high amounts of hemicelluloses.

2.3 Biochar and its applications

In this section, readers will be introduced to the term biochar and its potential for on carbon dioxide sequestration and soil amendment. It is important to classify biochar according to its soil amendment capacity, physical and chemical properties to evaluate its influence on soil chemistry. Here these properties are discussed with the aid of various studies done for soil amendment and adsorption purposes.

2.3.1 Biochar term

The application of the chars determines the terminology of either charcoal or biochar. Charcoal is used as fuel in boilers, as a filter, reductant in metallurgy, colouring material, fuel for cooking and for the production of chemicals. Biochar differs from charcoal due to its environmental management, especially by means of its soil application and production of activated carbon (AC) (Lehmann & Joseph, 2009; Grønli & Antal, 2003). Biochar has high carbon (C) content; six C atoms bonded together in the absence of oxygen (O) or hydrogen (H). Biochars are purer forms of carbon than most graphite (Grønli & Antal, 2003). Graphite is an allotrope of pure C, a highly ordered, electrically conducting structure of graphene sheets of indefinite size, whereas biochars are imperfectly stacked, extremely reactive and a packed bed of carbonised char (Preston & Schmidt, 2006). Figure 2.13 shows the structural changes with temperature. Low temperature applications (400°C) show the increased aromatic carbon with its highly amorphous structure (a). When temperature is increased

further (b), conjugated aromatic carbon sheets grow, and at very high temperatures such as 2500°C biochars present graphitic structures (c) (Lehmann & Joseph, 2009).

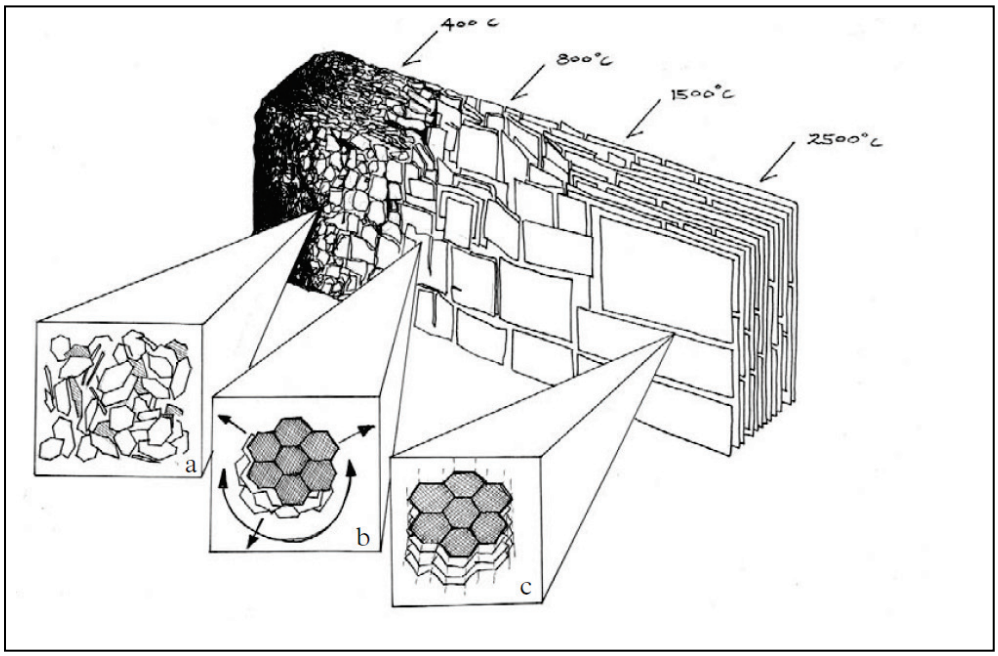

Figure 2.13: Change in biochar structure due to temperature increase (Lehmann & Joseph, 2009) (Granted permission from Earthscan)

Biochars from different biomasses and process conditions show differences in elemental composition (Table 2.3). Ultimate analyses of corn stalk char produced at 400°C and 500°C in the same reactor were compared. It can be seen that an increase in pyrolysis temperature leads to an increase in C content, as well as a decrease in H, N and O contents. If different pyrolysis conditions are compared, it is observed that corn stover char has higher C content when it is produced via slow pyrolysis and lower O and ash content than when produced by fast pyrolysis (Brewer *et al.,* 2009). Despite the increase of temperature for slow pyrolysis, vacuum pyrolysis leads to the highest C content.

Table 2.3: Process conditions and elemental analysis of various biochars (dry, wt.%)

Biochar Feedstock	Process Conditions	%C	%H	%N	%O*	Reference
Sugar cane bagasse	Slow pyrolysis T= 600°C, HR = 10°C/min	76.45	2.93	0.79	19.83	Inyang *et al.,* 2010
Sugar cane bagasse	Vacuum pyrolysis T= 500°C, HR= 12°C/min	85.60	2.90	1.30	10.2	Garcìa-Peréz *et al.*, 2002
Corn stalk	Slow pyrolysis T= 400°C, HR =10°C/min	61.51	3.55	3.23	31.41	Fu *et al.,* 2010
Corn stalk	Slow pyrolysis T = 500°C, HR = 10°C/min	63.10	2.82	3.10	30.70	Fu *et al.,* 2010
Corn stover	Slow pyrolysis T=500°C, HR= 15°C/min	62.80	2.90	1.30	32.95	Brewer *et al.,* 2009
Corn stover	Fast pyrolysis T= 750°C	37.80	2.50	0.80	58.84	Brewer *et al.,* 2009

*by difference

The difference between char and the widely used term activated carbon is the preparation (Figure 2.14). Activated carbons are prepared from carbon containing sources such as coal, lignite, wood, nut shell, petroleum and some polymers by thermal decomposition, followed by an activation step. The activation step can be achieved with steam above 800°C, carbon dioxide or their mixtures at higher temperatures (physical activation) or by using chemical activation agents such as $ZnCl_2$, KOH, H_3PO_4 (chemical activation) (Bansal, 1988; Lua & Yang, 2004). Activated carbons have been used for refining beet sugar, purification, remediation, filtration of drinking water, fuel storage, colour removal, etc. (Suzuki, 1990).

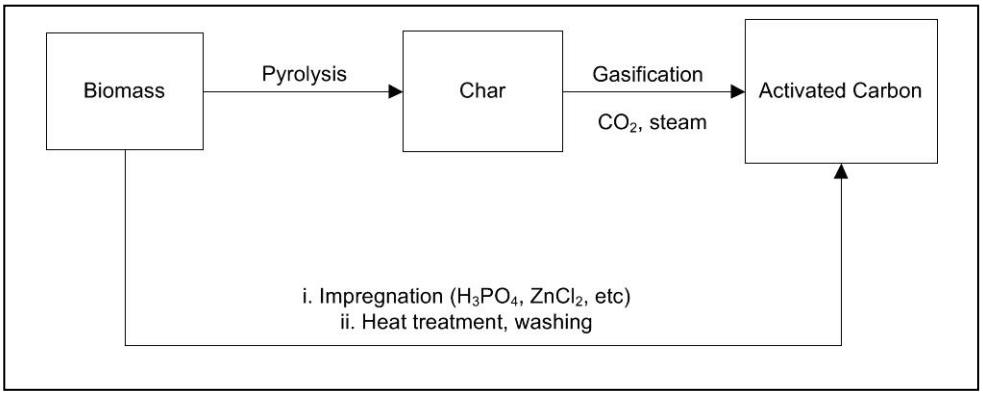

Figure 2.14: Production of activated carbon

The history of the carbon-rich solid products of pyrolysis (charcoal), goes back 38 000 years ago to Cro-Magnon men. Charcoal drawings indicate that charcoal was the first man-made material (Antal & Gronli, 2003). The application of char goes back to the Bronze Age when man used charcoal to smelt tin for the production of bronze tools (Antal & Gronli, 2003). As early as 1600 BC, wood chars were used for medicinal purposes in Egypt (Suzuki, 1990). Biochar has received the attention of the researchers due to the many advantages it provides. These advantages are namely; biomass waste management, carbon sequestration, energy generation and soil amendment (Roberts *et al.*, 2010).

Biochar can improve soil fertility, soil structure, nutrient availability, soil - water retention capacity and storage of carbon in soils for long term (Roberts *et al.*, 2010). Soil amendment by biochar is not a new concept. Charcoal was reported to be the reason for high soil organic matter contents and soil fertility of anthropogenic soils in the centre of Amazonia which is known as Terra Preta de Indio or Amazonian Dark Earths (Glaser *et al.*, 2002). Apparently, Terra Preta got this name due its black soil colour. The importance of this soil is that it has high soil nutrition and high carbon content. It is accepted that Terra Preta soils were created by human activities such as habitational activities or deliberate soil applications by Amerindians before arrival of Europeans in 1541. It is assumed that

Terra Preta soils were created between 500 and 8000 years ago. The discovery of carbon in Terra Preta has led researchers to further investigations of carbon added soils, especially the effects of carbon on fertilisation and possible contributions to the environment and agriculture (Lehmann & Joseph, 2009; Lehmann *et al.*, 2006).

2.3.2 Biochar as CO_2 sequester

The increasing CO_2 emissions have been a real challenge for the world. The reason for the increase is mainly the result of human activities. The total world CO_2 emission is 31 129.9 million tonnes according to the BP 2010 statistical report. The CO_2 emissions increased by about 19 200.4 million tonnes which is approximately 62% from 1965 to 2009. Considering South Africa, 1.5% of world CO_2 is emitted by South Africa (12th rank). The increase of CO_2 emissions in South Africa from 1965 to 2009 was 75% which explains the need for renewable energy with little emission or without any emission. CO_2 emissions in South Africa have decreased by 3% between 2008 and 2009 (British Petroleum, 2010); this could be attributed to biomass utilisation and economical recession during the past years. According to statistics of UNFCCC for 1994, the energy sector (Eskom) releases most of the CO_2 emissions to atmosphere in South Africa, followed by the agricultural, industrial (Sasol) and waste sectors (IEA, 2009).

Fossil fuel combustion releases approximately 5.5 gigatons of carbon (GtC) per year into the atmosphere and land-use changes contribute roughly 1.6 GtC per year. It has been estimated that 7.1 GtC is released per year from human activities. Approximately, 3.2 GtC remain in the atmosphere, which is the reason for increasing atmospheric CO_2 content. The oceans of the world can absorb approximately 2 GtC per year. Scientists are unsure about the remaining 1.9 GtC, but carbon sinks on land surface, which take up more carbon dioxide than is released each year is one of the possible explanations (Nasa Earth Science, 2010).

According to Lehmann (2007), emission reduction can be 12-84% greater if char is used as soil amendment rather than off-setting fossil-fuel use by burning the char. Steiner (2007) also reported that if the demand for renewable fuels, via pyrolysis, was met in 2100, sequestration by biochar could exceed the current emissions from fossil fuels (5.4 GtC/year). Figure 2.15 displays the schematic of carbon sequestration via photosynthesis (slow) and biochar amended soil by fixing carbon aboveground and belowground with 20% net carbon withdrawal difference. Biomass from unused agricultural wastes releases CO_2 and methane due to decomposition where as plants and

trees sequester CO_2 via photosynthesis, leading to a neutral carbon balance. The stability of carbon depends on the feedstock and biochar production conditions, but if the stable carbon is 80% as estimated by Roberts *et al.* (2010), the rest of the carbon will be stored in the soil and during thousand year's time, it will be released to the atmosphere. This process illustrates the carbon negative property of biochar from pyrolysis.

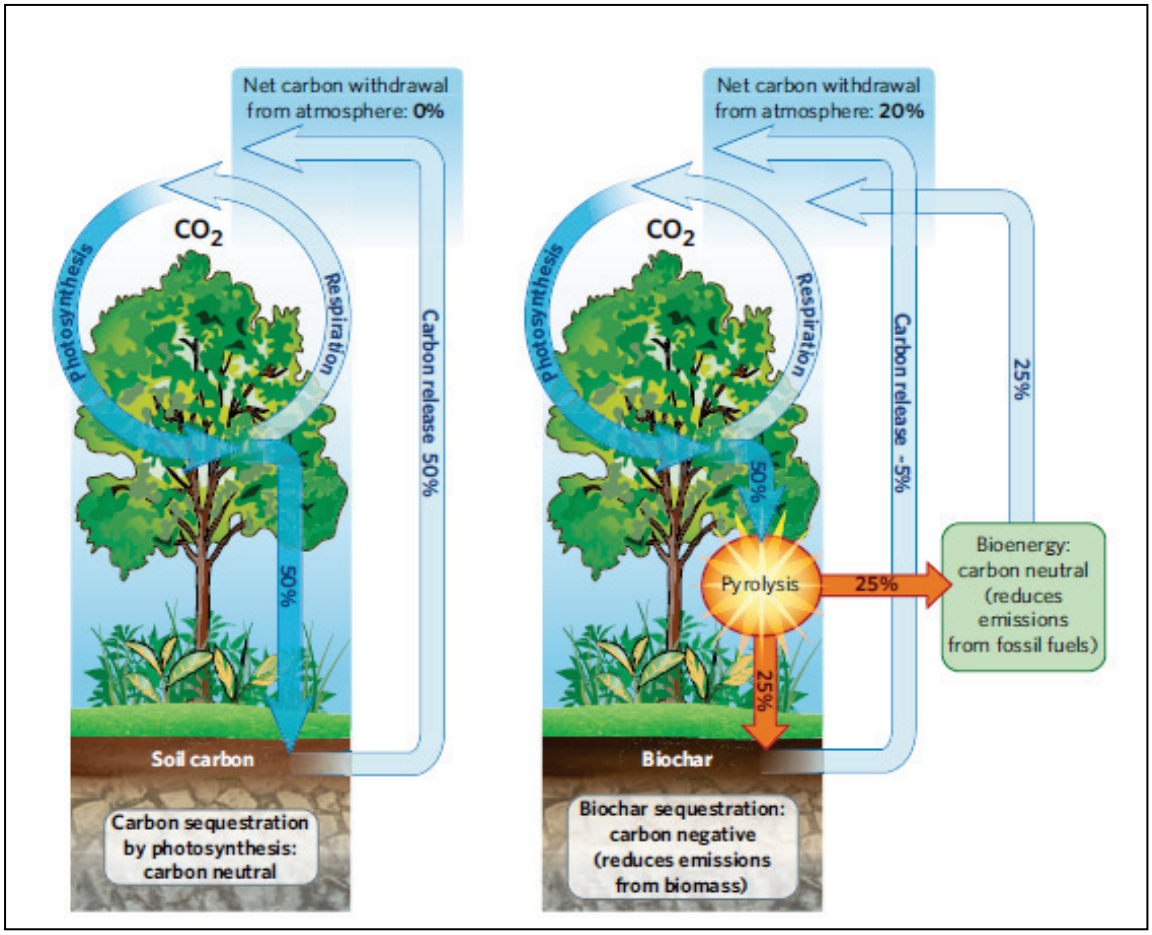

Figure 2.15: Schematic of carbon sequestration (Lehmann, 2007) (Granted permission from Nature Publishing Group)

Global biochar production varies around 0.05 to 0.3 GtC per year (Atkinson *et al.*, 2010), which equates to sequestration by biochar to 0.7 - 4% of the carbon released from human activities on annual basis. The estimation of biochar's ability to sequester carbon is 0.5-3 GtC per year, and at this level the global emissions would be sequestrated by roughly 5-30% on an annual basis (Biocharfarm, 2010).

2.3.3 Biochar as soil amendment

The soil amendment consists of improving the quality of soils through the reinforcement of the soil structure, pH control, nutrient mobility and water retention. Physical and chemical characterisation of biochar gives an understanding of biochar properties. With this information, it can be concluded what kind of biochar can be added to soil and whether the former is efficient as soil amendment regarding its nutrient content. These properties include surface acidity, basicity, pH, cation exchange capacity, nutrient content, electrical conductivity and BET surface area of the biochar.

2.3.3.1 Surface chemistry of biochar

The surface of biochars consists of spheroidal particles with graphene layers, which are piled up on top of each other by Van der Waals interactions and at the edges of the carbon layers heteroatoms, mostly H. Other than H, the most important element found is O in the form of various functional groups. Apart from H and O, combined S, N, Cl and other elements can be found (Biniak *et al.,* 1997). The concept of acidic and basic surface oxides was first introduced by Steenberg in 1944. The importance of surface functional groups is due to their effect on adsorption of ions, point of zero charge, wettability and electrical contact resistance (Pandolfo & Hollenkamp, 2006).

The existence of carboxyl groups, anhydrides, lactones, lactol groups and hydroxyl groups of phenolic character (Figure 2.16) gives carbon material its acidic surface chemistry (Boehm, 1994). Basic surface oxides, which give carbon material its basic surface chemistry, are considered to be more stable than acidic oxides. Figure 2.17 presents acid and basic groups which are grafted on the biochar's surface (Montes-Moran, 2004).

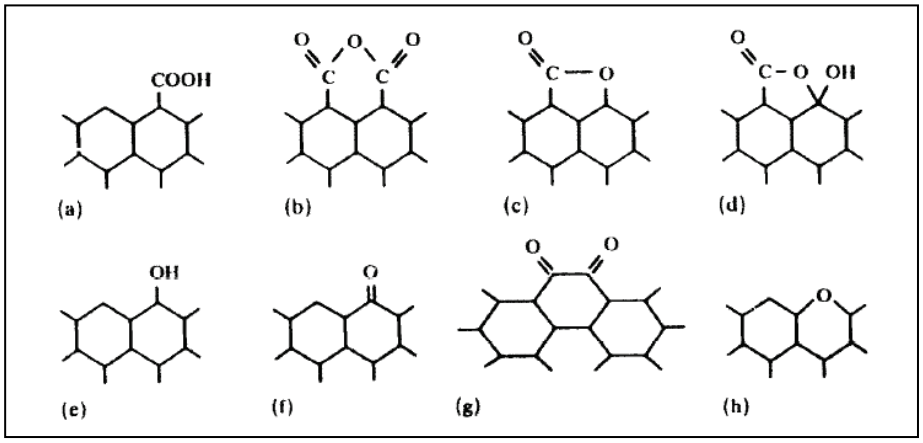

Figure 2.16: (a) carboxyl groups, (b) carboxylic anhydrides, (c) lactone groups, (d) lactols, (e) single hydroxyl groups, (f) carbonyl groups, (g) quinine-like groups, and (h) xanthenes-like groups (Boehm, 1994) (Granted permission from Elsevier Ltd.)

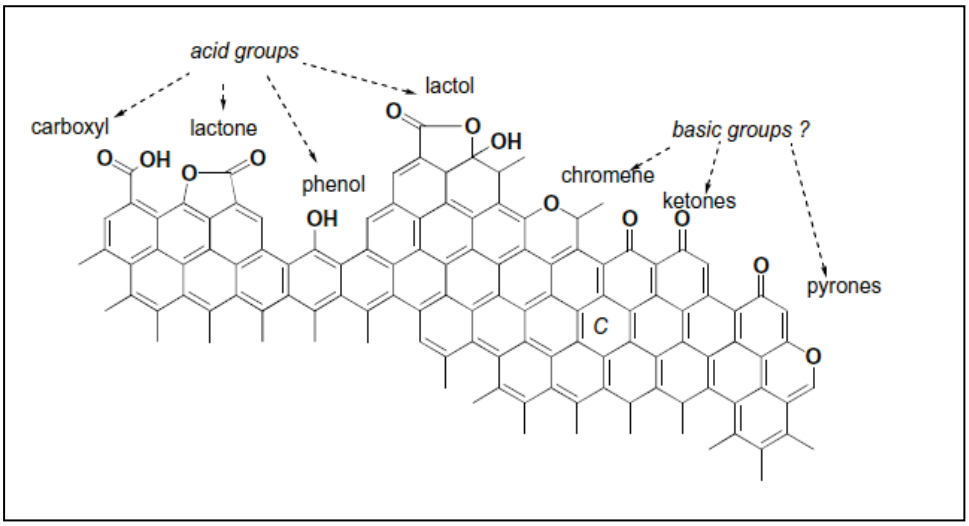

Figure 2.17: Surface groups of biochars (Montes-Moran, 2004) (Granted permission from Elsevier Ltd.)

Basic groups can be formed by heat treatment and exposure to oxygen at low temperatures. Papirer *et al.* (1987) reported that acidic functional groups are very sensitive to heat treatment such as pyrolysis. A carbon sample was exposed to O_2 and then treated with heat via pyrolysis. Above 400°C pyrone-type structures were formed, which react as basic centres in acid-base reactions, and when temperature reached 800°C, the pyrone structures were destroyed. Surface oxides decompose to CO_2 and CO on heating to high temperatures (Boehm, 2002). It is also well known that pH and oxygen content of carbon material are related. The higher the O content of the biochar, the more acidic an aqueous solution of the carbon material (Boehm, 1994). From this aspect, one would expect that

char from fast pyrolysis would be more alkaline than chars produced from low temperature pyrolysis such as slow and vacuum pyrolysis.

Basal sites should also be considered due to different chemistry compared to edge sites. Basal sites are the imperfections due to disordered stacking of graphene layers such as non-aromatic rings or structural carbon vacancies. Basal and edge sites in the graphene layers are called active sites, which show a great tendency to chemisorb heteroatoms (Bandosz & Ania, 2006). Edge sites are more reactive than basal sites with unpaired electrons (Pandolfo & Hollenkamp, 2006). Boehm (1994) also reported that basic properties of carbon materials were due to π-electron system of basal planes. Montes-Morán *et al.* (2004) also mentioned that overall basicity is caused by oxygen-containing functionalities (chromene, pyrone, and quinone) and non-heteroatomic Lewis base sites, characterised by regions of π-electron density on the carbon planes. A Lewis base is a compound with an available pair of electrons, either unshared or in a π-orbital. A Lewis acid is a compound with a vacant orbital. The strength of a bond of an acid and a base makes the reaction possible and that strength is called their hardness or softness. Classification of acids and bases is shown in Table 2.4.

Table 2.4: Classification of acids and bases (Reproduced from Alfarra, 2004)

Hard bases	**Soft bases**	**Borderline bases**
H_2O, OH^-, F^-, CH_3COO^-, SO_4^{2-}, Cl^-, CO_3^{2-}, NO_3^-, RO^-, RNH_2, ROH, R_2O	R_2S, RSH, RS^-, I^-, $(RO)_2P$, CO, C_2H_4, C_6H_6, H^-, R^-	$ArNH_2$, pyridine, NO_2^-
Hard acids	**Soft acids**	**Borderline acids**
H^+, Li^+, Na^+, K^+, Mg^{2+}, Ca^{2+}, Al^{3+}, Cr^{3+}, Fe^{3+}, BF_3, $AlCl_3$, CO_2, HX	Cu^+, Ag^+, Pd^{2+}, Pt^{2+}, Hg^{2+}, I_2	Fe^{2+}, Co^{2+}, Cu^{2+}, Zn^{2+}, Cd^{2+}, Sn^{2+}, Sb^{2+}, Sb^{3+}, Bi^{3+}

Hard bases are donor atoms, which have high electronegativity and low polarisability. They hold their valence electrons tightly, whereas soft bases have low electronegativity and high polarisability. Soft bases are easy to oxidise and they hold their valence electrons loosely. Hard acids are small acceptor atoms, which have a high positive charge density, low polarisability and low electronegativity. Soft acids are large acceptor atoms, which have low positive charge density, high polarisability and a low electronegativity. Hard acid atoms do not contain unshared pairs of electrons in their valence shells, whilst soft acid atoms contain unshared pairs of electrons (Alfarra, 2004). Hard acids and hard bases, or soft bases and soft acids, tend to bond and form strong acids and bases or weak acids and bases.

Other functionalities such as nitrogen can be introduced on carbon surfaces (Lahaye, 1997). Surface treatments on carbon surfaces, with the purpose of increasing their N content, resulted in enhancement of the surface basicity (Montes-Moran *et al.*, 2004). Nitrogen can be introduced in two ways:

- Reaction of a carbon with a N-containing reagent, e.g. ammonia, urea, melamine
- Preparation of a carbon from a N containing precursor

Figure 2.18 shows some of N-containing functional groups existing in biochars (Bandozs & Ania, 2006). The nature of N-containing functionalities differs depending on the heat treatment, for instance amides and aromatic amines dominate at low temperatures (400-700°C), while pyridine and pyrol dominate at higher temperature (>700°C) (Seredych, 2008; Bandozs & Ania, 2006). It is known that the introduction of N increases the polarity of the carbon surface and its specific interactions with polar species via electrostatic forces or hydrogen bonding (Stöhr *et al.*, 1991). Surface oxides can be determined by titration, infrared spectroscopy, X-ray photoelectron spectroscopy, thermal desorption spectroscopy and electrokinetic measurements (Boehm, 2001).

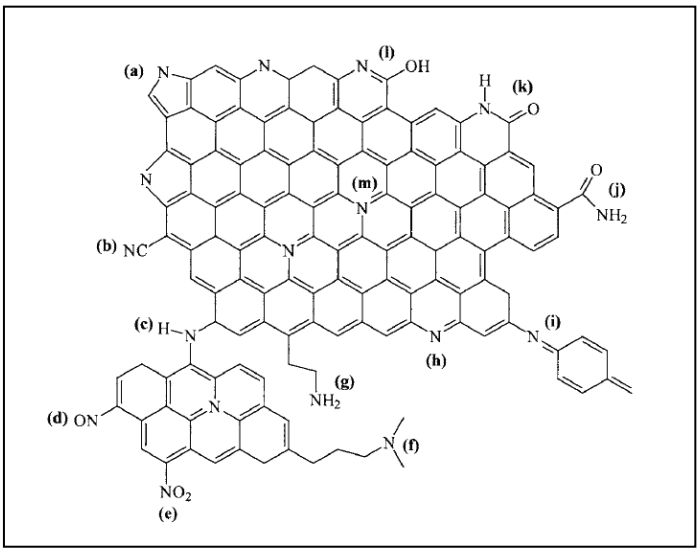

Figure 2.18: N-containing functionalities (Bandozs & Ania, 2006) (Granted permission from Elsevier Ltd.)

Carbon materials with acidic functional groups have cation exchange properties whereas basic functional groups have anion exchange properties due to faradaic reactions. Ion exchange properties have gained the attention because it is one of the most important driving forces in sorption (Biniak *et al.*, 1997). From Table 2.5, which presents some surface acidity and surface basicity values, it can be

seen that char from pine sawdust produced at high temperature (800°C) had a lower surface acidity (0.32 mmol/g) but a higher surface basicity (0.36 mmol/g) than the chars produced at lower temperatures (400°C). The surface acidity of sewage sludge (5.18 mmol/g) is much higher than the surface acidity of wheat residue char (1.13 mmol/g), even though the temperatures at which they were produced were close to each other (400-500°C). This could be due to the difference of the feedstock used and the activation process. Comparing the surface acidity of the activated carbons, chemically activated carbon has a higher surface acidity (0.731 mmol/g) than steam activated carbon (0.21 mmol/g).

Table 2.5: Surface acidity/basicity of various biochars

Product	Temperature (°C)	Surface acidity (mmol/g)	Surface basicity (mmol/g)	Reference
Pine sawdust char	800	0.32	0.36	Nowicki & Petrzak, 2010
Carbon black	n/a	0.21	0.605	Hulicova-Jurcakova *et al.*, 2010
Commercial phosphoric acid activated carbon from wood	n/a	0.731	0.123	Villacañas *et al.*, 2006
Steam activated activated carbon from wood	n/a	0.21	0.446	Villacañas *et al.*, 2006
Wheat residue char	400	1.13	0.11	Chun *et al.*, 2004
Chemically activated sewage sludge carbon	500	5.181	n/a	Chen *et al.*, 2002

Hulicova-Jurcakova *et al.* (2010) modified commercial carbon blacks with N-containing compounds. International Carbon Black Association defines carbon black as a virtually pure elemental carbon that is produced by thermal decomposition of gaseous and liquid hydrocarbons (ICBA, 2011). Before modification, initial carbon black samples were oxidised with 50% HNO_3 for 4h and washed with water to remove excess acid. After this oxidation treatment, samples were impregnated with urea or melamine, heated in nitrogen to 950°C and maintained at this temperature for 30 min. Afterwards, the samples were washed with boiling water to remove excess urea or melamine decomposition products and the acidity or basicity of the carbon surfaces determined. Results showed that oxidation of initial carbon caused 4 units decrease in pH due to higher surface area and increased

edges of graphene layers, which leads to more incorporated oxygen groups. It was found that N treatment made the surface character more basic. Urea treated carbon black contained fewer basic groups than melamine treated carbon black, expectedly the pH was lower. Modified carbon blacks showed four times higher sorption ability of anions than cations. Seredych *et al.* (2008) also reached the same conclusion with their research on activated carbons originating from wood.

Regarding the pyrolysis temperature effect on surface chemistry, Chun *et al.* (2004) showed that total acidity of the chars from wheat residues decreased and basicity increased with increased pyrolysis temperature. The temperature range tested was between 300°C and 700°C. Chars produced at low temperature (300°C and 400°C) showed a more polar and organic nature than the chars produced at 500°C, 600°C and 700°C due to partial carbonisation. Even though basicity increased with temperature, the total number of functional groups decreased with temperature. Regarding the sorption ability of chars, benzene and nitrobenzene were chosen as models for neutral organic contaminants (NOC). Chun *et al.* (2004) showed that surface polar groups reduced the uptake of non-polar NOCs (benzene) from water, which also affected sorption ability in combination with BET surface area of the chars. Carbons with a high amount of carbonyl groups among total acidic groups might improve the sorption of aromatic compounds via formation of electron acceptor-donor complexes (Chen *et al.*, 2002).

2.3.3.2 pH of biochar

Plants need nutrients to live, grow and reproduce. Plant roots require certain conditions to take up the nutrients from the soil. One of the conditions that are required is that the pH must be within a certain range for nutrients to be releasable from the soil (Hosier & Bradley, 1999). Soil pH is a measure of soil acidity (pH<7) or alkalinity (pH>7) by measuring the pH of a soil solution in water, or other solutions such as KCl, which is known as the active pH and that affects plant growth.

The reasons for pH change in soils were discussed by Sir John Russell (1954) and summarised as;

- Any substance in soil that is capable of changing their state by oxidation or reduction,
- The concentration of CO_2 in soil air,
- Hydrogen-ion concentration which is caused by base-exchange of the electric double layer surrounding the particles.

One of the problems that farmers face is low harvest yields in acidic soils, which affect the agriculture and economy. The most important reasons for soil acidity are H and Al concentrations. At low pH Al, Fe and Mn become more soluble which causes toxicity (Sparks, 1995). At pH values lower than 5.5, $Al(OH)_3$ begins to dissolve and release toxic aluminium hydroxy cations. As pH increases plants can suffer from nutrient deficiencies such as phosphate due to the decrease in solubility of phosphate. Soils can only have a pH above 8.5 if they contain enough exchangeable sodium for sodium carbonate formation (Russell, 1954; EPA, 2010). Different species of plants have different optimum conditions. Most plants perform best in a soil that is slightly acidic to neutral (pH 6 to 7).

Table 2.6 displays the values of pH obtained from different solutions, namely water ($pH(H_2O)$), potassium chloride (pH(KCl)) and calcium chloride ($pH(CaCl_2)$). The pH(KCl) is lower than $pH(H_2O)$ up to 1.35 units. $pH(H_2O)$ gives an indication of active acidity, while pH(KCl) or $pH(CaCl_2)$ refers to reserve acidity (Ahmed *et al.*, 2006). Since pH is due to the surface ionisation of the carbon and hydrolysis of the exchangeable base, one would suppose that the presence of salt would reduce hydrolysis, therefore the pH value is lower (Puri & Asghar, 1938).

Table 2.6: pH values of different biochars produced at different temperatures

Feedstock	Final process T(°C)	$pH(H_2O)$	pH(KCl)	$pH(CaCl_2)$	Reference
Acacia *mangium*	360	7.4	7.1	-	Yamato *et al,.* 2006
Oak wood	-	8.5	8.4	-	Cheng & Lehmann, 2009
Black locust	350	5.35	4	-	Cheng *et al,.* 2006
Greenwaste	450	-	-	9.4	Chan *et al.,* 2007
Eucalyptus deglupta	350	7	-	-	Rondon *et al.,* 2007
Poultry litter	450/550	9.9/13	-	-	Chan *et al.,* 2008
Pecanshell	700	7.5	-	-	Novak *et al.,* 2009
Wastewater sludge	550	-		8.2	Hossain *et al.,* 2010
Papermill waste 1/2	550	-	-	9.4/8.2	Van Zwieten *et al.,* 2010

When the $pH(H_2O)$ of a carbon solution is very high or low, ions might be present and the electrostatic interactions between them and charged surface functional groups could be significant (Villacañas *et al.*, 2006). Recent studies show that most biochars have an alkaline nature. The pH of biochar is related to feedstock nature and applied temperature in the production process. The effect of temperature (400, 600, 800, 900°C) and hold time (30 and 60 minutes) on $pH(H_2O)$ of biochar from sewage sludge is shown in Table 2.7.

Table 2.7: Effect of temperature and hold time on pH of biochar from sewage sludge (Bagreev *et al.*, 2001)

Temperature (°C)	Hold time (min)	pH(H_2O)
400	30	7.7
600	60	11.5
800	60	11.3
900	60	11.0

The pH of sewage sludge biochar decreased with an increase in temperature. Lower temperature and hold time resulted in low pH but still alkaline in nature. The significant pH change between biochars, which were produced at low and high temperatures, can be explained with the change of chemical structures during pyrolysis process. As can be seen from Table 2.6, the lowest pH of 7 was found for biochar produced at 350°C but the nature of the feedstock varied. The same trend was observed by Chan *et al.* (2008) who worked on two biochars produced from poultry litter at 450°C and 550°C. The pH of the biochar produced at 450°C was 3 units lower than the pH of biochar produced at 550°C.

Some researchers have studied the pH change in soil after addition of biochar. Novak *et al.* (2009) observed that when biochar from slow pyrolysis of pecan shells with a pH of 7.5 was added to acidic soil (40 t/h), the pH of soil increased from 4.8 to 6.3. Similarly, application of biochar (10 t/ha) from slow pyrolysis of sewage sludge with a pH of 8.2 increased soil pH from 4.3 to 4.6 units in the work of Hossain *et al.* (2010). Van Zwieten *et al.* (2010) produced two different biochars via slow pyrolysis at 550°C from paper mill sludge. The first biochar feedstock contained 32.6% enhanced solid reduction sludge (ESRS), 18.8 wt.% clarifier sludge and 48.6% waste wood chips. Second biochar was produced from 19.5 wt.% ESRS, 11.2 wt.% clarifier sludge and 69.3 wt.% waste wood chips. The pH of the biochars was determined as 9.4 and 8.2, respectively. Addition of 2% of the first biochar to acidic soil (ferrosol, with a pH of 4.2) resulted in approximately a 2 unit increase while the second biochar increased the pH by 1.2 units. Addition of 1.5% of the first biochar to slightly basic soil (calcarosol, with a pH of 7.67) did not cause any changes in pH. However, the second biochar increased the pH by 0.1 units. From this study, it could be concluded that alkaline natured biochars should be applied to acidic soils instead of alkaline soils due to interactions between biochar surface and soil.

As pH increases, the degree of negative charge increases due to deprotonation or dissociation of H from functional groups (Kumada, 1987). This is known as the positive liming effect of biochar. Through the liming effect, aluminium toxicity is prevented in acidic soils such as high rainfall region

soils and soils in the humid tropics (Glaser *et al.*, 2002). However, Chan *et al.* (2007b) could not find any correlation between the liming effect and pH of the biochar (Lehmann & Joseph, 2009).

2.3.3.3 Cation exchange capacity (CEC)

Cation exchange capacity (CEC) is a calculated value to estimate the soils ability to attract, retain and exchange cation elements. It is reported in millequivalents per 100 grams of soil (meq/100g). CEC also refers to the reversible process of stoichiometric binding of cations to negatively charged macromolecular compounds in the plant body (Buscher *et al.*, 1990). The sources of cation exchange are clay minerals, organic matter and amorphous minerals (Sparks, 1995). The chemical and physical processes more or less connected with ion exchange are; nutrient absorption by plants, swelling, shrinkage and leaching of electrolytes. In other words, the reasons for soil to have negative charge are permanent negative charges on clay, presence of minerals, which take place in isomorphous replacements, or hydrogen ions dissociation from hydroxyls attached to silicon atoms.

Carboxyl, phenol or hydroxyl groups are attached to various groups in soil solution that dissociate hydrogen ions (Russell, 1954). Cation exchange capacity is related to the pH of soil, which is discussed in Section 2.3.3.2. As the pH increases, negative charge grows and positive charge decreases due to an increase in ionisation of the acid groups and decreasing proton addition to basic groups. The opposite change would be expected when the pH decreases.

The electric charge on the soil particles is neutralized by an equivalent amount of oppositely charged ions and held to the surface by Coulomb forces. These ions are so-called exchangeable ions. The most common exchangeable cations in soils are Ca^{2+}, Mg^{2+}, H^{+}, K^{+}, Na^{+} and NH_4^{+}. Ca^{2+} is generally the most abundant ion. In alkaline soils, Na^{+} is the dominant ion but as in acid saline or sulfate soils, the concentration of SO_4^{2-} is very high (Bear, 1965). Coulomb's law is also used to explain the selectivity of the ion exchanger for one ion over another. For instance, the selectivity of the hydrated Group I elements in the periodic table would be $Cs^{+} > Rb^{+} > K^{+} > Na^{+} > Li^{+} > H^{+}$, because the smallest radius would be preferred, since the polarisation power would be greater. If the elements are with different valence, higher charged ion would be preferred; $Al^{3+} > Ca^{+2} > Mg^{2+} > K^{+}$ (Sparks, 1995).

Cation exchange reactions take place when the fertilisers such as ammonium sulphate, sodium nitrate, superphosphate of lime, potassium sulphate, sodium sulphate, magnesium sulphate, calcium oxide and calcium carbonate are used by farmers (Russell, 1954). It can be said that ion exchange can be considered as the most important process in the soils.

CEC of the soils in tropic regions is often low due to clay mineralogy (Glaser *et al.*, 2002). Hossain *et al.* (2010) reported that application of biochar to the soil increased CEC by up to 40% in the study of Mikan & Abrams in 1995 (Lehmann& Joseph, 2009). Tyron (1948) found that CEC increased after addition of 45% hardwood and conifer biochars to sandy and loamy soils. Lower amounts of added biochar would significantly increase the base cation availability in the soil, which could lead to an increase of nutrients in soil (Glaser *et al.*, 2002). Liang *et al*. (2006) mentioned that greater CEC could be reached with increasing degree of oxidation in soil organic matter or increasing the surface area for cation exchange sites. Glaser *et al.* (2003) suggested that major reasons for high CEC could be oxidation of aromatic carbon and formation of carboxyl groups. This same conclusion was made by Liang *et al.* (2006), reporting that surface oxidation led to a higher CEC per unit carbon. One would therefore expect that the ageing process of biochar would result in high CEC due to high surface acidity of biochar.

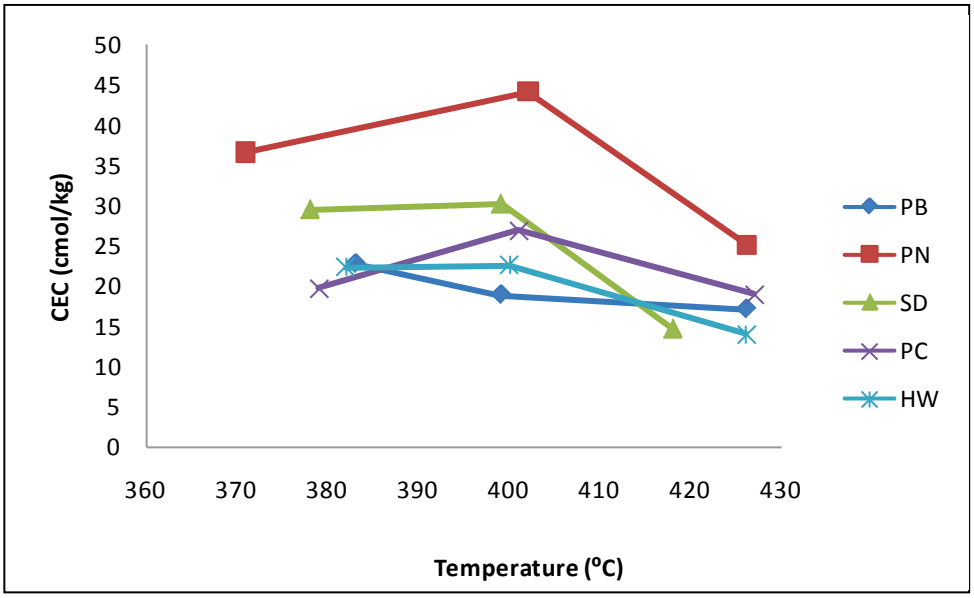

Figure 2.19: Effect of production temperature on CEC of pine bark (PB), peanut hull pellets (PN), pine sawdust (SD), pine chip pellets (PC) and hardwood (HW) (Redrawn from Gaskin *et al.*, 2007)

Gaskin *et al.* (2007) investigated CEC values of chars from different biomasses, namely pine bark (PB), peanut hull pellets (PN), pine sawdust (SD), pine chip pellets (PC) and hardwood (HW) at different temperatures (Figure 2.19). The highest CEC was reached around 400°C by all the biomasses except pine bark. For all biomasses the lowest CEC was observed at temperature above 420°C. The reason for this behaviour might be explained by the changes in plant available nutrients with temperature (Lehmann & Joseph, 2009). Unfortunately, there is very little information in the open literature regarding the correlation between temperature and CEC. The CEC of soil organic matter (SOM, same

as humus) is generally between 150 to 300 cmol/kg (Sparks, 1995). In comparison to SOM, CEC values of biochars from pyrolysis are very low.

2.3.3.4 Nutrients

The ash content of biochar is an indicator of nutrient concentration. Usually, the main minerals are silicon (Si), Calcium (Ca), Potassium (K), Sodium (Na), Magnesium (Mg) and smaller amounts of Sulphur (S), Phosphorus (P), Iron (Fe), Manganese (Mn) and Aluminium (Al). These elements are found in their oxides, silicates, carbonates, sulphate, chlorides and phosphate forms in the biochar (Ravedraan *et al.*, 1995). Metals that exist in biomass are mainly organically bound and highly volatile.

Previously (Section 2.2.2.6) the influence of the presence of inorganics on the product yields has been discussed, but it can also affect the biochar quality by plugging its pores and can cause a decrease in surface area, which is unwanted for activated carbon applications such as wastewater treatment. For soil amendment purposes, ash itself has already been used as a liming agent in soil and a fertiliser for nutrient deficient soils. Depending on the purpose of application, inorganics can be removed or not.

Nitrogen is a constituent of all proteins, therefore it is an essential macronutrient for plant growth. This element is taken up as ammonium (NH_4^+) or nitrate (NO_3^-) ions. The absorbed NO_3^- is rapidly broken down to NH_4^+ by molybdenum-containing enzymes. The NH_4^+ ions and synthesised carbohydrates are converted into amino acids in the leaves of the plant. Plant roots absorb more nutrients than they actually require. When excessive amounts of N are taken up, it renders large thin walled cells of the plant leaves, which are easily attacked by insect and fungus pests and ravaged by droughts and frosts. On the other hand, low N uptake gives leaves with small cells and thick walls and consequently, leaves are fibrous and light green in colour or even yellowishly, which affects photosynthesis (Russell, 1954; Hosier & Bradley, 1999).

Phosphorus, as ortho-phosphate, takes part in a number of enzymic reactions that depend on phosphorylation. Plants absorb P as inorganic phosphate ions, especially as $H_2PO_4^-$ ions and hence plants suffer from P deficiency in alkaline soils. The amounts of soluble phosphate ions decrease when the pH of the soil rises above 8. Excessive amount of phosphate uptake depresses crop yields. In plants with P deficiency, leaf tips look burnt and older leaves turn a dark green or reddish-purple colour (Russell, 1954; Hosier & Bradley, 1999).

Sulphur is an essential constituent of many proteins. It can also be found in the oils produced by certain plants. Plants absorb S in the form of sulphate (SO_4^{-2}). Excessive amounts of S may acidify the soil. Lack of S causes younger leaves turn to yellow, which is also known as “tea yellows” (Russell, 1954; Hosier & Bradley, 1999).

Potassium is very important in the nutrition of the plant, playing a role in plant metabolism. It has an effect on the synthesis of amino-acids and proteins from NH_4^+ ions, for instance, when plants grow in soil with high NH_4^+ concentrations but low K concentration, it results in tissue death. In the photosynthetic process, K shortage in the leaf leads to low rates of carbon dioxide assimilation. Plants absorb K in ion form. Potassium deficiencies cause older leaves to wilt and to look scorched. Excess K in soil reduces the uptake of other cations by the crop which results in deficiencies of other cations (Russell, 1954; Hosier & Bradley, 1999).

Calcium is essential for the growth of meristems, root tips and functioning of root tips. Ca deficiency causes stunting of the root system and also other substances to accumulate in the tissues, which harm the plant, making new leaves distorted. Ca deficiency generally occurs on very acid soils. Excess Ca limits the availability of Mg and K. Good Ca supply helps to neutralise the undesirable effects of an unbalanced distribution of soil nutrients that can be taken up by plants (Russell, 1954; Hosier & Bradley, 1999).

Magnesium is required by all green plants due to its role in chlorophyll synthesis. It also plays a part in the transport of phosphate in the plant, for instance phosphate content of a crop can be increased by addition of Mg. Plants absorb Mg in ion form. Mg deficiency usually occurs on acid sandy soils. Older leaves turn yellow at the edge leaving a green shape in the centre of the leaf (Russell, 1954; Hosier & Bradley, 1999).

Sodium is not really considered an essential nutrient. Some plants need Na for optimum growth, some benefit if there is Na available, some can tolerate part of their K supply being replaced by Na and some do not use Na. However, Na can help crops to grow in a potassium-deficient soil by preventing an accumulation of other cations which is toxic to the plant (Russell, 1954; Hosier & Bradley, 1999).

Plants need very small quantities of certain elements which are called trace elements; aluminium (Al), boron (B), bromine (Br), chlorine (Cl), cobalt (Co), copper (Cu), fluorine (F), iron (Fe), manganese (Mn), molybdenum (Mo), nickel (Ni), rubidium (Rb), silicon (Si), titanium (Ti), vanadium (V) and zinc

(Zn). These elements are important because they are involved in key metabolic events such as respiration, photosynthesis, fixation and assimilation of some major nutrients. Trace metals of the transition metal group activate enzymes or are incorporated into metalloenzymes as electron transfer system (Cu, Fe, Mn and Zn) and also catalyse valence changes in the substrate (Cu, Co, Fe and Mo). Some of the trace elements contribute to protection mechanisms of frost-hardy and drought-resistant plant species (Al, Cu, Co, Mo, Mn and Zn) (Kabata-Pendias, 2000).

Over long periods of time, nutrients are released to the solution phase through desorption, exchange, and dissolution from the solid mineral phase and biochemical mineralisation such as enzymatic hydrolysis, oxidation and reduction of the organic phase (Hedley, 2008).

Table 2.8 shows the differences of available amount of elements and C/N mass ratio between different biomass derived biochars and raw organic amendments. It is important to mention that total element amounts of soil amendments do not always show their available amount in the soil and the literature is quite limited regarding the available amount of nutrients in biochars from various feedstocks. It is apparent that animal feedstock based biochars have higher P content (e.g. sewage sludge and poultry litter) than plant origins. Similarly N content of biochar from sewage sludge is much higher than biochar derived from plant and wood origins, especially higher than oak wood and green wastes. Regarding K, poultry litter has the highest content.

C/N ratio is an indication of the ability of organic substrates to mineralise and release inorganic N when it is applied to soils (Lehman & Josephn, 2009). As can be seen from Table 2.8 the C/N ratios of the listed biochars have a wide range, from 7 to 759. Sewage sludge has the lowest C/N ratio and oak wood has the highest. Dias *et al.* (2010) and Topoliantz *et al*. (2005) reported C/N ratios of raw amendments such as poultry manure, coffee husk, manioc peels and sawdust. From this, it can be concluded that biochar has higher C/N ratio than other raw amendments such as poultry manure and manioc peels. Poultry manure and manioc peels have the higher N content and lower C/N ratios than wood origins. The difference in C/N ratios of two sawdusts is due to being different samples. For organic amendments with high C/N ratio, N immobilisation occurs; therefore plants cannot take up available N from the soil causing nitrogen shortages. However, the recalcitrant nature of biochar restricts N immobilisation (Kimetu *et al.*, 2008).

Table 2.8: Concentration of major elements present in soil amendments

Soil amendments	C (g/kg)	N (g/kg)	C/N (wt ratio)	P (g/kg)	K (g/kg)	Ca (g/kg)	Production (°C)	Reference
Pine chip biochar	728	19.0	38.3	2.2	19.3	5.4	400	Gaskin *et al.,* 2010
Oak wood biochar	759	1.0	759.0	-	2.2	0.7	350	Nguyen & Lehmann, 2009
Corn stover biochar	675	9.3	72.6	-	10.4	2.7	350	Nguyen & Lehmann, 2009
Poultry litter biochar	380	20.0	19.0	25.0	22.0		450	Chan *et al.,* 2008
Pine bark biochar	691	3.3	209.4	0.1	0.8	1.0	426	Gaskin *et al.,* 2007
Peanut hull pellets biochar	655	20.0	32.8	0.7	7.7	1.4	402	Gaskin *et al.,* 2007
Eucalyptus deglupta wood biochar	824	5.7	144.6	0.6	-	-	350	Rondon *et al.,* 2007
Green waste biochar	680	1.4	485.7	0.2	1.0	-	450	Chan *et al.,* 2007
Sugar cane bagasse biochar	710	17.7	40.1	-	-	-	500	Tsai *et al.,* 2006
Sewage sludge biochar	288	32.0	9.0	26.4	8.0	33	550	Yao *et al.,* 2010
Poultry manure	288	27.5	9.7	-	-	-	-	Dias *et al.,* 2010
Coffee husk	513	12.0	43.5	-	-	-	-	Dias *et al.,* 2010
Sawdust	454	9.5	49.6	-	-	-	-	Dias *et al.,* 2010
Manioc peels	356	24.2	14.7	-	-	-	-	Topoliantz *et al.,* 2005
Sawdust	521	5.13	102.0	-	-	-	-	Topoliantz *et al.,* 2005

Studies have demonstrated that application of biochar has many advantages including improvements in plant growth, organic carbon content in soil, exchangeable cations in soil, to reduce leaching of nutriens, water retention and microbial activity (Hossain *et al.,* 2010; Chan *et al.*, 2007; Van Zwieten *et al.,* 2010). Studies have also shown that the characteristics of biochar, which are essential to plant growth, can improve over time after its addition into soil (Cheng *et al.*, 2006). However, researchers have highlighted the improvements in plant growth after incorporation of biochar with fertiliser into soil (Hossain *et al.*, 2010; Chan *et al.*, 2007). Nevertheless, high rates of biochar application (22 t/ha) with N fertiliser has caused a depression in grain yield (Gaskin *et al.*, 2010) which points out the importance of both biochar and fertiliser application rates into soil. Optimum biochar application rate has been suggested to be 10 t/ha by Van Zwieten *et al.* (2010) for wastewater sludge biochar from slow pyrolysis.

Soil biota is essential for functioning soils (Verheijen *et al.*, 2010), therefore interactions between soil and biochar leads to the question of the effects of biochar on soil biology. Steiner *et al*. (2008) demonstrated that char application to soil increases microbial biomass as well as basal microbial activity. The increase in basal mictobial activity was associated with increased water holding capacity of soil along with increased microbial biomass. Steiner *et al.* (2008) also mentioned fertiliser addition along with biochar leads to further increase in microbial biomass. Rondon *et al.* (2007) reported an improvement in nitrogen fixation; hence increase in bean yields at biochar additions upto 50 g/kg. Most of the increase in biomass production by the N-fixing beans was caused by greater leaf biomass. Improved crop performance was a result of high values of P, K, Mg, Ca, Mo, and B availability and higher pH of biochar. However, biochar application at 90 g/kg caused a decrease in crop yields. Van Zwieten *et al.* (2010) reported biochar amendment along with fertiliser significantly increased microbial activity in soybean and radish in ferrosol. However, fertiliser and biochar amendment resulted in significant decreases in microbial activity in the calcarosol with wheat.

Regarding toxic elements in biochar, there is not enough information in the literature. Table 2.9 shows the comparison of the concentrations of toxic elements in biochar from sewage sludge and the concentration limits in biosolids given by the Environment Protection Agency (EPA). It can be seen that nickel is higher than the given limit, while the rest of the elements are lower. Toxic elemental content is highly dependent on the feedstock type. For instance Singh *et al.* (2010) showed that biochars from slow pyrolysis of *Eucalyptus saligna* at 400°C contained 1661, 21 and 4 mg/kg zinc, copper and nickel, respectively. Poultry litter biochar, which was produced under the same conditions, contained less zinc but more copper and nickel elements.

Table 2.9: Toxic elemental concentration in sewage sludge biochar (Hossain *et al.*, 2010)

Elements	Biochar (mg/kg)	EPA limits (mg/kg)
Arsenic	8.8	75
Cadmium	4.7	85
Chromium	230	3000
Copper	2100	4300
Lead	160	840
Nickel	740	420
Selenium	7	100
Zinc	3300	7500

Although biochar application to soil has many advantages, there are some negative effects of biochar as follows (Verheijen *et al*., 2010):

- soil loss by erosion,
- soil compaction during application,
- risk of contamination due to polycyclic aromatic hydrocarbons,
- heavy metals and dioxins that are present in biochar,
- incorporation of the crop residue into the soil due to residue removal,
- occupational health and fire hazards, and
- reduction in earthworm survival rates at high biochar application rates such as 67 t/ha.

However, these negative effects can be overcome with careful planning, engineering and management.

2.3.3.5 Electrical conductivity

Electrical conductivity (EC) gives an indication of the salinity. Electric current conducted by salt solution under standard conditions increases as the salt concentration of the solution increases. EC is expressed in dS/m (Sparks, 1995). The EC of biochar gives an indication of total soluble mineral, N and S contents (Lehmann & Joseph, 2009). Soil salinity and sodicity may have an effect on the structure of the soil and crop yields (Sparks, 1995).

Salinisation is one of the main causes of land degradation in arid and semi arid regions. Soluble salts accumulate in the soil when precipitation exceeds evaporation (Abdelfattah *et al.*, 2009). Salinity

causes loss of stand, reduces plant growth and crop yields. It limits water uptake by plants by reducing the osmatic potential and total soil water potentials. It causes ion toxicity related to Cl and Na and changes the nutritional balances. Additional to these, salinity reduces soil organic matter decomposition, mineralisation of C, N, S, P and activity of soil microorganisms (Corwin & Lesch, 2003; Rietz & Haynes, 2003). Salinity has compromised approximately 1 billion hectares, which is 7% of the earth's land, 20% of the world's irrigated lands and around 77 million hectares have been salinized due to human activities (Abdelfattah *et al.*, 2009). Each crop tolerates different levels soil salinity; for instance corn can tolerate soils EC up to 17 dS/m, while peanut only tolerates soil EC up to about 3.2 dS/m (Sparks, 1995).

Regarding EC values of biochar and the effect of biochar addition to soils, literature is limited. As it is shown in Table 2.10, EC values of biochars used for soil amendment are between 0.4 to 3.2 dS/m. Comparison to other amendments, EC of biochars are lower than poultry manure and coffee husk, suggesting that salt concentrations of these materials are higher than charred biomasses. Wood biochar has the lowest EC value with lowest pH among biochars. The high EC value of greenwaste biochar could be due to its high K content.

Table 2.10: EC and pH values of different soil amendments

Soil amendments	EC (dS/m)	pH	Reference
Greenwaste biochar	3.2	9.4[a]	Chan *et al.,* 2007
Biochar from *Eucalyptus grandis*	0.4	7.64	Dias *et al.,* 2010
Wastewater sludge biochar	1.9	8.2[a]	Hossain *et al.,* 2010
Poultry manure	5.02	9.64	Dias *et al.,* 2010
Coffee husk	5.99	4.81	Dias *et al.,* 2010
Sawdust	0.43	3.48	Dias *et al.,* 2010

[a] pH measured in $CaCl_2$, the rest is in water

Hossain *et al.* (2010) compared EC values of soil after addition of biochar from wastewater sludge, fertiliser and a combination of biochar and fertiliser. Biochar and fertiliser increased the soil EC approximately 0.24 and 0.28 units, respectively. The biochar with fertiliser application gave the highest increase of 0.48 units. Fertiliser resulted in higher EC increase in soil, but it should not be forgotten that in high rainfall regions, chemical fertilisers could easily be washed away.

2.3.3.6 BET and porosity

The BET surface area of char is very important because, like other physico-chemical characteristics, it may strongly affect the reactivity and combustion behaviour of the char (Ioannidou & Zabaniotou 2007). One of the important reasons for recent attention on activated carbons as double-layer capacitors is their high surface area properties (Seredych *et al.*, 2008).

Lua *et al.* (2004) studied the temperature effect on the BET surface area of pistachio nut shells. Increasing temperature from 250°C to 500°C improved the surface area due to the enhanced evolution of volatiles, which resulted in enhanced pore development in biochars. But it is widely known that very high temperatures, high pressure, high heating rate, high ash content and long residence times lead to loss of surface area due to plastic deformation, melting, fusion or sintering (Brown *et al.*, 2006). Similarly, Petrov *et al.* (2008) studied the temperature effect on surface areas of activated carbons and showed that surface areas increase with temperature, but it starts to decrease above 950°C. They compared the surface areas of carbons produced from oil-palm shells at atmospheric pressure and under vacuum. The results are 278 m^2/g and 368 m^2/g respectively. Other research by Jia & Lua (2008) showed that the BET surface area of steam activated carbons pyrolysed under vacuum were higher than the ones produced in nitrogen (Figure 2.20).

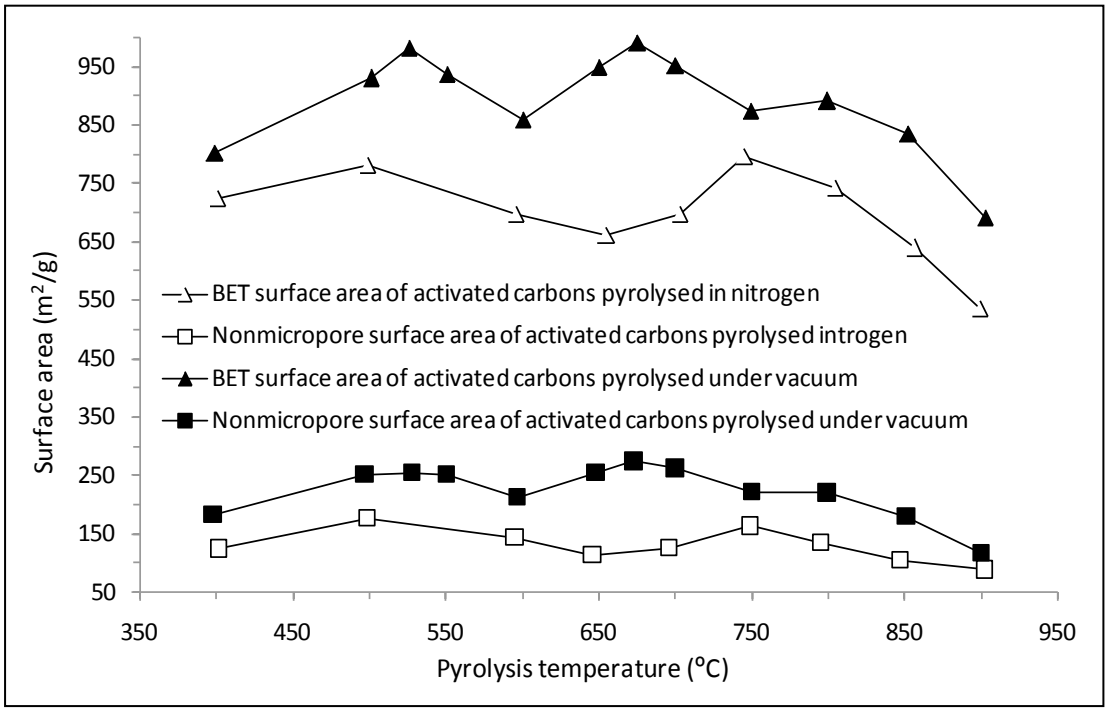

Figure 2.20: Effect of temperature on surface area (Redrawn from Jia & Lua, 2008)

For the nitrogen atmosphere, there was an increase in BET and non-micropore surface areas when temperature rose from 400°C to 500°C. From 500°C to 650°C, both surface areas decreased with an increase from 650°C to 750°C. Above 750°C, surface areas started to decrease with temperature. This change in surface areas with temperature supported the previous studies (Lua *et al.*, 2004; Guo & Lua, 2001). They also studied the effect of hold time (30-180 min) on surface area, a 120 min hold time yielded higher surface areas. The optimum conditions for vacuum pyrolysis of oil-palm shells were found as 675°C and 120 min hold time, resulting in a BET of 988 m^2/g.

Another important feature of adsorbents is the size and distribution of micropores, mesopores and macropores; these determine the adsorptive properties of adsorbents. For instance, small pores will not trap large adsorbate molecules and large pores will not be able to retain small adsorbates, whether they are charged or uncharged molecules, polar or non-polar compounds such as gases (Ioannidou & Zabaniotou, 2007; Suzuki, 1990). Mesopores have high adsorptive capacities in liquid-solid adsorption processes where macropores are important for aeration, hydrology of the soil, movement of roots through soil and being habitats for soil microbes (Lehmann & Joseph, 2009). Table 2.11 displays the pore sizes in typical activated carbons.

Table 2.11: Pore sizes in typical activated carbons (Particle density 0.6-0.9 g/cm^3; porosity 0.4-0.6)

	Micropore	**Mesopores or Transitional pores**	**Macropores**
Diameter (nm)	<2	2-50	>50
Pore volume (cm^3/g)	0.15-0.5	0.02-0.1	0.2-2
Surface area (m^2/g)	100-1000	10-100	0.5-2

*Reproduced from Ruthven (1994)

Materials with greater content of lignin e.g. grape seeds (49% lignin) and cherry stones (40% lignin) develop ACs with macroporous structure (Shopova *et al.*, 1997), whereas materials with greater content of cellulose e.g. apricot stones (39.75% cellulose, 25.75% lignin) (Mohamed *et al.*, 2010) almond shells (37.4% cellulose, 27.5% lignin) (González *et al.*, 2005), develop more microporous structure (Ioannidou & Zabaniotou 2007).

Lua *et al.* (2004) reported that pore size distribution to the micropore range make the biggest contribution to total surface area. Another study done by Li *et al.* (2008) investigated the effect of temperature on surface area and microporosity of coconut shell biochars via slow pyrolysis (Figure 2.21). Increased temperature resulted in increased surface area and microporosity. Zhang *et al.* (2004) mentioned that high temperature application destroys the walls between adjacent pores, which result in enlargement of micropores to macropores.

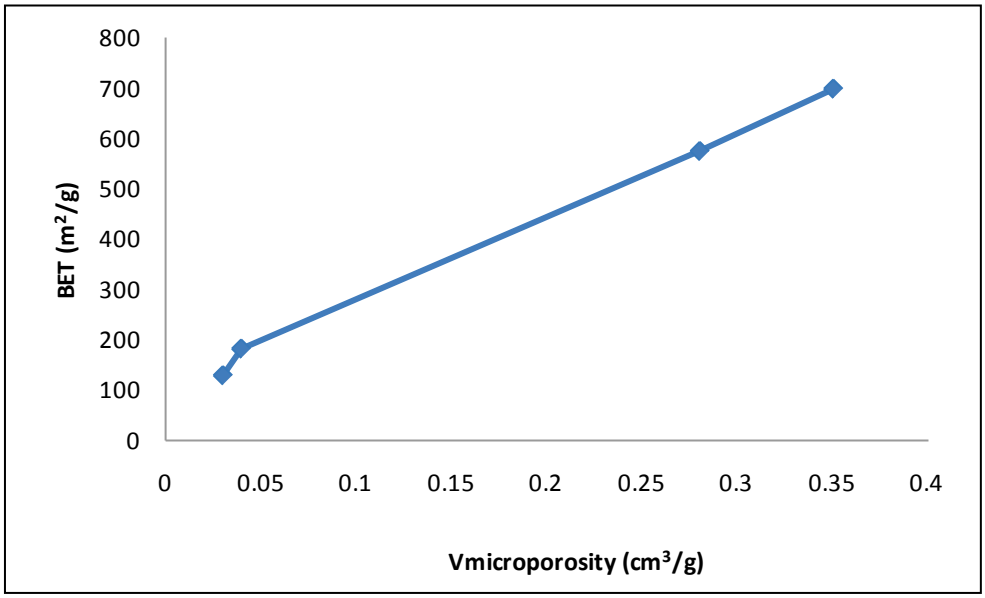

Figure 2.21: Relation between surface area and microporosity (Redrawn from Li *et al.*, 2008)

2.3.3.7. Conclusion

The physico-chemical properties of biochar are very important due to its interactions with soil and plant once it is added to soil. With these interactions, biochar can change the properties of soil by means of enhancing the soil fertility and CO_2 sequestration. Rather than enhancing soil structure, nutrient mobility and water retention, biochar provides accommodation for micro-organisms due its porosity. These physico-chemical properties are influenced by pyrolysis temperature as shown in Table 2.12.

The acidic functional groups of the biochar surface are very sensitive to heat treatment. With an increased temperature, the pH of biochar from sewage sludge decreased. However, an opposite trend was observed with poultry litter. The pH of biochar is highly related to the feedstock used. Above 400°C, CEC decreased but that is an expected result due to the decrease in acid functional groups. EC would be affected due to the change in chemistry and ash content. In Section 2.2.2.6 it was concluded that ash content increases with temperature. Higher ash content would give a higher EC value due to electrical current carried by a biochar solution.

Regarding surface area, high temperatures result in a decrease in BET surface area. Longer hold times could result in a decrease in surface acidity due to the removal of more volatiles from the

biochar surface. Low temperatures and low hold times result in biochar with a more acidic nature. Depending on the temperature used, hold time would affect the surface area of the biochar. At lower temperatures, longer hold times give higher surface areas. But a combination of high temperature and long hold time would cause a blockage of the pores, resulting in a decreasing surface area of the biochar. Activation hold time also has an effect on the surface oxides of the biochar. Increased activation hold time increases the acidic functional groups on the char surface and the pH values. The increase in pH is due to basic functionalities which are stronger than acidic functionalities on the surface.

Table 2.12: Effects of temperature (T) on surface acidity (SA), surface basicity (SB), pH, CEC, EC and BET surface area

	SA	SB	pH	CEC	EC	BET
T (+)	(-)	(+)	(-)/(+)	(-) above 400°C	(+)	(-) Above 750°C

2.3.4 Biochar as pollutant adsorbent

In this section, the adsorption term, adsorption isotherm and kinetic models will be given. Methylene blue adsorption and the effect of contact time and initial solution concentration on adsorption capacity will be discussed.

2.3.4.1 Adsorption

Atoms, ions and molecules present in a gasses or a liquid bulk adhere on the surface of a solid and this process is called adsorption. The term adsorption was introduced by Kayser in 1881 to describe the condensation of gases on free surfaces (Gregg & Sing, 1982). The solid used is called an adsorbent. The material in the adsorbed state is called adsorbate. The substance to be adsorbed (before it is on the surface) is called the adsorpt or adsorptive (Butt *et al.*, 2003).

There are two kinds of adsorption, namely physical adsorption and chemical adsorption. Physical adsorption (physisorption) is caused by van der Waals forces and electrostatic forces between adsorbate molecules and the atoms that compose the adsorbent surface. Chemical adsorption (chemisorption), on the other hand, involves formation of a chemical bond between sorbate molecules and the surface of the adsorbent (Table 2.13).

Table 2.13: Comparison of physical and chemical adsorption (Ruthven, 1994)

Physisorption	Chemisorption
Low heat of adsorption	High heat of adsorption
Non specific	Highly specific
Monolayer or multilayer	Monolayer only
No dissociation of adsorbed species	May involve dissociation
Reversible	Irreversible
Rapid, non-activated	Activated, may be slow
No electron transfer although polarisation of sorbate may occur.	Electron transfer leading to bond formation between sorbate and surface.

Van der Waals forces can be classified into three groups:

- Dipole-dipole forces,
- Dipole-induced dipole forces: In this case one molecule having a permanent dipole will induce a dipole in a non-polar atom, such as neon, and
- Dispersion forces.

2.3.4.2 Liquid adsorption isotherms

When an adsorbent is in contact with the surrounding fluid of a certain concentration, adsorption occurs and after a while the adsorbent and fluid reach equilibrium. The relation between amount adsorbed (mostly in micropores), q and concentration in the fluid phase, C and temperature T is called the adsorption isotherm. Adsorption isotherms are described in many mathematical forms. Well-known isotherms are Freundlich, Langmuir and BET (Branuer-Emmett-Teller) adsorption isotherms (Suzuki, 1990). Even though these isotherms were established long time ago, they are still the most used adsorption isotherm equations due to simplicity to use and ability to fit a wide range of experimental data. These isotherms can be used in linear and non-linear forms in order to find adsorption parameters (e.g. adsorption rate) (Kinniburgh, 1986).

Freundlich adsorption isotherm

The isotherm was named after Freundlich in 1932. The equation takes the following form:

$$q = KC^{1/n} \qquad (2.1)$$

q: The amount adsorbed per unit mass adsorbent (mg/g)

K: Equilibrium constant (function of temperature) ($mg^{1-1/n}L^{1/n}g^{-1}$)

n: Constant (function of temperature)

C: Concentration of the adsorbate in the liquid solution (mg/L)

n is usually greater than unity. The larger the value, the more non-linear the adsorption isotherm becomes as its behaviour deviates further away from the linear isotherm;

$$q = KC \tag{2.2}$$

The Freundlich equation is very commonly used for adsorption of organics from aqueous streams onto activated carbon. It is also applicable to gas phase systems onto heterogeneous surfaces in a narrow range of the adsorption data (Do, 1998; Kavitha & Namasivayam, 2007). Parameters of the Freundlich equation can be found by plotting $\log_{10}$ (q) versus $\log_{10}$ (C)

$$\log_{10}(q) = \log_{10}(K) + 1/n \log_{10}(C) \tag{2.3}$$

Langmuir adsorption isotherm

The Langmuir adsorption isotherm theory was introduced by Irving Langmuir in 1918 based on the theory of the adsorption of gases on plane surfaces such as glass. The assumptions of the Langmuir model are (Ruthven, 1994):

- Surface is homogeneous; that is adsorption energy is constant over all sites and there is no interaction between molecules adsorbed on neighbouring sites.
- Adsorption on the surface is localised, that is adsorbed atoms or molecules are adsorbed at definite, localised sites.
- Each site can accommodate only one adsorbate molecule or atom. Therefore, maximum adsorption corresponds to monolayer coverage.

This view is generally accepted for chemisorption and for physisorption at low pressures and moderately high temperatures (Shaw, 1970). However, liquid-phase adsorption is a more complex phenomenon than gas-phase adsorption. The reason is that the adsorbed molecules are not necessarily tightly packed with identical orientation in liquid phase adsorption. Furthermore, there can be other complications due to molecules of the solvent used and the formation of micelles from adsorbed molecules (Tien, 1994). The Langmuir isotherm is expressed as;

$$\frac{q}{q_m} = \frac{bC}{1+bC} \quad (2.4)$$

q_m: the maximum amount of adsorbate on the adsorbent (mg/g)

b: Langmuir constant (L/mg)

The larger the Langmuir constant is, the more adsorbate molecules cover the surface due to the stronger affinity of adsorbate molecules towards the surface (Do, 1998).

The Langmuir equation is widely used to estimate maximum adsorption capacity on the adsorbent surface (El-Halwany, 2010). In gas adsorption, at intermediate pressures, and low temperatures multilayers start to form. For that case, BET isotherms are applicable.

Brunauer-Emmett-Teller (BET) adsorption isotherms

Physical adsorption is not restricted to a monomolecular layer and it can continue to multimolecular layers due to forces acting in this process. The theory of Brunauer, Emmett and Teller is an extension of the Langmuir treatment to allow for multilayer adsorption on non-porous solid surfaces. The basic idea in the BET theory was to assume a Langmuir adsorption for each of the layers. Brunauer considered that there are five principal forms which are shown in Figure 2.22.

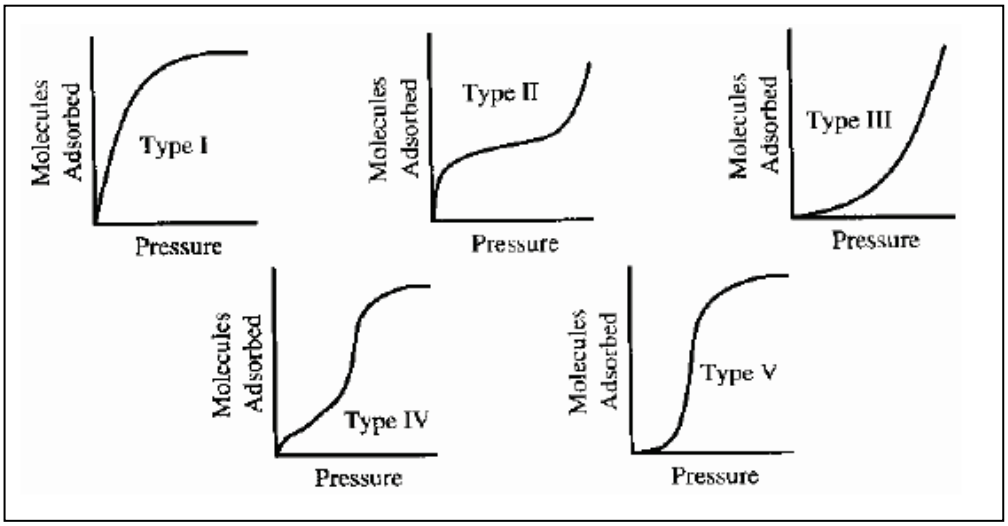

Figure 2.22: BET types (Masel, 1996) (Granted permission from John Wiley & Sons, Inc.)

Type I is the Langmuir type, roughly characterised by a monotonic approach to a limiting adsorption level that presumably corresponds to a complete monolayer. It is typical of adsorption in microporous solids, such as adsorption of oxygen on charcoal at -183°C.

Type II is very common in the case of physical adsorption and corresponds to multilayer formation. Usually the first concave part is attributed to the adsorption of a monolayer. For higher pressures more layers adsorb on top of the first one. Eventually, if the pressure reaches the saturation vapour pressure, condensation leads to macroscopically thick layers. The adsorption of nitrogen on iron catalysts at -195°C can be given as an example of this type.

Type III is the type typical of water adsorption on charcoal where the adsorption is not favourable at low pressures because of the non-polar nature of the charcoal surface. This type is expected if the binding of the first monolayer to an adsorbent is weaker than the binding of the molecules to already adsorbed molecules. This is the case if heat of adsorption is lower than the heat of condensation. Adsorption of bromine on silica gel at 79°C can be given as an example of this type.

Type IV and type V are the same as types II and III with the exception that they have a finite limit as the pressure tends to approach saturation vapour pressure due to the finite pore volume of porous solids. These types are considered to reflect capillary condensation phenomena in that they level off before the saturation pressure is reached and may show hysteresis effects. While adsorption of benzene on ferric oxide at 50°C is an example of type IV, adsorption of water on charcoal at 100°C can be given as an example of type V.

The BET equation was originally developed by Brunauer, Emmett and Teller in 1938 and is able to describe type I to type III. The type III isotherm can be produced from the BET equation when forces between adsorbate and adsorbent are smaller than that between adsorbate molecules in the liquid state. The BET equation does not cover type IV and type V because one of the assumptions of the BET theory is the allowance for infinite layers of molecules to build up on top of the surface. The BET equation for liquid adsorption can be written as;

$$\frac{q}{q_m} = \frac{C/C_s}{(1-C/C_s)[1+(\alpha-1)(C/C_s)]} \qquad (2.5)$$

q_m: the amount of adsorption corresponding to a complete monolayer coverage (mg/g)
C_s: saturated adsorbate concentration (mg/L).
α: BET equation constant which is related to the difference in the heat of adsorption of the first layer adsorbate and that of the other layers.

Wastewater treatment by adsorption is a preferred technique due to its cost, simplicity of design, ease of operation and insensitivity to toxic substances (Ugurlu *et al.*, 2007). It is important to emphasise that adsorption capacity is highly affected by physical nature of adsorbent pore, structure, ash content, functional groups, nature of adsorbate, its functional groups, polarity, molecular weight, size and solution conditions such as pH, ionic strength and adsorbate concentration (Wang & Zhu, 2007).

2.3.4.3 Adsorption kinetics

The kinetics of an adsorption system provides information on solute uptake rate which is necessary for the design and evaluation of an adsorption system. It also deals with the chemical changes on the adsorbent surface in time. Various adsorption kinetic models have been suggested to explain adsorption data. The kinetic models which describe the whole adsorption process are based on the overall adsorption process, whereas adsorption models focus on specific adsorption diffusions, namely; external (film) diffusion, intraparticle (internal) diffusion and the adsorption between the adsorbate and the active sites of adsorbent (Qui *et al.*, 2009). The latter is a rapid process, therefore the attention is drawn to film diffusion and intraparticle diffusion in order to estimate the rate limiting step of an adsorption process. The external diffusion determines the initial solute uptake rate and influenced by adsorption conditions such as agitation, initial solution concentration, and mass of the adsorbent, etc. (McKay *et al.*, 1988). The internal diffusion of solute is governed by pore diffusion where the adsorbate diffuses through the fluid-filled pores or solid phase diffusion where adsorbate is transferred in its adsorbed form along the pore walls (McKay *et al.*, 1988). Basically, it deals with the transport of molecules from the bulk of the solution to the solid phase. The intraparticle diffusion model was proposed by Weber & Morris in 1963 due to their studies suggesting solute uptake varies proportionally with $t^{1/2}$ rather than contact time t (Mahmoodi *et al.*, 2011).

$$q_t = k_p\, t^{1/2} + C \qquad (2.6)$$

where k_p is intraparticle rate constant (g/mg $min^{1/2}$) and C is a constant (mg/g) which is proportional to boundary thickness.

The pseudo-first-order adsorption kinetic model was introduced by Lagegren to describe the kinetics of oxalic acid and malonic acid adsorption onto charcoal in 1898. This model is based on the adsorption capacity. It is presented as follows:

$$\frac{dq_t}{dt} = k_1(q_e - q_t) \tag{2.7}$$

where k_1 is the rate constant of first order sorption (1/min), q_e is the amount of solute adsorbed at equilibrium (mg/g) and q_t is the amount of solute adsorbed on the surface of the adsorbent at any time *t* (mg/g).

Integrating Equation 2.7 with the boundary conditions of t=0 to t=t and q_t=0 to q_t=q_t and rearranging for linearized data plotting, the following is obtained (Ho & McKay, 1999);

$$\log(q_e - q_t) = \log(q_e) - \frac{k_1}{2.303}t \tag{2.8}$$

The adsorption kinetic rate law for a pseudo-second-order reaction model was proposed by Ho for adsorption of divalent metal ions onto peat in 1995 considering the cation exchange capacity of the peat between the functional groups on peat surface and divalent metal ions. Therefore, the assumption was that the adsorption may be second-order. The assumption was based on the fact that the rate limiting step of the adsorption process can be chemisorptions due to exchange of electrons between surface and cation. The rate equation can be written as follows (Ho & McKay, 1999):

$$\frac{dq_t}{dt} = k_2(q_e - q_t)^2 \tag{2.9}$$

where k_2 is the rate constant of adsorption (g/mg min), under the assumption that adsorption capacity is proportional to the number of active sites occupied on the adsorbent (Ho & McKay, 1999). Integrating the above equation and applying boundary conditions gives;

$$\frac{t}{q_t} = \frac{1}{h} + \frac{1}{q_e}t \tag{2.10}$$

Where h is the initial adsorption rate (mg/g min). Both of the kinetic models have been widely used to describe the adsorption of methylene blue from aqueous solution by activated carbons (Tan *et al.*,

2008; Gerçel *et al.*, 2007; Hameed *et al.*, 2007). However, Azizian *et al.* (2004) pointed out that the pseudo-second-order model is more suitable for analysis with low initial concentrations of solute, while the pseudo-first-order model shows a better fit for the adsorptions of solutions with high solute concentrations.

2.3.4.4 Adsorption of methylene blue (MB)

Dyes are aromatic organic compounds, including aryl rings which have delocalised electron systems. Dyes take their colours from the chromophore groups. Other existing structures are chromogens (aromatic structures) and auxochromes (ionising groups). Existence of auxochromes provides a bonding affinity that affects the adsorption capacity. It is estimated that over 7×10^5 tonnes of dyestuff is produced annually (Allen & Koumanova, 2005). Industries such as textile, leather, paper, plastics use dyes to colour their products and released wastewaters cause serious environmental problems (Rafatullah *et al.*, 2010; Wang & Zhu, 2007). The coloured wastewater reduces light penetration (Ugurlu *et al.*, 2007); is toxic to aquatic life, cancerogenic (Gercel *et al.*, 2007) and damages the aesthetic nature of the water.

MB has been studied by many researchers due to its toxicity and very high tinctorial value (less than 1 ppm of dye is visible in solution). When it is ionised in solution it forms cations, which have a high affinity for negatively charged adsorbent surfaces and facilitate adsorption process (El Qada *et al.*, 2008). The chemical formula of MB is $C_{16}H_{18}ClS.xH_2O$ (Figure 2.23). The minimum pore diameter of an adsorbent that MB molecules can enter is 1.3 nm (Gaspard *et al.*, 2007).

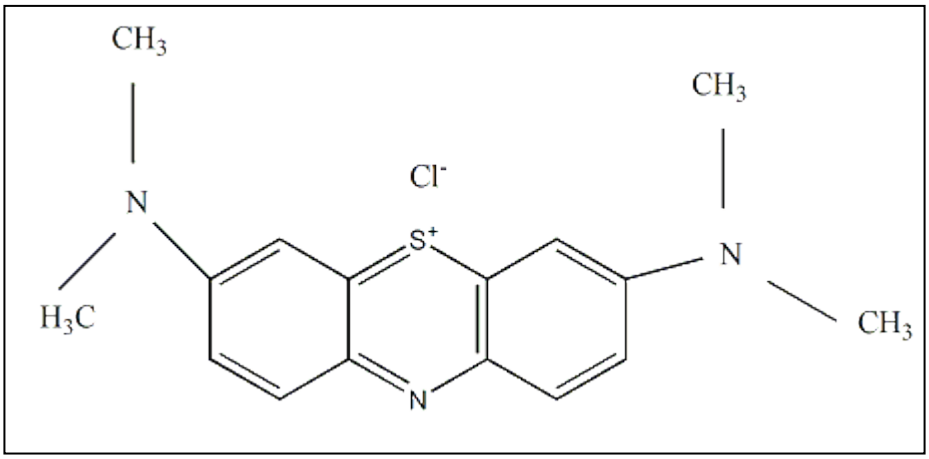

Figure 2.23: Chemical structure of methylene blue

Adsorption of MB has been studied on carbons from various biomasses such as bamboo, straw, coconut husk, corn cob, etc. (Rafatullah *et al.*, 2010). Table 2.14 shows the adsorption capacity and BET areas of various adsorbents.

Table 2.14: MB adsorption capacities and surface areas of biochars and activated carbons (AA: Activating Agent, T: Temperature, HT: Activation hold time)

Adsorbent	**Activation Process**	**BET surface area (m^2/g)**	**Adsorption capacity (mg MB/g)**	**Reference**
Bamboo	-	327	319	Mui *et al.* 2010
Rice husk	AA = $ZnCl_2$, T = 650°C, HT = 2h	181	10	Sharma & Uma, 2010
Rejected tea	-	4.2	147	Nasuha *et al.*, 2010
Rice hull	AA = H_2SO_4	n/d	60	El-Halwany, 2010
Pine cone	AA = H_3PO_4, T= 500°C, HT=1h	1402	≈350	Duman *et al.*, 2009
Commercial activated carbon	n/a	900	160	Karaca *et al.*, 2008
Olive stones	-	368	38	Petrov *et al.*, 2008
Olive pulp	-	396	46	Petrov *et al.*, 2008
Peach stones	AA = H_3PO_4 T = 500°C, HT = 2h	1300	412	Attia *et al.*, 2008

The amount adsorbed depends on the experimental conditions such as solution temperature, solution pH, initial solution concentration and contact time, etc. For instance, the adsorption capacity was (147 mg MB/g) with an initial solution concentration of 500 mg MB/L in the study of Nasuha et al. (2010), whereas Duman et al. (2009) reached an adsorption capacity of 350 mg MB/g for 350 mg MB/L initial solution concentration. In this project, the focus is on the effect of initial solution concentration and the contact time.

Effect of initial concentration and contact time

The adsorption capacity increases with an increase in the initial dye concentration. Authors attribute this to the increase in the mass transfer driving force of the concentration gradient to overcome all mass transfer resistances between the aqueous and solid phases. Tan *et al*., 2008 observed a slight decrease when the initial concentration was increased further. With increased contact time the amount of MB adsorbed onto carbon increases but at some point in time, it reaches a constant value where no more adsorption occurs. At this point, there is equilibrium between the amount of dye adsorbed from the solution and the amount of the dye desorbed from the carbon. The rate of adsorption decreases with time due to the gradual decrease in the driving force with time. Karaca *et al.* (2008) attributed the need of longer times to reach equilibrium for high initial concentrations to the lower intraparticle diffusion rate of dimeric forms and dimer de-aggregation. Table 2.15 represents some of the studies done on the effect of initial concentration and contact time on adsorption capacity.

Table 2.15: Effect of initial concentration and contact time on adsorption capacity

Adsorbent	Initial Concentration Range (mg/L)	Contact time (min)	Amount adsorbed (mg/g)	Reference
Coir pith carbon	10-40	40-120	1.6-5.4	Kavitha & Namasiyavam, 2007
Bamboo based activated carbon	100-500	360-1440	100-420	Hameed *et al.*, 2007
Oil palm fibre activated carbon	50-500	60-250	49-276	Tan *et al.,* 2007

2.4. General conclusion

The advantages of converting unused agricultural residues into solid, liquid and gaseous products via pyrolysis in terms of energy source have already been recognised worldwide. The solid product has mostly been used for its energy or production of activated carbon. However, the area of biochar application is not limited to energy production. From an environmental point of view, biochar is a

potential product that could help to overcome the issues such as pollution, land degradation and unproductive harvest due to its significant physico-chemical properties.

Biochar characteristics (e.g. surface area, porosity, cation exchange capacity, surface chemistry, and nutrients) determine the effects of biochar on soils. Recent studies have shown that biochar improves soil quality, structure and many other soil characteristics. On the other hand, negative effects are found to be avoidable with right planning and management. The physical and chemical characterisations of biochars have been focused on biochars from slow and fast pyrolysis. Therefore, there is a gap in literature regarding physico-chemical properties of biochars from vacuum pyrolysis for soil amendment purposes.

There are a few studies which focus on biochar as soil amendment and adsorbent. Therefore, the adsorption abilities of biochars will be tested by methylene blue adsorption. Considering methylene blue adsorption (wastewater treatment), activated carbons are mostly used but if biochars from vacuum pyrolysis are also efficient as adsorbents, it would reduce the cost by eliminating the activation step. In order to investigate the efficiency of biochars as adsorbents, Langmuir and Freundlich isotherms will be preferred by controlling the parameters such as initial concentration and contact time. For kinetic studies pseudo-first-order, pseudo-second-order and intraparticle diffusion kinetic models will be used. The best known and recently established analytical methods in soil science community will be used for the characterisation of biochars as soil amendment. These methods include pH, EC, surface acidity/basicity, CEC and plant available nutrients determinations.

CHAPTER 3: MATERIALS AND METHODS

3.1 Materials

The sugar cane bagasse was supplied by the Sugar Milling Research Institute in Durban, while the black wattle and vineyard prunings were provided by the Department of Soil Science, Stellenbosch University. The black wattle prunings were obtained from a 20 year old tree in the Pappagaaiberg public park, Stellenbosch. The tree itself was not fertilised and the woody parts were around 5 years old. The vineyard prunings were supplied from Nietvoorbij, Institute for Viticulture and Oenology Research, Stellenbosch from their Merlot cultivar. The vines were fertilised but not sprayed with pesticide for at least 6 months before pruning, which indicates that the pesticides should be gone due to the rainy season. The age of the prunings was around one year.

3.2 Preparation of materials

All the materials were air dried at ambient atmosphere and stored indoors. Before vacuum pyrolysis, sugar cane bagasse and vineyard prunings were milled in a Retsch ZM200 mill and sieved through a JEL (J. Engelsmann) sieve machine for 10 minutes. The black wattle was milled with a Retsch SM100 and put through a 10 mm sieve. The particle sizes used are shown in Table 3.1. For lignocellulosic composition determinations, +250 to -425 µm particle sizes according to British Standards DD CEN/TS-14780 were used.

The biochar samples were ball-milled to a particle size diameter of less than 1 mm with a Swissmade A10 Analysmühle Kinematica before their physical and chemical characterisation.

The size distribution of black wattle prunings is shown in Figure 3.1 due to its different particle size to sugar cane bagasse and vineyard prunings. For size distribution, the coning-and-quartering method was used to get a truly representative sample. The sample was shaked in a Retch AS200 shaker for 30 minutes.

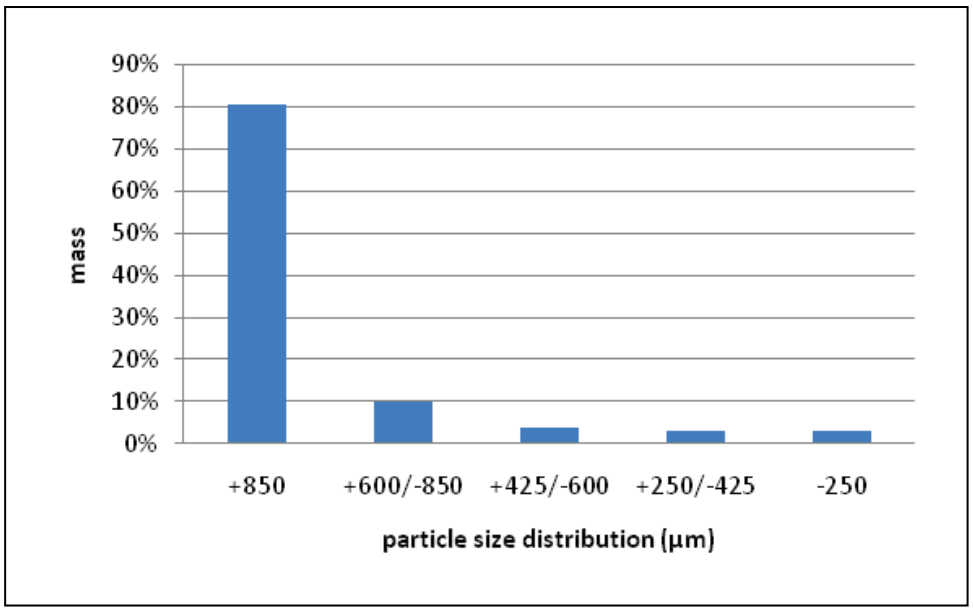

Figure 3.1: Size distribution of black wattle prunings

3.3 Vacuum pyrolysis procedure

The reactor consisted of a quartz tube and six, insulated and computer controlled, heating elements. The length of quartz tube was 1 m with diameter of 60 mm and the raw biomass was placed in the middle of the quartz tube. The reactor was connected to five condensation traps and a vacuum pump. The exit pipe from the reactor was maintained at 100-120°C to limit condensation before the first condenser. The vacuum pump removed the vapours and gas products from the reactor through the traps (condensers) and the condensable gases were condensed in the traps and recovered as liquid. The first condenser was kept at room temperature, the second and third at -10°C and the last two at dry ice temperature, -78°C as shown in Figure 3.2. The final pyrolysis temperature, heating rate and pyrolysis duration were controlled by a control system. Pressure was checked during the experiments and kept below 10 kPa_{abs}. The set-up was cooled down for 2h under vacuum after a 1 hour pyrolysis run, until the set-up was cold enough to disassemble. The set up was disassembled and condensers and solid residue were weighed. The solid residue (biochar) was stored in hermetically sealed containers to prevent moisture entering. The pyrolysis experimental conditions, particle size and mass of the biomasses used are shown in Table 3.1.

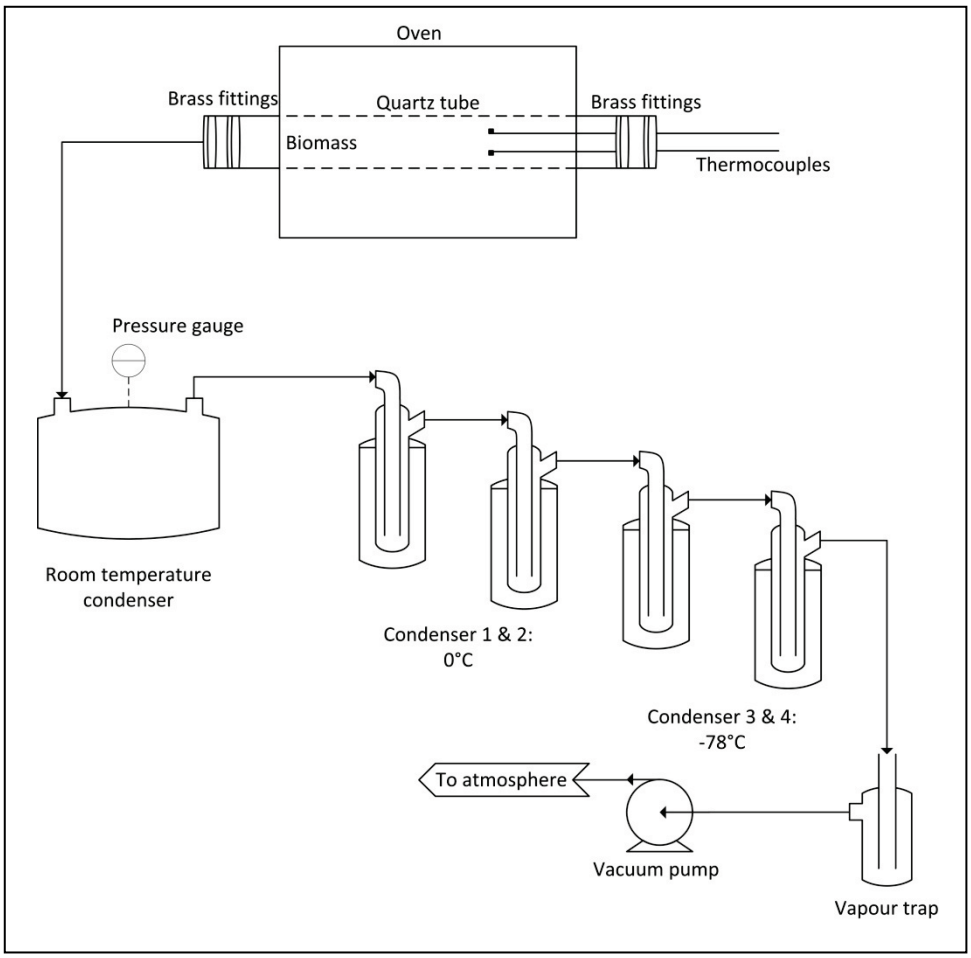

Figure 3.2: Vacuum pyrolysis experimental set-up

Table 3.1: Pyrolysis experimental conditions (T_f: Final temperature, HR: Heating rate, P: Pressure)

Biomass	Size (µm)	Mass (g)	T_f(°C)	HR (°C/min)	P $(kPa)_{abs}$
Vineyard	425-850	40	460	17	8
Sugar cane bagasse	425-850	40	460	17	8
Black wattle	+850	40	475	15-13	8.5

The experimental conditions were chosen with the help of previous results on the pyrolysis of sugar cane bagasse (Carrier *et al.*, 2011). Particle diameters between 425-850 µm were used. Nevertheless, it has been shown that a particle size of < 500 µm do not exert any influence on the rate of the process (Demirbaş, 2007). Larger particle sizes were used for black wattle in order to observe the effect of particle size on product yields. The temperature between 460 and 500 °C was the optimal temperature for production of biochars with high BET surface areas for a heating range of 8 - 24 °C/min. During experiments, the heating rate in the pyrolysis of black wattle could not be

controlled accurately due to problems with the control unit. However, it was decided to analyse biochar from pyrolysis of black wattle. The pyrolysis product yields (Y) were calculated on mass, dry and dry-ash free basis, using the following equations:

On a weight basis,

$$Y_{biochar} = \frac{m_f}{m_0} \times 100 \quad (3.1)$$

$$Y_{liquid} = \frac{m_{RTC} + m_{condensers} + m_{pipes}}{m_0} \quad (3.2)$$

$$Y_{gas+loss} = 100 - Y_{char} - Y_{liquid} \quad (3.3)$$

$$Y_{total\ water} = \frac{m_{RTC} \times \frac{WC_2}{100} + (m_{condensers} + m_{pipes}) \times \frac{WC_1}{100}}{m_0} \times 100 \quad (3.4)$$

$$Y_{bio-oil} = \frac{m_{RTC} + m_{condensers} + m_{pipes} - m_{total\ water}}{m_0} \quad (3.5)$$

$$Y_{pyrolytic\ water} = \frac{m_{total\ water} - m_0 \times \frac{WC_o}{100}}{m_0} \times 100 \quad (3.6)$$

where m_f (g) is the mass of the biochar, m_0 is the initial biomass mass, AC_0 is the ash content of initial material (% wt.), WC_0(% wt.) is the water content of initial material. WC_1 and WC_2 are the water contents of water phase and tarry phase, respectively.

The liquid is considered as a mixture of water and tarry phases. The water phase is made up by the initial water present in the raw materials and the water produced during pyrolysis. The tarry phase is collected from the first condenser at room temperature. The losses are the ones that cannot be recovered from the pyrolytic run. The standard deviations of experiments were calculated with the formula which was presented by Hugo (2010). The standard deviation calculations were based on measurement errors (Appendix A).

On a dry and ash-free basis,

$$Y_{biochar} = \frac{mf}{m_0 - m_0 \times AC_0/100 - m_0 \times WC_0/100} \times 100 \quad (3.7)$$

$$Y_{bio-oil} = \frac{m_{liquid} - m_{total,water}}{m_0 - m_0 \times \frac{AC_0}{100} - m_0 \times WC_0/100} \times 100 \quad (3.8)$$

$$Y_{pyrolytic\ \ water} = \frac{m_{total,water} - m_0 \times WC_0/100}{m_0 - m_0 \times \frac{AC_0}{100} - m_0 \times WC_0/100} \times 100 \quad (3.9)$$

$$Y_{liquid\ \ produced} = Y_{bio-oil} + Y_{pyrolytic\ \ water} \quad (3.10)$$

The ash devolatilisation percentages were calculated with the following equation:

$$Y_{ash\ devolatilisation} = \frac{m_0 \times \frac{AC_0}{100} - m_f \times \frac{AC_f}{100}}{m_0 \times \frac{AC_0}{100}} \quad (3.11)$$

where AC_f is the ash content of the biochar.

The same equations were used for yields on a dry basis, only excluding the moisture contents.

3.4 Analytical methods for chemical and physical characterisation of biochar

3.4.1 Moisture and ash content

The moisture content was determined according to the standard method of NREL/TP-510-42621. The ash content was determined according to the standard method of NREL/TP-510-42622. The biomass and biochar samples were scaled between 0.5-2.0 g for both analyses. The samples were heated in air to 105°C for 24 hours to dry. This temperature is high enough to eliminate free forms of water, with no loss of organic matter or salts. For the determination of ash content samples were heated to 575 ± 25 °C for 4 hours. The residues were weighed after they reached a constant weight. The ash and moisture content determinations were all done in triplicate. The following equations were used:

$$Moisture\ content(\%) = \left(m_{wet} - m_{dry}\right) \Big/ m_{dry} \times 100 \quad (3.12)$$

$$Ash(\%) = {}^{m_{ash}}/_{m_{original\ \ sample}} \times 100 \quad (3.13)$$

where m_{wet} is the weight of the sample before it was placed in the oven and m_{dry} is the weight after it was taken out of the oven. In Equation 3.13, m_{ash} is the weight of the ash and $m_{original\ sample}$ is the weight of the original sample which was put in the crucible.

The water contents of the tarry and pyrolytic water phases were determined by using a Metrohm Karl-Fisher Titrino, according to the standard method ASTM D1744. Between 0.02 to 0.2 g of sample was analyzed for water content by using Hydranal composite 5.

3.4.2 Total, major and trace elemental analyses

Major (Na_2O, MgO, SiO_2, K_2O, CaO, TiO_2, MnO, P_2O_5, Al_2O_3, Cr_2O_3 and Fe_2O_3) and trace elements (Cr, Ni, Zn, As, Ga, Co, V, Rb, Sr, Y, Zr, Nb, Ce, Nd, La, Th, U, Ba, S and Cl) of the raw materials were determined by X-ray fluorescence (XRF, PANalyticalAxios). The total contents of C, N and H were determined by Eurovector Elemental Analyser. The O content was determined by subtracting the ash and C, N, H and S contents from the total mass of the sample. Elemental analyses were done for both raw biomasses and the biochars.

3.4.3 Proximate analyses

The proximate analyses of the biomasses were done using a thermogravimetric method to determine water, volatile matter, fixed carbon and ash contents. TGA analyses were performed with a Perkin Elmer Pyris TGA 7. The sample was heated from 25°C to 600°C at 10°C/min and then from 600°C to 900°C at 20°C/min under nitrogen. After 7 minutes, oxygen at a 15 mL/min flow rate was introduced for the combustion stage.

3.4.4 Ethanol and water extractives

The ethanol-cyclohexane and water extractives were determined according to TAPPI Standard T-264 om-88. Firstly, approximately 5 g of biomass sample was put in a thimble, and then placed in a soxlet apparatus. A 200 mL mixture of ethanol (CH_3CH_2OH, 99.9% purity) (United Scientific Ltd.) and cyclohexane (C_6H_{12}, 98% purity) (Merck Chemicals Ltd.) was prepared in a ratio of 1:2. The 200 mL

solvent mixture was poured into a round bottom flask and placed in an Electrothermal ME 468 heating mantel. The heating mantel were switched on and left to distil overnight. After distillation, the solvent was evaporated until the flask was dry and the flask was placed in an oven at 105°C until it was dry. Afterwards, the flask was weighed. The following equation was used to calculate ethanol-cyclohexane extractives:

$$Ethanol - cyclohexane\ extractives\ (\%) = \left(\frac{m_{extractives}}{m_{wet\ \ ample}} \times 100\right) \times MCfactor \times Ash\ correction\ factor \quad (3.14)$$

where $m_{extractives}$ is the weight of the extractives in the flask and $m_{wetsample}$ is the weight of the sample which was placed in the thimble. The MC factor is moisture content correction factor and calculated according to the following equation:

$$Moisture\ content\ correction\ factor = {}^{1}\Big/\left(\frac{m_{dry}}{m_{wet}}\right) \quad (3.15)$$

where m_{dry} and m_{wet} are the same as Equation 3.12. The ash correction factor was calculated by using Equation 3.16.

$$Ash\ correction\ factor = {}^{1}\Big/_{(1 - oven\ dry\ ash\ content\ percentage)} \quad (3.16)$$

After ethanol-cyclohexane extractives determination, the thimble was used for water extractives determination. The same procedure and equations (Equation 3.13, 3.14 and 3.15) were used as for the ethanol-cyclohexane extractives procedure but using 220 mL distilled water instead of 200 mL of the above-mentioned solvent. At the end of the procedure, the sample in the thimble was extractive free and air dried overnight in a switched-on fume cabinet for determination of lignin.

3.4.5 Klason lignin determination

The Klason lignin was determined according to the standard method of NREL/TP-510-42618. Approximately 0.3 g of dry and extractive free sample was measured and 3 mL of 72% sulphuric acid (H_2SO_4) was added while stirring. The primary hydrolysis was performed at room temperature for 2 hours with stirring every 10 minutes. Two hours later, the sample was diluted to 3% sulphuric acid by

the addition of 84 mL of distilled water. Afterwards, the sample was transferred to an autoclave flask and autoclaved in an Eastern EA-630 vertical autoclave for 1 hour at a temperature of 120°C and 0.12 MPa (secondary hydrolysis). After secondary hydrolysis, the sample was transferred through a filtering crucible with 200 mL boiling water to wash off any residual reagents and sugars. The solid residue left in the filtering crucible was placed in the oven at 105°C overnight to dry and later on it was weighed. The filtering crucible was placed in a muffle furnace for a minimum of 4 hours at 575 ± 25 °C to determine the ash content left in the lignin. The acid insoluble lignin (AIL) was calculated on a dry and ash free basis with Equation 3.17:

$$AIL\ (\%) = \left({}^{m_{AIL} - m_{ash}}/_{m_{original\ \ sample}} \times 100 \right) \times MC\ factor \qquad (3.17)$$

where m_{AIL} is the mass of the residue left in the filtering crucible and m_{ash} is the weight of the ash after the filtering crucible has been placed in the muffle furnace and the MC factor was calculated by using Equation 3.15.

3.4.6 BET specific surface area

The BET surface area is an indication of the sorption capacity of a solid. The surface areas of the biochars were determined by using multipoint Brunauer, Emmett and Teller (BET) analysis on a Micrometrics ASAP2010 (Accelerated Surface Area and Porosimetry) system. For an accurate measurement, adsorbent surfaces should be prepared. Adsorbent surfaces are covered with an adsorbed film, which should be removed before analysis. This film can be readily removed if the solid is maintained at high temperature under a vacuum due to weak Van der Waals forces between the film and the adsorbent surface (Allen, 1997). Therefore, the first step in the procedure is the degassing of the adsorbent surface. A mass of between 0.2 and 0.5 g of sample was degassed on a VacPrep 061 system firstly at 90 °C for an hour, then for a minimum of 24 hours at 250 °C under a pressure between 6.7-9.3 Pa_{abs}.

Afterwards, the sample was introduced in the gas adsorption surface area analyser to study the adsorption of nitrogen at 77 K. The equilibrium points inside the 0.00-0.22 P/P_0 range were evaluated by the BET equation in order to determine the surface area of the biochar (Brunauer *et al.*, 1938). From BET analysis, not only surface areas are determined but, one can get information on the porosity of the biochar such as pore diameter, micropore, mesopore and macropore volumes and areas, which have great importance in sorption processes. The pore volume was taken at the

P/P_0=0.982 single point. The pore size distribution was calculated by the BJH (Barret-Joyner-Halenda) method (Barrett *et al.*, 1951) using the Harkins and Jura equation for multilayer thickness (Harkins & Jura, 1944).

3.4.7 pH determination

The determination of pH indicates the active (pH in water) and reserve (pH in KCl) acidity in the biochar. pH of a biochar can have a substantial effect on soil by changing the soil pH, therefore it could be a solution for soil acidity and aluminium toxicity. Potassium chloride solution was used because KCl could release the exchangeable protons from biochar into the solution due to its ionic nature. Two grams of biochar was shaken with 40 mL distilled water or 1 M KCl (99% purity) (Merck Chemicals Ltd.) solution for 30 min on an IKA®KS 260 basic shaker. The suspension was allowed to stand for 10 min before measuring the pH with a pH electrode, 827pH Lab, Metrohm (Cheng & Lehmann, 2009). The pH values of raw materials were measured with the same procedure in a distilled water suspension.

3.4.8 Cation exchange capacity (CEC)

The determination of CEC gives an indication of the abundance of negatively charged sites on the biochar that can attract, retain and exchange cation elements. The CEC of biochars were determined according to the method of CEC determination in alkaline soils (Rhoades, 1982). Firstly, biochar was saturated with a buffered solution of 0.1 N NaCl (99.9% purity) (Hopkin and Williams Ltd.). For saturation, 1 g of biochar was shaken for an hour with 20 mL of saturating solution (0.4 N NaOAc-0.1 N NaCl, 60% ethanol solution adjusted to pH 7.0 using 3 M HCl) in a 30 mL centrifuge tube. Then the tubes were centrifuged at 12 000 rpm in an Eppendorf AG 22331 Centrifuge 5810R to separate the biochar from the liquid and the supernatant was discarded. This procedure was repeated another three times to ensure complete saturation of cation exchange sites with Na. The Na/Cl molar ratio of saturating solution was determined by AAS (Na) (Varian AA 240FS Fast Sequential Atomic Absorption Spectrometer) and ion chromatography (Cl^-) (Dionex DX-120 Ion Chromatograph). Secondly, the Na was extracted with Mg. Twenty millilitres of extraction solution [0.25 M Mg (NO_3)] was added to Na saturated biochar and shaken for an hour. The suspension was centrifuged and the supernatant decanted into a 100 mL volumetric flask. This procedure was repeated twice with fresh extracting solution to ensure that all Na was exchanged and extracted. The collected supernatants were made up to 100 mL with distilled water. The Na and Cl concentrations in the solutions were determined

using AAS and ion chromatography, respectively. The CEC ($cmol_c/kg$) was calculated by determining the total amount of exchangeable Na as follows:

$$Exchangeable\ Na = Na_t - \left[(Cl_t) - (\frac{Na}{Cl})_{saturation\ \ solution}\right] \quad (3.18)$$

$$Exchangeable\ Na\ (mmoles) = \left[Na_t\ mg/L \times \frac{0.1\ L}{23\ mg\ /mmol}\right] - \left[Cl_t\ mg/L \times \frac{0.1\ L}{35.45\ mg\ /mmol}\right]\left[\left(\frac{Na\frac{mg}{L}\times 1L}{23\ mg\ /mmol}\right) \div \left(\frac{Cl\ mg\ /L\times 1L}{35.45\ mg\ /mmol}\right)\right]_{saturation\ \ solution} \quad (3\text{-}19)$$

$$CEC\ in \frac{mmol_c}{kg\ bioc\,har} = Exchangeable\ Na\ (mmoles)/1g\ biochar \quad (3.20)$$

$$CEC\ in \frac{cmol_c}{kg\ bioc\,har} = mmol_c/kg \div 10 \quad (3.21)$$

where Na_t and Cl_t is the Na and Cl concentrations in the final solution after the extraction step. Sodium acetate and hydrous magnesium nitrate were supplied from Merck Chemicals Ltd. with a purity of 99% and 99.5%, respectively.

3.4.9 Surface acidity and alkalinity

This determination provides an indication of the total surface acidity and alkalinity of the biochar. This method is based on the Boehm Titration method, which is well-known for determination of surface oxides on carbon material surfaces (Boehm, 1994). Surface acidity was determined by shaking 0.15 g of biochar with 15 mL of 0.1 N NaOH for 30 h. The slurry was filtered through Whatman No 2 filter paper. An aliquot of 5 mL of the NaOH filtrate was transferred to a 10 mL of 0.1 N HCl solution which neutralizes the unreacted base. The solution was back-titrated with 0.1 N NaOH in the presence of a phenolphthalein (PAL Chemicals) indicator. NaOH and HCl were supplied from Merck Chemicals Ltd.

The surface basicity was determined similarly to surface acidity. 0.15 g biochar was shaken with 15 mL of a 0.1 N HCl solution for 30 h. The slurry was filtered and an aliquot of 5 mL of HCl filtrate was transferred to 10 mL of a 0.1 N NaOH solution to neutralise the unreacted acid. The solution was back-titrated with a 0.1 N HCl solution. The base or acid uptake of biochar was converted into the

content of surface acidity or basicity (mmole/g), respectively (Cheng & Lehmann, 2009). For titration of the NaOH solutions, a Tim856 Titration Manager Autotitrator was used. The potentiometric endpoints were chosen as 4 for the back-titration with 0.1 N HCl. Surface acidity titrations were performed manually.

$$Surface\ acidity = \frac{mmol\ \ NaOH\ uptake}{g\ bioc\ har} = \frac{1.5\ mmol\ \ NaOH - [(1\ mmol - x)] \times \frac{15\ mL}{5\ mL}}{0.15\ g} \quad (3.22)$$

$$Surface\ basicity = \frac{mmol\ \ HCl\ uptake}{g\ bioc\ har} = \frac{1.5\ mmol\ \ HCl - [(1\ mmol - x)] \times \frac{15\ mL}{5\ mL}}{0.15\ g} \quad (3.23)$$

where x is the volume of NaOH or HCl consumed during titration.

3.4.10 Water soluble nutrients and electrical conductivity

This determination gives an indication of the water soluble nutrients (Ca^{2+}, Mg^{2+}, Na^{2+}, K^{+}, NO_3^{-}, PO_4^{3-}, Cl^{-}, F^{-}, SO_4^{2-}) and the total salinity in the biochar, which may affect clay dispersion and plant growth. One gram of biochar was shaken with 20 mL distilled water for an hour to extract water soluble anions and cations. The suspension was filtered through Whatman No 2 filter paper. The electrical conductivity was measured (Jenway, 4510 Conductivitymeter) and the concentrations of anions and cations were determined using ion chromatography (Dionex DX-120 Ion Chromatograph).

3.4.11 Citric acid-extractable nutrients

Citric acid-extractable nutrients determination provides information on nutrients potentially available for the plants and toxins present in the biochar. This method is based on the method described in “Handbook of Standard Soil Testing Methods for Advisory Purposes” (1990). Citric acid was chosen as solution because plant roots have citric acid in their roots; therefore the roots make some of the nutrients available to the plant. A 1 wt.% citric acid solution was prepared and heated up to 80°C in a water bath. One gram of biochar was shaken with 20 mL of warm 1 wt.% citric acid solution and put in an oven at 80°C for an hour, shaking every 10 min. Afterwards, the solution was filtered through Whatman No 2 filter paper.. The extractable macro-elements concentrations in the biochar such as Ca, N, Mg, P, K, S were determined by Inductively Coupled Plasma-Mass Spectrometer (ICP-MS Agilent 7700) and microelements such as B, Cu, Fe, Mn, Mo and Zn were

determined by Varian Liberty II Radical ICP instrument. The biggest difference in these instruments is their measuring range. ICP is capable of measuring the elements down to parts per billion, whereas ICP-MS measures down to parts per million.

3.4.12 Fourier transform infrared spectroscopy (FTIR)

Functional groups on the biochar surface are an indication of the biodegradability and play an important role in sorption processes. FTIR spectroscopy was chosen for the determination of functional groups because of its efficiency in the analysis of functional groups and its low cost also makes it attractive to use. Biochar is an opaque material; therefore it was diluted with a transparent medium to get sufficient signals to obtain spectra. KBr is one of the most widely used transparent media for FTIR analysis of carbonaceous materials. Biochar samples were dried in an oven overnight. Samples were mixed with spectrograde KBr (Merck Chemicals Ltd.) at the ratio of 1:200 (wt/wt), which allows preparing pellets which are transparent enough to absorb beam light. Pellet thickness was kept constant by fixing the sample-KBr mixture weight using a hydraulic press and pelletising under the same pressures. The pellets were analysed by using Thermoelectron Nexus 6700 FTIR spectroscopy. The OMNIC® software package that was used for analysis of the FTIR detector data automatically corrects for the background material that is used as medium to measure the FTIR spectra.

3.4.13 Solid-state ^{13}C nuclear magnetic resonance (NMR)

The NMR analyses of the biochars were performed for determination of the percentages of functional groups, by means of the aromacity and acidic functional groups present on the biochar surface (Table 3.2). The solid state NMR spectra were acquired on a Varian VNMRS 500 MHz two-channel spectrometer using 4 mm zirconia rotors and a 4 mm Chemagnetics™ T3 HX MAS probe. The cross-polarisation spectrum was recorded at ambient temperature without proton decoupling using a recycle delay of 2s. The power parameters were optimised for the Hartman-Hahn match; the radio frequency fields were $\gamma_C B_{1C} = \gamma_H B_{1H} \approx 56$ kHz.

The contact time for cross-polarisation was 1.5 ms. Magic-angle-spinning (MAS) was performed at 15 kHz and Adamantane was used as an external chemical shift standard where the downfield peak was referenced to 38.3 ppm. The setting of the integral ranges and the assignment of the integrals

according to functional groups was based on the papers by Wang *et al.* (2007) and Cheng *et al.* (2010).

Table 3.2: The assignments of integrals to functional groups

Integral range	Functional group
220 to 190 ppm	Carbonyl C
190 to 163 ppm	Carboxyl C
163 to 145 ppm	Phenolic C
145 to 90 ppm	Aromatic C
90 to 50 ppm	Substituted C (including alcohol, amines, carbohydrates, ethers, methyl and acetal groups)
50 to 0 ppm	Paraffinic C

3.5 Methylene blue adsorption

The determination of adsorption efficiency of biochars was quantified by a methylene blue adsorption process to quantify the quality of the biochars as adsorbents. Concentrations of 1.0 to 20 mg/L of methylene blue (MB) (supplied from Sugar Milling Research Institute, Durban) were made up and their absorbance values were measured at 630 nm with a Cary IE Varian UV-Visible spectrophotometer. The maximum absorbance of MB was obtained at 630 nm. Firstly calibration curves of absorbance against concentration of MB were drawn. The calibration curve is an indication of the Beer-Lambert law which shows a linear relationship between the concentration of a solution and the absorbance value at a constant wavelength. Calibration curves were drawn for each newly prepared stock solution. The calibration curves are presented in Appendix C.

To determine the adsorption of MB on biochar and the effect of contact time on adsorption, around 0.27 g (Wirsam Analytical Plus microbalance) of biochar samples were added to 300 mL of 20, 15, 10 and 5 mg/L MB solutions and stirred on magnetic stirrers (Lasec MH–4 hotplate stirrer). Around 3 mL of aliquots were taken using a syringe and immediately filtered through a 0.45 µm PTFE syringe filter. The filtrate was introduced in a disposable cuvette and the absorbance was determined by using a Secomam Anthelie Light UV spectrophotometer. During experiments, temperature and pH were measured with a Cyberscan 200 pH meter. The pH values of the initial MB solutions were between pH 5 – 6, indicating its acidic cationic chemistry. Experiments were done in duplicate for the repeatability of the results and average values were used for equilibrium and kinetic calculations (Appendix D). Temperature could not be controlled during the experiments.

The absorbance values were converted into concentrations by the calibration equations. From the determined concentrations, the percentage of removal (%) and the amount of MB solution removed per gram biochar (q) were calculated.

$$q\ (mg/g) = \frac{(C_0 - C).V}{m} \quad (3.24)$$

$$Removal\ \% = \frac{(C_0 - C)}{C_0} \times 100 \quad (3.25)$$

Where C_0 is initial concentration (mg/L), C is the concentration at t (min), V is the volume of the solution (L) and m is the mass of the biochar used in gram. The effect of contact time and adsorption time were determined by a plot of q (mg/g) versus t (min) for all concentrations. For adsorption equilibrium model fittings, Freundlich (Equation 3.27) and Langmuir adsorption isotherm equation (Equation 3.26) were used to interpret the experimental data which were obtained at 1, 15, 150 minutes, assuming the adsorption occurs at a heterogeneous surface and at the homogenous sites of the biochar without any interaction between sorbed molecules, respectively. These two isotherm models are the most widely used equilibrium models to determine the efficiency of the carbon in solid-liquid adsorption in the scientific world.

$$\frac{C_e}{q_e} = \frac{1}{q_{max}\ b} + \frac{C_e}{q_{max}} \quad (3.26)$$

Where C_e is the equilibrium dye concentration (mg/L), q_{max} is the monolayer adsorption capacity of the biochar (mg/g), and b is the Langmuir adsorption constant (L/mg) which is related to energy of sorption. Plotting C_e/q_e versus C_e gives a straight line where q_{max} and b values can be calculated. The maximum adsorption capacity was used to compare the adsorption efficiencies of the biochars.

$$\log q_e = logK_F + \left(\frac{1}{n}\right) logC_e \quad (3.27)$$

where K_F (mg/g(L/mg)$^{1/n}$) and n are Freundlich constants.

For the understanding of mass transfer in the processes, kinetic models were tested to determine adsorption rates. These models are the pseudo-first-order kinetic model by Lagergren, pseudo-second-order and intraparticle diffusion kinetic model by Weber and Morris (Hameed *et al.*, 2007). For the kinetic calculations, 1350 minutes of adsorption process were fitted to models. Firstly, the pseudo-first-order model was tested with the following equation:

$$\ln(q_e - q_t) = lnq_e - k_1 t \quad (3.28)$$

where q_e is the amount of MB solution removed per gram biochar at equilibrium time, q_t is the amount of MB solution removed per gram biochar at time t and k_1 is the rate constant of adsorption (1/min). A plot was of ln (q_e-q_t) versus t was made and q_e and k_1 values were calculated. Secondly, the pseudo-second-order kinetic model was tested with the following equation:

$$t/q_t = (1/k_2 {q_e}^2) + (1/q_e) \times t \quad (3.29)$$

Plotting $1/q_t$ against t gives a straight line from which q_e and k_2 (g/mg min) were calculated. Finally, the intraparticle diffusion model was tested to check if it was involved as a rate limiting step in the adsorption process with the following equation;

$$q_t = k_p\, t^{1/2} + C \quad (3.30)$$

where k_p is the intraparticle rate constant (g/mg $min^{1/2}$) and C is a constant. Plotting q_t against $t^{t/2}$ should give a straigt line where q_e and k_p can be calculated. The calculated q_e values were compared to experimental q_e values for the validity of the kinetic models by sum of squared errors (SSE, %) given by:

$$SSE, \% = \sqrt{\frac{(q_e,experiment - q_{e,calculated})^2}{N}} \quad (3.31)$$

where N is the number of the data points (Hameed *et al.*, 2007).

CHAPTER 4: RESULTS AND DISCUSSION

4.1 Chemical characterisation of raw materials

During a pyrolysis process thermo-chemical conversion occurs; therefore it is important to analyse the major elements in biochar to understand the chemical changes. Organic matter mainly consists of carbon, hydrogen, nitrogen and oxygen, as well as small amounts of inorganics which is termed ash. Table 4.1 presents the elemental and proximate analyses of the raw materials.

Table 4.1: Chemical analysis of raw biomasses

	Black wattle	Vineyard	Sugar cane bagasse
Elemental Analysis (dry, wt.%)			
Moisture (wt. %)	5.1	5.7	8.8
[a]Ash	1.3	3.1	3.5
C	52.3	50.2	52.7
N	0.43	0.5	1.1
H	6.1	6.7	5.8
[c]O+S	39.9	39.5	36.9
Proximate Analysis			
Moisture (wt.%)	5.7	5.4	8.8
[b]Ash	1.2	2.57	5.6
Volatiles	72.7	77.3	82.5
[c]Fixed carbon	26.1	20.1	11.9

[a] determined by analytical method
[b] determined by proximate analysis
[c] by difference

Moisture in biomass is the mineralised water content in living cells, containing anions, cations and non-charged species. The moisture contents of the woody biomasses were similar to each other, whereas sugar cane bagasse had relatively higher moisture content. The moisture content in the raw biomass would affect the energy consumption and decrease the efficiency of the conversion process and also increase the cost of transport. The harvesting conditions of the biomasses as well as the cropping season would affect the moisture contents, for instance the extraction step would increase the moisture content of bagasse as well as the elements of the biomass (Hugo, 2010). Pretreatments such as drying of biomass are generally used to decrease the moisture in the biomass.

The major elemental component of biomass and biochar is carbon. Some is "fixed carbon" in terms of proximate analysis, and some present in a remaining volatile portion (Brownsort, 2009). The fixed carbon values are actually more important for biochar regarding its usage as fuels. However, volatile matter and fixed carbon together can be an indication of stability (fixed) or its labile carbon content, which is also considered to be important for soil amendment purposes (Lehmann & Joseph, 2009). On a dry basis the volatile matter yield of biomass includes light hydrocarbons, CO, CO_2, H_2 and tars (Stanislav *et al.*, 2010). The highest volatile matter was observed in sugar cane bagasse with low fixed carbon content. The volatile matter content (db) in biomass ranged from 48-86%, where fixed carbon content varied between 1-38% (Stanislav *et al.*, 2010). The results from ultimate and proximate analyses were more or less in agreement with literature (Chapter 2, Table 2.1). Stanislav *et al.* (2010) pointed out that the ratio of the volatile matter and the fixed carbon content of biomasses are commonly higher than 3.5, however, for black wattle this ratio was 2.7. Therefore, this value could be accepted as an indication of its stability against decomposition.

Regarding ash contents, vineyard prunings and sugar cane bagasse had higher ash contents than black wattle prunings. This could be due to environmental conditions (e.g. soil type, rain, fertilisers used, etc.). The ash contents, which were determined by proximate analysis, were lower for woody biomasses but higher for sugar cane bagasse. The reason for this could be the inhomogeneous structure of the bagasse. The chemical compositions of the ash in the biomasses were given in Table 4.2. During sample preparation, black wattle biomass did not fuse into the glass bead; therefore ash composition could not be determined.

Table 4.2: Normalised inorganic composition of biomasses, dry wt.% of the ash

Biomass	SiO_2	CaO	K_2O	P_2O_5	Al_2O_3	MgO	Fe_2O_3	MnO	Na_2O	TiO_2
Vineyard	bd	42.79	26.44	12.02	bd	16.83	0.96	0.48	bd	0.48
Bagasse	68.70	2.67	4.20	1.53	8.02	3.82	9.54	0.38	bd	1.15

The major inorganic components of bagasse were silica and iron, while calcium and potassium were the main constituents for vineyard prunings. The results suggested that composition varied depending on the biomass type, namely woody biomass and herbaceous industrial residue and their growing and environmental conditions. Moreover, biochar from bagasse would be expected to have higher silicon and iron content than the biochar from vineyard prunings (Table 4.16). In the sugar industry, leftover bagasse after extraction is used as fuel in boilers for heat generation leaving 8-10% ash. Goyal *et al.* (2007) analysed sugar cane bagasse ash and also observed high silicon dioxide (62.43%) and around 7% ferric oxide contents, which was in agreement with Table 4.2. Although

silica is preferable for the production of glass, cement and ferrosilicon for the steel industry, it could also be useful to increase the amount of available phosphate in the soil when it is in the form of silicate (Russell, 1954). High Si and Al contents of sugar cane bagasse could be associated with contamination by soil (Stanislav *et al.*, 2010), whereas high Fe could be as a result of the mechanical processing of the biomass (Devnarain *et al.*, 2002). Demeyer *et al.* (2001) pointed out that wood ash consisted of mostly calcium and potassium oxides, similar to the ash components of vineyard prunings.

4.2 Vacuum pyrolysis yields and physico-chemical characterisation of biochars

In this section the results from vacuum pyrolysis of black wattle, vineyard prunings and sugar cane bagasse will be given and the biochar characteristics will be discussed.

4.2.1 Vacuum pyrolysis yields and elemental compositions of biochars

The vacuum pyrolysis of the prunings and bagasse led to the production of biochar, liquid (mixture of tarry and water phases) and gases in different yields. Table 4.3 revealed average product yields obtained by pyrolysis of the biomasses.

Table 4.3: Average product yields from vacuum pyrolysis on wt.% (T: 460/475°C, HR: 17/15°C/min, P: 8/8.5 kPa_{abs}, HT: 1 h)

Biomass	$Y_{biochar}$	Y_{liquid}	$^{*}Y_{gas+losses}$
Black wattle	23.5±0.3	58.1±8.1	18.4
Vineyard	31.0±0.3	35.2±11.6	33.8
Sugar cane bagasse	19.7±0.3	50.0±7.7	30.3

*by difference

Vacuum removes the primary volatiles from the reaction zone, restricting further reactions such as conversion of tar products into gas or small amounts of biochar (Garcìa-Pérez *et al.*, 2002; Shafizadeh, 1982). As a result, less gas and biochar are produced, but higher liquid yields are obtained than those from slow pyrolysis are obtained. Vacuum pyrolysis of black wattle biochar resulted in higher amounts of liquid and lesser amounts of gas and losses. The reason for that is the biomass particle size used for the experiments was much larger (+850 µm) than the particle sizes of

bagasse and vineyard prunings (425-850 µm). Larger particle size and slow heating rate enhanced the residence time of the vapours inside the particles; therefore secondary reactions were increased favouring the formation of biochar (Antal & Varhegyi, 1995). Islam *et al.* (2010) reported that larger particle sizes lead to a decrease in gas due to a lower reaction surface, which results in slower decomposition of the biomass. The reason for high liquid yield could be the higher moisture content of black wattle prunings due to its higher particle size. The combination of higher temperature and lower heating rate might have enhanced the pyrolytic water production due to increased reactions on the biomass.

The yields were in the same range with vacuum pyrolysis of various biomasses in literature (Chapter 2, Table 2.2). In case of sugar cane bagasse, Garcìa-Pérez *et al.* (2002) observed higher gas content but lower liquid content. Indeed, different pyrolysis reactors, conditions and biomasses resulted in different product yields. The product yields on a dry basis can be found in Appendix C.

Comparing the product yields from vineyard prunings and bagasse, which were produced under the same conditions, the effect of biomass type was significant. Dry and ash-free biochar yields and lignocellulosic compositions of biomasses were presented in Table 4.4 showing the influence of the lignocellulosic composition on product yields.

Table 4.4: The biochar yields and lignocellulosic compositions of biomasses on daf,wt.%

Biomass	Y_{ash}	$Y_{biochar}$	Y_{lignin}	$Y_{extractives\ (water)}$	$Y_{extractives\ (ethanol:cyclohexane)}$	$*Y_{holocellulose}$
Black wattle	1.3	25.1	23.9±0.02	4.8±0.004	14.9±0.02	56.4
Vineyard	3.1	35.5	27.7±0.02	2.9±0.02	9.8±0.02	59.6
Sugar cane bagasse	3.5	26.2	21.4±0.002	0.9±0.002	2.6±n.d	75.1

*by difference

The lignin compositions of the biomasses were slightly higher than the literature data, which was presented in Chapter 2 (Table 2.1). The cellulose and hemicelluloses yields could not be determined due to an inadequate HPLC column that was used that could not separate the sugar monomers and gave incorrect hemicelluloses content that resulted in a summative analysis of less than 100%. The presences of inorganic salts such as potassium, sodium and magnesium suppress the formation of tar and favour the char-forming secondary reactions (Raveedran *et al.*, 1995). Inorganic species especially act on hemicelluloses and reduce their decomposition temperature, which favours carbonisation (DeGroot & Shafizadeh, 1984). The combination of the higher ash and lignin content of vineyard prunings resulted in higher biochar yield, whereas the higher holocellulose composition of

bagasse resulted in lower biochar yield. As was mentioned in the literature review (Section 2.2.2.7), holocellulose starts to decompose at lower temperatures than lignin. During pyrolysis high concentration of cellulose decomposes to form biochar but with increased temperature, degradation of biochar occurs resulting in an increase in liquid yield (Antal & Varhegyi, 1995). One would expect that biochar yield from black wattle prunings would be higher than bagasse. However, higher maximum temperature during pyrolysis (515°C) of black wattle prunings might have enhanced the degradation of biochar. Black wattle was rich in extractives (19 daf,%) compared to bagasse, vineyard prunings and even softwood bark (17.7 wt.%) (Garcìa-Pérez *et al.*, 2007). Roy *et al.* (1990) studied the effect of extractives on vacuum pyrolysis yields and found that the presence of extractives slows down the levoglucosan production and reduces the yield of oil. However, it is difficult to make a conclusion whether there was an influence of extractives on the water phase of the liquid yield from the vacuum pyrolysis of black wattle. If the aim is biochar production, it would be better to use vineyard prunings, but for substantial production of biochar and bio-oil, black wattle is a potential biomass to be preferred under optimised conditions.

In general, the elemental analysis of biochar shows an increase in carbon and ash content, but a decrease in O, H, and N compare to elemental contents of biomass, due to the mass loss of organics during volatilisation. However, N and H percentages showed an increase in the results reported in Table 4.5. The increased H contents could be due to the presence of moisture in biochars. As H and O contents decreased, it would be expected that N percentages in biochars are higher than the ones in biomass as nitrogen could be acting like an inorganic element. In Table 4.1, the ash percentages of the biomasses were shown. More ash means more minerals in the biomass indicating a more effective catalytic role during pyrolysis (by means of the temperature reduction effect (Jun *et al.*, 2006)). The ash devolatilisation percentages (wt.%) were found to be 12.5%, 19.3% and 32.0% for black wattle, vineyard and sugar cane bagasse, respectively. During pyrolysis, major elements of biomass such as O, H, N are removed as volatile gaseous products leaving a residue with a high carbon content, where these carbon atoms are grouped into stacks of flat aromatic sheets with a disordered structure. The disordered structural arrangement of aromatic sheets gives biochar its unique physico-chemical characteristics (Bandosz & Ania, 2006).

Table 4.5: Elemental composition and ash content of biochars on wt.%

Biochar	C	N	H	S	*O	Ash	C/N	O/C	H/C
Black Wattle	70.14±2.24	2.17±0.67	8.31±3.43	0.01	19.37	4.84	32.3	0.28	0.12
Vineyard	74.19±5.62	2.51±1.04	7.39±0.89	0.02	15.89	8.08	29.6	0.21	0.10
Sugar cane bagasse	59.49±2.13	1.39±0.58	9.79±3.37	0.01	29.33	12.06	42.8	0.49	0.16

*by difference

The C/N, O/C and H/C atomic ratios are important for biochar characterisation. O/C and H/C ratios indicate the degree of functionalisation. Functional groups consist mainly of O or H, therefore O/C and H/C ratios indicate the presence of functional groups which increase biological degradability (Lehmann & Joseph, 2009; Bandosz & Ania, 2006). Sugar cane bagasse biochar showed the highest O/C, H/C ratios, while lowest O/C and H/C ratios were observed for vineyard biochar. Therefore, more surface functionalities would be expected on sugar cane bagasse biochar surface than black wattle and vineyard biochars.

The Van Krevelen plot of elemental ratios (all values are given on a moisture and ash free basis) for cottonseed hull (CH), sewage sludge (SS) and black wattle (BW), vineyard (V) and sugar cane bagasse (SCB) were shown in Figure 4.1. The data for cottonseed hull and sewage sludge biochars were obtained from Uchiyama *et al.* (2011) and Hossain *et al.* (2011), respectively.

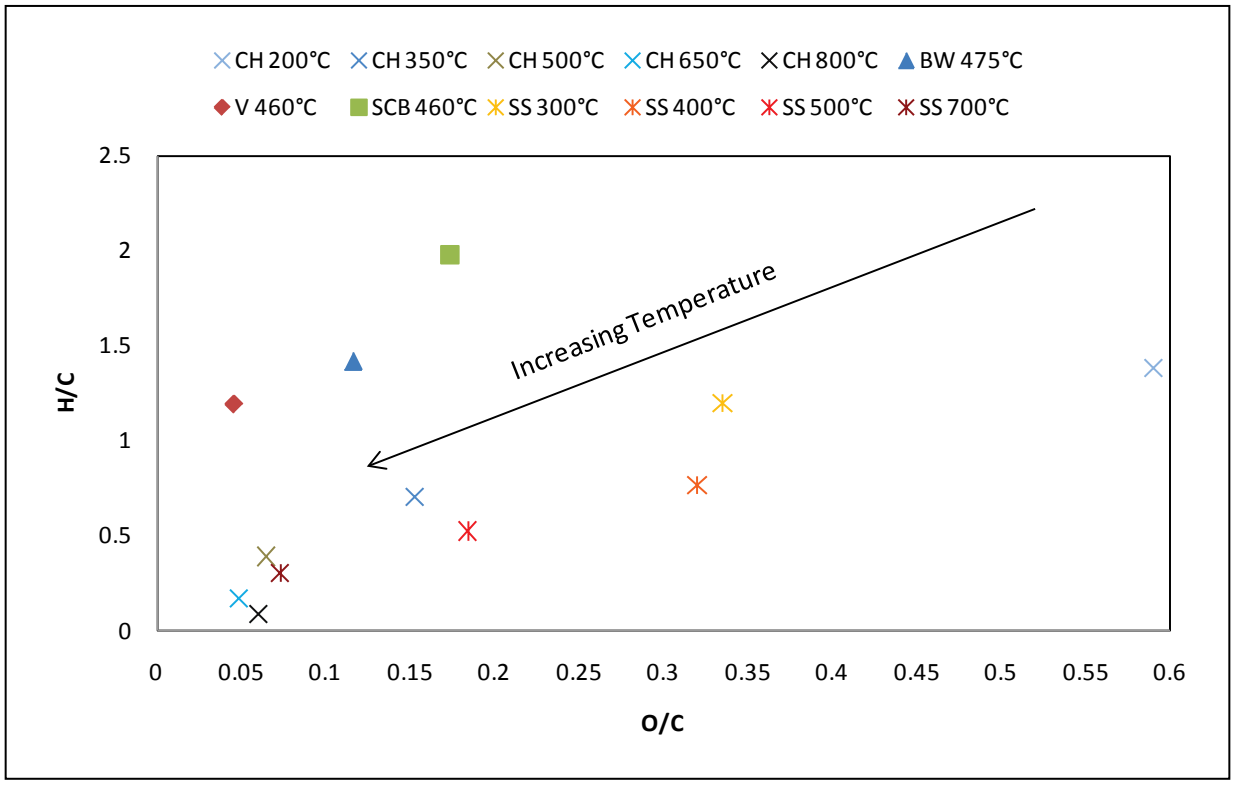

Figure 4.1: The van Krevelen plot of elemental ratios for biochars produced from various biomass sources at different pyrolysis temperatures.

The Van Krevelen diagram (molar ratios of H/C and O/C) is generally used to understand structural changes (Uchiyama *et al.*, 2011). As can be seen, the H/C and O/C molar ratios of biochars tend to decrease for increased pyrolysis temperatures due to reactions that take place during pyrolysis. Vacuum pyrolysis of black wattle, vineyard and sugar cane bagasse resulted in higher H content

compared to the biochars from slow pyrolysis, indicating that more carbon atoms were attached to a hydrogen atom. From the Van Krevelen diagram it can be deduced that the aromacity of the biochars would be in order of sugar cane bagasse < black wattle < vineyard biochar (Section 4.3.2). Under the same pyrolysis conditions, wood based biomass tends to show a higher degree of carbonisation compared to herbaceous industrial biomass. The lower degree of carbonisation of black wattle compared to vineyard could be a result of the particle size used.

The C/N ratio of a biochar is more related to the recalcitrant properties of the biochar or it could be used to understand how much nitrogen could be mineralised. The C/N ratios of biochars varied between 30 and 43 (Table 4.5). Fast pyrolysis of sugar cane bagasse resulted in a C/N ratio of 40.1 (Tsai *et al.*, 2006), which was similar to the C/N ratio of sugar cane bagasse biochar from vacuum pyrolysis. The C/N ratios of the wood based biochars were lower than the biochars produced from slow pyrolysis of wood based biomasses such as pine chip, pine bark, oak wood and *Eucalyptus deglupta* (Chapter 2, Table 2.8). In Chapter 2 (Table 2.3), it was observed that vacuum pyrolysis leads to higher C content than the C contents from slow and fast pyrolysis. Therefore lower C/N ratios of the biochars can be attributed to the nature of the biomasses. Generally C/N ratios higher than 20 is assumed to result in inorganic N immobilisation by microbial biomass, which induces N deficiencies for plants (Lehmann & Joseph, 2009). However, the aromatic nature of biochar provides high recalcitrance against microbial decay; therefore it is unlikely that biochars would cause N immobilisation (Kimetu *et al.*, 2008).

4.2.2 Surface acidity and basicity of the biochars

The pyrolysis conditions as well as the nature of the biomass influence the heterogeneous structure of the biochar; therefore the chemistry of biochar surfaces differs from one another. The surface chemistry of the biochars was determined in two ways: the Boehm titration method and infrared spectroscopy (Chapter 3). These two methods enable one to determine the surface nature, in terms of acidic or basic and hydrophilic or hydrophobic character.

The acidic or basic nature of the surface is caused by oxygen containing functional groups, which are mostly located on the edge of the graphene layers with an uneven distribution. The presence of heteroatoms as well as the mentioned functional groups is the main reasons for the heterogeneous nature of the biochar surface. Table 4.6 shows the surface acidity and alkalinity of the biochars.

Table 4.6: Surface acidity and basicity of biochars

Biochar	Surface acidity (mmol/g)	Surface basicity (mmol/g)
Blackwattle	1.28±0.1	1.04±0.06
Vineyard	0.70±0.3	1.67±0.20
Sugar cane bagasse	2.30±0.2	0.31±0.004

The acidic surface functionalities are caused by the presence of carboxyl groups, lactones and phenols. Boehm titration can be conducted with different solutions to determine different functional groups. It is generally assumed that $NaHCO_3$ neutralizes only carboxylic groups, Na_2CO_3 neutralizes carboxylic and lactonic groups and NaOH neutralizes carboxylic, phenolic and lactonic groups. Therefore, the surface acidity determined by titration with NaOH will be termed as "total acidity". On the other hand, surface alkalinity is more a controversial topic since the cause of surface alkalinity is still controversial (Pastor-Villegas *et al.*, 2010). However, it is assumed that the chromene and pyrone type groups cause the surface alkalinity. Therefore, it is accepted that titration with HCl neutralizes the basic functionalities including ketones, as well as the carbonates and other alkalinity causing species due to the presence of ash on the biochar surface (Singh *et al.*, 2010; Boehm, 1994).

There were less alkaline functional groups than acidic functional groups on the surfaces of black wattle and sugar cane bagasse biochars. However, biochar from vineyard prunings had a different chemistry with its higher amount of alkaline functional groups than acidic functional groups on the surface. The highest surface acidity was found in sugar cane bagasse biochar, whereas vineyard biochar had the lowest. Regarding surface alkalinity, the highest number of basic functional groups was found on vineyard biochar surface, whilst sugar cane bagasse biochar had the lowest (Table 4.6). The presence of acidic surface functionalities makes biochar more acidic and hydrophilic, whereas basic surface functional groups make biochar more basic and hydrophobic. Therefore, it could be said that sugar cane bagasse was more hydrophilic than the other biochars and expected to be more acidic than the rest of the biochars (Section 4.2.3).

The surface acidity values of biochars in this study were relatively higher than the values reported for biochars in the literature (Chapter 2, Table 2.5). Nevertheless, chemically activated carbons in Table 2.5 had higher surface acidities than the discussed biochars. Surface alkalinity of the biochars was higher, but the basicity of biochar from sugar cane bagasse was in the same range as the literature values.

The FTIR spectra of the biochars were shown in Figure 4.2, wavelength ranging from 400 cm^{-1} to 4000 cm^{-1} for vineyard and 400 cm^{-1} to 2500 cm^{-1} for sugar cane bagasse and black wattle. However, the wavelength range important to this research was between 400 and 2500 cm^{-1}.

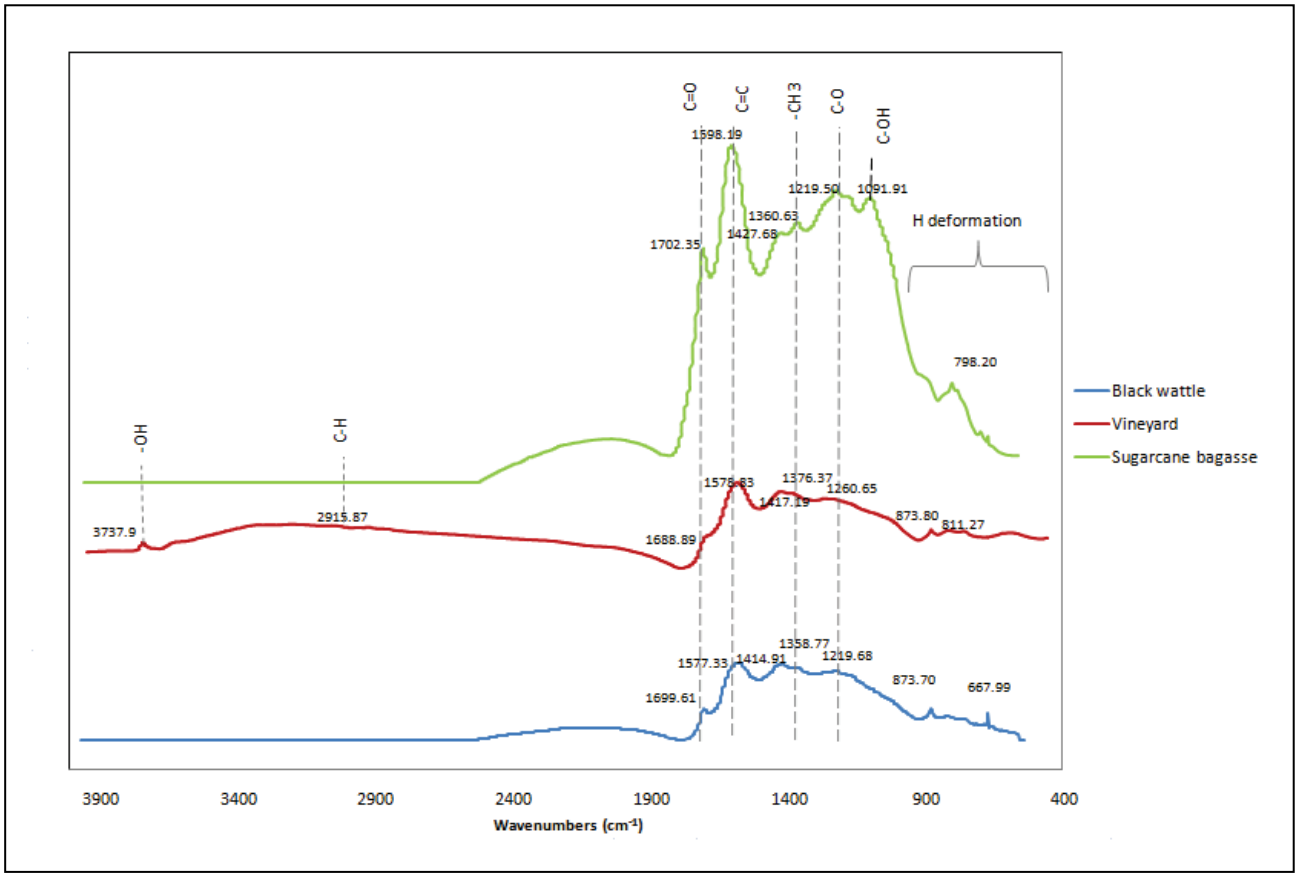

Figure 4.2: FTIR analyses of biochars

As can be noticed immediately, the FTIR analysis of sugar cane bagasse biochar was different from those of black wattle and vineyard biochars regarding the intensity. The peaks between 1688 and 1702 cm^{-1} correspond to C=O stretching, which is an indication of carboxylic and lactonic groups (Fuente *et al.*, 2003). It can be seen that the above-mentioned peaks were very weak for vineyard biochar which was in agreement with its lower surface acidity.

Aromatic C=C ring stretching were observed between 1414 and 1598 cm^{-1} and the peaks between 1219 and 1260 cm^{-1}, corresponding to aromatic CO- stretching, were observed for all biochars. Aromatic C=C peaks are an indication of benzene-like rings. Aromatic molecules have extra stability caused by the nature of their structure (Section 4.2.3). However, Ahmad *et al.* (2007) observed the same peak (1578 cm^{-1}) on biochar derived from oil palm wood and attributed it to C=O stretching of

carbonyl group in quinone and pyrone type structures which were the main causes for surface alkalinity in the case of vineyard and black wattle biochars.

The peaks between 1376 and 1358 cm^{-1} correspond to aliphatic CH_3 deformation. Biochar from sugar cane bagasse showed a peak at 1091 cm^{-1}, which could be due to aliphatic ether C-O or alcohol C-O stretching. That peak could also be an indication of asymmetric Si-O-Si stretching, which could also be attributed to the high Si content of sugar cane bagasse biomass, shown in Table 4.2 (Coates, 2000). The peaks between 873 and 798 cm^{-1} correspond to changes in aromatic structures such as aromatic hydrogen.

Biochar from black wattle showed a peak at 667 cm^{-1}, which could be S-O stretching (Gerçel *et al.*, 2007). The peak observed at 3737 cm^{-1} is probably alcohol or phenol free OH stretching vibrations on biochar from vineyard. The reason for this peak could be water content due to insufficient cleaning of the equipments used. A weak peak around 2915 cm^{-1} corresponds to aliphatic CH stretching (Özçimen & Ersoy-Meriçboyu, 2010).

Bouchelta *et al.* (2008) studied the surface chemistry of raw date pits and biochars produced from slow pyrolysis at different final process temperatures ranging from 500 °C to 700 °C via FTIR analysis. Comparing the surface chemistry of raw date pits and biochar produced at 500 °C, it was clear that biochar and raw biomass had similar surface functional groups, however some of the peaks such as those at 3400, 2926, 2870 and 1640 cm^{-1} disappeared. These peaks correspond to stretching in hydroxyl groups, stretching in alkyl groups and stretching in olefins. The disappearance of these peaks was an indication of decreases in water and aliphatic compounds. Not only was the disappearance of the peaks observed, but a new peak around 1540 cm^{-1}, corresponding to aromatic C=C stretching, appeared on the biochar surface. This indicates an increase in aromacity during pyrolysis as temperature increased. Similar observations were made by Özçimen & Ersoy-Meriçboyu (2010) for the FTIR analyses of raw chestnut shell and its biochar produced at 477 °C. The peaks at 3324 and 1018 cm^{-1} corresponding to –OH stretching and aliphatic ether C-O and alcohol C-O stretching disappeared, but new peaks from 700 to 900 cm^{-1} corresponding to an aromatic C-H stretching appeared on the biochar surface. It is evident that the temperature applied has an important effect on the aromatic nature of the biochar as it increases with temperature due to the decomposition of unsaturated chemical structures during pyrolysis (Guo & Bustin, 1998).

As was mentioned in Section 4.2.1, in general, pyrolysis results in a decrease in oxygen content compared to the raw biomass. The decrease in oxygen causes disappearance of phenolic and alcoholic groups, therefore –OH stretching vibrations disappear on the biochar surface (Sharma *et al.*, 2004). Nevertheless, Özçimen & Ersoy-Meriçboyu (2010) observed that a new peak appeared around 3387 cm^{-1} on the biochar surface of hazelnut shell, produced at 477°C. To get a better understanding of chemical changes on biochar surfaces, the FTIR spectra of raw materials from literature have been compared to FTIR spectra of biochars from vineyard, black wattle and sugar cane bagasse (Figure 4.2). Indeed, environmental conditions would cause differences between the biomasses used and the biomasses from the literature. Table 4.7 shows functional groups on the surface of vineyard prunings and the wavenumbers observed in vineyard biochar. From the FTIR spectra obtained by Yasar *et al.* (2010), raw vineyard had similar surface functionalities as vineyard biochar. However, there is a shift that might have occurred for carboxyl C=O and C-O stretching due to the pyrolysis process.

Table 4.7: Comparison of surface functionalities on vineyard prunings (Yasar *et al.*, 2010) to biochar

Wavenumber (cm^{-1})	Assignments	Biochar wavenumber (cm^{-1})
3450	-OH stretching	3738
2950	Aliphatic CH stretching vibration	2916
1710	Aromatic carbonyl/carboxyl C=O stretching	1689
1150	Aromatic CO- stretching	1261

Table 4.8: Surface functionalities on sugar cane bagasse (Garg *et al.*, 2007)

Wavenumber (cm^{-1})	Assignments	Biochar Wavenumber (cm^{-1})
3778 - 3407.9	-OH stretching	n/d
2921	Aliphatic CH stretching vibration	n/d
1727	Aromatic carbonyl/carboxyl C=O stretching	1702
1428	Aromatic C=C ring stretching	1598
1374	Aliphatic CH_3 deformation	1360
1326	Aliphatic CH_2 deformation	-
1249	Aromatic C-O stretching	1219
1161	Aromatic C-O stretching	-
1051	Aliphatic ether C-O and alcohol C-O stretching	1091

The OH stretching vibrations (Garg *et al.*, 2007) as well as the peak at 2921 cm^{-1} was not determined on the surface of sugar cane bagasse biochar. But, the same functional groups at different wavenumbers were observed for the biochar.

There is no available data on FTIR spectra of black wattle prunings, therefore spectra for black wattle fibre was compared to spectra for black wattle biochar in Table 4.9. As can be seen from Table 4.9, the same functional groups were observed on the biochar surface with similar wavenumbers.

Table 4.9: Surface functional groups on black wattle fibre (Klash et al., 2009)

Wavenumber (cm^{-1})	Assignments	Biochar Wavenumber (cm^{-1})
1690	Aromatic carbonyl/carboxyl C=O stretching	1699
1590	Aromatic C=C ring stretching	1577
1450	Aromatic C=C ring stretching	1415
1360	Aliphatic CH_3 deformation	1359
1220	Aromatic C-O stretching	1219

As stated previously, the surface chemistry of the biochars are related to the precursor. The chemical composition of the precursor influences the surface functionalities. In the pyrolysis process, hemicelluloses start to degrade first (197-257°C), then cellulose (237-347°C) and lastly lignin (277-497°C) (Demirbas, 2007). Bilba & Ouensanga (1996) studied the thermal degradation of sugar cane bagasse and the FTIR analyses of the biochars produced. They mentioned that signals around 1700 cm^{-1} in raw material were due to lignin and holocellulose. The structural alterations appeared at 200°C, which is the temperature where hemicelluloses degradation starts and this alteration increased with increased temperature (300-400 °C). They also observed a decrease in intensities of the O-H, C-O and C=C vibration signals. It is well known that phenolic groups on biochar surfaces are due to the degradation of lignin (Souza et al., 1996). Sharma *et al.* (2004) mentioned that firstly carbohydrates (Bilba & Ouensanga, 1996) and lignin dehydrate at 350°C, and then carbonyl groups form with temperature. With increased temperature, these groups are eliminated. Finally aliphatic groups decompose resulting in carbon structures with a high aromatic content.

The FTIR analyses of the biochars (Figure 4.2) had similar results as the results of the pistachio-nut shell biochar, produced at 500°C by vacuum pyrolysis (Lua & Yang, 2004). However, they observed bands at 3389 cm^{-1}, 2922 cm^{-1}, 2338 cm^{-1}, which could not be shown for black wattle and sugar cane bagasse biochars due to computer error with an exception of the peak around 2951 cm^{-1} for vineyard biochar. One of the important findings from the study of Lua & Yang (2004) was that the biochars, which were produced from 350 to 600°C via vacuum pyrolysis, had similar FTIR spectra, indicating the surface functional groups were the same. When they increased the pyrolysis temperature, the spectra of biochars produced between 700°C and 1000°C changed, displaying a flatter profile and weaker peaks. Therefore, it could be deduced that pyrolysis temperature is the key element in surface functionalities in biochars.

4.2.3 NMR results

Solid state NMR analysis gives a better determination of structural groups in the biochar that cannot be exactly determined by FTIR analysis. Figure 4.3 presents the ^{13}C NMR spectra of black wattle, vineyard and sugar cane bagasse biochars.

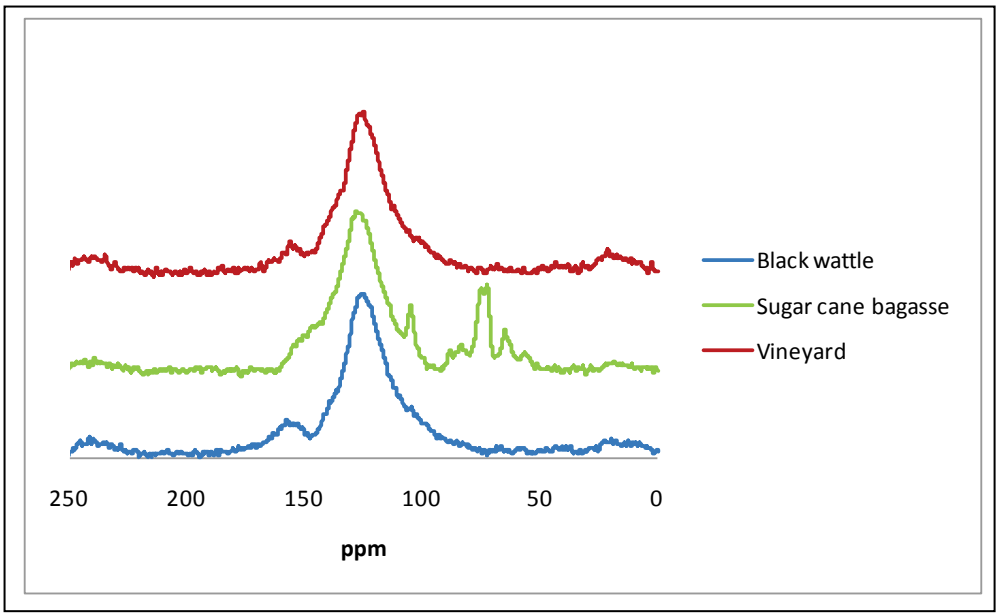

Figure 4.3: Solid state ^{13}C NMR spectra of black wattle, vineyard and sugar cane bagasse biochars

The different chemical structure of sugar cane bagasse which was also observed in Figure 4.2 is clearer in Figure 4.3. The chemical structure of black wattle and vineyard biochars were quite similar to each other. The chemical shift regions were utilised for quantification of the dominant functional groups in the biochars in Table 4.10.

Table 4.10: The distribution of percentage C for structural groups as determined by ^{13}C NMR of black wattle, vineyard and sugar cane bagasse biochars

Chemical shift and structural group	0-50 ppm Paraffinic C	50-90 ppm Substituted C	90-145 ppm Aromatic C	145-163 ppm Phenolic C	163-190 ppm Carboxyl C	190-220 ppm Carbonyl C
Black wattle	4	1	84	10	3	0
Vineyard	5	1	86	8	1	0
Sugar cane bagasse	3	18	64	13	1	0

Error margins: ±3%

Aliphatic C content (0-90 ppm) of sugar cane bagasse biochar was relatively higher than vineyard and black wattle biochars. Polar C content (50-90 ppm and 145-220 ppm) of biochars were in an order: vineyard < black wattle < sugar cane bagasse. This order was in agreement with their polarity [molar (O+N)/C] values; 0.19, 0.23 and 0.39 for vineyard, black wattle and sugar cane bagasse biochars, respectively (Wang *et al.*, 2007) and FTIR peak intensities at C=O stretching bands, around 1700 cm^{-1} (Figure 4.2). The sharp peaks between 50-90 ppm can be attributed to aliphatic polar C in sugar cane bagasse biochar (18%). Aromatic C contents of biochars were in order of sugar cane bagasse < black wattle < vineyard, which indicates that wood based biochars had higher aromacity hence higher stability for microbial degradation than herbaceous industrial residue based biochar, produced under the same pyrolysis conditions. The stability of the biochar from vineyard could also be attributed to the relatively higher lignin content of the feedstock. The stability determines not only how long C is applied to soil as biochar would remain sequestered in soil, but also determines how long biochar could provide benefits to soil and water quality (Lehmann & Joseph, 2009). Therefore, the contribution of vineyard and black wattle biochars to the mitigation of GHG emissions and soil productivity would be expected to be higher than sugar cane bagasse biochar.

Phenolic C contents of the biochars were higher than their carboxyl carbon contents. Phenolic and carboxylic C contents vary in order of the vineyard < black wattle < sugar cane bagasse was in agreement with surface acidity values (Table 4.6), FTIR analyses (Figure 4.2), O/C and H/C ratios (Table 4.5). This finding suggests that sugar cane bagasse biochar would result in better cation exchange ability.

Brewer *et al.* (2009) studied quantitative NMR spectral analysis of switchgrass biochars from slow and fast pyrolysis at 500°C. Aromatic content of switchgrass biochar from slow pyrolysis was 87%, whereas fast pyrolysis of switchgrass resulted in lower aromatic C content (73%). The reason was attributed to the longer hold time (2h) on slow pyrolysis to that of fast pyrolysis (<2 s). Therefore, it could be deduced that longer hold times in vacuum pyrolysis would result in higher aromaticities, especially for wood based biomasses. They also reported that the types of carbon present seem to depend on process temperature as well.

In conclusion, elemental and NMR analyses showed consistently that biochar produced from sugar cane bagasse contained more oxygen in various functional groups. The higher acidic functionalities which were observed by FTIR and NMR analyses and Boehm titration on sugar cane bagasse indicate its higher cation exchange capacity. However, aromatic C of sugar cane bagasse was found to be lower than that of black wattle and vineyard biochars. Therefore, high aromaticity of black wattle and vineyard biochars would make them more preferable in soil applications if the purpose is carbon

sequestration. However, sugar cane bagasse would be more preferable if the aim is to help improve nutrient retention in soil.

4.2.4 pH of the biochars

Thermo-chemical conversion of the raw materials resulted in an increase in the pH of the biochar product (Table 4.11). pH determination of the raw materials were done with the same method used for the pH determination of biochars. Determination of the pH of sugar cane bagasse was difficult due to its hydrophilic nature. Depending on the pyrolysis conditions and the nature of the feedstock, different pH values, ranging from pH 4 to 13 can be reached (Chan *et al.*, 2008; Cheng *et al.*, 2006). Biochars from pyrolysis processes are usually alkaline in nature ranging from pH 7.5-9.4 (Van Zwieten *et al.*, 2010; Novak *et al.*, 2009; Cheng & Lehmann, 2009). In this sense, biochars from vacuum pyrolysis at 460-475°C with 60 min hold time resulted in the same pH range for wood based feedstocks. The highest pH was observed for biochar from vineyard prunings.

Table 4.11: pH of the raw materials and biochars

Biomass	pH(H_2O) raw	pH (H_2O) biochar	pH(KCl) biochar
Black wattle	5.12±0.02	9.74±0.01	8.79
Vineyard	5.79±0.04	10.43±0.02	9.82
Sugar cane bagasse	6.19±0.09	6.56±0.04	5.15

Biochar from sugar cane bagasse was slightly acidic in nature, which is in contrast to other biochars, but in agreement with Figure 4.2 (C=O stretching). From Table 4.11, it can be concluded that under the same pyrolysis conditions, pH values of biochars are dependent on the nature of the feedstock. It is known that high temperatures lead to alkaline biochars due to the destruction of acidic functional oxides on the biochar surface due to further decomposition of biochar, whereas low pyrolysis temperatures result in biochars with lower pH values. Shinogi & Kanri (2003) observed a substantial increase in pH during the pyrolysis of sugar cane bagasse, rice husk, activated sludge and cow biosolids between 300 and 500°C, where alkaline character biochars were obtained with carbonisation temperature above 600°C. The O content of the biochars was in order of vineyard biochar < black wattle biochar < sugar cane bagasse, which is relevant to pH values of the biochars as the higher the oxygen content is, the more acidic the aqueous solution.

The alkaline nature biochars (vineyard, black wattle) would be useful to increase the pH of acidic soils at risk of aluminium toxicity. Yuan *et al.* (2010) reported that the presence of carbonates and

anions in biochar leads to a decrease in soil acidity by reacting with soil H^+. Carbonates generally show a peak between 880-860 cm^{-1} (Coates, 2000), which can be observed significantly for vineyard biochar in Figure 4.2. On the other hand, sugar cane bagasse could be used to balance the pH of slightly basic soils since the optimum nutrient availability of the soils are between pH 6.5 – 7 (Ashman & Puri, 2002).

Biochars showed lower pH in 1 M KCl solution, which was an indication of reserve acidity. In soil science 1 M KCl solution is used to test for the presence of exchangeable aluminium. Aluminium and H^+ are displaced by K^+ on the exchange complex, which consumes OH^- ions and the concentration of H^+ increases, therefore solution pH decreases if pH KCl is below 5.2. Sugar cane bagasse was the only biochar that has pH (KCl) lower than pH 5.2, which was an indication of higher aluminium content than other biochars (Table 4.2). In biochars with pH values higher than pH 5.2, aluminium is not exchanged but other exchangeable groups are. The difference between pH (H_2O) and pH (KCl) was more than 1 pH unit for sugar cane bagasse, while the difference was 0.51 for vineyard biochar. In literature this difference was up to 1.35 pH units for black locust biochar (Chapter 2, Table 2.6). It could be deduced that the higher the difference between pH (H_2O) and pH (KCl), the more ion groups tend to be exchanged. On the other hand, the ash content of biochar, which increases with temperature (up to 600-700°C), could affect the pH of the biochars, as it could block the pores and cause a decrease in surface area resulting in higher pH than their actual pH (Shinogi & Kanri, 2003).

pH of biochar is also useful for the determination of the surface charge, which is very important in sorption processes. The pH of the point of zero charge (PZC), where the net surface charge is zero, should be determined. Biochars are considered as amphoteric solids due to the nature of their surface, therefore depending on the solution pH, both negative and positively charged surfaces exist within the solution. The surface of the biochar is negatively charged when pH > pH_{PZC}. When the surface is negatively charged, it attracts cations from the solution. When the surface is positively charged, it attracts anions from the solution. Uchiyama *et al*. (2011) has determined the pH and pH_{PZC} values of biochars which were produced at different pyrolysis temperatures. The pH_{PZC} of cottonseed hull biochars were higher than their pH when the pyrolysis temperature was 500 °C and above, indicating positively charged surface of the biochars. The pH_{PZC} of the biochars were lower than their pH when the production temperature was below 350°C, indicating the surfaces were negatively charged. From the mentioned study, they concluded that the greater electrostatic interactions would be expected between cationic heavy metal species and negatively charged surfaces once biochar from slow pyrolysis temperature is added into soil. Therefore, it can be

concluded that biochar from sugar cane bagasse would be more effective to retain cationic heavy metals when it is applied to soil.

Comparing Tables 4.6 and 4.11, lower pH was observed for bagasse biochar with its high surface acidity and very low surface basicity, whereas higher pH was observed for vineyard biochar with its high surface basicity and low acidity. Although black wattle biochar had more surface acidity than its basicity (0.24 mmol/g net), the pH of the biochar slurry was alkaline. The reason for this could be that surface basic functionalities are considered to be stronger than surface acidic functionalities (Nowicki & Pietrzak, 2010) or the presence of high amounts of water soluble ions such as K and Na resulted in higher pH values.

4.2.5 Cation Exchange Capacity (CEC) of biochars

Cation Exchange Capacity is an important indicator for potential application of biochar into soil and carbon sequestration. The presence of charged, hard Lewis ligand functional groups on the biochar surface gives biochar its ability to attract, retain and exchange basic cations (readily available for plants to absorb), which can be used to enhance nutrient holding capacity of the soil, minimising nutrient losses by leaching. Briefly, as Lee *et al.* (2010) reported CEC is the amount of exchangeable cations such as K, Ca, Mg, etc. Table 4.12 shows the potential CEC results of the biochars produced.

Table 4.12: Potential CEC and O/C ratios of the biochars

Biochar	CEC ($cmol_c$ /kg)	O/C
Black wattle	101	0.28
Vineyard	65	0.21
Sugar cane bagasse	122	0.49

Bagasse biochar showed the highest CEC value, whereas vineyard biochar had the lowest cation exchange capacity. The CEC value of sugar cane bagasse biochar is similar to CEC of common soil mineral montmorillonite (80 - 150 $cmol_c$/kg). The CEC values of all biochars are comparable to the CEC of another common soil mineral, dioctahedral vermiculite (10 – 150 $cmol_c$/kg). Kaolinite is the typical clay mineral found in subtropical regions such as the Western Cape. When comparing the CEC values of the biochars to kaolinite (2-15 $cmol_c$/kg), it was seen that the value of the vineyard biochar is four times as high as kaolinite. The CEC of soil organic matter or humic substances range between 150 and 200 $cmol_c$/kg which is much higher than the CEC values of the biochars produced (Sparks, 1995). In Table 4.12, O/C values are presented as an indication of the presence of more hydroxyl,

carboxylate and carbonyl groups which could contribute to a higher CEC value (Lee *et al.*, 2010). As can be seen, CEC values correlated well with the O/C ratios. This finding suggests that higher CEC values could be reached if the pyrolysis conditions are optimised for a particular biomass.

Table 4.13: CEC values from literature

Precursor	Process Conditions	CEC ($cmol_c/kg$)	Reference
Eucalyptus saligna	Slow pyrolysis, T= 400°C	7.3	Singh *et al.*, 2010
Poultry litter	Slow pyrolysis, T= 400°C	14.5	Singh *et al.*, 2010
Cow manure	Slow pyrolysis, T= 400°C	22.2	Singh *et al.*, 2010
Paper mill waste	Slow pyrolysis, T= 550°C	9 - 18	Van Zwieten *et al.*, 2010
Wastewater sludge	Slow pyrolysis, T= 550°C	35	Hossain *et al.*, 2010

Comparing CEC values (Table 4.12) to recent studies (Table 4.13), all the biochars produced from vacuum pyrolysis had much higher CEC values than the values in literature. It can be concluded that biochars from vacuum pyrolysis would contribute more to soil as amendment and carbon sequesteration compared to the ones produced via slow pyrolysis by producing higher acidic surface functionalities. However, it might be useful to study the CEC values of biochars produced at different temperatures for optimisation of the process for soil amendment purposes. From the study of Gaskin *et al.* (2007), it was observed that CEC values decreased with an increase in temperature, however in the study of Singh *et al.* (2010), there was only a small increase (0.8 $cmol_c/kg$) in CEC values of the biochars from *Eucalyptus saligna* when temperature was increased from 400°C to 550°C.

As CEC is correlated with the presence of acidic functional groups, the CEC values of the biochars were compared to surface acidity values. As expected, the bagasse biochar, which had the highest surface acidity, showed the highest CEC, while the vineyard biochar had the lowest CEC with is low surface acidity. Therefore, it would be expected that CEC values would decrease with an increase in temperature because higher pyrolysis temperatures cause loss of acidic surface functional groups. Biochars from fast pyrolysis has recently received attention for soil amendment purposes. Lee *et al.* (2010) and Silber *et al.* (2010) reported the CEC values of biochars from the fast pyrolysis of corn stovers as 26.4 and 17.9 $cmol_c/kg$, respectively. These values are relatively lower than the values from biochars produced in this study. All in all, it could be deduced that vacuum pyrolysis has contributed to higher acidic functionalities due to lesser secondary reactions.

In conclusion, biochars produced during vacuum pyrolysis would increase the CEC of soils due to their inherently high CEC values and furthermore, as they age in the soils, the cation exchange

abilities would increase due to the oxidation of biochar. Therefore, one would expect that the soil application of the biochar from sugar cane bagasse would lead to the greatest improvement in soil fertility.

4.2.6 Electrical conductivity and nutrients of biochars

The EC value is an indication of the salinity of the biochar. Salinity refers to the presence of the major dissolved ions, which is very important because each plant tolerates different salinity levels in soil. However, in most of the cases, high salinity of the soil adversely affects the rate of plant growth and harvest yield by causing ion toxicity and reducing water uptake by plants. Soils with EC values above 4 dS/m are considered to be saline soil (Sparks, 1995).

Table 4.14: EC values and water soluble ions of biochars

Biochar	EC	Ca^{+2}	Mg^{+2}	Na^{+}	K^{+}	Cl^{-}	PO_4^{-3}	SO_4^{2-}	NO^{-3}	NO^{-2}
	dS/m				mg/kg					
Black wattle	0.67±0.02	60	113± 12	1140± 40	2300± 69	460± 35	1033± 64	520± 87	0	0
Vineyard	0.83±0.05	428± 24	421± 26	233± 21	4380± 191	247± 23	n/d	813± 70	n/d	n/d
Sugar cane bagasse	0.17±0.01	32±7	25±8	173± 5	560± 65	84± 4	317± 20	335± 34	0	0

The EC values of biochars were between 0.2 and 0.8 dS/m. Biochar from vineyard prunings showed the highest EC value, whereas sugar cane bagasse showed the lowest EC value indicating its low salinity. These values were compared to EC values of various biochars from literature in Table 4.15.

Table 4.15: EC values of various biochars

Biochar	Process conditions	Pyrolysis Temperature (°C)	EC (dS/m)	Reference
Eucalyptus saligna	HR=5-10°C/min; HT=40 min	550	0.16	Singh *et al.*, 2010
Poultry litter	HR=5-10°C/min; HT=40 min	400	6.32	Singh *et al.*, 2010
Cow manure	HR=5-10°C/min; HT=40 min	400	9.18	Singh *et al.*, 2010
Eucalyptus grandis	n/a	450	0.4	Dias *et al.*, 2010
Wastewater sludge	HR=10°C/min	550	1.9	Hossain *et al.*, 2010
Greenwaste	n/a	450	3.2	Chan *et al.*, 2007

The EC values of biochars produced in this study are lower than the EC values of most of the biochars in literature (Table 4.15). It can be seen that biochars from animal based precursors had much higher EC values than plant based biochars. Wood based biochars showed higher EC values than sugar cane bagasse. Chan *et al.* (2008) added biochar produced from poultry litter with EC value of 5.6 dS/m into soil with an EC value of 0.11 dS/m at different rates. The EC of the soil significantly increased with biochar application at 10 t/ha (36%). Similar substantial increase in soil EC by the addition of biochar was also observed by Novak *et al.* (2009). The recommended biochar application rate is 10 t/ha (Chan *et al.*, 2007). When they increased the biochar application rate to 50 t/ha, the EC of the soil increased from 0.11 to 0.29 dS/m, which means the percentage increase was 164%. Based on the mentioned study, one would expect that biochars produced in this study would increase the soil EC less due to their lower EC values. The amount of biochar should be calculated carefully before addition into soil to prevent any soil salination problems and nutrient imbalances.

Singh *et al.* (2010) studied the pyrolysis temperature effect on the EC values of the biochars. While biochar from slow pyrolysis of *Eucalyptus grandis* at 400°C had an EC value of 0.09 dS/m, the biochar which was produced at 550°C had an EC value of 0.16 dS/m. However, a recent study by Hossain *et al.* (2011) showed that with increased pyrolysis temperature, the EC values of wastewater sludge biochar decreased. Comparing EC values of raw biomass to EC values of biochars, an increase in EC values was observed during the pyrolysis process of sugar cane bagasse and black wattle while the EC value of vineyard biochar decreased. This might be due to the presence of fine particles in the raw vineyard pruning sample, which increased the amount of dissolved ions in water. Therefore, it can be concluded that an increase in the pyrolysis temperature results in an increase in EC values of biochars from lignocellulosic materials, unlike wastewater sludge.

The pH and EC values of the biochars were compared (Table 4.11 and 4.14). The EC values of sugar cane bagasse, black wattle and vineyard biochars were in the same order as the pH values namely; sugar cane bagasse < black wattle < vineyard.

Nutrient contents of biochars make them potential soil amendment agents. Water soluble ions in the biochar give an indication of readily available nutrients in the biochar. Plants use the inorganic forms of N (ammonium and nitrate), P (phosphate) and S (sulphate) as nutrients from the soil.
The biochars contained little or no NO_3^-, which is an essential nutrient for plant growth (Table 4.14). N starts to volatilise at low temperatures (above 200°C). Wang *et al.* (2010) observed that the primary nitrogen species produced from straw were NH_3 and HNCO (isocyanic acid). N containing

groups were not observed from the FTIR analyses of biochars. The reason for low or non-detected NO_3^- content of biochars could be due to the formation of N-heterocylic aromatic structures from the condensation of N containing structures (Koutcheiko *et al.*, 2007).

Phosphorus starts to volatilise around 700°C, however during pyrolysis phosphocarbonaceous structures are created at low temperatures, and these structures decompose due to bond scission at high temperatures to form phosphate (Bandosz & Ania, 2006). During pyrolysis very little phosphorus is lost, however with increased temperature its plant availability decreases (Silber *et al.*, 2010). The phosphate content of biochars from vineyard could not be determined; however PO_4^{-3} content of black wattle biochar was three times higher than that of sugar cane bagasse biochar (Table 4.14). The availability of phosphate is strongly pH dependent. Under acidic conditions, the phosphate availability decreases due to the fixation of phosphate as precipitation of highly insoluble iron and aluminium phosphates in soils that are high in Al and Fe oxides or aluminosilicate clays. If the pH of the soil solution is too high, precipitation of insoluble calcium phosphates occurs; therefore availability of phosphate decreases. The greatest phosphate availability is found to be around pH 6 to 7 for most agricultural soils (Bohn *et al.*, 1979).

Sulphur is an essential nutrient, which is absorbed in the form of sulphate. C-O-S was found to be the major sulphur species during the pyrolysis of straw and the release of C-O-S and H_2S from the decomposition of organic sulphur occured below 400°C (Wang *et al.*, 2010). Biochar from vineyard showed the highest sulphate content.

Potassium, calcium and magnesium are the major macronutrients. The highest water soluble K was found in vineyard biochar, whereas sugar cane bagasse had the lowest K content, approximately 1/8 that of vineyard biochar. During pyrolysis of straw, the major species are found to be HCl. The formation of Cl_2 was mainly at temperatures between 300-350°C for straw pyrolysis (Wang et al., 2010). Black wattle biochar had the highest Cl content, whereas sugar cane bagasse had the lowest. Cl^- is considered a hard base which means it would bond with a hard acid such as potassium. Wang *et al.* (2010) concluded that potassium was vaporized as KCl or other kind of potassium containing species during pyrolysis of straw and coal. Calcium and magnesium contents of biochars are relatively lower than the K contents.

In conclusion, the water soluble nutrient contents of biochars were as follow; vineyard > black wattle > sugar cane bagasse which is in the same order as the EC values. Apparently, EC values were mostly affected by K contents of the biochars due to the higher relative solubility of K containing salts and

carbonates in water. Regarding ash content, of which EC is an indication, it can be concluded that ash percentages of biochars increased due to the pyrolysis process which was also shown in Table 4.5.

There is no available data in the open literature on water soluble nutrients and thus makes it difficult to compare the results in this study to the literature (Table 4.14). Plant roots secrete weak acids such as citric acid to take up nutrients (Hinsinger, 2001). Wet acid digestion is commonly used for the determination of plant available nutrients. Recently, microwave assisted wet acid digestion method has been preferred for this determination (Novak *et al.*, 2009; Hossain *et al.*, 2011). However, available phosphorus cannot be determined with this method; therefore citric acid available nutrients were determined and presented in Table 4.16.

Biochars contained substantial amounts of plant available nutrients such as K, Ca, and Mg. Pyrolysis influences the availability of the base cations such as K, Ca, and Mg by increasing the solubility (Silber *et al.*, 2010). The sugar cane bagasse contained less major nutrients than the other biochars. This property of sugar cane bagasse makes it less attractive as a soil amendment agent. The soluble form of Al could be toxic for soil biota in very acidic soils. The Al content of bagasse biochar was very high compared to the rest of the biochars. The typical range of Al in soils vary from 10 000 to 300 000 mg/kg (EPA, 2003). The Al content of biochar from *Eucalyptus saligna* wood produced via slow pyrolysis at 400°C was found to be 103 mg/kg (Singh *et al.*, 2010). Black wattle biochar had a relatively high Ca content compared to other nutrients. That would be a problem if it is added to soil as excess Ca could limit the availability of Mg and K which could make black wattle biochar undesirable to use, unless it is used on very acid soils suffering from Ca deficiency. A similar study was done by Singh *et al.* (2010) and very high Ca contents of biochars from various feedstocks were also observed. The Ca and K contents of biochars from vineyard were similar to ones produced from the activation of *Eucalyptus saligna* and poultry litter, respectively. However, P content of poultry litter was much higher (Singh *et al.*, 2010). As was also pointed out by Singh *et al.* (2010), biochars from biosolids have much higher P and N contents compare to biochars from agricultural wastes. However, high P and N contents could cause eutrophication of surface water, which is one of the potential environmental problems. If the optimum application rate, 10 t/ha, is taken as basis, the plant available P would be 19.88 kg/ha for vineyard biochar, where P from black wattle biochar would only be 3.97 kg/ha. Phosphorus uptake of crops such as sugar beet and potato are between 4 and 39 kg/ha (Silber *et al.*, 2010). However, these are low input crops, the needs for high input crops will be more than the values given. Therefore, P and N addition would be necessary in biochar

applications into soil. All in all, biochar from vineyard should be a better fertiliser compared to the rest of the biochars.

Table 4.16: Macro, micro nutrient and heavy metals concentration in biochars (citric acid digestion) in mg/kg

Element	Black wattle	Vineyard	Sugar cane bagasse	*Concentration limits for all biosolids (EPA,2010)
		Macronutrients		
P	397±4	**1989±102**	451±32	
Ca	**13783±120**	**17177±1367**	**2181±128**	
Mg	**1349±73**	**3908±255**	**1158±71**	
K	**5670±42**	**15746±982**	**3463±271**	
Na	2205±15	672±18	289±9	
		Micronutrients		
Fe	24±2	102±7	**3953±192**	
Al	82±3.5	83±11	2955±102	
Mn	10±0.3	78±8	162±8	
Zn	**7±0.3**	**179±20**	**42±4**	**7500**
Cu	b/d	1.37±0.3	**9±0.2**	**4300**
Co	0.02±0.004	0.06±0.01	1.9±0.1	
Mo	0.1±0.003	0.02±0.01	0.01	75
		Heavy metals		
As	0.06±0.001	0.2±0.01	0.4±0.03	75
Cd	b/d	0.09±02	0.03	85
Cr	**0.13±0.02**	**0.5±0.1**	**13±1.4**	**3000**
Pb	**b/d**	**0.8±0.2**	**3.6±0.7**	**840**
Ni	**0.46±0.05**	**0.8±0.2**	**4.5±0.7**	**420**
Se	0.07±0.06	0.06±0.01	b/d	100

*on dry basis

Plants need very small amounts of micronutrients such as Mn, Fe, Co, Cu, Zn and Mo. Generally, the availability of the micronutrients and toxic cations increase with increased soil acidity. However, the availability of molybdenum decreases with increased acidity of soil pH. For instance, Mo is needed for N fixation by legumes (Bohn *et al.*, 1979). Biochars have very low contents of toxic elements compared to authorised limits given by the Environment Protection Agency (EPA) (Table 4.16). Some of the toxic elements of biochars compared to potential soil amendment biochars from slow pyrolysis of sewage sludge (Hossain *et al.*, 2011; Hossain *et al.*, 2010), *Eucalyptus saligna* wood, leaves, paper sludge, poultry litter and cow manure (Singh *et al.*, 2010) are much lower.

Silber et al. (2010) reported that CEC is strongly dependent on pH as in their study CEC of acidified biochar increased by 11.5 $cmol_c$/kg for every increased pH unit. They mentioned that exchangeable P was increased by 6.7 $cmol_c$/kg as the pH decreased from 8.9 to 4.5 pH units. At pH 4.5, approximately 90% of total Ca and Mg contents of biochar were released and under alkaline conditions the opposite trend was observed. This study reveals that exchangeable cations (Ca^{+2}, Mg^{+2}, Na^{+}, K^{+}) are released at different soil solution pH.

In conclusion, biochars contained high amounts of nutrients and trace amounts of toxic elements which make them potential soil amendments. Biochar addition with nitrogen fertiliser would be recommended due to their low nitrate content. However, using soil analytical methods on biochar is a bit of a concern since the applicability of these methods is unknown (Singh *et al.*, 2010). Further study is needed to compare different analytical methods. Further investigation on the influence of temperature, hold time and heating rate on different biomasses should be done with focus on the nutrient properties of the biochars produced.

4.2.7 BET surface areas of biochars

The BET surface areas of the biochars indicate the physical evolution of biochar during pyrolysis and are generally connected with their sorption abilities. The surface areas and porosity characteristics of the biochars are presented in Table 4.17.

Table 4.17: BET surface areas and microporosity of the biochars

Biochar	Surface area (m^2/g)	Micropore volume (cm^3/g)	Internal Surface Area (m^2/g)	Single Point Total volume of pores (cm^3/g)	Average pore diameter (nm)
Sugar cane bagasse	259	0.088	194	0.14	2.09
Black wattle	241	0.082	184	0.12	2.05
Vineyard	92	0.029	64	0.05	2.47

Biochars from sugar cane bagasse and black wattle showed high surface areas, whereas biochar from vineyard showed very low surface area. The surface area of biochar from vacuum pyrolysis of sugar cane bagasse at 530°C was found to be 529 m^2/g (Garcìa-Peréz *et al.*, 2002). Similarly, study of Carrier *et al.* (2011) showed that between temperatures of 460-540°C, the surface areas of biochars varied between 396-418 m^2/g for the vacuum pyrolysis of sugar cane bagasse. Biochars from vacuum

pyrolysis had higher surface areas than biochars from slow pyrolysis due to the higher reaction rate, therefore greater devolatilisation by using vacuum. Similar observations were made by other researchers (Nuithitikul *et al.*, 2010; Petrov *et al.*, 2007).

The activation process is commonly preferred to increase the surface area by creating new pores and enhancing pore volumes and pore diameters of existing pores that were created during pyrolysis. The surface area of sugar cane biochar can be increased up to 931- 1394 m^2/g by steam activation (Bernardo, 1997). However, using different activation agents and pre-treatment and post-treatments enhance the surface areas up to 2289 m^2/g for biochar from sugar cane bagasse (Liou, 2010). The surface area of biochar from vineyard stalks reached 1500 m^2/g by chemical activation in the study of Deiana *et al.* (2009).

The ash content of biochar could plug the pores; therefore surface areas of biochars could decrease (Shinogi & Kanri, 2003). Liou (2010) pointed out that the ash content can be reduced significantly by base leaching. Hence removal of ash allows a better interaction between the activation agent and pores, resulting in an efficient increase in mesoporous structure of biochar with a high surface area.

Comparing the surface areas of the biochars (Table 4.17) to surface areas of other adsorbents presented in Section 2.3.4.4, Table 2.14, it can be concluded that biochars from sugar cane bagasse, vineyard and black wattle do not have very high surface areas, but is likely to obtain high surface areas by an activation process. Especially for the case of vineyard biochar, the pyrolysis temperature should be increased to above 460°C to obtain a higher BET surface area.

Biochar consists of different pore sizes which give biochar its adsorption characteristics. Nitrogen adsorption on biochar was used for the porosity determination as it is commonly used for the determination of surface areas and porosity (Önal, 2006). Figure 4.4 presents the hysteresis loops in the nitrogen adsorption-desorption isotherms.

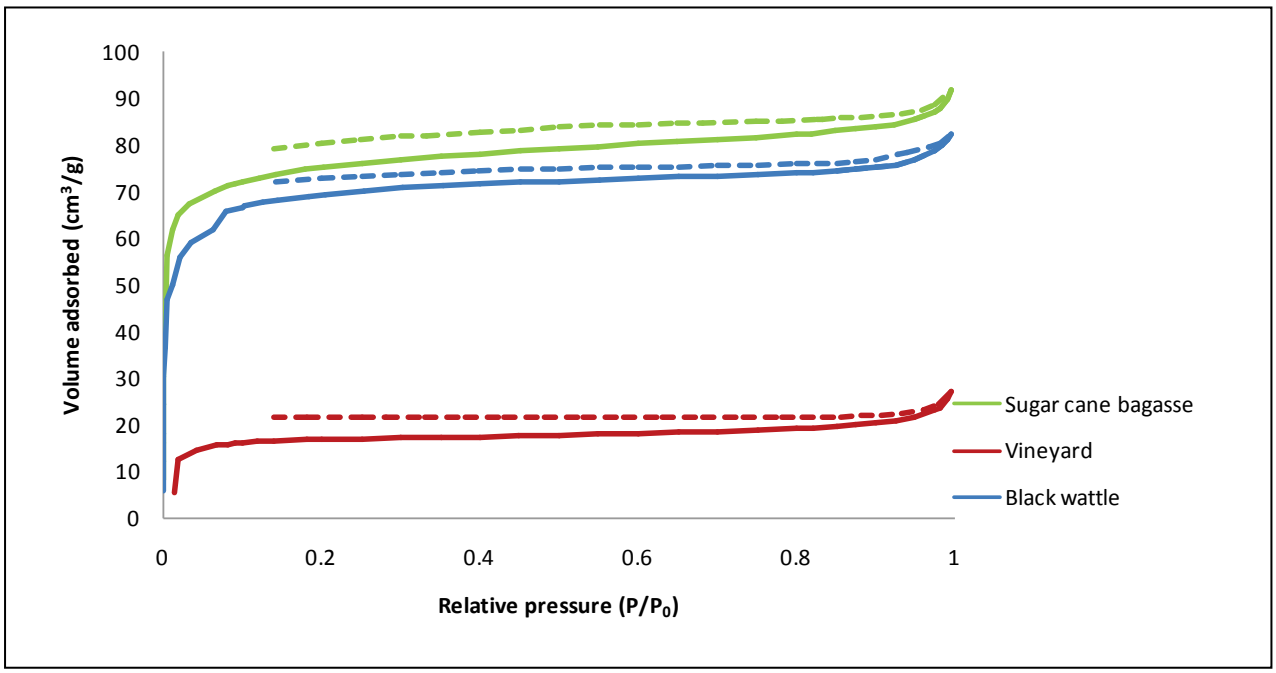

Figure 4.4: Hysteresis loops shown in the nitrogen adsorption (77K) isotherm of sugar cane bagasse, vineyard and black wattle biochars: the lower branch represents the adsorption isotherm and the upper branch represents the desorption isotherm

The adsorption-desorption isotherms of biochars were typical type I isotherms (Section 2.3.4.2, Figure 2.22) in nature, which are characteristic of microporous materials, according to the IUPAC classification (Gregg & Sing, 1982).

The adsorption curves rose sharply at relative pressures up to 0.1. Beyond this value of P/P_0 the isotherms presented a plateau with increasing relative pressure. Also the adsorption and desorption branches were parallel over relative pressure range and formed a "tail" as saturation pressure was approached. It can also be seen that the amount of nitrogen adsorbed by sugar cane bagasse biochar was slightly higher than black wattle biochar, but much higher than vineyard biochar, indicating the order of pore volumes of the biochars. The characteristic of the hysteresis loops in Figure 4.4 indicated the presence of mesopores, which is typical of Type IV hysteresis and associated with capillary condensation (Gregg & Sing, 1982).

Micropores have diameters less than 2 nm and most of the adsorption takes place due to the proximity of graphite-like walls. Mesopores and macropores on the other hand have larger diameters, 2-50 nm and >50 nm, respectively. Comparing micropore volumes of the biochars from Table 4.17, vineyard biochar had a relatively smaller micropore volume; indeed the surface area was lower. Interestingly, the meso-macropore volume of vineyard biochar was almost the same as its

micropore volume, whereas micropore volumes of other biochars were significantly higher than their meso-macropore volumes. This is in agreement with the finding of Ioannidou & Zabaniotou (2007) who emphasised that lignocellulosic composition of the biomass is related to the porosity of the biochar. Sugar cane bagasse, which is rich in cellulose, led to the production of more microporous biochar. The higher lignin content of vineyard prunings led to the production of more macroporous biochar. Macropores allow the rapid movement of water and gas through the soil. Therefore, macroporosity of the biochars would be a key function for soil aeration and hydrology. Moreover, they could provide a habitat for microbes. Mesopores hold water, thus water is stored for plants to use, whereas micropores are more involved with molecule adsorption and transport (Atkinson *et al.*, 2010; Ashman & Puri, 2002). Therefore, biochar from vineyard would not be efficient enough to provide the needs of plants by means of mineral transport.

Internal surface area refers to the micropore area, which represents the walls of slits, mainly caused by surface particle imperfections such as cracks that penetrate deeply into the interior. Internal and external surface area form total surface area, where external surface area (ESA) is non-microporous area including walls of mesopore and macropore, as well as the edges and aromatic sheets facing the outside. For typical activated carbon, ESA varies between 10 and 200 m^2/g of solid, and the discussed biochars are in the same range, indicating that with an activation process meso-macroporosity would be developed. The average pore diameters are in the range of mesopore diameters, indicating their potential in liquid-solid adsorptions such as wastewater treatments.

Liang *et al.* (2006) reported that cation exchange capacity is a function of charge density and the surface area of a biochar. Charge density of biochar is calculated by dividing its CEC value with the surface area. The charge densities of the biochars were in the following order; vineyard (0.007 $mmol/m^2$) > sugar cane bagasse (0.005 $mmol/m^2$) > black wattle (0.004 $mmol/m^2$). Surface charge is caused by negatively charged functional groups, therefore due to high charge density and CEC, nutrient retention enhances.

4.3 Methylene blue adsorption by using biochars

Adsorption from dilute aqueous solutions onto solid surfaces is an attractive separation method for many purification processes such as wastewater treatments, drinking water, and industrial effluent purification (Ioannidou & Zabaniotou, 2007). Methylene blue is used for many colourisation purposes including leather, plastics, cotton, etc. Methylene blue is commonly the preferred model

compound for adsorption purposes in the scientific world to determine quality of the adsorbent. In this section, the quality of biochars by means of methylene blue removal efficiency will be investigated.

4.3.1 Effect of initial solution concentration and contact time on adsorption

The effects of initial solution concentration and contact time on adsorption were investigated. The temperature could not be controlled within a range of ±1°C due to technical problems. But all the adsorption experiments have been done at the same time in order to work under the same temperature conditions.

Methylene blue is a basic solution. However; in this study low concentrations of the MB solutions showed acidic characteristics, meaning more H^+ ions were available in the solution. According to Weber, adsorption of a solute to the interior surfaces of an adsorbent may involve four steps; bulk transport, film transport, intraparticle transport and adsorption on the active sites of the adsorbent (Abdelrasoul, 2006).

It was observed that the amount of dye adsorbed (mg/g) increased for all biochars as the contact time was increased and reached equilibrium (Figure 4.5). The graphs for 15, 10 and 5 ppm MB solutions were magnified in Figure 4.5 in order to clarify the adsorption for these concentrations. The overall adsorption of MB by vineyard, black wattle and sugar cane bagasse at different concentrations (20 to 5 ppm) can be found in Appendix C. The standard deviations were very low to be shown on the graphs; hence the deviations were given in Appendix D.

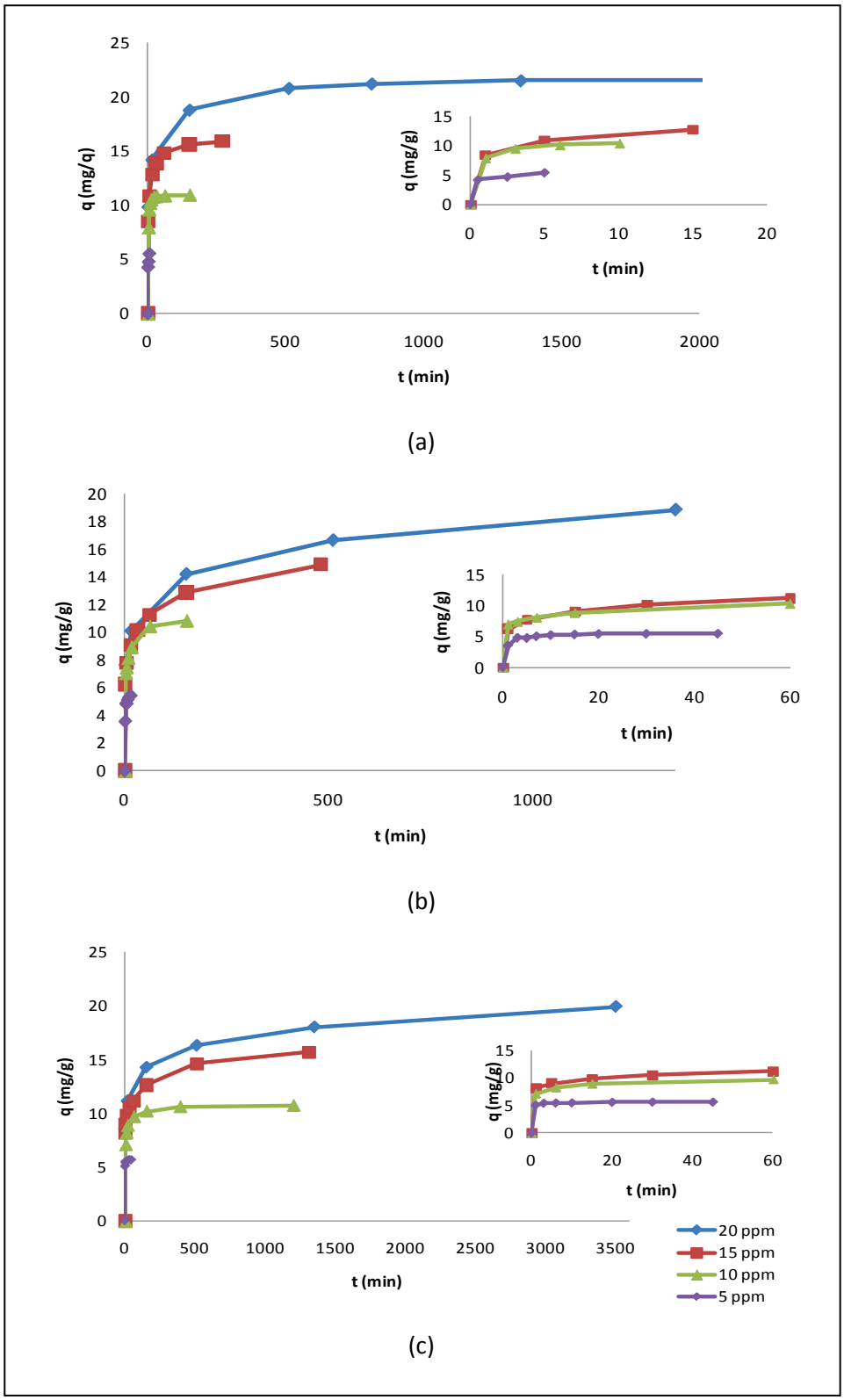

Figure 4.5: Adsorption capacities of biochars at different initial solution concentrations with increased contact time; (a) sugar cane bagasse, (b) black wattle and (c) vineyard

The equilibrium time was determined from the experimental data based on the study of Gerçel *et al.* (2007). They defined the equilibrium point as the last data just before stabilisation of the q (mg/g) versus t (min) graph. The equilibrium times found to be 3505 min for 20 ppm dye solution for vineyard biochar. The equilibrium time decreased as the initial solution concentration decreased. The equilibrium time was 1315, 1200 and 45 min for 15, 10 and 5 ppm dye solutions, respectively. For black wattle biochar, equilibrium time was relatively lower. The equilibrium time was 1350, 480, 150 and 15 min for 20, 15, 10, 5 ppm dye solutions, respectively. For sugar cane bagasse biochar, the equilibrium time was much lower; 150, 60, 20 and 5 min for 20, 15, 10 and 5 ppm dye solutions, respectively. The amount of dye removed at equilibrium increased from 5.7 to 19.9 mg/g, 5.4 to 18.8 mg/g and 10.8 to 18.8 mg/g with the increase in the dye concentration from 5 to 20 ppm for vineyard, black wattle and sugar cane bagasse biochar, respectively. It is important to note that these equilibrium values were decided with available data points and with more data points, more accurate equilibrium times can be obtained.

It was also observed that the initial stage of adsorption was rapid, and as soon as biochar was in contact with dye solution, approximately 40% of dye removal occurred in a minute for maximum dye concentration. As contact time was increased, adsorption rate was decreased and reached a plateau. This may be attributed to the gradual decrease in the concentration driving force with an increase in contact time (Karaca *et al.*, 2008). The same trend was also observed by other researchers (Tan *et al.*, 2007; Kavitha & Navasivayam, 2007). This might be attributed to the amount of available vacant sites on the biochar surface, which with the aid of rapid mixing increases the external mass transport (Kavitha & Navasivayam, 2007). From Figure 4.5, it is clear that adsorption rate was in order of sugar cane bagasse > black wattle > vineyard. The adsorption characteristic of a biochar is determined by its porous structure and surface chemistry. The reason for long contact time for vineyard biochar could be attributed to its surface area (smaller internal surface area), which would take a relatively longer time for all dye particles to diffuse into active sites of the biochar. It can be deduced that the adsorption rate is related to surface areas of the adsorbents, which enhance the adsorption process excluding the effect of temperature and initial solution pH.

While the amount of adsorbed methylene blue increased with contact time, the percentage of MB removal also increased with contact time (Figure 4.6). The percentage of MB removal increased from 0 to 89% in 3505 min and as contact time was increased, the removal increased to 96% for vineyard biochar with 20 ppm initial solution concentration. The same trend occurred for black wattle and sugar cane bagasse biochars.

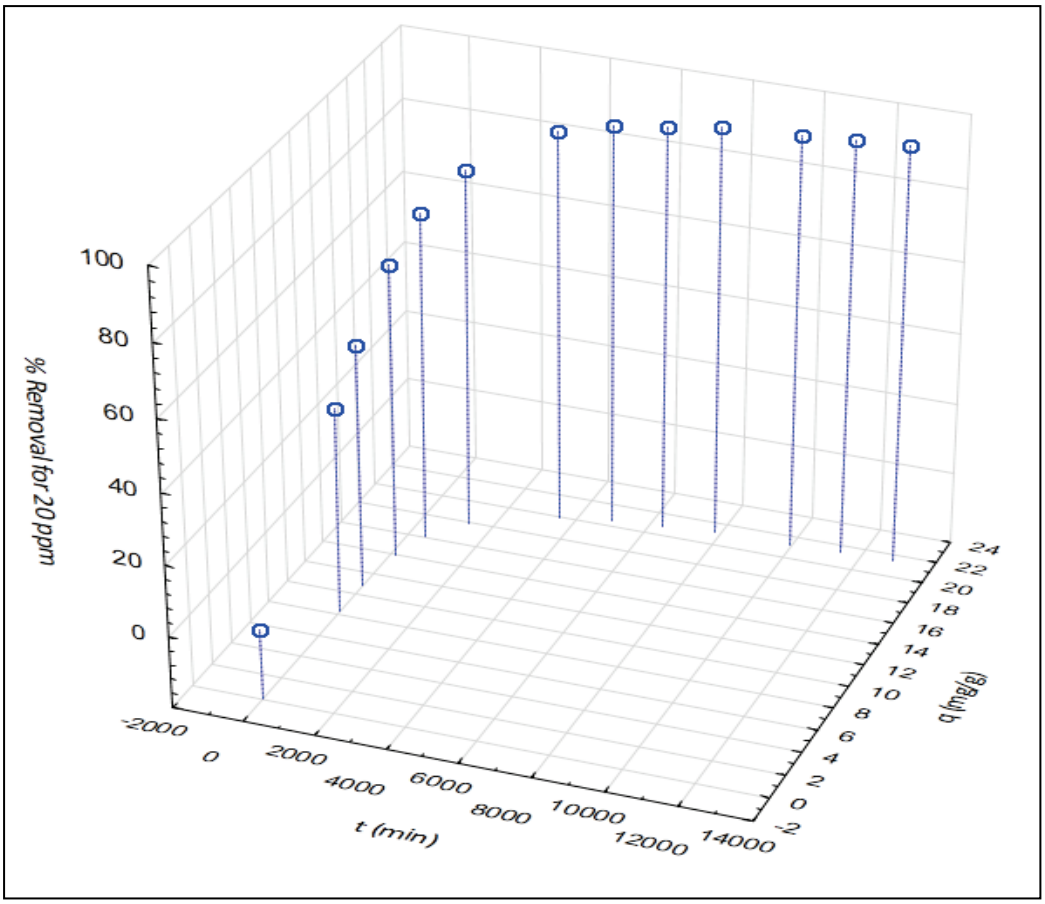

Figure 4.6: Percentage removal versus time and adsorption capacity for vineyard biochar with 20 ppm initial dye concentration

The percentage removal at equilibrium decreased from 98% to 89%, 98% to 85% and almost 100% to 85% when the initial solution concentration increased from 5 to 20 ppm for vineyard, black wattle and sugar cane bagasse biochars, respectively. As the solution concentration increases, the mass transfer driving force becomes larger to overcome mass transfer resistance, resulting in higher adsorption (Nasuha *et al.*, 2010).

During the experiments the pH values of the solutions were measured, but the methylene blue solution-biochar mixture has a complex matrix. It has been observed that the initial pH of the solutions were increased from pH 5-6 to pH 8-9, once black wattle and vineyard biochars were added to the solutions. The pH of the methylene blue solution-biochar mixture stayed between pH 5-6 when sugar cane bagasse biochar was added, which means sugar cane bagasse biochar did not have an influence on pH due to its low pH, 6.56. For black wattle and vineyard biochars, as contact time increased, the pH of the mixture started to decrease. The pH of the mixtures at equilibrium is

shown in Figure 4.7. Higher equilibrium pH values were observed for lower initial solution concentrations.

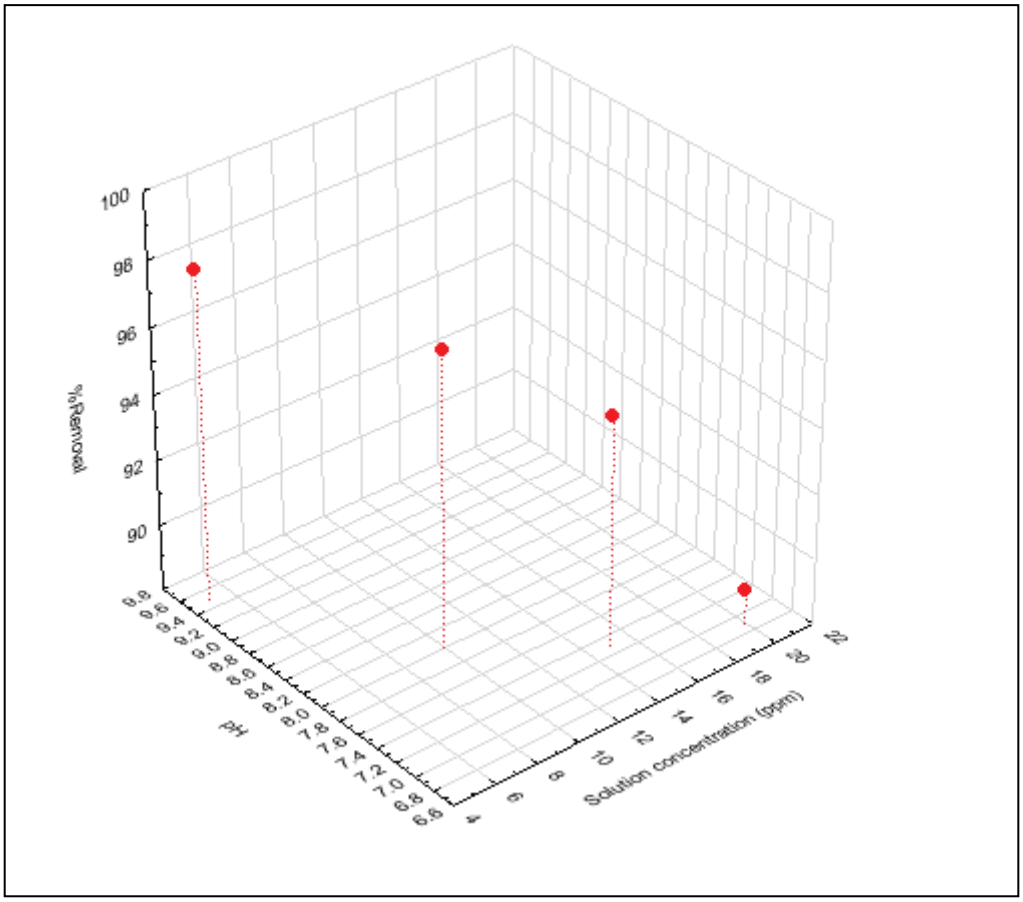

Figure 4.7: Percentage removal versus initial solution concentration and pH of the mixture for vineyard biochar at equilibrium

The initial pH of methylene blue solution was 5-6 which was also observed by Wang *et al.* (2005), who observed relatively longer equilibrium times (longer than 21000 min for the adsorption of methylene blue by commercial activated carbons). Here the pH of the initial solution gained importance. As biochar is considered to be an amphoteric solid, both negative and positive surface charges exist in aqueous solution. However, the availability of surface charges to interact with dye ions depend on the initial solution pH. If the pH of the solution is higher than the aforementioned pH point of zero charge value of biochar, the surface of biochar tends to be negatively charged; therefore more cations would be attracted to the biochar surface due to the electrostatic attractions. When solution pH < pH_{PZC}, the inverse charge appears on the biochar surface; therefore biochar attracts more anions. Many researchers studied the effect of initial solution pH on the adsorption of methylene blue and concluded that high pH increases the attraction between cations and a negatively charged surface, hence adsorption capacity increased (Nasuha *et al.*, 2010; Gerçel

et al., 2007). The optimum pH values vary in literature; Nasuha *et al.* (2010) suggested a pH value between 4 and 8, whereas Ravikumar *et al.* (2005) observed the optimum pH value as 13.4. However, it can be assumed that low pH would increase the H^+ ions in the solution, resulting in a competition between H^+ ions and the cation groups on the dye for adsorption sites (Nasuha *et al.*, 2010).

4.3.2 Adsorption isotherms

The experimental data are analysed according to the Freundlich and Langmuir isotherms as an indication of how the adsorption molecule distribute between the liquid phase and the biochar when the adsorption process reaches equilibrium. The plot of log amount of dye adsorbed (q_e) versus log concentration (C_e) has been shown in Figure 4.8 for the Freundlich isotherm. For the Langmuir isotherm C_e/q_e has been plotted against C_e in Figure 4.9. The fourth data point (5 ppm) could not be used because the adsorption was already completed for 5 mg/L MB solution in 150 minutes. Therefore, three data points represent 20, 15, 10 mg/L initial MB concentrations right to left, respectively. The applicability of the isotherm models to the adsorption study done was compared by judging the correlation coefficients (R^2 values) which are shown in Table 4.18.

Table 4.18: Freundlich and Langmuir isotherm model constants and correlation coefficients

Isotherms	**Biochar**	**Constants**		R^2	**p**
		K_F (mg/g(L/mg)$^{1/n}$)	1/*n*		
Freundlich	Vineyard	10.54	0.15	0.997	0.013
	Black wattle	11.58	0.10	0.995	0.014
	Sugar cane bagasse	16.59	0.12	0.999	0.011
Langmuir	**Biochar**	q_{max} (mg/g)	*b* (L/mg)	R^2	**p**
	Vineyard	15.15	1.83	0.998	0.013
	Black wattle	14.49	4.06	0.996	0.014
	Sugar cane bagasse	19.23	8.67	0.995	0.011

t-test at a confidence level of 95%, $p < 0.05$

The Freundlich isotherm is based on the assumption of heterogeneous surface energies (Tan *et al.*, 2007). K_F can be defined as the adsorption coefficient, which represents the amount of dye adsorbed onto biochar for a unit of equilibrium concentration. The K_F results show that the highest amount of dye adsorbed on the sugar cane bagasse biochar, whilst the lowest amount of dye adsorbed onto vineyard biochar. The value 1/*n* is a measure of adsorption intensity or surface heterogeneity. The values of 1/*n* shows more heterogeneous biochar as the value gets closer to zero (Hameed *et al.*,

2007), hence black wattle biochar can be considered to be a little bit more heterogeneous than the rest of the biochars. The *n* values are higher than 1 which suggests that adsorption of MB by biochars is favourable. Tan *et al.* (2007) observed that K_F increased when temperature was increased from 30 to 40°C, but as temperature was increased to 50°C, the K_F value for adsorption by oil palm fibre activated carbon decreased. On the other hand, Gerçel *et al.* (2007) observed an increase in K_F value when the adsorption temperature was increased from 20 to 40°C for adsorption by *Euphorbia rigida* activated carbon. Kavitha & Namasivayam (2007) reported that higher initial solution pH leads to an increase, but higher solution concentration causes a decrease in K_F value for adsorption by coir pith carbon. In their study the K_F and 1/n values were determined as 0.845 mg/g(l/mg)$^{1/n}$ and 1.38 for 20 ppm initial solution, respectively.

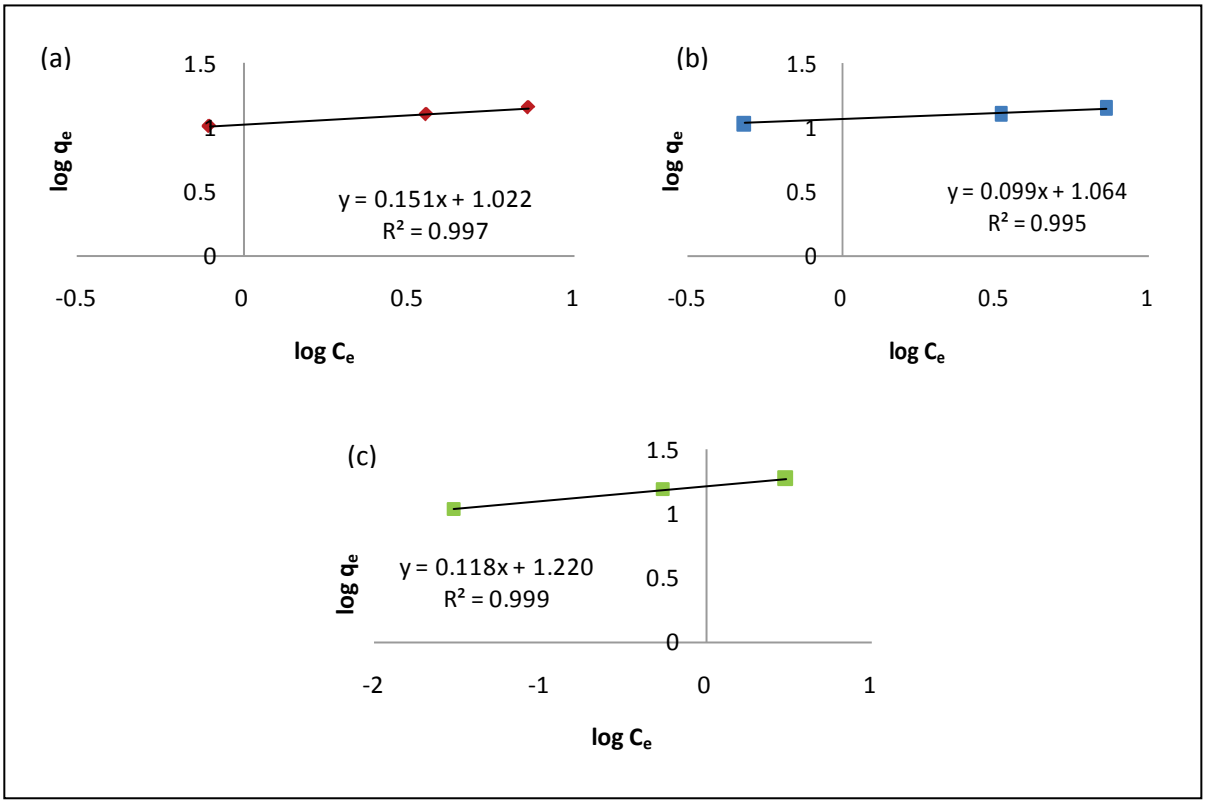

Figure 4.8: Freundlich isotherms for the adsorption of MB by (a) vineyard, (b) black wattle and (c) sugar cane bagasse biochars

The Langmuir isotherm suggests that the maximum adsorption capacity corresponds to a complete monolayer of dye molecules on the biochar surface with constant energy and no transmission of adsorbate in the plane of the biochar surface (Hameed *et al.*, 2007).

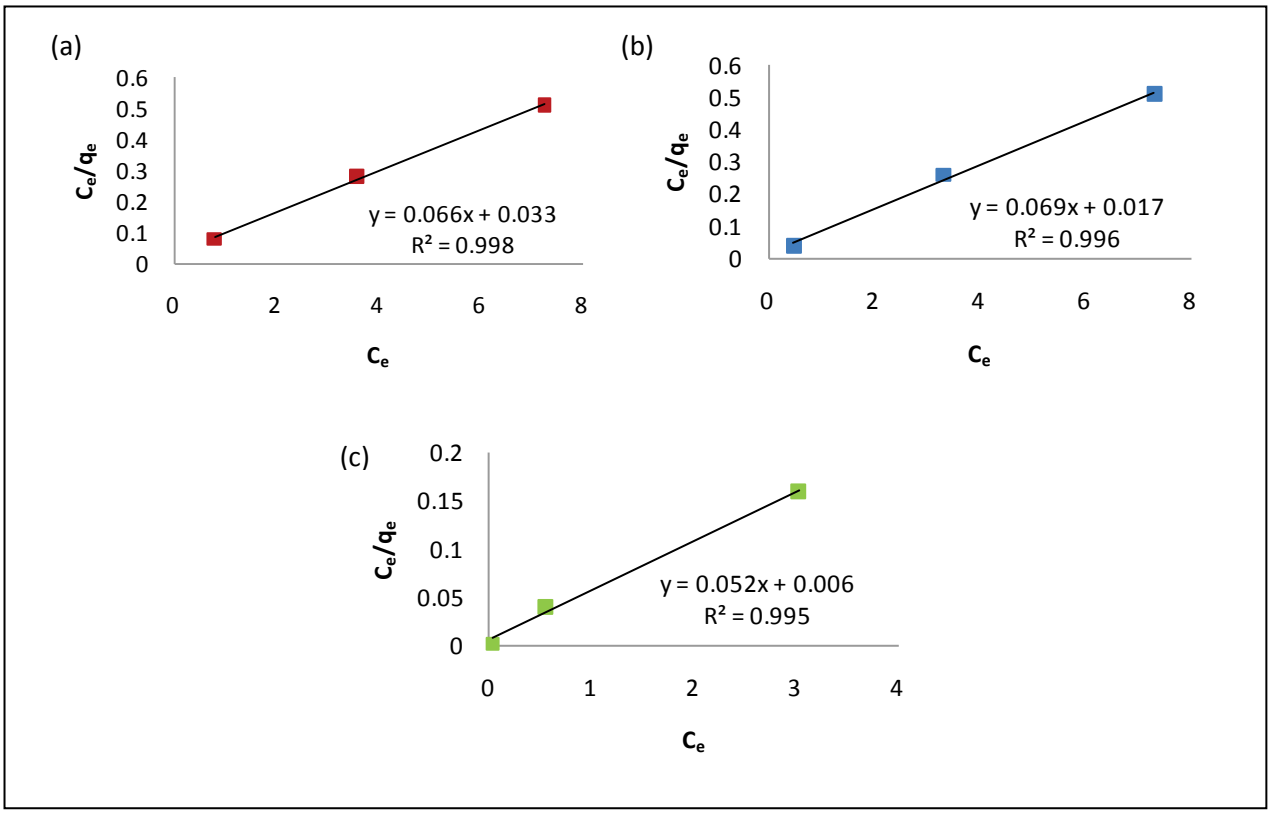

Figure 4.9: Langmuir isotherms for the adsorption of MB by (a) vineyard, (b) black wattle and (c) sugar cane bagasse biochars

Biochar from sugar cane bagasse showed the highest maximum adsorption capacity (19.23 mg/g) due to its negatively charged surface and high BET area. However, one would expect black wattle biochar to have higher adsorption capacity than vineyard biochar, which cannot be seen in Table 4.18. The reason for this is that a lower adsorption capacity of black wattle biochar was observed for a 20 ppm initial solution concentration. The maximum adsorption capacities were compared to literature data in Table 4.19. It can be deduced that the biochars produced in this study are better adsorbents than the ones which were shown in Table 4.19. However, the differences in experimental conditions would have an influence on adsorption capacities. The maximum adsorption capacities of adsorbents vary from 2.4 mg/g (Kadirvelu *et al.*, 2003) to 412 mg/g (Attia *et al.*, 2008) and even higher depending on the experimental conditions and the physico-chemical characteristics of the adsorbent.

Table 4.19: Comparison of adsorption capacities of different activated carbons for the removal of methylene blue

Activated carbon source	q_{max} (mg/g)	Reference
Rice husk	9.83	Sharma & Uma, 2010
Coconut coir	15.59	Sharma *et al.*, 2009
Coconut tree sawdust	4.7	Kadirvelu *et al.*, 2003
Silk cotton hull	2.4	Kadirvelu *et al.*, 2003
Corn cob	5	Kadirvelu *et al.*, 2003
Banana pith	4.67	Kadirvelu *et al.*, 2003
Vineyard biochar	15.15	This study
Black wattle biochar	14.49	This study
Sugar cane bagasse biochar	19.23	This study

The Langmuir constant *b* is an indication of adsorption energy and rate of adsorption. The highest *b* value was observed for adsorption by biochar from sugar cane bagasse, while the lowest b value was observed for adsorption by biochar from vineyard. During the experiments, faster removal of MB by sugar cane bagasse biochar was also observed, followed by black wattle and vineyard. This observation is supported by the Langmuir constants. The values for the dimensionless equilibrium parameter, R_L for the biochars are 0.02, 0.01 and 0.004 for vineyard, black wattle and sugar cane bagasse biochars, respectively. These values confirmed that biochars are favourable ($0<R_L<1$) for adsorption of MB under the conditions used in this study. It can be seen in Table 4.18 that both models fit the MB adsorption by biochars as illustrated by R^2 values. However the Freundlich model showed a better fit for biochar from sugar cane bagasse, whereas the Langmuir model could be a better model to be used for vineyard and black wattle biochars. Therefore it could be deduced that the Langmuir isotherm model tends to show a better fit for the adsorption sytems with a high energy uptake rate due to the low solution concentration.

4.3.3 Adsorption kinetics

The adsorption kinetics describes the rate of solute uptake, which is important for designing effective adsorption plants (Ho & McKay, 1999). Several models can be used to express the adsorption mechanism. The simplified models; pseudo-first-order (Lagergren, 1898), pseudo-second-order (Ho & McKay, 1999) and intraparticle diffusion (Weber & Morris, 1963) have been widely applied. Table 4.20 reveals the kinetic constants for MB adsorption at 20 ppm dye concentration, assuming 1350 min is the equilibrium time needed. It should be noted that the limited time used

does not correspond to a true equilibrium state since vineyard biochar requires a longer period, whereas sugar cane bagasse requires a shorter period which was mentioned in Section 4.3.1.

Table 4.20: Comparison of the pseudo-first-order, pseudo-second-order and intraparticle diffusion models for 20 ppm solution concentration

	Pseudo-first-order kinetic model					
	$q_{e,exp}$ (mg/g)	**k_1 (1/min)**	**$q_{e,cal}$ (mg/g)**	**R^2**	**SSE (%)**	**p**
Vineyard	17.93	0.003	7.78	0.934	5.07	0.01
Black wattle	18.77	0.003	9.18	0.950	4.80	0.02
Sugar cane bagasse	21.57	0.005	8.64	0.936	6.47	0.05
	Pseudo-second-order kinetic model					
	$q_{e,exp}$ (mg/g)	**k_2 (g/mg min)**	**$q_{e,cal}$ (mg/g)**	**R^2**	**SSE (%)**	**p**
Vineyard	17.93	0.002	18.18	0.998	0.11	0.01
Black wattle	18.77	0.002	18.87	0.998	0.04	0.02
Sugar cane bagasse	21.57	0.004	21.74	1.000	0.08	0.05
	Intraparticle diffusion model					
	$q_{e,exp}$ (mg/g)	**k_p (mg/g $min^{1/2}$)**	**$q_{e,cal}$ (mg/g)**	**R^2**	**SSE (%)**	**p**
Vineyard	17.93	0.253	18.87	0.910	0.42	0.01
Black wattle	18.77	0.296	19.90	0.916	0.51	0.02
Sugar cane bagasse	21.57	0.305	23.48	0.759	0.86	0.05

t-test at a confidence level of 95%, $p < 0.05$

Reversible reactions of MB ions and biochar may be represented as (Ho & McKay, 2000):

$$A^- + (MB)^+ \overset{k_a}{\leftrightarrow} AMB$$

or

$$HA + (MB)^+ \overset{k_a}{\leftrightarrow} AMB + H^+$$

The pseudo-first order kinetic model is based on solid capacity (Ho & McKay, 1999). The k_a refers to adsorption rate which is represented as k_1 in Table 4.20. The adsorption rates for vineyard and black wattle were approximately the same according to the pseudo-first order model. The adsorption rate for sugar cane bagasse was a little bit higher. The calculated q_e values did not agree with experimental q_e values. The validity of each model was determined by the sum of error squares (SSE, %). The lower the value of SSE and higher the correlation coefficient (R^2) is, the better the model fits. However, the correlation coefficient values can be considered as low. This indicates that the adsorption is not likely to be a first-order reaction. The linearised plots for adsorption by biochars are shown in Figure 4.10. Comber *et al.* (1996) reported a complex multi-step process for long equilibrium times. This multi-step process is essentially based on three independent first order

reactions for short (5 min), long (600 min), very long (12 000 min) periods of times. However, Ho & McKay (1999) suggested that the pseudo-second order model could be used for short or long equilibrium times.

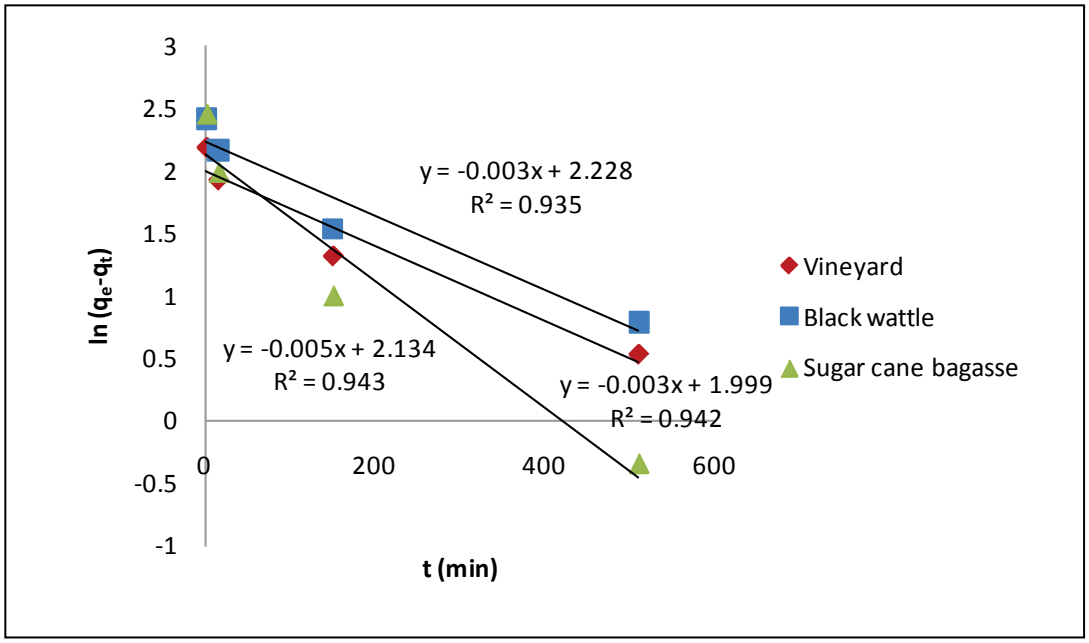

Figure 4.10: Pseudo-first-order adsorption kinetics of MB onto vineyard, black wattle and sugar cane bagasse biochars

The pseudo-second-order kinetic model is based on solid phase sorption, which describes a chemisorption rather than physical adsorption. Here k_a refers to k_2 in Table 4.20. It can be observed that the adsorption rate of sugar cane bagasse was relatively higher than vineyard and black wattle. The rate of pseudo-second-order reaction is assumed to be dependent on chemisorptions involving valence forces through exchange of electrons between adsorbent and sorbate (Ho & McKay, 1999). Although the acidic surface functionalities of black wattle was higher than vineyard (NMR studies, Section 4.2.3), according to calculations adsorption rate of vineyard was the same as the adsorption rate of black wattle. The reason for this could be higher film diffusion of solute from the solution onto the external surface across the boundary layer of vineyard biochar (Kavitha & Namasivayam, 2007). Ho & McKay (1999) reported that q_e is a function of temperature, initial ion concentration, adsorbent dose and nature of solute-adsorbent interaction. In this study temperature, initial ion concentration and adsorbent doses were the same. Therefore, solute-sorbent interaction gains importance regarding q_e values. The calculated q_e values were in order of sugar cane bagasse> black wattle> vineyard, which was the same order as the surface acidity of the biochars. The correlation coefficient values were above 0.99 (Figure 4.11); indicating pseudo-second order kinetic model is the correct model to explain the dynamics of adsorption processes of MB with these biochars. The SSE

(%) values are close to zero indicating the experimental and calculated q_e values were close to each other. The pseudo-second-order adsorption kinetic model is one of the best models to determine the overall adsorption kinetics. Therefore; the graphs for pseudo-second-order adsorption kinetics were shown in Appendix F. These graphs clearly indicated the differences of adsorption rates.

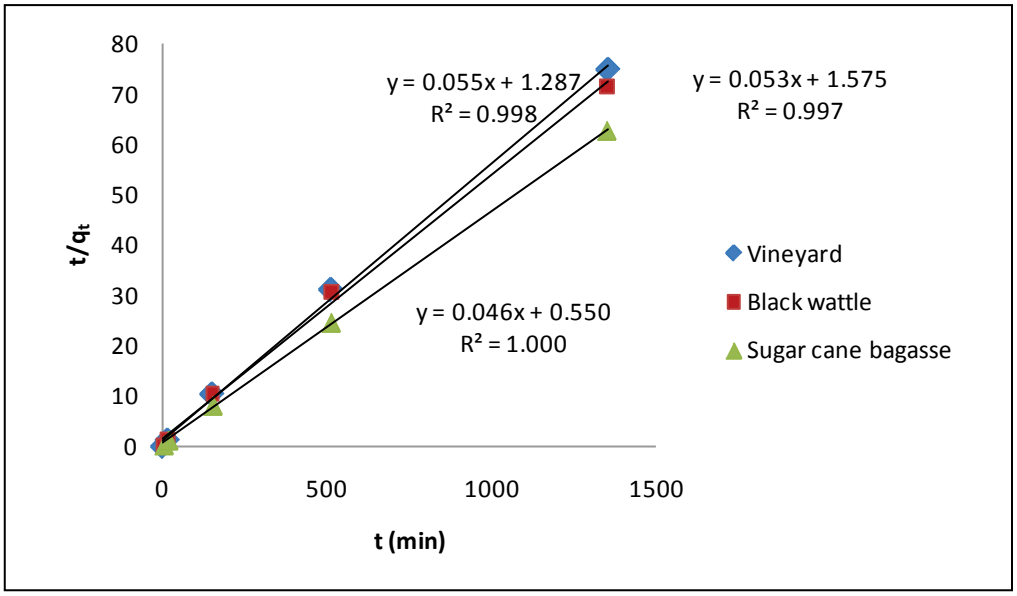

Figure 4.11: Pseudo-second-order adsorption kinetics for MB onto vineyard, black wattle and sugar cane bagasse biochars.

The adsorption kinetic data was further processed to determine if intraparticle diffusion was rate limiting, therefore intraparticle rate constants were calculated (Table 4.21) via Figure 4.12. The boundary layer diffusion gives the initial part of the plot and the gradual adsorption stage represents the rate limiting intraparticle diffusion and finally the equilibrium stage takes place where intraparticle diffusion slows down due to the low concentration of the solute (Sun & Yang, 2003). If the plot passes through the origin, it is accepted that intraparticle diffusion is the rate controlling step (Gerçel *et al.*, 2007). When the plot does not pass through the origin, it indicates some degree of boundary layer control. That means intraparticle diffusion is involved in the adsorption process, but it is not the only rate limiting step (Mahmoodi *et al.*, 2011). The intercept (*C*) which is termed as the intraparticle diffusion constant (mg/g), indicated the thickness of the boundary layer; 12.28, 9.57 and 9.02 for adsorption by sugar cane bagasse, vineyard and black wattle respectively. The boundary layer thickness can be defined as the distance from the adsorbent where the concentration of the diffusing species reaches 99% of the bulk concentration (Fogler, 2006). It indicates the tendency of ions to adsorb on the adsorbent surface. High thicknesses show higher adsorption capacities (Igwe *et al.*, 2008), which can also be observed from Figure 4.12. The highest intraparticle adsorption rate

was observed for adsorption of MB by sugar cane bagasse. As is known, the rate of transport is affected by the structure of the adsorbent and its interaction with the solute (Itodo *et al.*, 2010). In general, adsorption is controlled by the intraparticle diffusion due to the microporosity of the adsorbent. Considering micropore volumes of the biochars, it would also be expected that diffusion rate for sugar cane bagasse would be higher than black wattle and vineyard. Therefore, the micropore volumes of the biochars were in agreement with the intraparticle diffusion rates. However, intraparticle diffusion model did not really agree with the experimental data.

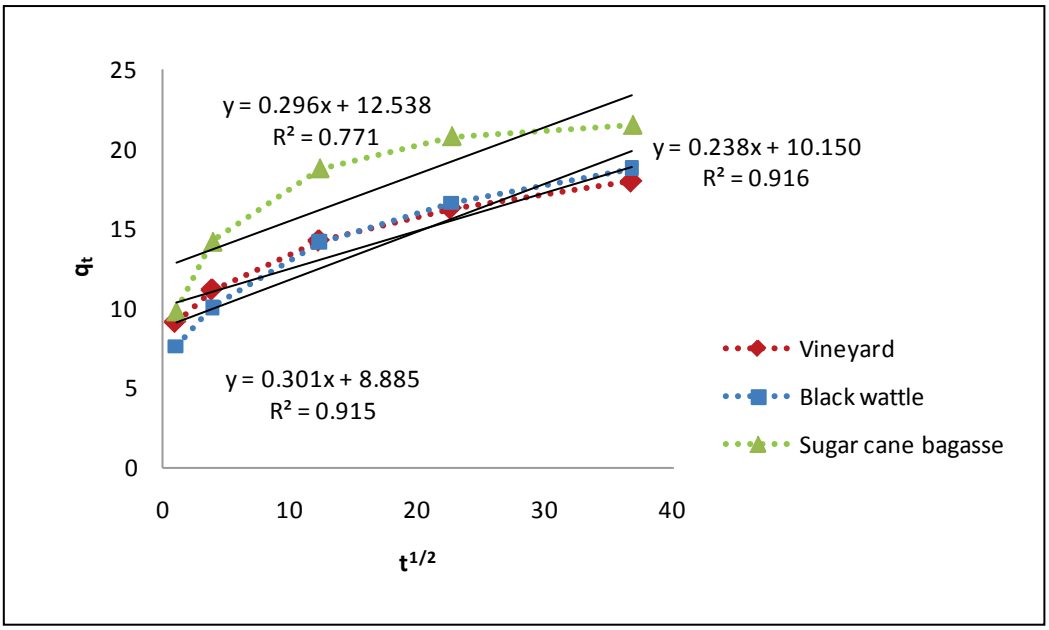

Figure 4.12: Intraparticle diffusion models for adsorption of MB by vineyard, black wattle and sugar cane bagasse biochars.

As was mentioned earlier, initial ion concentration affects the adsorption kinetics. Figure 4.13 shows the effect of initial solution concentration on adsorption rate and adsorption amount for pseudo-second-order kinetics and intraparticle diffusion rate and C values (intervals) of MB adsorption by vineyard biochar.

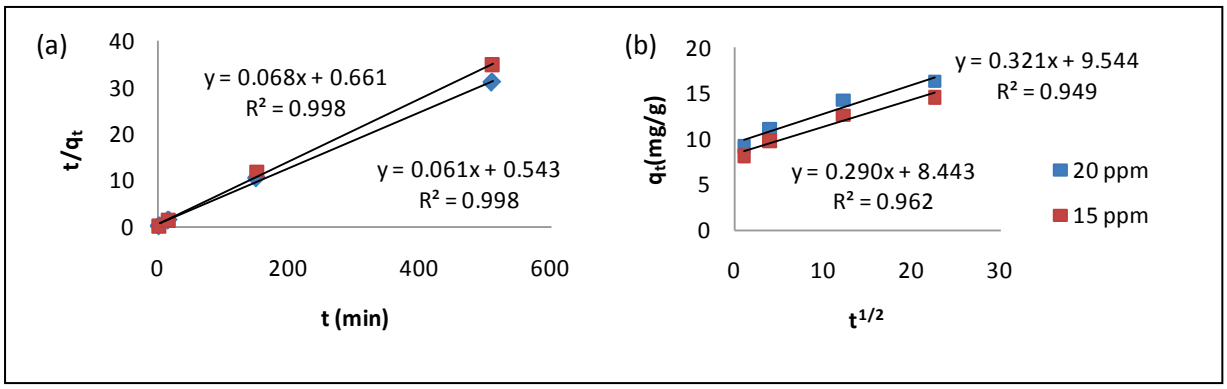

Figure 4.13: (a) Pseudo-second-order kinetics, (b) intraparticle diffusion kinetic models for 20 and 15 ppm MB adsorption by vineyard biochar

As the solution concentration increased, adsorption capacity (q_e) increased. This was also discussed in Section 4.3.1. However, the adsorption rate decreased for the pseudo-second-order model due to the increase in solution concentration. The intraparticle diffusion rate and interval thickness of the boundary layer showed an increase with increased solution concentration (Table 4.21,) indicating that as initial concentration increases, the possibility of the adsorbate to diffuse into the interior pores of the biochar increases due to the increased driving force of diffusion. These trends were also reported by other researchers (Mahmoodi *et al.*, 2011; Hameed *et al.*, 2007; Kavitha &Namasivayam, 2007).

Table 4.21: Kinetic constants for dye adsorption at 20 and 15 ppm

Dye concentration(ppm)	q_e (mg/g)	k_2	R^2	k_p	C	R^2	p
	Pseudo-second-order			Intraparticle diffusion			
15	14.71	0.0067	0.998	0.298	8.151	0.967	0.02
20	16.13	0.0066	0.998	0.341	8.928	0.938	0.01

t-test at a confidence level of 95%, $p < 0.05$

In conclusion, contact time and initial solution concentration had a great effect on adsorption. Percentage removal and adsorption capacity increased with contact time. However, percentage removal decreased with initial solution concentrations due to the larger mass driving forces to overcome mass transfer resistances. The Langmuir and the Freundlich adsorption models have fitted the adsorption by biochars. However, Freundlich isotherm was a better model for adsorption by sugar cane bagasse biochar, while the Langmuir showed a slightly better fit than the Freundlich for the adsorption by black wattle and vineyard biochars. The order of maximum adsorption capacity

was: vineyard < black wattle < sugar cane bagasse, suggesting sugar cane bagasse biochar was a better adsorbent than the rest of the biochars.

The pseudo-second-order reaction model was found to be the best model to explain the adsorption kinetics. The rates of adsorption were in order of vineyard < black wattle < sugar cane bagasse. The rate of adsorption by sugar cane bagasse was found to be much higher than the ones of vineyard and black wattle biochars. This information was supported by pseudo-second-order overall adsorption kinetics and presented in Appendix F. It was also deduced that intraparticle diffusion was not the only rate controlling step during adsorption and initial solution concentration had an effect on adsorption kinetics.

CHAPTER 5: CONCLUSIONS AND RECOMMENDATIONS

This study focused on the potential of biochars from vacuum pyrolysis of black wattle, vineyard prunings and sugar cane bagasse (460-475°C, 8-8.5 kPa, 13-17°C/min) as soil amendment and adsorbent.

5.1 Conclusions

- The major ash components of sugar cane bagasse were found to be silicon (68.7% SiO_2) and iron (9.54% Fe_2O_3), while calcium (42.79% CaO) and potassium (26.44% K_2O) was the main elements in the ash of vineyard prunings. The inorganics depend on the type of the biomass, growing, harvesting and environmental conditions.

- The vacuum pyrolysis of the biomass resulted in the production of biochar, liquid and gas. The biochar yields were 23.5 %, 31.0% and 19.7% on weight basis for black wattle, vineyard and sugar cane bagasse, respectively. The pyrolysis conditions as well as biomass nature influenced the pyrolytic product yields.

- Comparing the products from wood based biomasses, namely black wattle and vineyard prunings, it was concluded that larger particle size leads to a decrease in gas, but an increase in biochar production, due to the enhanced secondary reactions.

- The higher biochar yield from vineyard prunings was due to the influence of higher lignin and ash composition of the biomass.

- The percentages of carbon, nitrogen, hydrogen and ash increased, whereas oxygen percentage decreased in biochars in comparison to raw materials as a result of the pyrolysis process. Biochars from black wattle and vineyard prunings contained higher amounts of carbon than biochar from sugar cane bagasse, whereas biochar from sugar cane bagasse contained higher amounts of oxygen.

- The O/C and H/C values can be used as an indication of presence of functional groups and aromatic carbon structures. The Van Krevelen diagram was used to show the influence of pyrolysis temperature on O/C and H/C values and it was deduced that sugar cane bagasse

biochar exhibits a low degree of carbonisation, whereas biochar from vineyard prunings exhibits a higher degree of carbonisation.

- The highest surface acidity was observed for sugar cane bagasse (2.3 mmol/g), whereas the highest basicity was observed for vineyard (1.67 mmol/g). These results were in agreement with pH, FTIR and NMR analysis.

- The nature of the biomass as well as pyrolytic conditions influenced surface functional groups present on the biochar surface. Vacuum pyrolysis of biomasses at 460 °C resulted in higher acidic functional groups on biochar surfaces compared to slow and fast pyrolysis studies from literature.

- The aromaticity of biochars was in the order of vineyard > black wattle > sugar cane bagasse, implying vineyard and black wattle biochars would take longer to decay in soil which would be advantageous by means of nutrient availability and water retention as well as contribution to greenhouse gas mitigation via storage of carbon for long terms.

- Under the same pyrolysis conditions, wood based biochar had higher aromacity than herbaceous industrial residue based biochar.

- Sugar cane bagasse biochar was rich in aliphatic carbon, whereas aliphatic carbon percentages of black wattle and vineyard were very low. Higher aliphatic content of sugar cane bagasse biochar was also correlated with FTIR analysis. Polar carbon content of biochars were in the order of sugar cane bagasse > black wattle > vineyard which was in agreement with molar (O+N)/C ratios.

- The pH values of biochars were 6.56, 9.74 and 10.43 for sugar cane bagasse, black wattle and vineyard, respectively. Slightly acidic character of sugar cane bagasse biochar was in contrast with literature.

- The C/N ratios of biochars were found to be 32.3, 29.6, and 42.8 for black wattle, vineyard and sugar cane bagasse, respectively. These values were an indication of nitrogen immobilisation; however the recalcitrant nature of biochars is able to overcome this problem.

- The cation exchange capacities of biochars were in order of sugar cane bagasse (122 cmol/kg) > black wattle (101 cmol/kg) > vineyard (65 cmol/kg), which can be considered as high compared to biochars from slow and fast pyrolysis. The CEC values correlate well with O/C ratios of the biochars. Vacuum pyrolysis contributed to the presence of functional groups, which was the reason for their high cation exchange abilities compared to literature.

- Electrical conductivities were found to be more correlated with feedstock nature. The results were in order: vineyard (0.83 dS/m) > black wattle (0.67 dS/m) > sugar cane bagasse (0.17 dS/m). The EC values correlated well with pH values of the biochars.

- Biochars contained substantial amounts of plant-available nutrients. However, plant available NO_3^- was low. Biochars are low in toxic elements. Lesser amount of nutrients in sugar cane bagasse makes it unattractive as soil amendment.

- BET surface areas were found to be 259 m^2/g, 241 m^2/g and 91 m^2/g for sugar cane bagasse, black wattle and vineyard respectively, which would improve the soil properties such as nutrient retention.

- The nitrogen adsorption isotherms were typical of type I, which was indicative of microporosity and hysteresis loops were typical of type IV indicating the presence of mesopores. Since the micropores in biochars are more involved with molecular transport, vineyard biochar would not be as efficient as black wattle and sugar cane bagasse in molecular transport in soil due to its lower amounts of micropores.

- Vacuum pyrolysis is a preferable pyrolysis technique for biochar production for soil amendment purposes by producing biochars with high CEC, plant available nutrients and more surface functionalities.

- Batch methylene blue (model compound) adsorption studies showed that the amount of dye adsorbed increased when initial solution concentrations were increased. The adsorption capacities increased with initial increased contact time and reached equilibrium. Considering experimental data points that were obtained, the experimental equilibrium time were found to be approximately 3505 min, 1350 min, 150 min for adsorption of 20 mg/L methylene blue solution for vineyard, black wattle and sugar cane bagasse, respectively. These results were

attributed to the chemical structure of the biochars as well as physical structures such as BET surface areas, particularly internal surface areas.

- The experimental equilibrium fitted the Langmuir and Freundlich models. The Freundlich model showed a better fit for sugar cane bagasse, whereas the Langmuir model had a better fit for vineyard and black wattle biochars. However, these models should be investigated with more data points at different solution temperatures and higher solution concentrations. The maximum adsorption capacities of biochars were found to be 15.15 mg/g, 14.49 mg/g and 19.23 mg/g for vineyard, black wattle and sugar cane bagasse. These values suggest that the mentioned biochars are better adsorbents than some of the activated carbons such as rice husk (9.83 mg/g) and corn cob (5 mg/g). However, these values are highly dependent on experimental conditions and physico-chemical characteristics of the adsorbents.

- Methylene blue adsorption onto biochars followed the pseudo-second-order kinetic model. The second-order adsorption rates were found to be the same for adsorption by vineyard and black wattle biochars (0.002 g/mg min), whereas adsorption rate was 0.004 g/mg min for adsorption by sugar cane bagasse biochar. The calculated q_e values were similar to the experimental ones and in order of sugar cane bagasse> black wattle > vineyard, which was in the order of the presence of surface acidity on the biochars. The intraparticle diffusion model was found to be involved in the adsorption process, but it was not the only rate limiting step. As solution concentration was increased, the second-order adsorption rate decreased, but the intraparticle diffusion rate and the interval which indicated the thickness of the boundary layer increased. These findings could be used as baseline data to conduct further investigations on adsorption kinetics and thermodynamics.

- All in all, sugar cane bagasse was found to the best adsorbent for the removal of cationic dyes due to its high BET surface area and the presence of hard Lewis acidic functionalities. Sugar cane bagasse could be also more preferable for nutrient retention purposes. Nevertheless, black wattle and vineyard biochars were found to be a better soil amendment due to higher amounts of nutrients. However, higher CEC and BET surface area of black wattle make it more preferable to vineyard biochar. Therefore, it can be said that black wattle was the best biochar for soil amendment purposes.

Table 5.1: Summary of physico-chemical properties of biochars and their intended usage

Physico-chemical property	Intended application	Suitable biochar	Result	Expected effect	Additional requirements
pH in water	Addition to acidic soils	Vineyard & Black wattle	$pH_{Vineyard}$ =10.43; $pH_{Black\ wattle}$= 9.74	Liming effect	none
pH in water	Addition to slightly basic soils	Sugar cane bagasse	pH=6.56	Neuralisation of soil pH	none
Cation Exchange Capacity (CEC)	Addition into nutrient deficient soils	Sugar cane bagasse & Black wattle	$CEC_{Sugar\ cane\ bagasse}$= 122 cmol/kg; $CEC_{Black\ wattle}$= 101 cmol/kg	Nutrient retention	none
Oxygen containing functional groups	-	Sugar cane bagasse	O/C = 0.49	Increase in CEC	none
Aromatic C content	Addition to soils	Vineyard & Black wattle	Vineyard= 86%; Black wattle= 84%	Resistance to microbial decay; therefore restriction for C/N immobilisation. Longer sequestration of carbon in soil	none
Electrical Conductivity (EC)	Addition into soils	Vineyard & Black wattle& Sugar cane bagasse	$EC_{Vineyard}$= 0.83 dS/m; $EC_{Black\ wattle}$= 0.67 dS/m; $EC_{Sugar\ cane\ bagasse}$= 0.17 dS/m	Not a substantial change is expected	None

Physico-chemical property	Intended application	Suitable biochar	Result	Expected effect	Additional requirements
Water Soluble Nutrients	Addition into soils	Vineyard & Black wattle	Vineyard= 6522 mg/kg; Black wattle= 5626 mg/kg	Increase in water soluble nutrients	Nitrogen fertilizer addition is essential.
Citric acid soluble macro and micro nutrients	Addition into nutrient deficient soils	Vineyard & Black wattle	Vineyard= 39263 mg/kg; Black wattle= 23527 mg/kg	Increase in plant available nutrients	Nitrogen fertilizer addition is essential.
BET surface area	Addition into soils	Sugar cane bagasse & Black wattle	$BET_{Sugar\ cane\ bagasse}$= 259 m^2/g; $BET_{Black\ wattle}$= 241 m^2/g	Increase in mineral transport from soil to plant and sorption of heavy metals from soils to biochar	none
BET surface area	Adsorption of wastewater (Model compound= Cationic methylene blue solution)	Sugar cane bagasse	$BET_{Sugar\ cane\ bagasse}$= 259 m^2/g	Efficient adsorption of cationi wastewaters	Steam activation can improve surface area. For vineyard and black wattle biochars chemical activation can lead a better improvement on surfaces of abovementioned biochars

Table 5.2: Production conditions for application based biochars

Application	The best biochar	Production conditions
Soil amendment	Black wattle	Biomass particle size= +850 nm; T_f= 475^{0}C; HR= 15-13^{0}C/min; P= 8.5 kPa_{abs}
Wastewater treatment	Sugar cane bagasse	Biomass particle size= 425-850 nm; T_f= 460^{0}C; HR= 17^{0}C/min; P= 8 kPa_{abs}

5.2 Recommendations

- If the aim is biochar production, it would be better to use vineyard prunings, but for substantial production of biochar and bio-oil, black wattle is a potential biomass to be preferred under optimised conditions. Both vineyard and black wattle biochars should be tested in pot trials to observe soil-biochar-plant interactions.

- Sugar cane bagasse can be used to balance the pH of slightly basic soils due to its slightly acidic pH. It could be beneficial to balance soil pH around pH 6-7 as most nutrients are plant available in this range of pH.

- Nitrogen fertiliser should be supplemented when applying the biochars into soil and the amount of biochar should be calculated carefully before addition into soil to prevent any soil salinisation problems and nutrient imbalances. Another suggestion is pyrolysis of a biomass with a nitrogen resource to increase the plant available nitrate in biochar. It could be advantageous for waste management of both agricultural residues and animal waste.

- Citric acid and nitric acid digestion methods should be compared in order to evaluate the analytic methods for biochar characterisation as soil amendments.

- Further study on the effect of pyrolysis conditions (e.g. temperature, hold time) on the chemical properties of biochars which are essential for soil properties (e.g. cation exchange capacity, surface acidity, pH, plant available nutrient content) is needed to produce high quality biochars for soil amendment.

- Further studies on economy and energy are required to ensure that biochar as soil amendment is beneficial.

- Further investigations on adsorption equilibrium, kinetics and thermodynamics are needed to optimise the adsorption by biochars. Higher initial concentrations of solution should be used in order to use equilibrium and kinetic models more efficiently. Different wastewaters should be tested to obtain maximum adsorption abilities of the biochars.

REFERENCE LIST

ABDELFATTAH, M.A., SHAHID, S.A., OTHMAN, Y.R. 2009. Soil salinity mapping model developed using RS and GIS- a case study from Abu-Dhabi, United Arab Emirates. *Europian Journal of Scientific Research*, 26: 342-351.

ABDELRASOUL, F. 2006. Application of adsorption model for dye removal. *Tenth International Water Technology Conference*, Alexandria, Egypt, 2006.

ABDULLAH, H., MEDIASWANTI, K.A., WU, H. 2010. Biochar as a fuel: 2. Significant differences in fuel quality and ash properties of biochars from various biomass components of Mallee trees. *Energy & Fuels*, 24: 1972-1979.

AHMAD, A.L., LOH, M.M., AZIZ, J.A. 2007. Preparation and characterisation of activated carbon from oil palm wood and its evaluation on Methylene blue adsorption. *Dyes and Pigments*, 75: 263-272.

AHMED, A., PAKDEL, H., ROY, C., KALIAGUINE, S. 1989. Characterization of the solid residues of vacuum pyrolysis of *Populus tremuloides*. *Journal of Analytical and Applied Pyrolysis*, 14: 281-294.

AHMED, M.S., ZAMIR, M.R., SANAULLAH, A.F.M. 2006. Active acidity, reserve acidity, clay content and CEC of some tea soils of Bangladesh. *International Journal of Agriculture and Biology*, 8: 89-92.

ALFARRA, A., FRACKOWIACK, E., BÉGUIN, F. 2004. The HSAB concept as ameant to interpret the adsorption of metal ions onto activated carbons. *Applied Surface Science*, 228: 84-92.

ALLEN, T. 1997. Particle size measurement: Volume 2. 5th Ed. USA: Chapman & Hall.

ALLEN, S.J., KOUMANOVA, B. 2005. Decolourisation of water/wastewater using adsorption. *Journal of the University of Chemical Technology and Metallurgy*, 40(3): 175-192.

ANTAL, M.J., VARHEGYI, G. 1995. Cellulose pyrolysis kinetics: the current state of knowledge. *Industrial and Engineering Chemical Research*, 34: 703-717.

ASHMAN, M.R., PURI, G. 2002. Essential soil science: a clear and concise introduction to soil science. UK: Blackwell Science.

ATKINSON, C.J., FITZGERALD, J.D., HIPPS, N.A. 2010. Potential mechanisms for achieving agricultural benefits from biochar application to temperate soils: a review. *Plant Soil*, 337: 1-18.

ATTIA, A.A., GIRGIS, B.S., FATHY, N.A. 2008. Removal of methylene blue by carbons derived from peach stones by H_3PO_4 activation: batch and column studies. *Dyes and Pigments*, 76: 282-289.

BAGREEV, A., BANDOSZ, T.J., LOCKE, D.C. 2001. Pore structure and surface chemistry of adsorbents obtained by pyrolysis of sewadge sludge-derived fertilizer. *Carbon*, 39: 1971-1979.

BANDOSZ, T.J., ANIA, C.O. 2006. Surface chemistry of activated carbons and its characterization. *In* Activated Carbon Surfaces in Enviromental Remediation. USA: Elsevier, 159:229.

BANSAL, R.C. 1988. Active Carbon. New York: Dekker.

BARRETT, E.P., JOYNER, L.G., HALENDA, P.P. 1951. The determination of pore volume and area distributions in porous substances: I. Computations from nitrogen isotherms. *Journal of American Chemical Society*, 73: 373-380.

BEAR, F.E. 1965. Soils in relation to crop growth. USA: Reinhold Publishing Co.

BEAUMONT, O., SCHWOB, Y. 1984. Influence of physical and chemical parameters on wood pyrolysis. *Industrial and Engineering Chemistry Process Design and Development*, 23: 637-641.

BENALLAL, B., ROY, C., PAKDEL, H., CHABOT, S., POIRIER, M.A. 1995. Characterization of pyrolytic light naphta from vacuum pyrolysis of used tyres comparison with petroleum naphta. *Fuel*, 74: 1589-1594.

BIERMAN, C.J. 1996. Handbook of pulping and paper making. 2nd Ed. USA: Academic Press.

BILBA, K., OUENSANGA, A. 1996. Fourier transform infrared spectroscopic study of thermal degradation of sugar cane bagasse. *Journal of Analytical and Applied Pyrolysis*, 38: 61-73.

BINIAK, S., SZYMAŃSKI, G., SIEDLEWSKI, J., ŚWIATKOWSKI, A. 1997. The characterization of activated carbons with oxygen and nitrogen surface groups. *Carbon*, 35: 1799-1810.

BOEHM, H.P. 1994. Some aspects of the surface chemistry of carbon blacks and other carbons. *Carbon*, 32: 759-769.

BOEHM, H.P. 2002. Surface oxides on carbon and their analysis: a critical assessment. *Carbon*, 40: 145-149.

BOHN, H.L., MCNEAL, B.L., O'CONNOR, G.A. 1979. Soil Chemistry. New York, USA: Wiley.

BOUCHELTA, C., MEDJRAM, M.S., BERTRAND, O., BELLAT, J.P. 2008. Preparation and characterization of activated carbon from date stones by physical activation with steam. *Journal of Analytical and Applied Pyrolysis*, 82: 70-77.

BOUCHER, M.E., CHAALA, M., ROY, C. 2000. Bio-oils obtained by vacuum pyrolysis of softwood bark as a liquid fuel for gas turbines. Part I: properties of bio-oil and its blends with methanol and a pyrolytic aqueous phase. *Biomass and Bioenergy*, 19: 337-350.

BREWER, C.E., SCHMIDT-ROHR, K., SATRIO, J.A., BROWN, R.C. 2009. Characterization of biochar from fast pyrolysis and gasification systems. *Environmental Progress and Sustainable Energy*, 28: 386-396.

BRIENZO, M., SIQUEIRA, A.F., & MILAGRES, A.M.F. 2009. Search for optimum conditions of sugarcane bagasse hemicelluloses extraction. *Biochemical Engineering Journal*, 46: 199-204.

BRIDGWATER, A.V. 1994. Advances in thermochemical biomass conversion. Volume 2. London: Blackie Academic.

British Petroleum Statistical Review of World Energy. 2010. http://www.bp.com/statisticalreview Date of Access: 18 Aug. 2010.

BROWN, A.G., KO, H.C. 1997. Black wattle and its utilization- Abridged English edition. Rural industries research and development corporation. http://www.dpie.gov.au/rirdc Date of access: 9 Sep. 2010.

BROWN, R.A., KERCHER, A.K, NGUYEN, T.H., NAGLE, D.C., BALL, W.P. 2006. Production and characterization of synthetic wood chars for use as surrogates for natural sorbents. *Organic Geochemisty*, 37: 321-333.

BROWNING, B.L. 1969. The chemistry of the wood. New York: John Wiley and sons Interscience Publishers.

BROWNSORT, P.A. 2009. Biomass pyrolysis processes: performance parameters and their influence on biochar system benefits. University of Edinburgh. Edinburgh. UK. (Thesis-M.Sc.). http://www.era.lib.ed.ac.uk/bitstream/1842/3116/1/Brownsort%20PA%20MSc%202009.pdf. Date of Access: 10 Sep 2010.

BRUNNER, R., & ROBERTS, P.V. 1980. The significance of heating rate on char yield and char properties in the pyrolysis of cellulose. *Carbon*, 18: 217-224.

BRUNAUER, S., EMMETT, P.H., TELLER, E. 1938. Adsorption of gases in multimolecular layers. *Journal of American Chemical Society*, 60: 309-319.

BUAH, W.K., CUNLIFFE, A.M., WILLIAMS, P.T. 2007. Characterization of products from the pyrolysis of municipal solid waste. *Process Safety and Environmental Protection*, 85: 450-457.

BÜSCHER, P., KOEDAM, N., VAN SPEYBROECK, D. 1990. Cation-exchange properties and adaptation to soil acidity in bryophytes. *New Phytology*, 115: 177-186.

BUSTOS, G., MOLDES, A.B., CRUZ, J.M., DOMÍNGUEZ, J.M. 2004. Production of fermentable media from vine-trimming wastes and bioconversion into lactic acid by *Lactobacillus pentosus*. *Journal of the Science of Food and Agriculture*, 84: 2105-2112.

BUTT, H.J., GRAF, K., KAPPL, M. 2003. Physics and chemistry of interfaces. Weinheim: Wiley-VHC.

ÇAĞLAR, A. 2007. Catalytic pyrolysis of biomass: influence on the yields of liquid product of structural composition of biomass. *Kastamonu Education Journal*, 15: 651-660.

CAO, N., DARMSTADT, H., SOUTRIC, F., ROY, C. 2002. Thermogravimetric study on the steam activation of charcoals obtained by vacuum and atmospheric pyrolysis of softwood bark residues. *Carbon*, 40: 471-479.

CARRIER, M., HUGO, T., GORGENS, J., KNOETZE, H. 2011. Comparison of slow and vacuum pyrolysis of sugar cane bagasse. *Journoul of Analytical and Applied Pyrolysis*, 90: 18-26.

CAVALAGLIO, G., COTANA, S. 2007. Recovery of vineyards pruning residues in an agro-energetic chain. *15th Biomass Conference and Exhibition*, Berlin, 2007.

CETIN, E., MOGHTADERI, B., GUPTA, R., WALL, T.F. 2004. Influence of pyrolysis conditions on structure and gasification reactivity of biomass chars. *Fuel*, 83: 2139-2150.

CHAN, K.Y., VAN ZWIETEN, L., MESZAROS, I., DOWNIE, A., JOSEPH, S. 2007. Agronomic values of greenwaste biochar as a soil amendment. *Australian Journal of Soil Research*, 45: 629-634.

CHAN, K.Y., VAN ZWIETEN, L., MESZAROS, I., DOWNIE, A., JOSEPH, S. 2008. Using poultry litter biochars as soil amendments. *Australian Journal of Soil Research*, 46:437-444.

CHEN, X., JEYASEELAN, S., GRAHAM, N. 2002. Physical and chemical properties study of activated carbon made from sewadge sludge. *Waste Management*, 22: 755-760.

CHENG, H.N., WARTELLE, L.H., KLASSON, T.K., EDWARDS, J.C. 2010. Solid-state NMR and ESR studies of activated carbons produced from pecan shells. *Carbon*, 48: 2455-2469.

CHENG, C.H., LEHMANN, J. 2009. Ageing of black carbon along a temperature gradient. *Chemosphere*, 75: 1021-1027.

CHENG, C.H., LEHMANN, J., ENGELHARD, M.H. 2008. Natural oxıdatıon of black carbon in soils: changes in molecular form and surface along a climosequence. *Geochimica et Cosmochimica Acta*, 72: 1598-1610.

CHENG, C.H., LEHMANN, J., THIES, J.E., BURTON, S.D., ENGELHARD, M.H. 2006. Oxidation of black carbon by biotic and abiotic processes. *Organic Geochemistry*, 37: 1477-1488.

CHENJE, M., MOHAMMED-KATERERE, J. 2006. Invasive alien species. *Africa Environment Outlook 2*. United Nations Environment Program, 331-347.

CHUN, Y., SHENG, G., CHIOU, C.T., XING, B. 2004. Compositions and sorptive properties of crop residue-derived chars. *Environmental Science and Technology*, 38: 4649-4655.

COATES, J. 2000. Interpretation of Infrared Spectra, a practical approach. *In* Encyclopedia of Analytical Chemistry. USA: John Wile & Sons Ltd, 10815-10837.

COMBER, S.D.W., GARDNER, M.J., GUNN, A.M., WHALLEY C. 1996. Kinetics of trace metal sorption to estuarine suspended particulate matter. *Chemosphere*, 33: 1027-1040.

CORCHO-CORRAL, B., OLIVARES-MARÍN, M., FERNÁNDEZ-GONZÁLEZ, C., GÓMEZ-SERRANO, V., MACÍAS-GARCÍA, A. 2006. Preparation and textural characterization of activated carbon from vine shoots (*Vitis vinifera*) by H_3PO_4- chemical activation. *Applied Surface Science*, 252: 5961-5966.

CORWIN, D.L., LESCH, S.M. 2003. Application of soil electrical conductivity to precision agriculture: theory, principles, and guidelines. *Agronomy Journal*, 95: 455-471.

DARMSTADT, H., GARCIA-PEREZ, M., CHAALA, A., CAO, N., ROY, C. 2001. Co-pyrolysis under vacuum of sugar cane bagasse and petroleum residue: properties of char and activated char products. *Carbon*, 39: 815-825.

DARMSTADT, H., PANTEA, D., SUMMCHEN, L., ROLAND, U., KALIAGUINE, S., ROY, C. 2000. Surface and bulk chemistry of charcoal obtained by vacuum pyrolysis of bark: influence of feedstock moisture content. *Journal of Analytical and Applied Pyrolysis*, 53: 1-17.

DEGROOT, W.F., SHAFIZADEH, F. 1984. The influence of exchangeable cations on the carbonization of biomass. *Journal of Analytical and Applied Pyrolysis*, 6: 217-232.

DE JONGH, W.A. 2001. Possible applications for vacuum pyrolysis in the processing of waste materials. Stellenbosch: SU. (Thesis-M.Sc.)

DE NEERGAARD, A., SAARNAK, C., HILL, T., KHANYILE, M., BERSOZA, A.M., BIRCH-THOMSEN, T. 2005. Australian wattle species in the Darkensberg region of South Africa- An invasive alien or a natural resource. *Agricultural Systems*, 85: 216-233.

DEIANA, A.C., SARDELLA, M.F., SILCA, H., AMAYA, A., TANCREDI, N. 2009. Use of grape stalk, a waste of viticulture industry, to obtain activated carbon. *Journal of Hazardous Materials*, 172: 13-19.

DEMEYER, A., VOUNDI NKANA, J.C., VERLOO, M.G. 2001. Characteristics of wood ash and influence on soil properties and nutrient uptake: an overview. *Bioresource Technology*, 77: 287-295.

DEMIRBAS, A. 2004. Effects of temperature and particle size on bio-char yield from pyrolysis of agricultural residues. *Journal of Analytical and Applied Pyrolysis*, 72: 243-248.

DEMİRBAŞ, A. 2007. The influence of temperature on the yields of compounds existing in bio-oils obtained from biomass samples via pyrolysis. *Fuel Processing Technology*, 88: 591-597.

DEMIRBAS, A. 2008. Bio-fuels from agricultural residues. *Energy Resources*, 30: 101-109.

DEMİRBAŞ, A.& ARIN, G. 2002. An overview of biomass pyrolysis. *Energy Sources*, 24: 471-482.

DEVNARAIN, P.B., ARNOLD, D.R., DAVIS, S.B. 2002. Production of activated carbon from South African sugarcane bagasse. *Proceedings of South African Sugar Technologists Association*, 76: 477-489.

DI BLASI, C., BRANCA, C., & GALGANO, A. 2010. Biomass screening for the production of furfural via thermal decomposition. *Industrial and Engineering Chemistry Research*, 49: 2658-2671.

DIAS, B.O., SILVA, C.A., HIGASHIKAWA, F.S., ROIG, A., & SÁNCHEZ-MONEDERO, M.A. 2010. Use of biochar as bulking agent for the composting of poultry manure: effect on organic matter degradation and humification. *Bioresource Technology*, 101: 1239-1246.

DUMAN, G., ONAL, Y., OKUTUCU, C., ONENC, S., YANIK, J. 2009. Production of activated carbon from pine cone and evaluation of its physical, chemical, and adsorption properties. *Energy & Fuels*, 23, 2197-2204.

EL QADA, E.N., ALLEN, S.J., WALKER, G.M. 2008. Adsorption of basic dyes from aqueous solution onto activated carbons. *Chemical Engineering Journal*, 135: 174-184.

EL-HALWANY, M.M. 2010. Study of adsorption isotherms and kinetic models for methylene blue adsorption on activated carbon developed from Egyptian rice hull (Part II). *Desalination*, 250: 208-213

ENCINAR, J.M., BELTRÁN, F.J., BERNALTE, A., RAMIRO, A., GONZÁLEZ, J.F. 1996. Pyrolysis of two agricultural residues: olive and grape bagasse. Influence of particle size and temperature. *Biomass and Bioenergy*, 11: 397-409.

ERTAŞ, M., ALMA, M.H. 2010. Pyrolysis of laurel (*Laurus nobilis L.*) extraction residues in a fixed-bed reactor: characterization of bio-oil and bio-char. *Journal of Analytical and Applied Pyrolysis*, 88: 22-29.

FENGEL, D., WEGNER, G. 2003. Wood. Germany: Kessel Verlag, Remagen.

FIGUEIREDO, J.L. 1989. Pyrolysis of olive wood. *Biological Wastes*, 28: 217-225.

FISHER, T., HAJALIGOL, M., WAYMACK, B., KELLOGG, D. 2002. Pyrolysis behaviour and kinetics of biomass derived materials. *Journal of Analytical and Applied Pyrolysis*, 62: 331-349.

FOGLER, H.S. 2006. Elements of chemical reaction engineering. USA: Pearson Education, Inc.

FU, P., HU, S., XIANG, J., LI, P., HUANG, D., JIANG, L., ZHANG, A., ZHANG, J. 2010. FTIR study of pyrolysis products evolving from typical agricultural residues. *Journal of Analytical and Applied Pyrolysis*, 88: 117-123.

FU, P., HU, S., XIANG, J., SUN, L., YANG, T., ZHANG, A., WANG, Y. 2009. Structural evolution of maize stalk particles during pyrolysis.

FUENTE, E., MENÉNDEZ, J.A., DÍEZ, M.A., SUÁREZ, D., MONTES-MORÁN, M.A. 2003. Infrared spectroscopy of carbon materials: a quantum chemical study of model compounds. *Journal of Physical Chemistry*, 107: 6350-6359.

GARCÌA-PÉREZ, M., CHAALA, ROY, C. 2002. Vacuum pyrolysis of sugarcane bagasse. *Journal of Analytical and Applied Pyrolysis*, 65: 111-136.

GARCÌA-PÉREZ, M., CHAALA, A., PAKDEL, H., KRETSCHMER, D., ROY, C. 2007. Vacuum pyrolysis of softwood and hardwood biomass comparison between product yields and bio-oil properties. *Journal of Analytical and Applied Pyrolysis*, 78: 104-116.

GARG, U.M., KAUR, M.P., GARG, V.K., SUD, D. 2007. Removal of hexavalent chromium from aqueous solution by agricultural waste biomass. *Journal of Hazardous Materials*, 140: 60-68.

GASKIN, J.W., SPEIR, A., MORRIS, L.M., OGDEN, L., HARRIS, K., LEE, D., DAS, K.C. 2007. Potential for pyrolysis char to affect soil moisture and nutrient status of a loamy sand soil. *Proceedings of the 2007 Georgia Water Resources Conference*. Georgia.

GASKIN, J.W., SPEIR, R.A., HARRIS, K., DAS, K.C., LEE, R.D., MORRIS, L.A., FISHER, D.S. 2010. Effect of peanut hull and pine chip biochar on soil nutrients, corn nutrient status, and yield. *Agronomy Journal*, 102: 623-633.

GASPARD, S., ALTENOR, S., DAWSON, E.A., BARNES, P.A., OUENSANGA, A. 2007. Activated carbon from vetiver roots: gas and liquid adsorption studies. *Journal of Hazardous Materials*, 144: 73-81.

GERÇEL, Ö., ÖZCAN, A., ÖZCAN, A.S., GERÇEL, H.F. 2007. Preparation of activated carbon from a renewable bio-plant of *Euphorbia rigida* by H_2SO_4 activation and its adsorption behavior in aqueous solutions. *Applied Surface Science*, 253: 4843-4852.

GLASER, B., HAUMAIER, L., GUGGENBERGER, G., ZECH, W. 2001. The Terra Preta phenomenon: a model for sustainable agriculture in the humid tropics. *Naturwissenschaften*, 88: 37-41.

GLASER, B., LEHMANN, J., ZECH, W. 2002. Ameliorating physical and chemical properties of highly weathered soils in the tropics with charcoal- a review. *Biology and Fertility of Soils*, 35: 219-230.

GONZÁLEZ, J.F., RAMIRO, A., GONZÁLEZ-GARCÍA, C.M., GAÑÁN, J., ENCINAR, J.M., SABIO, E., RUBIALES, J. 2005. Pyrolysis of almond shells: energy applications of fractions. *Industrial and Engineering Chemistry Research*, 44: 3003-3012.

GOYAL, H.B., SEAL, D., SAXENA, R.C. 2008. Bio-fuels from thermochemical conversion of renewable resources: a review. *Renewable and Sustainable Energy Reviews*, 12: 504-517.

GOYAL, A., ANWAR, A.M., KUNIO, H., HIDEHIKO, O. 2007. Properties of sugarcane bagasse ash and its potential as cement-Pozzolana Binder. *Twelfth International Colloquium on Structural and Geotechnical Engineering*, Cairo: Egypt.

GRACE, J. 2004. Understanding and managing global carbon cycle. *Journal of Ecology*: 92: 189-202.

GRAY, M.R., CORCORAN, W.H., GAVALAS, G.R. 1985. Pyrolysis of a wood-derived material: effects of moisture and ash content. *Industrian and Engineering Chemistry Process Development*, 24: 646-651.

GREGG, S.J., SING, K.S.W. 1982. Adsorption, surface area and porosity. 2nd Ed. London: Academic Press.

GRØNLI, M., ANTAL, M.J. 2003. The art, science, and technology of charcoal production. *Industrial and Engineering Chemical Research*, 42: 1619-1640.

GUO, Y., BUSTIN, R.M. 1998. FTIR spectroscopy and reflectance of modern charcoals and fungal decayed woods: implications for studies of inertinite in coals. *International Journal of Coal Geology*, 37: 29-53.

GUO, J., LUA, A.C. 2001. Experimental and kinetic studies on pore development during CO_2 activation of oil-palm-shell char. *Journal of Porous Materials*, 8: 149-157.

HAMEED, B.H., DIN A.T.M., AHMAD, A.L. 2007. Adsorption of methylene blue onto bamboo-based activated carbon: kinetics and equilibrium studies. *Journal of Hazardous Materials*, 141: 819-825.

HARKINS, W.D., JURA, G. 1944. Surfaces of solids: XIII. A vapor adsorption method for the determination of the area of a solid without the assumption of a molecular area, and the areas

occupied by nitrogen and other molecules on the surface of a solid. *Journal of American Chemical Society*, 66: 1366- 1373.

HEDLEY M.J. 2008. Techniques for assessing nutrient bioavailability in soils: current and future issues. *Developmenst in Soil Science*, 32: 283-327.

HERNÁNDEZ, J.J., ARANDA, G., SAN MIGUEL, BULA, A. 2010. Gasification of grapevine pruning waste in an entrained-flow reactor: gas products, energy efficiency and gas containing alternatives. *Global NEST Journal*, 12: 215-227.

HINSINGER, P. 2001. Bioavailability of soil inorganic P in the rhizosphere as affected by root-induced chemical changes: a review. *Plant and Soil*, 237: 173-195.

HO, Y.S., MCKAY, G. 2000. The kinetics of sorption of divalent metal ions onto sphagnum moss peat. *Water Research*, 34: 735-742.

HO, Y.S., MCKAY, G. 1999. Pseudo-second order model for sorption processes. *Process Biochemistry*, 34: 451-465.

HOSIER, S., BRADLEY, L. 1999. Guide to symptoms of plant nutrient deficiencies. http://ag.arizona.edu/garden/az1106.pdf Date of Access: 15 Aug 2010.

HOSSAIN, M.K., STREZOV, V., CHAN, K.Y., ZIOLKOWSKI, A., NELSON, P.F. 2011. Influence of pyrolysis temperature on production and nutrient properties of wastewater sludge biochar. *Journal of Environmental Management*, 92: 223-228.

HOSSAIN, M.K., STREZOV, V., CHAN, K.Y., NELSON, P.F. 2010. Agronomic properties of wastewater sludge biochar and bioavailability of metals in production of cherry tomato (*Lycopersicon esculentum*). *Chemosphere*, 78: 1167-1171.

HUGO, T.J. 2010. *Pyrolysis of sugarcane bagasse*. University of Stellenbosch. Stellenbosch. (Thesis-M.Sc.)

HULICOVA-JURCAKOVA, D., SEREDYCH, M., JIN, Y., LU, G.Q., BANDOSZ, T.J. 2010. Specific anion and cation capacitance in porous carbon blacks. *Carbon*, 48: 1767-1778.

IGWE, J.C., ABIA, A.A., IBEH, C.A. 2008. Adsorption kinetics and intraparticle diffusivities of Hg, As and Pb ions on unmodified and thiolated coconut fiber. *International Journal of Environmental Science Technology*, 5: 83-92.

International Carbon Black Association. 2011. http://www.carbon-black.org Date of access: 14 Nov. 2011.

International Energy Agency. 2010. Sustainable production of second-generation biofuels: potential and perspectives in major economies and developing countries http://www.iea.org Date of access: 18 Aug. 2010.

International Energy Agency. 2009. CO_2 emissions from fuel combustion: highlights. http://www.iea.org Date of Access: 18 Aug. 2010.

INYANG, M., GAO, B., PULLAMMANAPPALLIL, P., DING, W., ZIMMERMAN, A.R. 2010. Biochar from anearobically digested sugarcane bagasse. *Bioresource Technology*, 101: 8868-8872.

IOANNADIO, O., ZABANIOTOU, A. 2007. Agricultural residues as precursors for activated carbon production- a review. *Renewable and Sustainable Energy*, 11: 1966-2005.

IOANNIDOU, O., ZABANIOTOU, A., ANTONAKOU, E.V., PAPAZISI, K.M., LAPPAS, A.A., ATHANASSIOU, C. 2009. Investigating the potential for energy, fuel, materials, and chemicals production from corn residues (cobs and stalks) by non-catalytic and catalytic pyrolysis in two reactor configurations. *Renewable and Sustainable Energy Reviews*, 13: 750-762.

ISLAM, M.R., PARVEEN, M., HANIU, H. 2010. Properties of sugarcane waste-derived bio-oils obtained by fixed-bed fire-tube heating pyrolysis. *Bioresource Technology*, 101: 4162-4168.

ISMADJI, S., SUDARYANTO, Y., HARTONO, S.B., SETIAWAN, L.E.K., AYUCITRA, A. 2005. Activated carbon from char obtained from vacuum pyrolysis of teak sawdust: pore structure development and characterization. *Bioresource Technology*, 96: 1364-1369.

ITODO, A.U., ABDULRAHMAN, F.W., HASSAN, L.G., MAIGANDI, S.A., ITODO, H.U. 2010. Intraparticle diffusion and intraparticulate diffusivities of herbicide on derived activated carbon. *Researcher*, 2: 74-86

IZABEL, R., MOURA, A.B.D., MORISSO, F.D.P., DE SOUZA MELLO, F. 2008. Thermogravimetric analysis of the pyrolysis of black wattle (*Acacia mearnsii* de Wild.) grown in Rio Grande do Sul, Brazil. *Revista Árvore*, 32: 533-543.

JENKINS, B.M., EBELING, J.M. 1985. Thermochemical properties of biomass fuels. *California Agriculture*, 14-16.

JIA, Q., LUA, A.C. 2008. Effects of pyrolysis conditions on the physical characteristics of oil-palm-shell activated carbons used in aqueous phase phenol adsorption. *Journal of Analytical and Applied Pyrolysis*, 83: 175-179.

JUN, W., MINGXU, Z., MINGQIANG, C., FANFEI, M., SUPING, Z., ZHENGWEI, R., YONGJIE, Y. 2006. Catalytic effects of six inorganic compounds on pyrolysis of three kinds of biomass. *Thermochimica Acta*, 444: 110-114.

KABATA-PENDIAS, A. 2000. Trace elements in soils and plants. 3rd ed. USA: CRC Press.

KADIRVELU, K., KAVIPRIYA, M., KARTHIKA, C., RADHIKA, M., VENNILAMANI, N., PATTABHI, S. 2003. Utilization of various agricultural wastes for activated carbon preparation and application for the removal of dyes and metal ions from aqueous solutions. *Bioresource Technology*, 87: 129-132.

KARACA, S., GÜRSES, A., AÇIKYILDIZ, M., KORUCU., M.E. 2008. Adsorption of cationic dye from aqueous solutions by activated carbon. *Microporous and Mesoporous Materials*, 115: 376-382.

KAVITHA, D., NAMASIVAYAM, C. 2007. Experimental and kinetic studies on methylene blue adsorption by coir pith carbon. *Bioresource Technology*, 98: 14-21.

KAWAMOTO, H., MURAYAMA, M., SAKA, S. 2003. Pyrolysis behaviour of levoglucosan as an intermediate cellulose pyrolysis: polymerisation into polysaccharide as a key reaction to carbonised product formation. *Journal of Wood Science*, 49: 469-473.

KIMETU, J.M., LEHMANN, J., NGOZE, S.O., MUGENDI, D.N., KINYANGI, J.M., RIHA, S., VERCHOT, L., RECHA, J.W., PELL, A.N. 2008. Reversibility of soil productivity decline with organic matter of differing quality along a degradation gradient. *Ecosystems*, 11: 726-739.

KLASH, A., NCUBE, E., MEINCKEN, M. 2009. Localization and attempted quantification of various functional groups on pulpwood fibres. *Applied Surface Science*, 255: 6318-6324.

KOUTCHEIKO, S., MONREAL, C.M., KODAMA, H., MCCRACKEN, T., KOTLYAR, L. 2007. Preparation and characterization of activated carbon derived from the thermo-chemical conversion of chicken manure. *Bioresource Technology*, 98: 2459-2464.

KUMADA, K. 1987. Chemistry of soil organic matter. Tokyo: Japan Scientific Societies Press.

LAHAYE, J. 1997. The chemistry of carbon surfaces. *Fuel*, 77: 543-547.

LEE, J.W., KIDDER, M., EVANS, B.R., PAIK, S., BUCHANAN III, A.C., GARTEN, C.T., BROWN, R.C. 2010. Characterization of biochars produced from cornstovers for soil amendment. *Environmental Science Technology*, 44: 7970-7974.

LEHMANN, J. 2007. A handful of carbon. *Nature*, 447: 143-144.

LEHMANN, J. 2009. Terra preta di Indio. (*In* Encyclopedia of Soil Science, 1: 1-4.)

LEHMANN, J. JOSEPH, S. 2009. Biochar for environmental management: science and technology. London: Earthscan.

LEHMANN, J., DA SILVA, J.P., STEINER, C., NEHLS, T., ZECH, W., GLASER, B. 2003. Nutrient availability and leaching in an archeological Anthrosol and a Ferrasol of the Central Amazon basin: fertilizer, manure, charcoal amendments. *Plant and Soil*, 249: 343-357.

LEHMANN, J., GAUNT, J., RONDON, M. 2006. Bio-char sequestration in terrestrial ecosystems- a review. *Mitigation and Adaptation Strategies for Global Change*, 11: 403-427.

LI, W., YANG, K., PENG, J., ZHANG, L., GUO, S., XIA, H. 2008. Effects of carbonization temperatures on characteristics of porosity in coconut shell chars and activated carbons derived from carbonized coconut shell chars. *Industrial Crops and Products*, 28: 190-198.

LIANG, B., LEHMANN, J., SOLOMON, D., KINYANGI, J., GROSSMAN, J., O'NEILL, B., SKJEMSTAD, J.O., THIES, J., LUIZÃO,F.J., PETERSON, J., NEVES, E.G. 2006. Black carbon increases cation exchange capacity in soils. *Soil Science Society of America Journal*, 70: 1719-1730.

LIOU, T.H. 2010. Development of mesoporous structure and high adsorption capacity of biomass-based activated carbon by phosphoric acid and zinc chloride activation. *Chemical Engineering Journal*, 159: 129-142.

LU, G.Q., LOW, J.C.F, LIU, C.Y., LUA, A.C. 1995. Surface area development of sewadge sludge during pyrolysis. *Fuel*, 74: 344-348.

LUA, A.C., YANG, T. 2004. Effects of vacuum pyrolysis conditions on the characteristics of activated carbons derived from pistachio-nut shells. *Journal of Colloid and Interface Science*, 276: 364-372.

LV., D., XU, M., LIU, X., ZHAN, Z., LI, Z., YAO, H. 2010. Effect of cellulose, lignin, alkali and alkaline earth metallic species on biomass pyrolysis and gasification. *Fuel Processing Technology*, 91: 903-909.

MAHMOODI, N.M., HAYATI, B., ARAMI, M., LAN, C. 2011. Adsorption of textile dyes on Pine Cone from colored wastewater: kinetic, equilibrium and thermodynamic studies. *Desalination*, 268: 117-125.

MANI, T., MURUGAN, P., ABEDI, J., MAHINPEY, N. 2010. Pyrolysis of wheat straw in a thermogravimetric analyzer: effect of particle size and heating rate on devolatilization and estimation of global kinetics. *Chemical Engineering Research and Design,* 88: 952-958.

MASEL, R.I. 1996. Principles of adsorption and reaction on solid surfaces. New York: John Wiley & Sons, Inc.

MCKAY, G., EL GUNDI, M., NASSAR, M.M. 1988. External mass transport processes during the adsorption of dyes onto bagasse pith. *Water Research*, 22: 1527-1533.

MIRANDA, R., PAKDEL, H., ROY., C., DARMSTADT, H., VASILE, C. 1999. Vacuum pyrolysis of PVC II: product analysis. *Polymer Degradation and Stability*, 66: 107-125.

MOHAMED, A.R., MOHAMMADI, M., DARZI, G.N. 2010. Preparation of carbon molecular sieve from lignocellulosic biomass: a review. *Renewable and Sustainable Energy Reviews*, 14: 1591-1599.

MOHAN, D., PITTMAN, C.U., STEELE, P.H. 2006. Pyrolysis of wood/biomass for bio-oil: a critical review. *Energy & Fuels*, 20: 848-889.

MOK, W.S.L., ANTAL, M.J. 1983a. Effects of pressure on biomass pyrolysis I. Cellulose pyrolysis products. *Thermochimica Acta*, 68: 165-186.

MOK, W.S.L., ANTAL, M.J. 1983b. Effects of pressure on biomass pyrolysis II. Heats of reaction of cellulose pyrolysis. *Thermochimica Acta*, 68: 165-186.

MONTES-MORÁN, M.A., SUÁREZ, D., MENÉNDEZ, J.A., FUENTE, E. 2004. On the nature of basic sites on carbon surfaces: an overview. *Carbon*, 42: 1219-1225.

MOYO, H.P.M., DUBE, S., FATUNBI, A.O. 2009. Impact of the removal of black wattle (*Acacia mearnsii*) in the Tsomo Valley in Eastern Cape: consequences on the water recharge and soil dynamics (an ongoing study). *Grassroots: Newsletter of the Grassland Society of Southern Africa*, 9: 38-41.

MUI, E.L.K, CHEUNG, W.H., CALIX, M., MCKAY, G. 2010. Dye adsorption onto char from bamboo. *Journal of Hazardous Materials*, 177: 1001-1005.

NASA Earth Observatory. The carbon cycle. http://earthobservatory.nasa.gov Date of Access: 9 Sep. 2010.

NASUHA, N., HAMEED, B.H., DIN A.T.M. 2010. Rejected tea as potential low-cost adsorbent for the removal of methylene blue. *Journal of Hazardous Materials*, 175: 126-132.

Non-Affiliated Soil Analysis Work Committee. 1990. Handbook of standard soil testing methods for advisory purposes. Soil Science Society of South Africa, Pretoria.

NOVAK, J.F., BUSSCHER, W.J., LAIRD, D.L., AHMEDNA, M., WATTS, D.W., NIANDOU, M.A.S. 2009. Impact of biochar amendment on fertility of a Southeastern coastal plain soil. *Soil Science*, 174: 105-112.

NOWICKI, P., PIETRZAK, R. 2010. Carbonaceous adsorbents prepared by physical activation of pine sawdust and their application for removal of NO_2 in dry and wet conditions. *Bioresource Technology*, 101: 5802-5807.

NTALOS, G.A., GRIGORIU, A.H. 2002. Characterization and utilisation of vine prunings as a wood substitute for particleboard production. *Industrial Crops and Products*, 16: 59-68.

NUITHITIKUL, K., SRIKHUN, S., HIRUNPRADITKOON, S. 2010. Influences of pyrolysis condition and acid treatment on properties of durian peel-based activated carbon. *Bioresource Technology*, 101: 426-429.

OKUNO, T., SONOYAMA, N., HAYASHI, J., Li, C., SATHE, C., CHIBA, T. 2005. Primary release of alkali and alkaline earth species during the pyrolysis of pulverized biomass. *Energy and Fuels*, 19: 2164-2171.

ÖNAL, Y. 2006. Kinetics of adsorption of dyes from aqueous solution using activated carbon prepared from waste apricot. *Journal of Hazardous Materials*, B137: 1719-1728.

ÖZÇİMEN, D., ERSOY-MERİÇBOYU, A. 2010. Characterization of biochar and bio-oil samples obtained from carbonization of various biomass materials. *Renewable Energy*, 35: 1319-1324.

PAKDEL, H., ROY, C., KALKREUTH, W. 1999. Oil production by vacuum pyrolysis of Canadian oil shales and fate of the biological markers. *Fuel*, 78: 365-375.

PANDOLFO, A.G., HOLLENKAMP, A.F. 2006. Carbon properties and their role in supercapacitors: review. *Journal of Power Sources*, 157: 11-27.

PAPIRER, E., LI, S., DONNET, J.B. 1987. Contribution to the study of basic surface groups on carbons. *Carbon*, 25: 243-247.

PARIHAR, M.F., KAMIL, M., GOYAL, H.B., GUPTA, A.K., BHATNAGAR, A.K. 2007. An experimental study on pyrolysis on biomass. *Process Safety and Environmental Protection*, 85: 458-465.

PASSÉ-COUTRIN, N., ALTENOR, S., GASPARD, S. 2009. Assessment of the surface area occupied by molecules on activated carbon from liquid phase adsorption data from a combination of the BET and the Freundlich theories. *Journal of Colloid and Interface Science*, 332: 515-519.

PASTOR-VILLEGAS, J., RODRÍGUEZ, J.M.M., PASTOR-VALLE, J.F., ROUQUEROL, J., DENOYEL, R., GARCÍA, M.G. 2010. Adsorption-desorption of water vapour on chars prepared from commercial wood charcoals, in relation to their chemical composition, surface chemistry and pore structure. *Journal of Analytical and Applied Pyrolysis*, 88: 124-133.

PETROV, N., BUDINOVA, T., RAZVIGOROVA, PARRA, J., GALIATSATOU, P. 2008. Conversion of olive wastes to volatiles and carbon adsorbents. *Biomass and Bioenergy*, 32: 1303-1310.

PISKORZ, J., RADLEIN, D., SCOTT, D.S. 1986. On the mechanism of the rapid pyrolysis of cellulose. *Journal of Analytical and Applied Pyrolysis*, 9: 121-137.

PRATT, K., MORAN, D. 2010. Evaluating the cost-effectiveness of global biochar mitigation potential. *Biomass and Bioenergy*, 34: 1149-1158.

PRESTON, C.M., SCHMIDT, M.W.I. 2006. Black (pyronegic) carbon: a synthesis of current knowledge and uncertainties with special consideration of boreal regions. *Biogeosciences*, 3: 397-420.

PURI, A.N., ASGHAR, A.G. 1938. Influence of salts and soil-water ratio on pH value of soils. *Soil Science*, 46: 249-257.

PÜTÜN, A.E., KOÇKAR, Ö.M., YORGUN, S., GERÇEL, H.F., ANDRESEN, J., SNAPE, C.E., PÜTÜN, E. 1996. Fixed-bed pyrolysis and hydropyrolysis of sunflower bagasse: Product yields and compositions. *Fuel Processing Technology*, 46: 49-62.

RAFATATULLAH, M., SULAIMAN, O., HASHIM, R., AHMAD, A. 2010. Adsorption of methylene blue on low-cost adsorbents: a review. *Journal of Hazardous Materials*, 177: 70-80.

RAPOSO, F., DE LA RUBIA, M.A., BORJA, R. 2009. Methylene blue number as useful indicator to evaluate the adsorption capacity of granular activated carbon in batch mode: influence of adsorbate/adsorbent mass ratio and particle size. *Journal of Hazardous Materials*, 165: 291-299.

RAVEDRAAN, K., GANESH, A., KHILAR, K.C. 1996. Pyrolysis characteristics of biomass and biomass components. *Fuel*, 75: 987-998.

RAVEEDRAN, K., GANESH, AN., KHILAR, K.C. 1995. Influence of mineral matter on biomass pyrolysis characteristics. *Fuel*, 74: 1812-1822.

RAVIKUMAR, K., DEEBIKA, B., BALU, K. 2005. Decolourization of aqueous dye solutions by a novel adsorbent: application of statistical designs and surface plots for the optimization and regression analysis. *Journal of Hazardous Materials*, B122: 75-83.

RHOADES, J.D. 1982. Cation exchange capacity. *In* Methods of soil analysis Part 2. Chemical and microbial properties. ASA and SSA: Madison.

ROBERTS, K.G., GLOY, B.A., JOSEPH, S., SCOTT, N.R., LEHMANN, J. 2010. Life cycle assessment of biochar systems: estimating the energetic, economic, and climate change potential. *Environmental Science Technology*, 44: 827-833.

RONDON, M.A., LEHMANN, J., RAMÍREZ, J., HURTADO, M. 2007. Biological nitrogen fixation by common beans (*Phaseolus vulgaris L.*) increases with bio-char additions. *Biology and Fertility of Soils*, 43: 699-708.

ROY, C., PAKDEL, H., BROUILLARD, D. 1990. The role of extractives during vacuum pyrolysis of wood. *Journal of Applied Polymer Science*, 41: 337-348.

RUSSELL, E.J. 1954. Soil conditions and plant growth. London: Longmans, Green and Co.

RUTHVEN, D.M., S., FAROOQ, S., KNAEBEL, K.S. 1994. Pressure swing adsorption. New York: VCH.

ŞENSÖZ, S., DEMİRAL, İ., GERÇEL, H.F. 2006. Olive bagasse (*Olea europea* L.) pyrolysis. *Bioresource Technology*, 97: 429-436.

South Africa Wine Industry Information and Systems (SAWIS). 2009. http://www.sawis.co.za Date of Access: 15 March 2011.

SEREDYCH, M., HULICOVA-JORCAKOVA, D., LU, G.Q., BANDOSZ, T.J. 2008. Surface functional groups of carbons and the effects of their chemical character, density and accessibility to ions on electrochemical performance. *Carbon*, 46: 1475-1488.

SHAFIZADEH, F. 1982. Introduction to pyrolysis of biomass. *Journal of Analytical and Applied Pyrolysis*, 2: 283-305.

SHARMA, Y.C., UMA. 2010. Optimization of parameters for adsorption of methylene blue on a low-cost activated carbon. *Journal of Chemical Engineering Data*, 55: 435-439.

SHARMA, T.C., UMA, UPADHYAY, S.N. 2009. Removal of a cationic dye from wastewaters by adsorption on activated carbon developed from coconut coir. *Energy and Fuels*, 23: 2983-2988.

SHARMA, R.K., WOOTEN, J.B., BALIGA, V.L., LIN, X., CHAN, W.G., HAJALIGOL, M.R. 2004. Characterization of chars from pyrolysis of lignin. *Fuel*, 83: 1469-1482.

SHAW, D.J. 1970. Introduction to colloid and surface chemistry. London: Butterworths.

SHEN, D.K., GU, S., LUO, K.H., WANG, S.R., FANG, M.X. 2010. The pyrolytic degradation of wood-derived lignin from pulping process. *Bioresource Technology,* 101: 6136-6146.

SHINOGI, Y., KANRI, Y. 2003. Pyrolysis of plant, animal and human waste: physical and chemical characterization of pyrolytic products. *Bioresource Technology*, 90: 241-247.

SHOPOVA, N., MINKOVA, V., MARKOVA, K. 1997. Evaluation of the thermochemical changes in agricultural by-products and in the carbon adsorbents obtained from them. *Journal of Thermal Analysis*, 48: 309-320.

SILBER, A., LEVKOVITCH, I., GRABER, E.R. 2010. pH-dependent mineral release and surface properties of cornstraw biochar: agronomic implications. *Environmental Science Technology*, 44: 9318-9323.

SINGH, B., SINGH, B.P., COWIE, A.L. 2010. Characterization and evaluation of biochars for their application as a soil amendment. *Australian Journal of Soil Research*, 48: 516-525.

SJOSTROM, E. 1981. Wood chemistry: fundamentals and applications. USA: Academic Press.

SOUZA, B.S., MOREIRA, A.P.D., TEIXEIRA, A.M.R.F. 2009. TG-FTIR coupling to monitor the pyrolysis products from agricultural residues. *Journal of Thermal Analysis and Calorimetry*, 97: 637-642.

SPARKS, D.L. 1995. Environmental soil chemistry. USA: Academic Press.

STANISLAV, V.V, BAXTER, D., ANDERSEN, L.K., VASSILEVA, C.G. 2010. An overview of the chemical composition of biomass. *Fuel*, 89: 913-933.

STEINER, C. 2007. Soil charcoal amendments maintain soil fertility and establish a carbon sink-research and prospects. In: *Soil Ecology Research Developments*. Edited by: Liu, T., Nova Science Publishers, Inc.

STEINER, C., GLASER, B., TEIXEIRA, W.G., LEHMANN, J., BLUM, W.E.H, ZECH, W. 2008. Nitrogen retention and plant uptake on a highly weathered central Amazonian Ferralsol amended with compost and charcoal. *Journal of Plant Nutrition and Soil Science*, 171: 893-899.

STÖHR, B., BOEHM, H.P., SCHLÖGL, R. 1991. Enhancement of the catalytic activity of activated carbons in oxidation reactions by thermal treatment with ammonia or hydrogen cyanide and observation of a superoxide species as a possible intermediate. *Carbon*, 29: 707-720.

SUN, Q., YANG, L. 2003. The adsorption of basic dyes from aqueous solution on modified peat-resin particle. *Water Research*, 37: 1535-1544.

SUZUKI, M. 1990. Adsorption engineering. Tokyo: Kodansha.

TAN, I.A.W., AHMAD, A.L., HAMEED, B.H. 2008. Adsorption of basic dye using activated carbon prepared from oil palm shell: batch and fixed bed studies. *Desalination*, 225: 13-28.

TAN, I.A.W., HAMEED, B.H., AHMAD, A.L. 2007. Equilibrium and kinetic studies on basic dye adsorption by oil palm fibre activated carbon. *Chemical Engineering Journal*, 127: 111-119.

TARTARELLI, R., GIORGINI, M., GHETTI, P., BELLI, R. 1987. DTG combustion behavior of charcoals. *Fuel*, 66:1737-1738.

TOPOLIANTZ, S., PONGE, J.F., BALLOF, S. 2005. Manioc peel and charcoal: a potential organic amendment for sustainable soil fertility in the tropics. *Biology and Fertility of Soils*, 41: 15-21.

TSAI, W.T., LEE, M.K., CHANG, Y.M. 2006. Fast pyrolysis of rice straw, sugarcane bagasse and coconut shell in an induction –heating reactor. *Journal of Analytical and Applied Pyrolysis*, 76: 230-237.

TYRON, E.H. 1948. Effect of charcoal on certain physical, chemical, and biological properties of forest soils. *Ecological Monographs*, 18: 81-115.

UCHIMIYA, M., WARTELLE, L.H., KLASSON, K.T., FORTIER, C.A., LIMA, I.M. 2011. Influence of pyrolysis temperature on biochar property and function as a heavy metal sorbent in soil. *Journal of Agricultural and Food Chemistry*, 59: 2501-2510.

UGURLU, M., GÜRSES, A., DOGAR, C. 2007. Adsorption studies on the treatment of textile dyeing effluent by activated carbon prepared from olive stone by $ZnCl_2$ activation. *Coloration Technology*, 123:106-114.

UZUN, B.B., APAYDIN-VAROL, E., ATEŞ, F., ÖZBAY, N., PÜTÜN, A.E. 2010. Synthetic fuel production from tea waste: Characterization of bio-oil and bio-char. *Fuel*, 89: 176-184.

VALMARI, T., LIND, T.M., KAUPPINEN, E.I. 1999. Field study on ash behavior during circulating fluidized-bed combustion of biomass: ash formation. *Energy & Fuels*, 13: 379-389.

VAN ZWIETEN, L., KIMBER, S., MORRIS, S., CHAN, K.Y., DOWNIE, A., RUST, J., JOSEPH, S., COWIE, A. 2010. Effects of biochar from slow pyrolysis of paper mill waste on agronomic performance and soil fertility. *Plant and Soil*, 327: 235-246.

VERHEIJEN, F., JEFFERY, S., BASTOS, A.C., VAN DER VELDE, M., DIAFAS, I. 2010. Biochar application to soils: a critical scientific review of effects on soil properties, processes and functions. JRC Europian Commission Scientific and Technical Report, Luxembourg, 1-166.

VILLACAÑAS, F., PEREIRA, M.F.R., ÓRFÃO, J.J.M., FIGUEIREDO, J.L. 2006. Adsorption of simple aromatic compounds on activated carbons. *Journal of Colloid and Interface Science*, 293: 128-136.

WANG, X., SI, J., TAN, H., MA, L., POURKASHANIAN, M., XU, T. 2010. Nitrogen, sulfur, and chlorine transformations during the pyrolysis of straw. *Energy Fuels*, 24: 5215-5221.

WANG, X., COOK, R., TAO, S., XING, B. 2007. Sorption of organic contaminants by biopolymers: role of polarity, structure and domain spatial arrangement. *Chemosphere*, 66: 1476-1484.

WANG, S., ZHU, Z.H. 2007. Affects of acidic treatment of activated carbons on dye adsorption. *Dyes and Pigments*, 75:306-314.

WANG, S., ZHU, Z.H., COOMES, A., HAGHSERESHT, F., LU, G.Q. 2005. The physical and surface chemical characteristics of activated carbons and the adsorption of methylene blue from wastewater. *Journal of Colloid and Interface Science*, 284: 440-446.

WARD, S.M., BRASLAW, J. 1985. Experimental weight loss kinetics of wood pyrolysis under vacuum. *Combustion and Flame*, 61: 261-269.

WOOLF, D. 2008. Biochar as a soil amendment: a review of the environmental implications. http://orgprints.org Date of Access: 9 Sep 2010.

WORASUWANNARAK, N., SONOBE, T., TANTHAPANICHAKOON, W. 2007. Pyrolysis behaviors of rice straw, rice husk, and corncob by TG-MS technique. *Journal of Analytical and Applied Pyrolysis*, 78: 265-271.

YAMATO, M., OKIMORI, Y., WIBOWO, I.F., ANSHORI, S., OGAWA, M. 2006. Effects of the application of charred bark *Acacia mangium* on the yield of maize, cowpea and peanut, and soil chemical properties in South Sumatra, Indonesia. *Soil Science and Plant Nutrition*, 52: 489-495.

YAO, F.X., ARBESTAIN, M.C., VIRGEL, S., BLANCO, F., AROSTEGUI, J., MACIÁ-AGULLÓ, J.A., MACÍAS, F. 2010. Simulated geochemical weathering of a mineral ash-rich biochar in a modified soxhlet reactor. *Chemosphere*, 80: 724-732.

YASAR, S., GUNTEKIN, E., CENGIZ, M., TANRIVERDI, H. 2010. The correlation of chemical characteristics and UF-Resin ratios to physical and mechanical properties of particleboard manufactured from vine prunings. *Scientific Research and Essays*, 5: 737-741.

YUAN, J.H, XU, R.K., ZHANG, H. 2010. The forms of alkalis in the biochar produced from crop residues at different temperatures. *Bioresource Technology*, 102: 3488-3497.

ZHANG, T., WALAWENDER, W.P., FAN, L.T., FAN, M., DAUGAARD, D., BROWN, R.C. 2004. Preperation of activated carbon from forest and agricultural residues through CO_2 activation. *Chemical Engineering Journal*, 105: 53-59.

APPENDIX A: VACUUM PYROLYSIS EXPERIMENTAL RUNS

Table A.1: Vacuum pyrolysis product yields on mass basis

	$Y_{biochar}$	Y_{liquid}	$Y_{totalwater}$	$Y_{bio-oil}$	$Y_{pyrolyticwater}$
			Black wattle		
Run 1	23.51	60.36	39.48	20.88	34.38
Run 2	23.11	58.44	35.42	23.02	30.31
Run 3	23.89	55.63	32.20	23.43	27.09
			Vineyard		
Run 1	31.44	36.87	25.73	11.15	15.91
Run 2	29.58	33.85	21.01	12.83	11.19
Run 3	31.25	34.14	23.38	10.76	13.56
Run 4	31.55	36.04	26.44	9.60	10.81
			Sugar cane bagasse		
Run 1	18.49	53.27	22.23	31.03	1.56
Run 2	18.51	44.82	26.97	17.85	6.30
Run 3	22.07	51.89	25.13	26.76	4.46

* The symbol Y denotes yield percentage.

Error analysis

The products were scaled at the end of each run. Therefore, the error analysis is based on the errors which arise from multi scaling. It has been shown by Hugo (2010) as follows:

$$A = a \pm \Delta a$$
$$B = b \pm \Delta b$$
$$A + B = (a \pm \Delta a) + (b \pm \Delta b)$$
$$A + B = (a + b) + (\pm \Delta a \pm \Delta b)$$
$$A + B = (a + b) \pm (\Delta a + \Delta b)$$
$$E_{relative} = \frac{E}{Value} = \frac{\Delta a + \Delta b}{a + b} \approx \frac{\Delta a}{a} \approx \frac{\Delta b}{b}$$

$$(if - \Delta a \approx \Delta b)$$

The multiplication of errors is calculated as follows:

$$E_{relati\ ve} = \frac{E}{Value} = \frac{b\Delta a + a\Delta b}{ab} = \frac{\Delta a}{a} + \frac{\Delta b}{b}$$

The laboratory scale was assumed to have an error of ±0.1 g. For instance, ±0.1 g error would be caused by the weighing both the biomass and the biochar. If Run 1 from black wattle is taken as an example with a value of 40.54 g of biomass and 9.53 g biochar, the error calculation for biochar yield would be as follows:

$$E_{bioc\ har\ \ yield} = (\frac{\pm 0.1}{m_{biomass}} + \frac{\pm 0.1}{m_{bioc\ har}}) \times Yield_{bioc\ har}$$

$$E_{bioc\ har\ \ yield} = (\frac{\pm 0.1}{40.54\ g} + \frac{\pm 0.1}{9.53\ g}) \times 23.51 = \pm 0.3$$

APPENDIX B: VACUUM PYROLYSIS PRODUCT YIELDS

Table B.1: Vacuum pyrolysis product yields

	$Y_{biochar}$	Y_{liquid}	$Y_{totalwater}$	$Y_{bio-oil}$	$Y_{pyrolyticwater}$
on weight basis					
Black wattle	23.5±0.3	58.1±8.1	35.7±10.1	22.4±6.4	30.6±9.2
Vineyard	31.0±0.3	35.2±11.6	24.1±10.8	11.1±4.7	14.3±6.6
Sugar cane bagasse	19.7±0.3	50.0±7.7	24.8±6.6	25.2±6.7	4.1±1.1
on dry weight basis					
Black wattle	24.8±0.8	61.3±9.7	37.6±11.3	23.7±7.2	32.2±9.7
Vineyard	34.3±0.7	39.1±13.2	26.8±12.2	11.4±5.0	15.9±7.4
Sugar cane bagasse	24.8±0.5	63.0±10.0	31.2±8.4	31.8±8.6	5.2±1.4
on dry and ash free weight basis					
Black wattle	25.1±2.8	62.1±14.9	38.1±14.6	24.0±9.3	32.7±12.5
Vineyard	35.5±2.0	40.3±15.0	27.7±13.6	12.7±6.0	16.4±8.2
Sugar cane bagasse	26.2±1.2	66.5±12.2	32.9±9.7	33.5±9.9	5.5±1.6

* The symbol Y denotes yield percentage.

APPENDIX C: CALIBRATION CURVES USED FOR CALCULATION OF MB CONCENTRATION

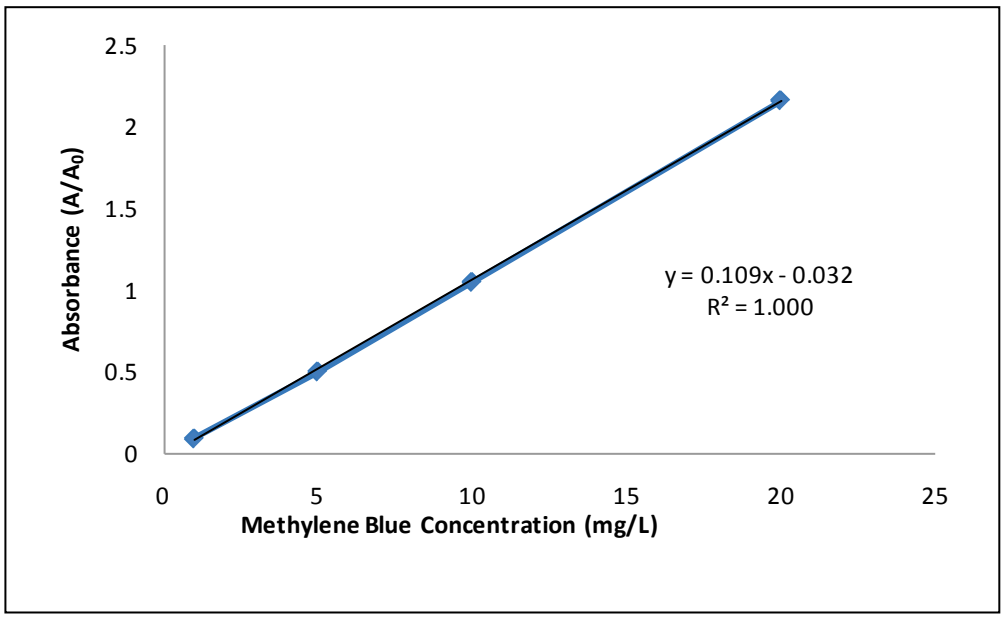

Figure C.1: Calibration curve using 20 ppm methylene blue solution

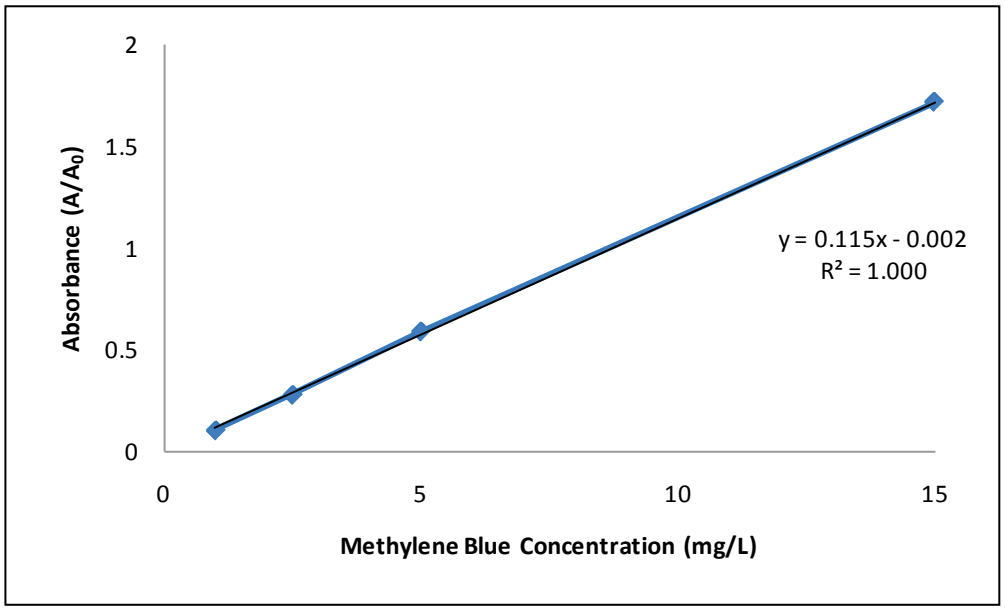

Figure C.2: Calibration curve using 15 ppm methylene blue solution

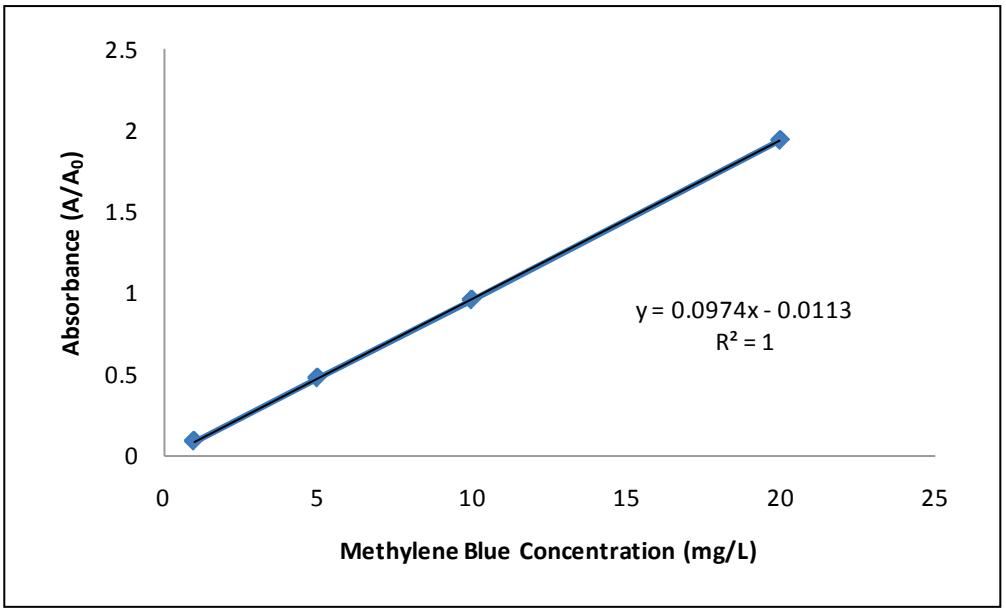

Figure C.3: Calibration curve using 10 ppm methylene blue solution

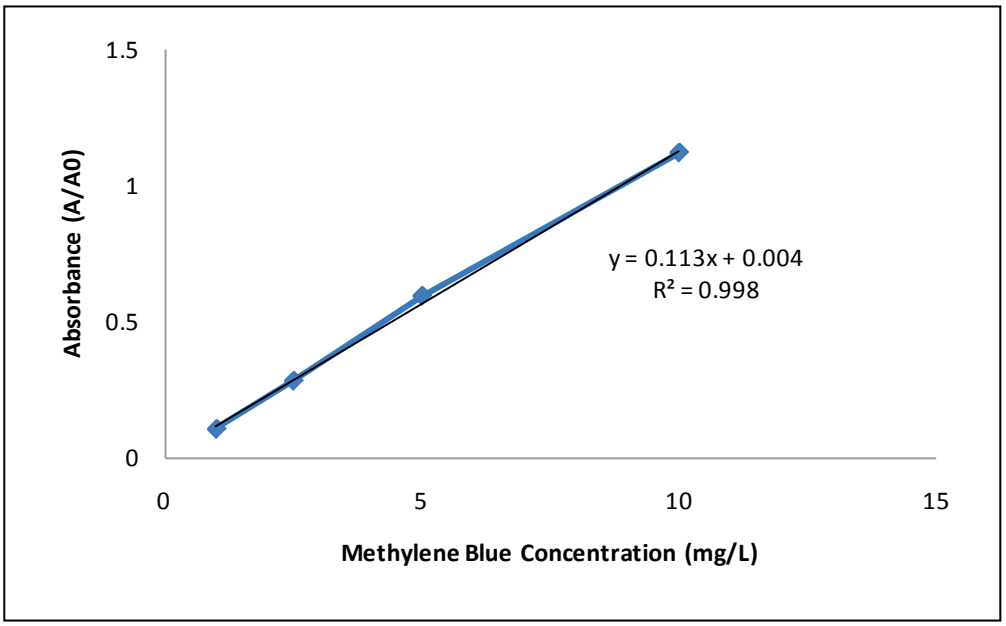

Figure C.4: Calibration curve using 5 ppm methylene blue solution

APPENDIX D: ADSORPTION RAW DATA

Table D.1: Adsorption data for vineyard (20 mg/L MB)

	No .1				No. 2									
t (min)	**A/A_0**	**[MB] mg/L**	**q (mg/g)**	**%Removal**	**A/A_0**	**[MB]**	**q (mg/g)**	**% Removal**	**std dev [MB]**	**std dev for q**	**std for % Removal**	**Avg. [MB]**	**Avg. q (mg/g)**	**Avg. %Removal**
0	2.163	20.14	0.00	0.00	2.163	20.14	0.00	0.00	0.00	0.00	0.00	20.14	0.00	0.00
1	1.265	11.90	9.14	40.92	1.416	13.28	7.60	34.0	0.98	1.09	4.86	12.59	8.37	37.48
15	1.064	10.06	11.18	50.07	1.139	10.74	10.42	46.7	0.49	0.54	2.42	10.40	10.80	48.37
150	0.758	7.25	14.29	64.01	0.819	7.81	13.67	61.2	0.40	0.44	1.96	7.53	13.98	62.62
510	0.558	5.41	16.33	73.12	0.605	5.84	15.85	71.0	0.30	0.34	1.51	5.63	16.09	72.05
1350	0.39	3.87	18.04	80.78	0.411	4.06	17.82	79.8	0.14	0.15	0.68	3.97	17.93	80.30
3505	0.203	2.16	19.94	89.30	0.21	2.22	19.87	89.0	0.05	0.05	0.23	2.19	19.90	89.14
4945	0.127	1.46	20.71	92.76	0.173	1.88	20.24	90.7	0.30	0.33	1.48	1.67	20.48	91.71
6385	0.114	1.34	20.84	93.35	0.132	1.50	20.66	92.5	0.12	0.13	0.58	1.42	20.75	92.94
7825	0.094	1.16	21.05	94.26	0.096	1.17	21.03	94.2	0.01	0.01	0.06	1.17	21.04	94.21
9985	0.076	0.99	21.23	95.08	0.082	1.05	21.17	94.8	0.04	0.04	0.19	1.02	21.20	94.94
11425	0.061	0.85	21.38	95.76	0.073	0.96	21.26	95.2	0.08	0.09	0.39	0.91	21.32	95.49
12865	0.056	0.81	21.43	95.99	0.053	0.78	21.46	96.1	0.02	0.02	0.10	0.79	21.45	96.06

Table D.2: Adsorption data for vineyard (15 mg/L)

	No .1				No. 2									
t (min)	**A/A_0**	**[MB] mg/L**	**q (mg/g)**	**% Removal**	**A/A_0**	**[MB]**	**q (mg/g)**	**% Removal**	**std dev [MB]**	**std dev for q**	**std for % Removal**	**Avg. [MB]**	**Avg. q (mg/g)**	**Avg. %Removal**
0	1.717	14.95	0.00	0.00	1.717	14.95	0.00	0.00	0.00	0.00	0.00	14.95	0.00	0.00
1	0.87	7.58	8.17	49.28	0.855	7.45	8.32	50.15	0.09	0.11	0.62	7.52	8.25	49.72
5	0.782	6.82	9.02	54.40	0.765	6.67	9.19	55.39	0.10	0.12	0.70	6.74	9.10	54.89
15	0.694	6.05	9.87	59.52	0.679	5.92	10.02	60.39	0.09	0.11	0.62	5.99	9.94	59.95
30	0.627	5.47	10.51	63.41	0.623	5.43	10.56	63.65	0.02	0.03	0.16	5.45	10.54	63.53
60	0.561	4.90	11.15	67.25	0.548	4.78	11.28	68.01	0.08	0.09	0.53	4.84	11.22	67.63
150	0.409	3.57	12.62	76.09	0.415	3.63	12.57	75.75	0.04	0.03	0.25	3.60	12.59	75.92
510	0.201	1.77	14.62	88.19	0.227	1.99	14.38	86.68	0.16	0.17	1.07	1.88	14.50	87.44
1315	0.091	0.81	15.68	94.59	0.101	0.90	15.60	94.01	0.06	0.06	0.41	0.85	15.64	94.30
1420	0.08	0.71	15.79	95.23	0.092	0.82	15.69	94.53	0.07	0.07	0.49	0.77	15.74	94.88
1615	0.072	0.64	15.87	95.70	0.088	0.78	15.72	94.77	0.10	0.10	0.66	0.71	15.80	95.23
1735	0.06	0.54	15.98	96.39	0.072	0.64	15.88	95.70	0.07	0.07	0.49	0.59	15.93	96.04

Table D.3: Adsorption data for vineyard (10 mg/L)

	No .1				No. 2									
t (min)	**A/A_0**	**[MB] mg/L**	**q (mg/g)**	**% Removal**	**A/A_0**	**[MB]**	**q (mg/g)**	**% Removal**	**std dev [MB]**	**std dev for q**	**std for % Removal**	**Avg. [MB]**	**Avg. q (mg/g)**	**Avg. %Removal**
0	0.957	9.98	0.00	0.00	0.957	9.98	0.00	0.00	0.00	0.00	0.00	9.98	0.00	0.00
1	0.337	3.59	7.09	64.05	0.294	3.14	7.58	68.49	0.31	0.35	3.14	3.37	7.33	66.27
6	0.241	2.60	8.18	73.97	0.237	2.56	8.23	74.38	0.03	0.03	0.29	2.58	8.21	74.18
15	0.182	1.99	8.86	80.06	0.187	2.04	8.80	79.55	0.04	0.04	0.37	2.02	8.83	79.80
60	0.111	1.26	9.67	87.40	0.114	1.29	9.64	87.09	0.02	0.02	0.22	1.27	9.65	87.24
150	0.066	0.79	10.18	92.05	0.058	0.71	10.28	92.87	0.06	0.07	0.58	0.75	10.23	92.46
390	0.03	0.42	10.60	95.76	0.032	0.44	10.58	95.56	0.01	0.01	0.15	0.43	10.59	95.66
1200	0.02	0.32	10.71	96.80	0.018	0.30	10.74	97.00	0.01	0.02	0.15	0.31	10.72	96.90

Table D.4: Adsorption data for vineyard (5 mg/L)

	No .1				No. 2									
t (min)	**A/A_0**	**[MB]**	**q (mg/g)**	**% Removal**	**A/A_0**	**[MB]**	**q (mg/g)**	**% Removal**	**std dev [MB]**	**std dev for q**	**std for % Removal**	**Avg. [MB]**	**Avg. q (mg/g)**	**Avg. %Removal**
0	0.594	5.22	0.00	0.00	0.594	5.22	0.00	0.00	0.00	0.00	0.00	5.22	0.00	0.00
1	0.076	0.64	5.08	87.79	0.081	0.68	5.03	86.95	0.03	0.03	0.60	0.66	5.05	87.37
3	0.039	0.31	5.44	94.07	0.051	0.42	5.32	92.03	0.08	0.08	1.44	0.36	5.38	93.05
6	0.034	0.27	5.49	94.91	0.043	0.35	5.40	93.39	0.06	0.06	1.08	0.31	5.45	94.15
10	0.032	0.25	5.51	95.25	0.038	0.30	5.45	94.24	0.04	0.04	0.72	0.27	5.48	94.74
20	0.021	0.15	5.62	97.12	0.025	0.19	5.58	96.44	0.03	0.03	0.48	0.17	5.60	96.78
30	0.017	0.12	5.66	97.80	0.018	0.12	5.65	97.63	0.01	0.01	0.12	0.12	5.65	97.71

Table D.5: Adsorption data for black wattle (20 mg/L)

	No .1				No. 2									
t (min)	**A/A_0**	**[MB] mg/L**	**q (mg/g)**	**%Removal**	**A/A_0**	**[MB]**	**q (mg/g)**	**% Removal**	**std dev [MB]**	**std dev for q**	**std for % Removal**	**Avg. [MB]**	**Avg. q (mg/g)**	**Avg. %Removal**
0	2.272	20.10	0.00	0.00	2.272	20.10	0.00	0.00	0.00	0.00	0.00	20.10	0.00	0.00
1	1.487	13.21	7.64	34.28	1.443	12.82	8.06	36.20	0.27	0.30	1.36	13.02	7.85	35.24
15	1.234	10.99	10.10	45.32	1.220	10.87	10.23	45.93	0.09	0.09	0.43	10.93	10.17	45.62
150	0.813	7.30	14.20	63.69	0.816	7.32	14.16	63.56	0.02	0.03	0.09	7.31	14.18	63.62
510	0.562	5.10	16.64	74.64	0.535	4.86	16.89	75.82	0.17	0.18	0.83	4.98	16.76	75.23
1350	0.336	3.11	18.84	84.51	0.349	3.23	18.70	83.94	0.08	0.10	0.40	3.17	18.77	84.22
2060	0.16	1.57	20.55	92.19	0.191	1.84	20.23	90.84	0.19	0.22	0.96	1.71	20.39	91.51
3500	0.154	1.52	20.61	92.45	0.177	1.72	20.37	91.45	0.14	0.17	0.71	1.62	20.49	91.95
6385	0.06	0.69	21.52	96.55	0.081	0.88	21.30	95.64	0.13	0.16	0.65	0.79	21.41	96.09
7370	0.06	0.69	21.52	96.55	0.070	0.78	21.41	96.12	0.06	0.08	0.31	0.74	21.47	96.33
10250	0.06	0.69	21.52	96.55	0.060	0.69	21.51	96.55	0.00	0.01	0.00	0.69	21.52	96.55

Table D.6: Adsorption data for black wattle (15 mg/L)

	No .1				No. 2									
t (min)	**A/A_0**	**[MB] mg/L**	**q (mg/g)**	**%Removal**	**A/A_0**	**[MB]**	**q (mg/g)**	**% Removal**	**std dev [MB]**	**std dev for q**	**std for % Removal**	**Avg. [MB]**	**Avg. q (mg/g)**	**Avg. %Removal**
0	1.717	14.95	0.00	0.00	1.717	14.95	0.00	0.00	0.00	0.00	0.00	14.95	0.00	0.00
1	1.069	9.31	6.25	37.71	1.042	9.08	6.51	39.28	0.17	0.19	1.11	9.20	6.38	38.49
5	0.913	7.96	7.75	46.78	0.92	8.02	7.69	46.37	0.04	0.04	0.29	7.99	7.72	46.58
15	0.778	6.78	9.05	54.63	0.777	6.77	9.07	54.69	0.01	0.01	0.04	6.78	9.06	54.66
30	0.664	5.79	10.15	61.26	0.667	5.82	10.13	61.09	0.02	0.02	0.12	5.80	10.14	61.17
60	0.549	4.79	11.26	67.95	0.534	4.66	11.41	68.82	0.09	0.11	0.62	4.73	11.33	68.39
150	0.379	3.31	12.90	77.84	0.372	3.25	12.97	78.25	0.04	0.05	0.29	3.28	12.94	78.04
480	0.169	1.49	14.92	90.05	0.166	1.46	14.96	90.23	0.02	0.03	0.12	1.47	14.94	90.14
1764	0.048	0.43	16.09	97.09	0.058	0.52	16.00	96.51	0.06	0.06	0.41	0.48	16.04	96.80

Table D.7: Adsorption data for black wattle (10 mg/L)

	No .1				No. 2									
t	**A/A_0**	**[MB] mg/L**	**q (mg/g)**	**%Removal**	**A/A_0**	**[MB]**	**q (mg/g)**	**% Removal**	**std dev [MB]**	**std dev for q**	**std for % Removal**	**Avg. [MB]**	**Avg. q (mg/g)**	**Avg. %Removal**
0	0.982	10.24	0.00	0.00	0.982	10.24	0.00	0.00	0.00	0.00	0.00	10.24	0.00	0.00
1	0.366	3.89	7.04	62.04	0.374	3.97	6.95	61.24	0.06	0.06	0.57	3.93	7.00	61.64
3	0.33	3.52	7.45	65.67	0.31	3.31	7.69	67.68	0.15	0.17	1.42	3.41	7.57	66.68
7	0.271	2.91	8.13	71.61	0.251	2.70	8.36	73.62	0.15	0.17	1.42	2.80	8.24	72.62
15	0.203	2.21	8.90	78.46	0.186	2.03	9.10	80.17	0.12	0.14	1.21	2.12	9.00	79.31
60	0.071	0.85	10.41	91.74	0.07	0.84	10.43	91.85	0.01	0.01	0.07	0.84	10.42	91.79
150	0.036	0.48	10.81	95.27	0.034	0.46	10.84	95.47	0.01	0.02	0.14	0.47	10.83	95.37
475	0.022	0.34	10.97	96.68	0.018	0.30	11.03	97.08	0.03	0.04	0.28	0.32	11.00	96.88
1475	0.017	0.29	11.03	97.18	0.023	0.35	10.97	96.58	0.04	0.04	0.43	0.32	11.00	96.88

Table D.8: Adsorption data for black wattle (5 mg/L)

	No .1				No. 2									
t (min)	**A/A_0**	**[MB] mg/L**	**q (mg/g)**	**%Removal**	**A/A_0**	**[MB]**	**q (mg/g)**	**% Removal**	**std dev [MB]**	**std dev for q**	**std for % Removal**	**Avg. [MB]**	**Avg. q (mg/g)**	**Avg. %Removal**
0	0.565	4.96	0.00	0.00	0.565	4.96	0.00	0.00	0.00	0.00	0.00	4.96	0.00	0.00
1	0.203	1.76	3.55	64.49	n/d	n/d	n/d	n/d	n/d	n/d	n/d	1.76	3.55	64.49
3	0.072	0.60	4.84	87.87	0.059	0.49	4.96	90.19	0.08	0.09	1.64	0.54	4.90	89.03
5	0.076	0.64	4.80	87.15	0.065	0.54	4.90	89.12	0.07	0.08	1.39	0.59	4.85	88.14
7	0.047	0.38	5.08	92.33	0.038	0.30	5.17	93.93	0.06	0.06	1.14	0.34	5.12	93.13
10	0.028	0.21	5.27	95.72	0.021	0.15	5.34	96.97	0.04	0.05	0.88	0.18	5.30	96.34
15	0.017	0.12	5.38	97.68	0.014	0.09	5.40	98.22	0.02	0.02	0.38	0.10	5.39	97.95
20	0.009	0.04	5.45	99.11	0.009	0.04	5.45	99.11	0.00	0.00	0.00	0.04	5.45	99.11
30	0.006	0.02	5.48	99.64	0.006	0.02	5.48	99.64	0.00	0.00	0.00	0.02	5.48	99.64

Table D.9: Adsorption data for sugar cane bagasse (20 mg/L)

	No .1				No. 2									
t (min)	**A/A_0**	**[MB] mg/L**	**q (mg/g)**	**%Removal**	**A/A_0**	**[MB]**	**q (mg/g)**	**% Removal**	**std dev [MB]**	**std dev for q**	**std for % Removal**	**Avg. [MB]**	**Avg. q (mg/g)**	**Avg. %Removal**
0	2.163	20.00	0.00	0.00	2.163	20.00	0.00	0.00	0.00	0.00	0.00	20.00	0.00	0.00
1	1.201	11.09	9.87	44.54	1.31	12.10	8.76	39.49	0.71	0.78	3.57	11.60	9.32	42.01
15	0.777	7.17	14.22	64.17	0.778	7.18	14.23	64.12	0.01	0.00	0.03	7.17	14.23	64.14
150	0.329	3.02	18.82	84.91	0.335	3.07	18.78	84.63	0.04	0.03	0.20	3.05	18.80	84.77
510	0.133	1.20	20.83	93.98	0.136	1.23	20.82	93.84	0.02	0.01	0.10	1.22	20.83	93.91
810	0.093	0.83	21.24	95.83	0.091	0.81	21.29	95.93	0.01	0.03	0.07	0.82	21.26	95.88
1350	0.064	0.56	21.54	97.18	0.061	0.54	21.59	97.31	0.02	0.04	0.10	0.55	21.57	97.25
2070	0.062	0.55	21.56	97.27	0.072	0.64	21.48	96.81	0.07	0.06	0.33	0.59	21.52	97.04

Table D.10: Adsorption data for sugar cane bagasse (15 mg/L)

	No .1				No. 2									
t (min)	**A/A_0**	**[MB] mg/L**	**q (mg/g)**	**%Removal**	**A/A_0**	**[MB]**	**q (mg/g)**	**% Removal**	**std dev [MB]**	**std dev for q**	**std for % Removal**	**Avg. [MB]**	**Avg. q (mg/g)**	**Avg. %Removal**
0	1.681	14.63	0.00	0.00	1.681	14.63	0.00	0.00	0.00	0.00	0.00	14.63	0.00	0.00
1	0.803	7.00	8.46	52.15	1.007	8.77	6.49	40.03	1.25	1.39	8.57	7.89	7.48	46.09
5	0.552	4.82	10.88	67.07	0.588	5.13	10.54	64.93	0.22	0.24	1.51	4.97	10.71	66.00
15	0.353	3.09	12.80	78.90	0.371	3.24	12.63	77.83	0.11	0.12	0.76	3.17	12.71	78.36
30	0.239	2.10	13.90	85.68	0.256	2.24	13.74	84.67	0.10	0.11	0.71	2.17	13.82	85.17
60	0.141	1.24	14.84	91.50	0.153	1.35	14.73	90.79	0.07	0.08	0.50	1.30	14.79	91.14
150	0.061	0.55	15.61	96.26	0.057	0.51	15.66	96.49	0.02	0.03	0.17	0.53	15.63	96.37
270	0.03	0.28	15.91	98.10	0.023	0.22	15.98	98.51	0.04	0.05	0.29	0.25	15.95	98.31

Table D.11: Adsorption data for sugar cane bagasse (10 mg/L)

	No .1				No. 2									
t (min)	**A/A_0**	**[MB] mg/L**	**q (mg/g)**	**%Removal**	**A/A_0**	**[MB]**	**q (mg/g)**	**% Removal**	**std dev [MB]**	**std dev for q**	**std for % Removal**	**Avg. [MB]**	**Avg. q (mg/g)**	**Avg. %Removal**
0	1.12	9.88	0.00	0.00	1.12	9.88	0.00	0.00	0.00	0.00	0.00	9.88	0.00	0.00
1	0.312	2.73	7.94	72.41	0.222	1.93	8.81	80.47	0.56	0.62	5.70	2.33	8.38	76.44
3	0.145	1.25	9.58	87.37	0.117	1.00	9.84	89.88	0.18	0.19	1.77	1.12	9.71	88.62
6	0.083	0.70	10.19	92.92	0.065	0.54	10.35	94.54	0.11	0.12	1.14	0.62	10.27	93.73
10	0.051	0.42	10.50	95.79	0.042	0.34	10.58	96.60	0.06	0.06	0.57	0.38	10.54	96.19
20	0.025	0.19	10.76	98.12	0.02	0.14	10.80	98.57	0.03	0.03	0.32	0.16	10.78	98.34
30	0.02	0.14	10.80	98.57	0.019	0.13	10.81	98.66	0.01	0.00	0.06	0.14	10.81	98.61
60	0.014	0.09	10.86	99.10	0.011	0.06	10.88	99.37	0.02	0.02	0.19	0.08	10.87	99.24
150	0.007	0.03	10.93	99.73	0.01	0.05	10.89	99.46	0.02	0.03	0.19	0.04	10.91	99.60

Table D.12: Adsorption data for sugar cane bagasse (5 mg/L)

	No .1				No. 2									
t (min)	**A/A_0**	**[MB] mg/L**	**q (mg/g)**	**%Removal**	**A/A_0**	**[MB]**	**q (mg/g)**	**% Removal**	**std dev [MB]**	**std dev for q**	**std for % Removal**	**Avg. [MB]**	**Avg. q (mg/g)**	**Avg. %Removal**
0	0.565	4.96	0.00	0.00	0.565	4.96	0.00	0.00	0.00	0.00	0.00	4.96	0.00	0.00
0.5	0.131	1.12	4.25	77.34	0.176	1.52	3.82	69.31	0.28	0.31	5.68	1.32	4.04	73.33
2.5	0.08	0.67	4.76	86.44	0.07	0.58	4.86	88.22	0.06	0.07	1.26	0.63	4.81	87.33
5	0.004	0.00	5.50	100	0.005	0.01	5.50	99.82	0.01	0.00	0.13	0.00	5.50	99.91

APPENDIX E: TIME (MIN) VERSUS Q (MG/G) EQUILIBRIUM GRAPHS FOR MB ADSORPTION

E.1 Vineyard

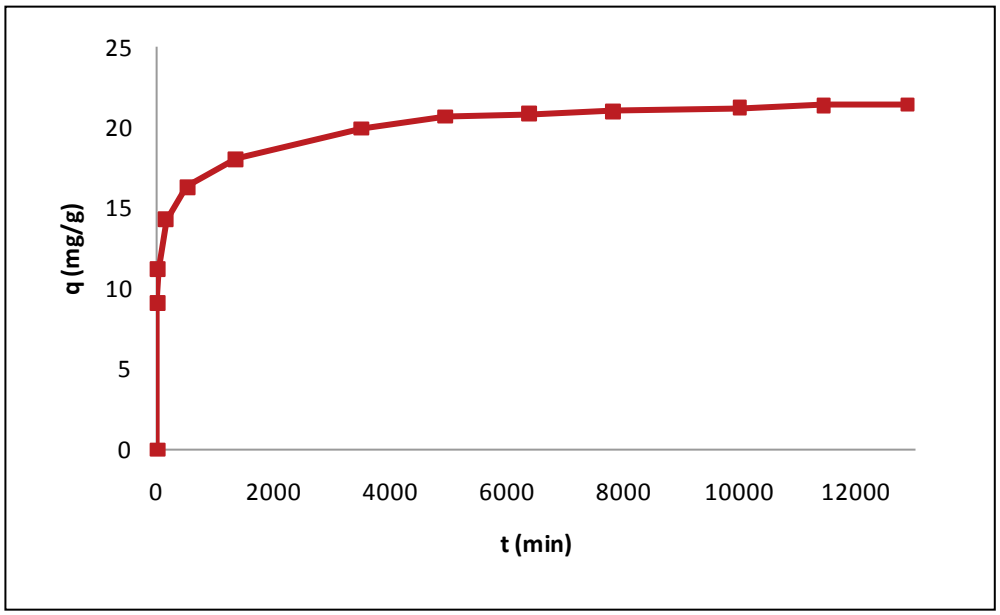

Figure E.1: Methylene blue adsorption by vineyard for a concentration of 20 ppm

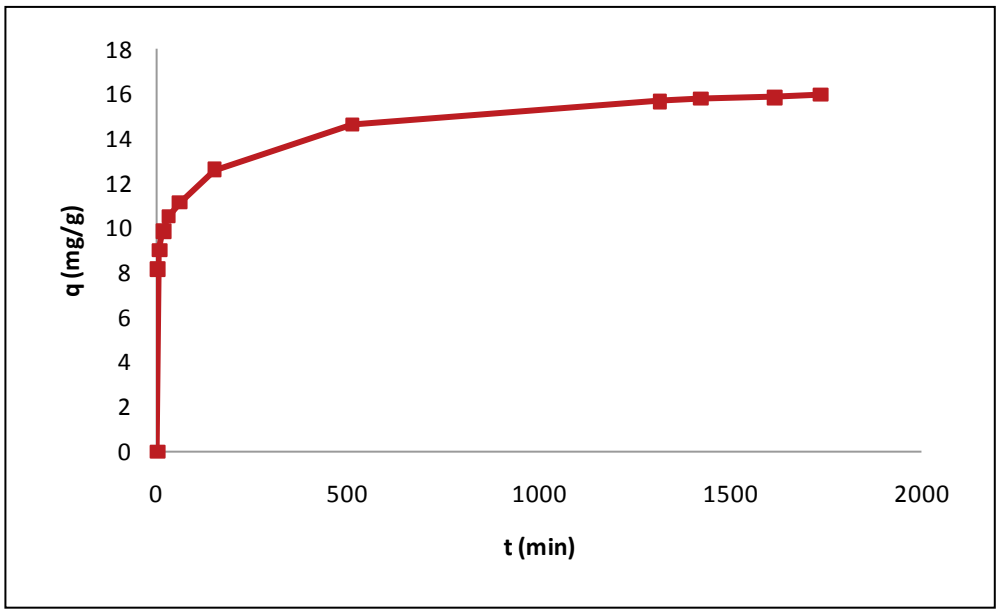

Figure E.2: Methylene blue adsorption by vineyard for a concentration of 15 ppm

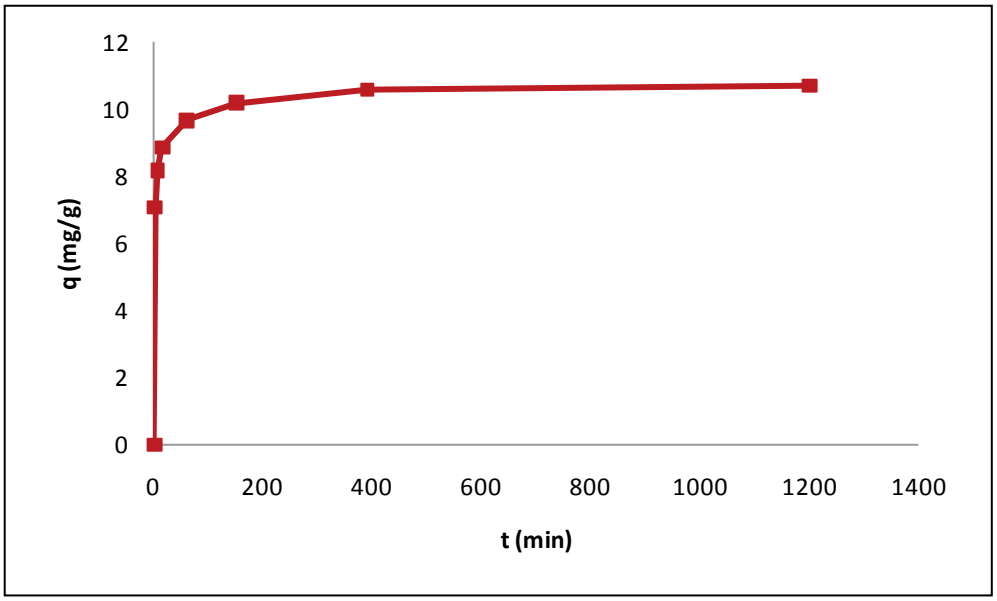

Figure E.3: Methylene blue adsorption by vineyard for a concentration of 10 ppm

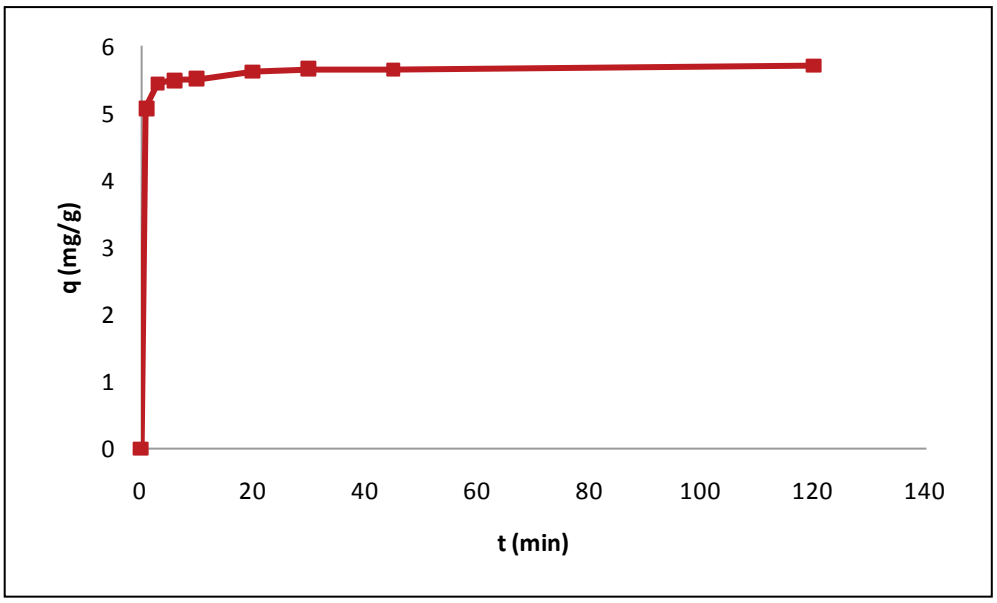

Figure E.4: Methylene blue adsorption by vineyard for a concentration of 5 ppm

E.2 Black Wattle

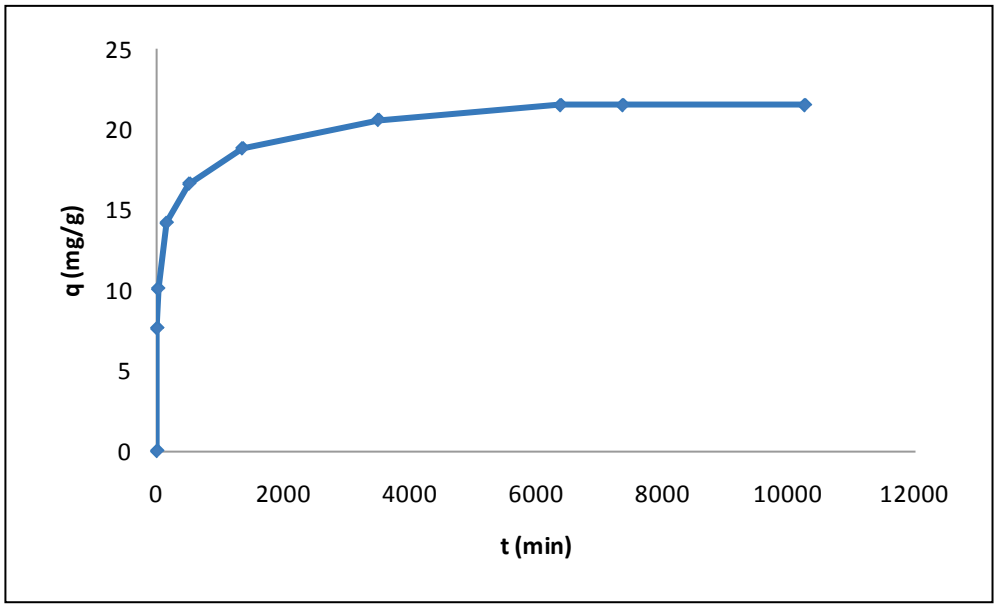

Figure E.5: Methylene blue adsorption by black wattle for a concentration of 20 ppm

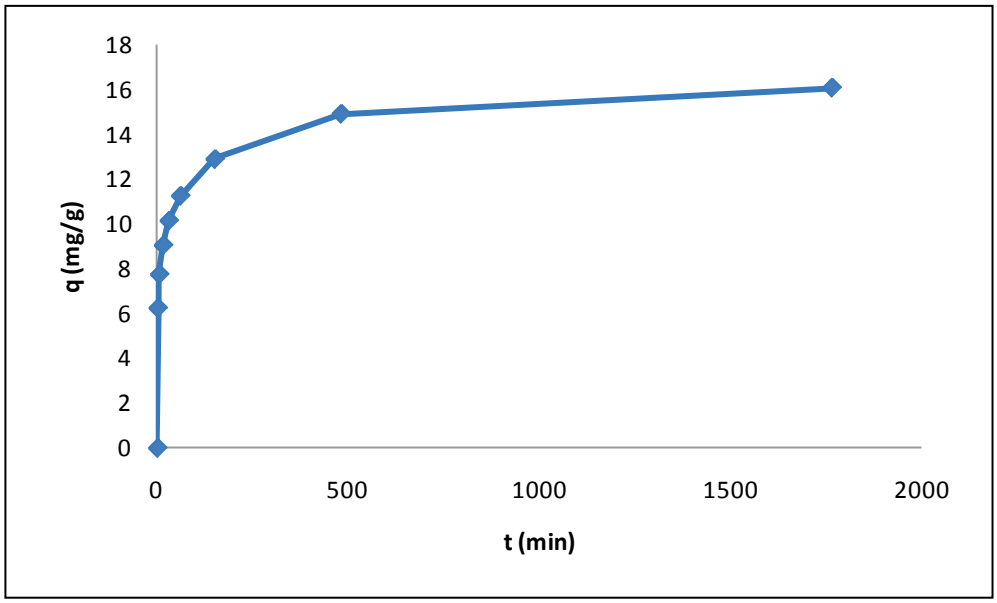

Figure E.6: Methylene blue adsorption by black wattle for a concentration of 15 ppm

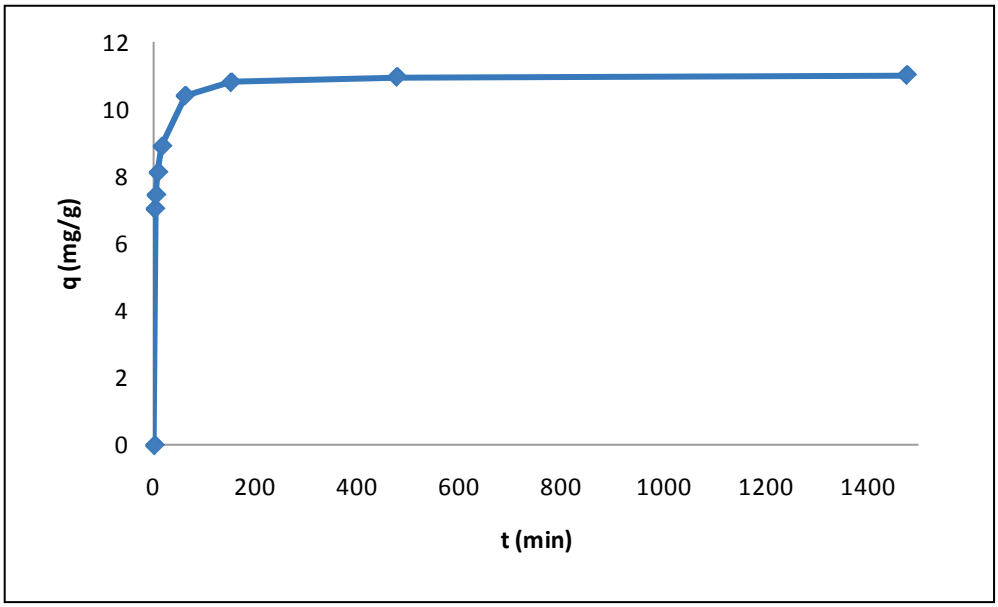

Figure E.7: Methylene blue adsorption by black wattle for a concentration of 10 ppm

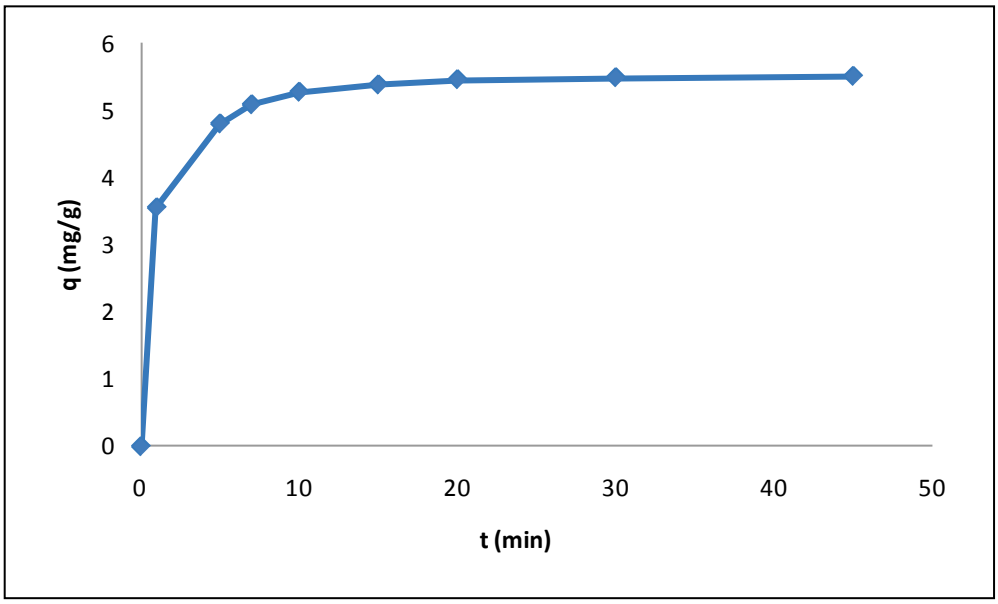

Figure E.8: Methylene blue adsorption by black wattle for a concentration of 5 ppm

E.3 Sugar cane bagasse

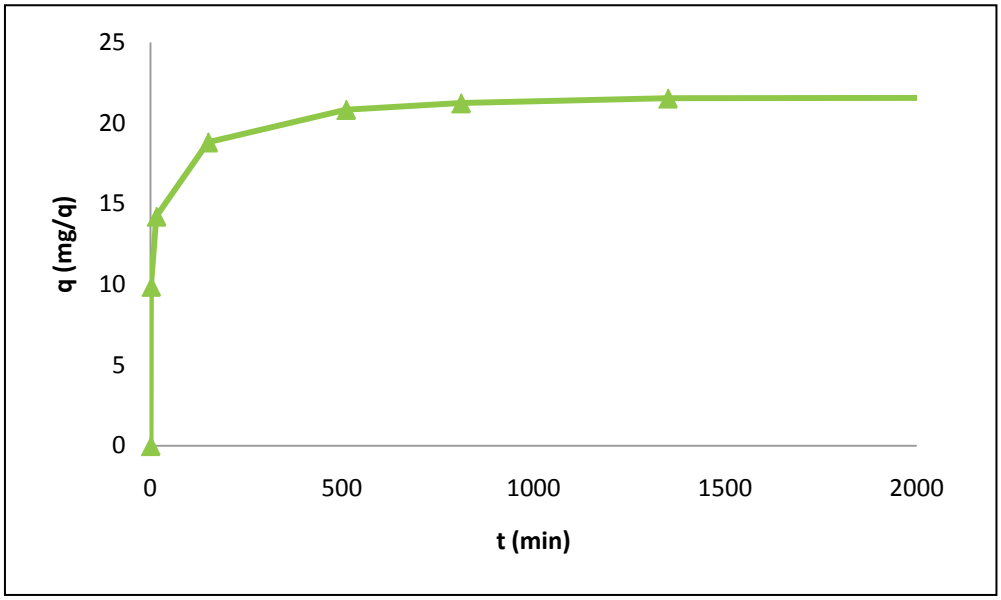

Figure E.9: Methylene blue adsorption by sugar cane bagasse for a concentration of 20 ppm

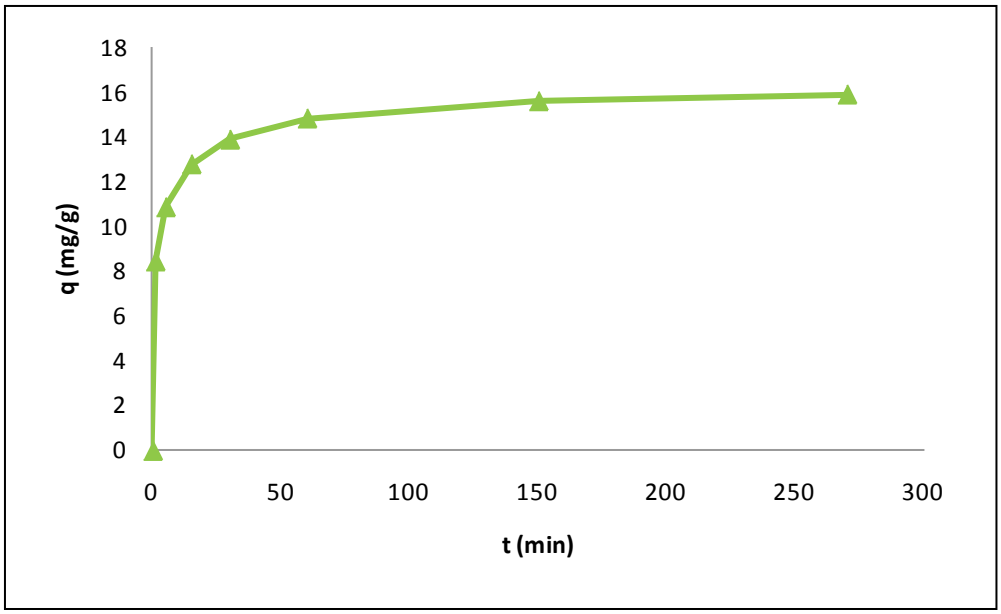

Figure E.10: Methylene blue adsorption by sugar cane bagasse for a concentration of 15 ppm

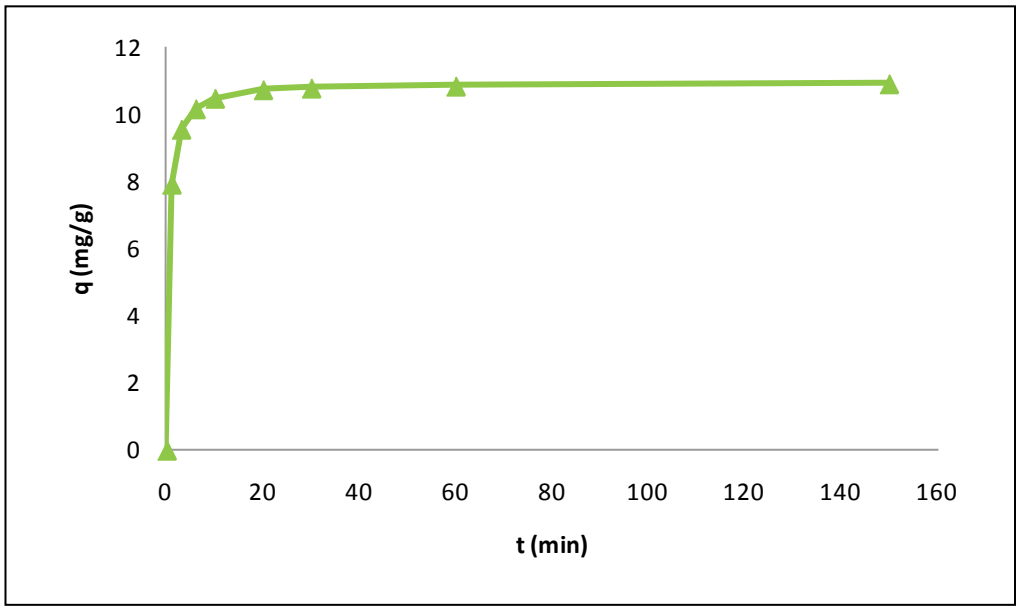

Figure E.11: Methylene blue adsorption sugar cane bagasse for a concentration of 10 ppm

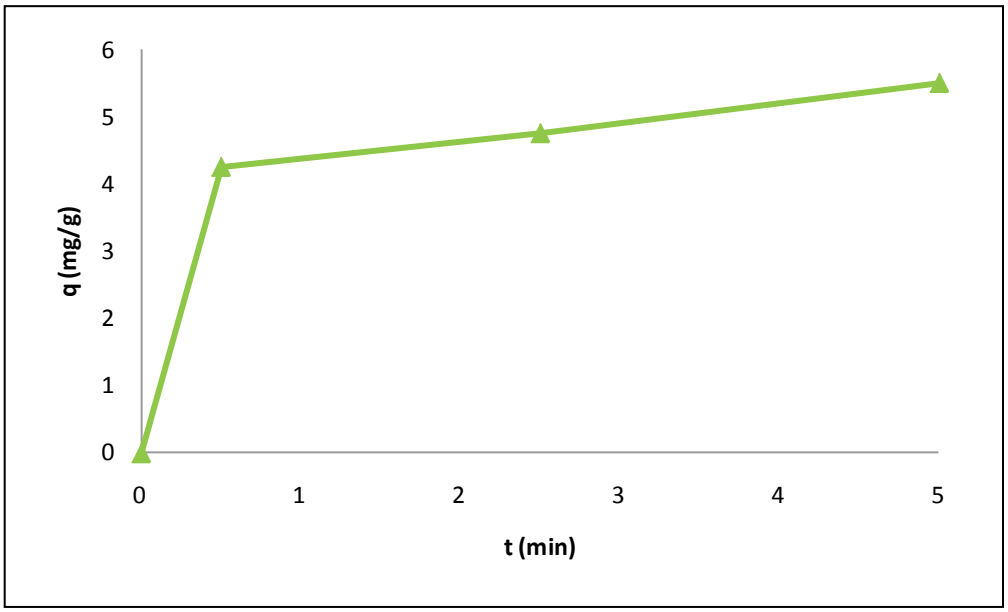

Figure E.12: Methylene blue adsorption sugar cane bagasse for a concentration of 5 ppm

APPENDIX F: PSEUDO-SECOND-ORDER ADSORPTION KINETICS FOR OVERALL ADSORPTION OF 20 PPM MB

F.1 Vineyard

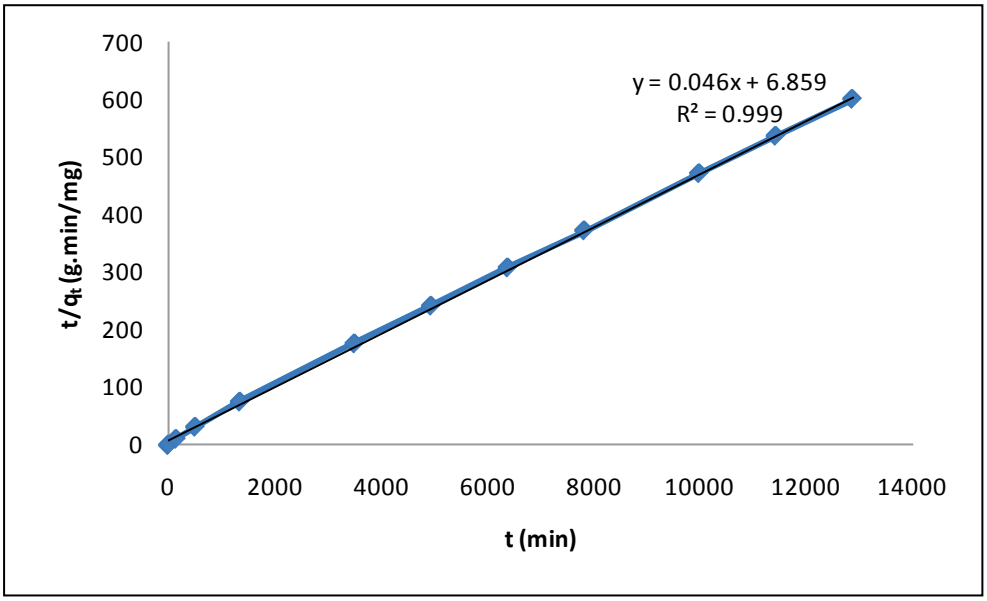

Figure F.1: Pseudo-second-order kinetics for overall adsorption of 20 ppm MB by vineyard biochar

The overall adsorption of 20 ppm MB by vineyard biochar resulted with a q_e of 21.74 mg/g and k_2 of 0.0003 g/mg.min.

F.2 Black wattle

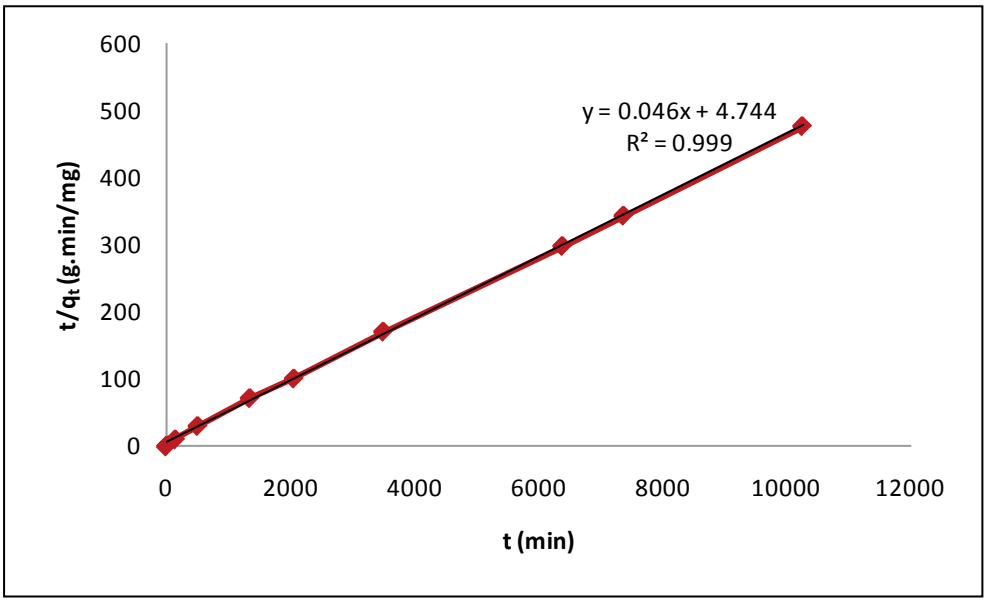

Figure F.2: Pseudo-second-order kinetics for overall adsorption of 20 ppm MB by black wattle biochar

The overall adsorption of 20 ppm MB by black wattle biochar resulted with a q_e of 21.74 mg/g and k_2 of 0.0005 g/mg.min.

F.3 Sugar cane bagasse

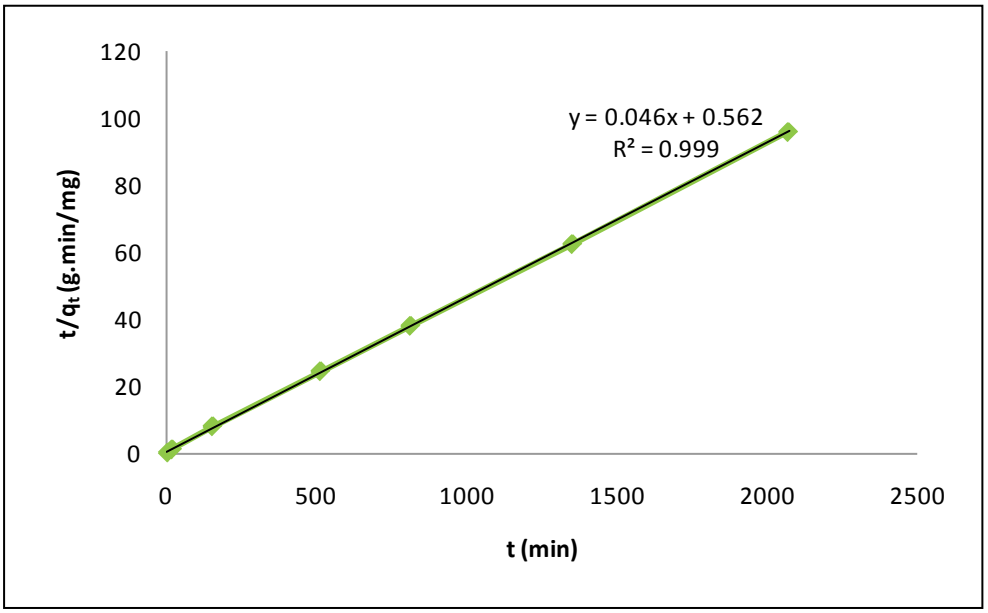

Figure F.3: Pseudo-second-order kinetics for overall adsorption of 20 ppm MB by sugar cane bagasse biochar

The overall adsorption of 20 ppm MB by sugar cane bagasse biochar resulted with a q_e of 21.74 mg/g and k_2 of 0.004 g/mg.min.